Gravitational Lensing Astronomy

Masamune Oguri
Center for Frontier Science, Chiba University

CHIBA UNIVERSITY
Center for Frontier Science

2026/5-6 Intensive lecture@U.Tokyo

Plan

- schedule
  - 5/27 (Wed) 2nd, 3rd, 4th periods
  - 6/5 (Fri) 2nd, 3rd, 4th, 5th periods
  - 6/10 (Wed) 2nd, 3rd, 4th periods
  - 6/12 (Fri) 2nd, 3rd, 4th periods
- use both blackboard and slides (slides are uploaded to UTOL)
- questions are very much welcome, please interrupt me at any time!

Reference

- M. Oguri, “Gravitational lensing” (in Japanese), Asakura Publishing Co.

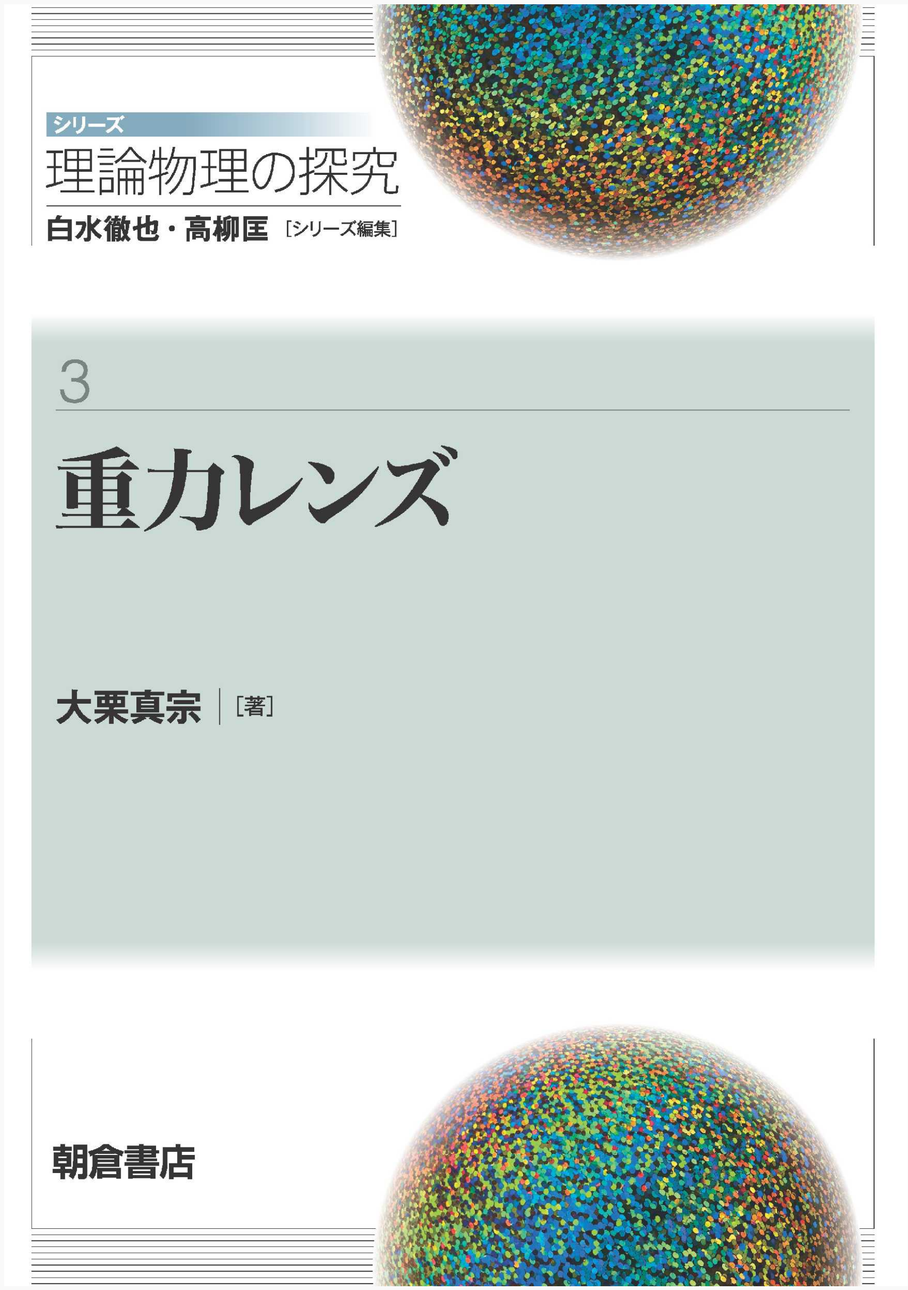

1. Introduction

Standard model of cosmology

- Standard model of cosmology assumes dark matter and dark energy, and consistently explains many different observations
  - cosmic background radiation (CMB)
  - Type Ia supernova
  - galaxy clustering
  - gravitational lensing
  - …

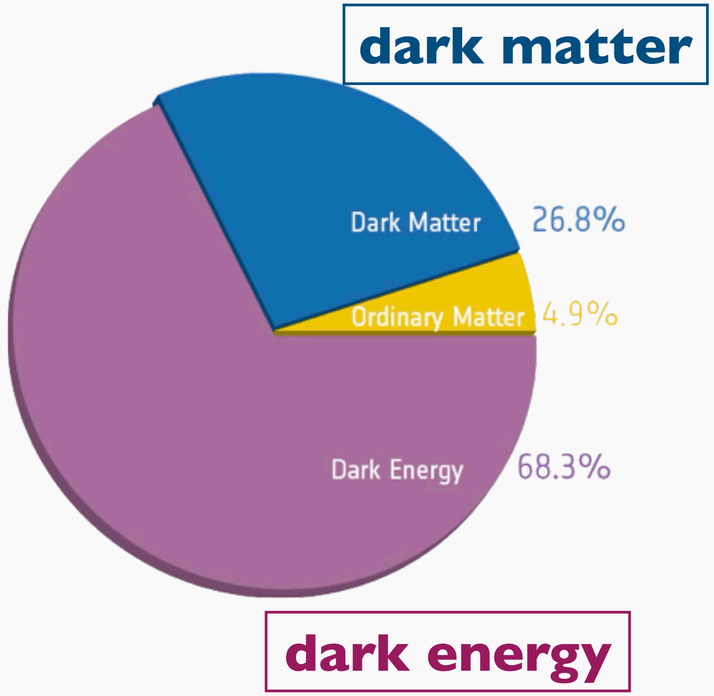

(ESA/Planck)

Gravitational lensing

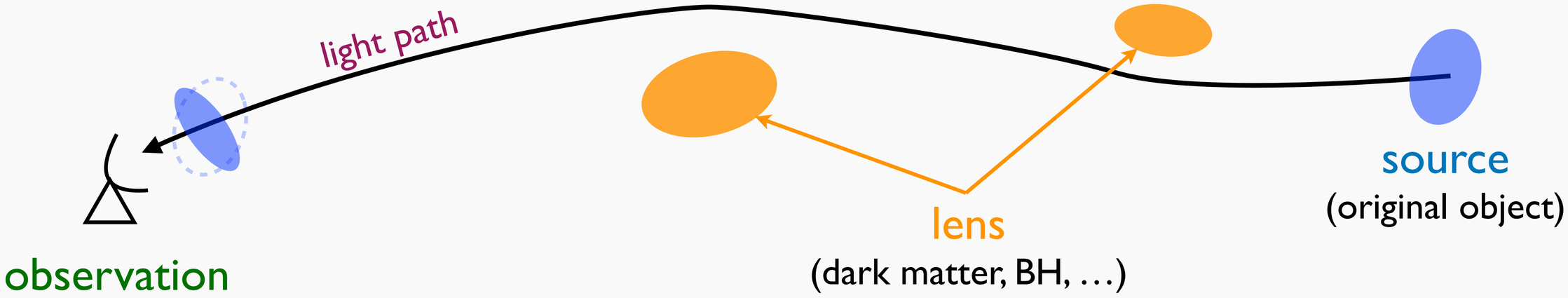

- predicted by general relativity
- deflection of light ray path due to density inhomogeneity
- multiple images, distortion of images, magnification, etc.

Gravitational lensing in Newtonian gravity

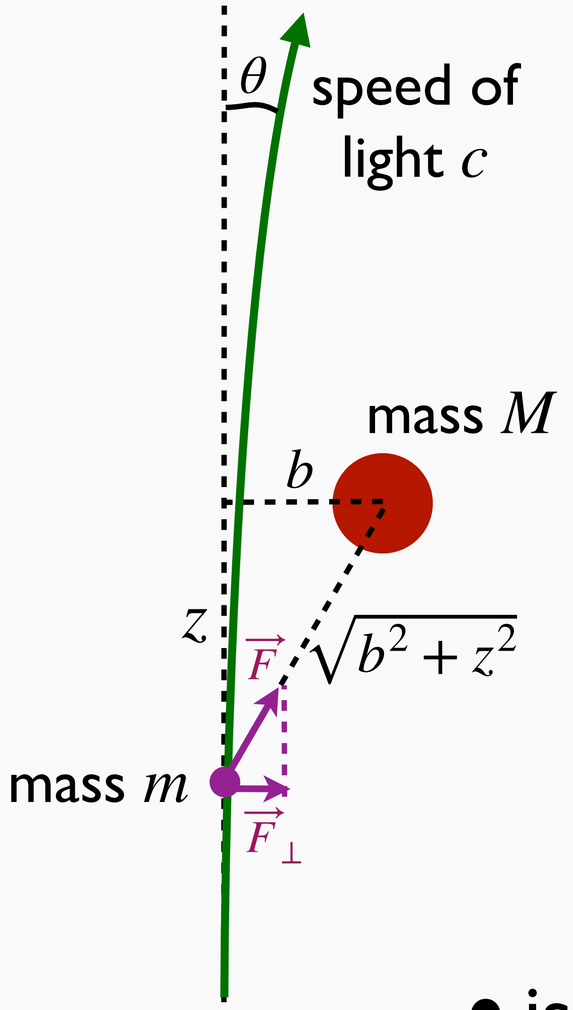

$$m\vec{a} = \vec{F}$$ equation of motion

$$\left|\vec{F}_\perp\right| = \frac{GMmb}{(b^2+z^2)^{3/2}}$$ force perpendicular to propagation direction

deflection angle

$$\theta \simeq \frac{v_\perp}{c} \simeq \frac{1}{c^2}\int_{-\infty}^{\infty} a_\perp dz$$

$$= \frac{GMb}{c^2}\int_{-\infty}^{\infty} \frac{1}{(b^2+z^2)^{3/2}} dz = \frac{2GM}{c^2 b}$$

- is light path really deflected? ($m = 0$?)

Gravitational lensing in general relativity

- unambiguously calculated from geodesic equation

$$\frac{d^2x^\mu}{d\lambda^2} + \Gamma^\mu{}_{\alpha\beta}\frac{dx^\alpha}{d\lambda}\frac{dx^\beta}{d\lambda} = 0$$

- deflection angle factor of 2 larger than Newtonian case

$$\theta = \frac{4GM}{c^2 b} = 1.74'' \left(\frac{M}{M_\odot}\right)\left(\frac{b}{R_\odot}\right)^{-1}$$

when pass through the surface of Sun

Gravitational lensing in general relativity

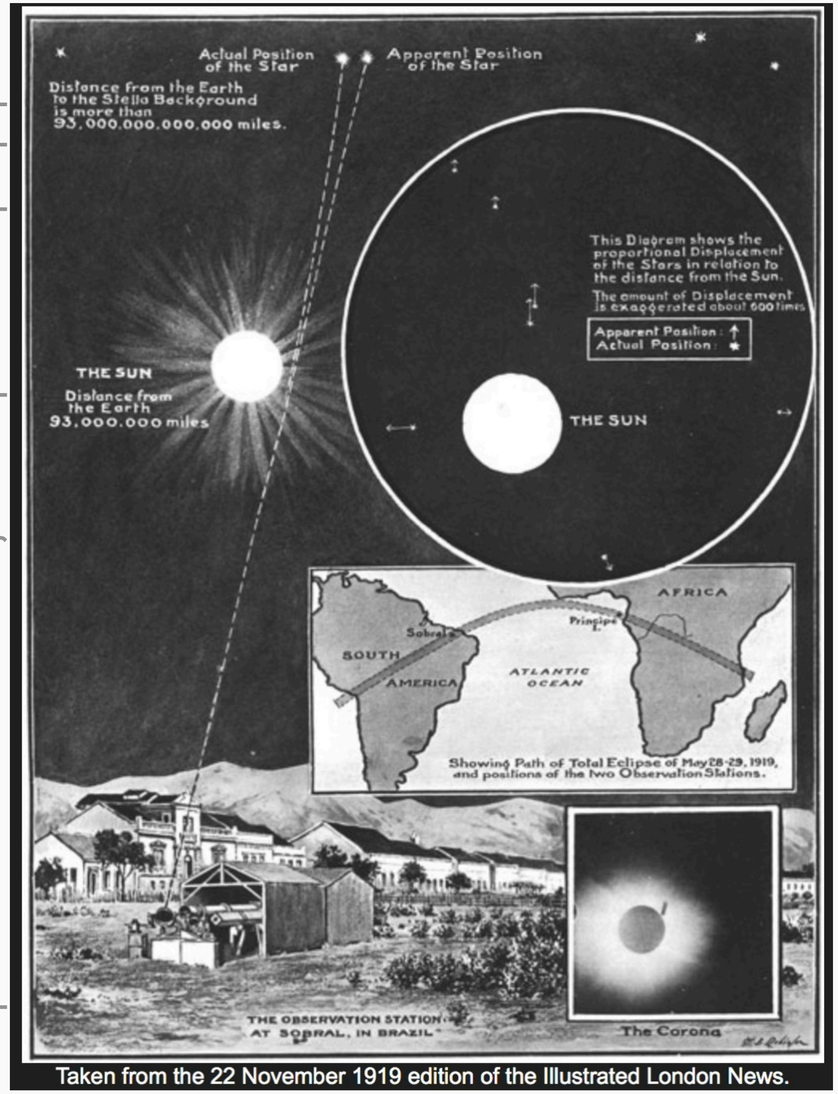

Taken from the 22 November 1919 edition of the Illustrated London News.

http://www.astro.caltech.edu/~rjm/Principe/1919eclipse.php

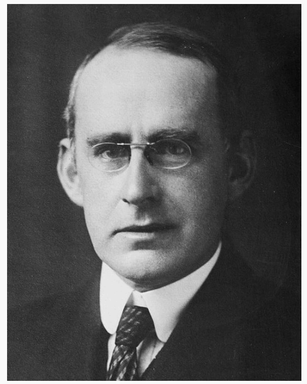

Arthur Eddington (Wikipedia)

- observation of deflection angle in 1919 solar eclipse
  - 1.61″±0.40″ @Principe
  - 1.98″±0.16″ @Sobal

➡ general relativity is correct!

e.g., Cole, astro-ph/0102462

Inconvenient truth?

- Sobal result is based on a backup 4 inch telescope as main 10 inch telescope data was in trouble
- 10 inch data indicates 0.93″, closer to Newtonian value
- Principe data was not so accurate as weather was not good
- not clear if data was good enough to conclude that general relativity is correct

Recent measurement

- deflection angle is tested with accuracy of 10^{-4} from observations of radio sources behind Sun

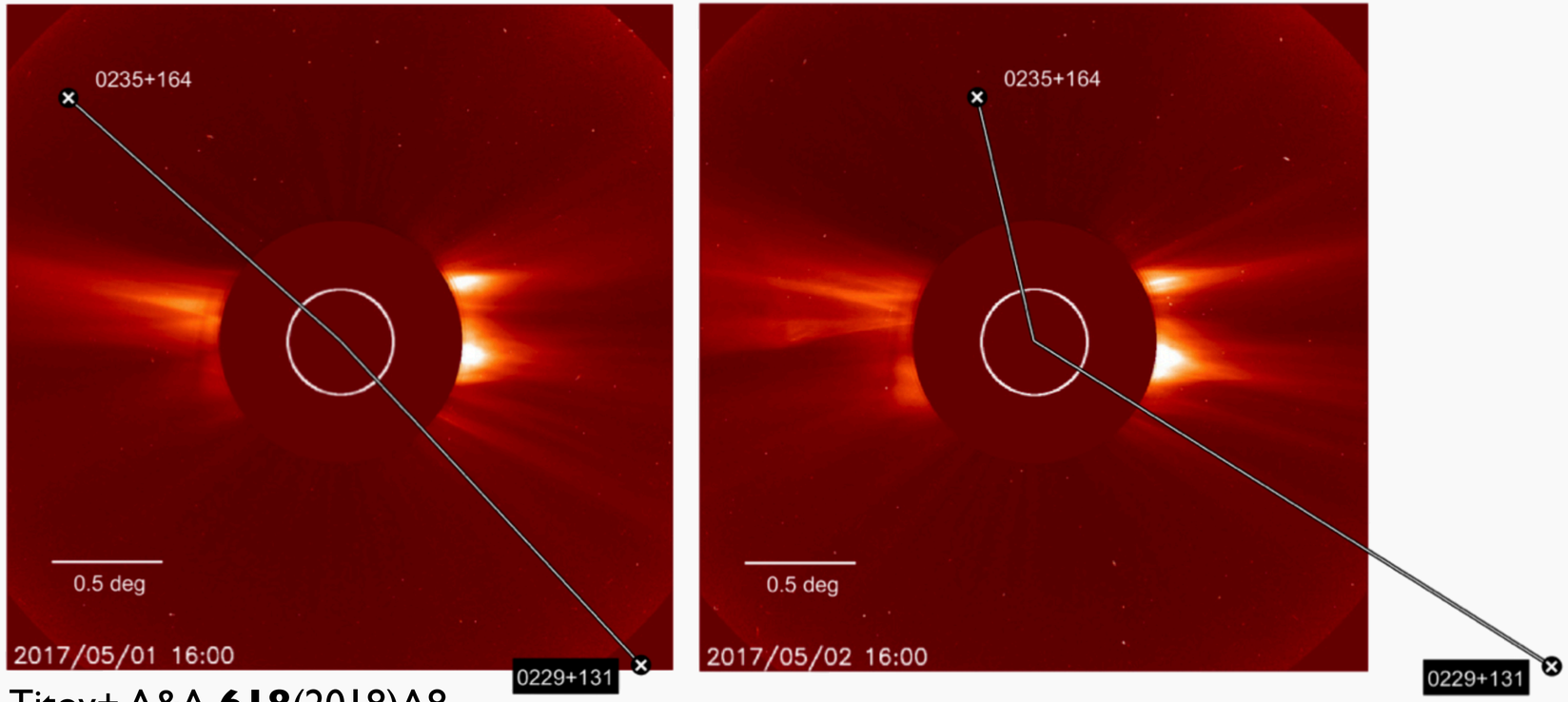

Titov+ A&A **618**(2018)A8

Example of gravitational lensing (I)

Q0957+561

first strong gravitational lensing reported in 1979 Walsh+ Nature **279**(1979)381

double images of quasar

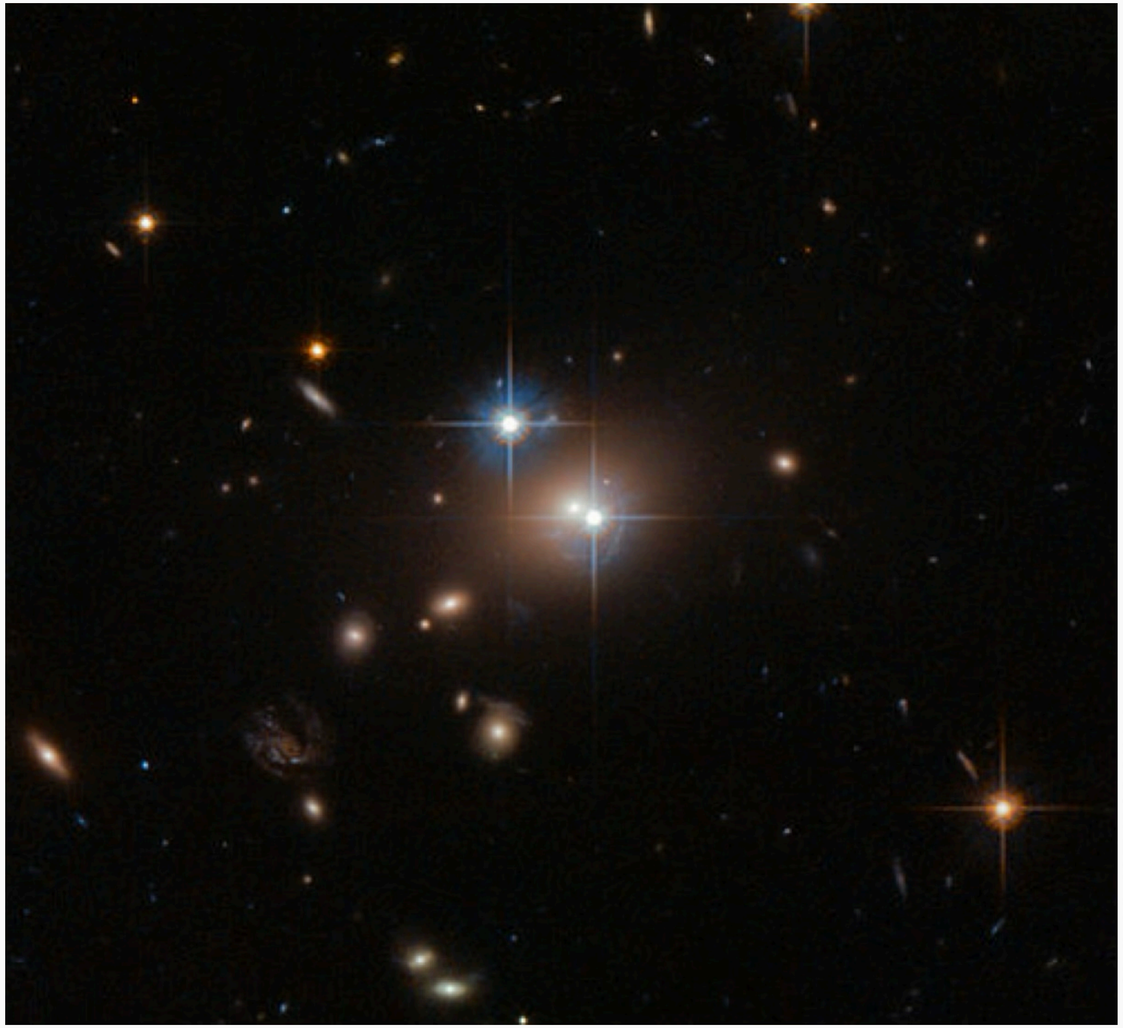

Hubble/ESA/NASA

Example of gravitational lensing (I)

Q0

first

repo

dou

Walsh+ Nature **279**(1979)381

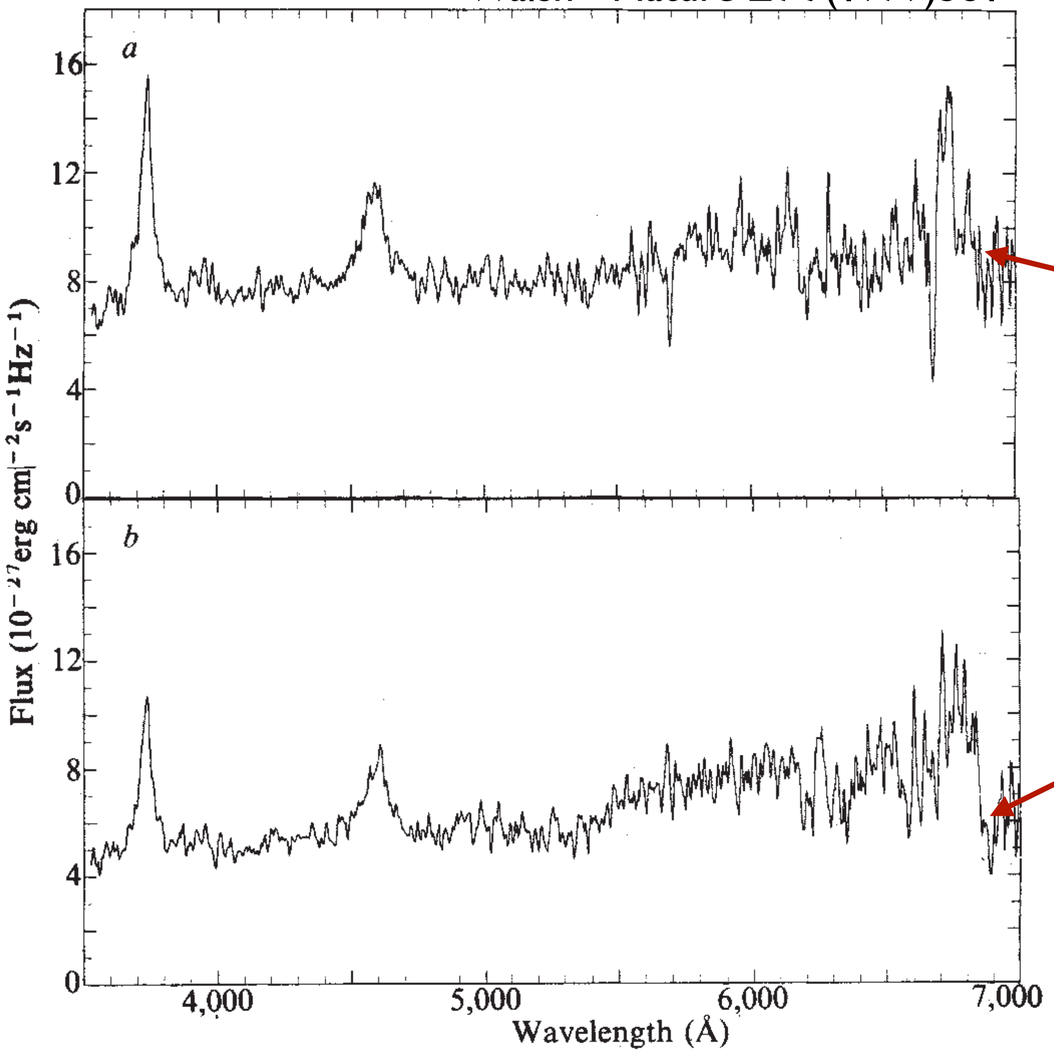

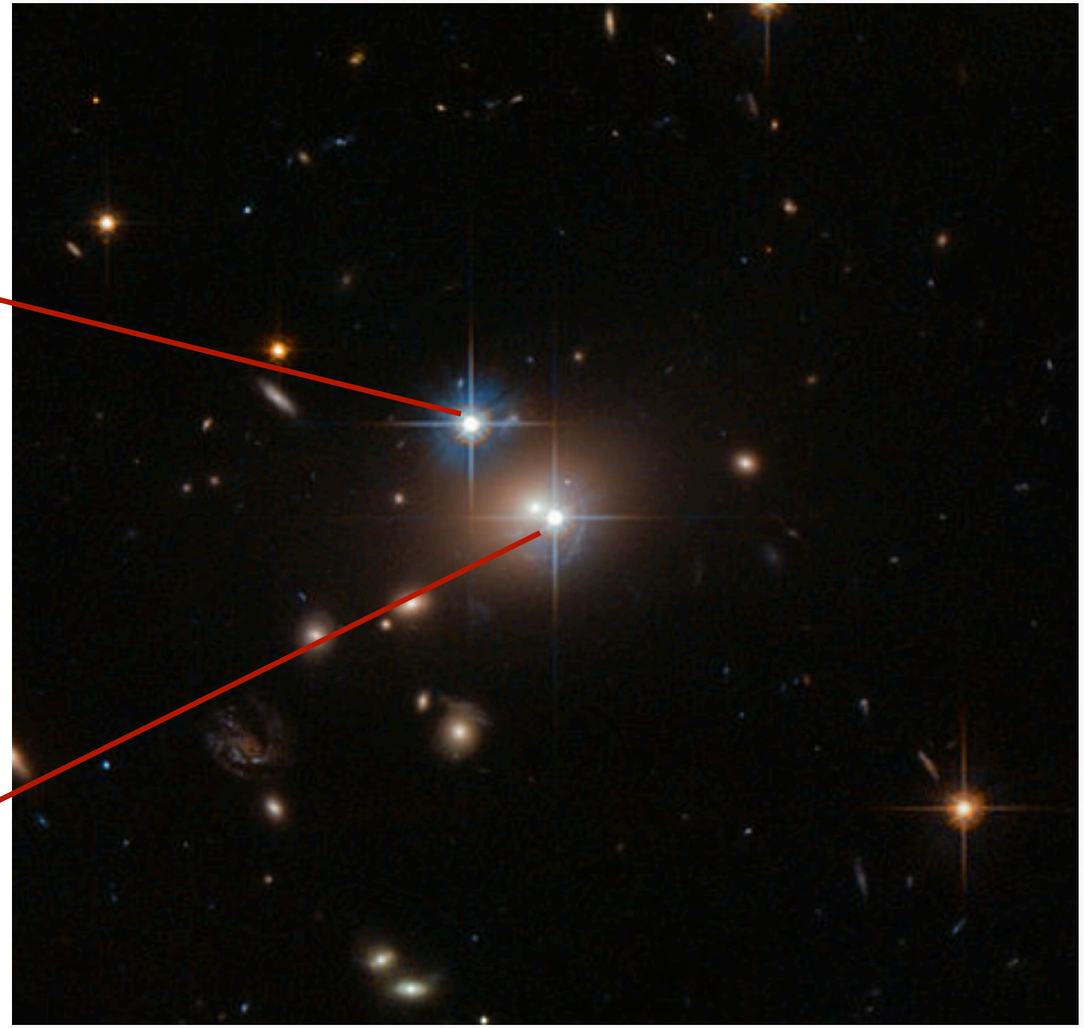

Hubble/ESA/NASA

Example of gravitational lensing (II)

SDSS J1004

large-separation gravitationally lensed quasar produced by cluster

Inada, MO+ Nature, **426**, 810 (2003)

quintuple images of quasar

ESA/NASA/K. Sharon/E. Ofek

Example of gravitational lensing (III)

SMACS J0723

one of first targets of James Webb Space Telescope (JWST)

image released in 2022

many lensed arcs behind cluster

NASA/ESA/CSA/STScI

Applications of strong gravitational lensing

- strong gravitational lensing produce multiple images and high magnifications
- representative applications
  - Hubble constant measurement with time delays
  - small-scale dark matter distribution with flux ratios and shapes of multiple images
  - distant objects with help of lensing magnifications

Hubble constant (H_0) problem

distance ladder

combine various distance indicators such as Cepheid and Type Ia supernovae

CMB

derive from observed CMB temperature fluctuation pattern assuming standard cosmology

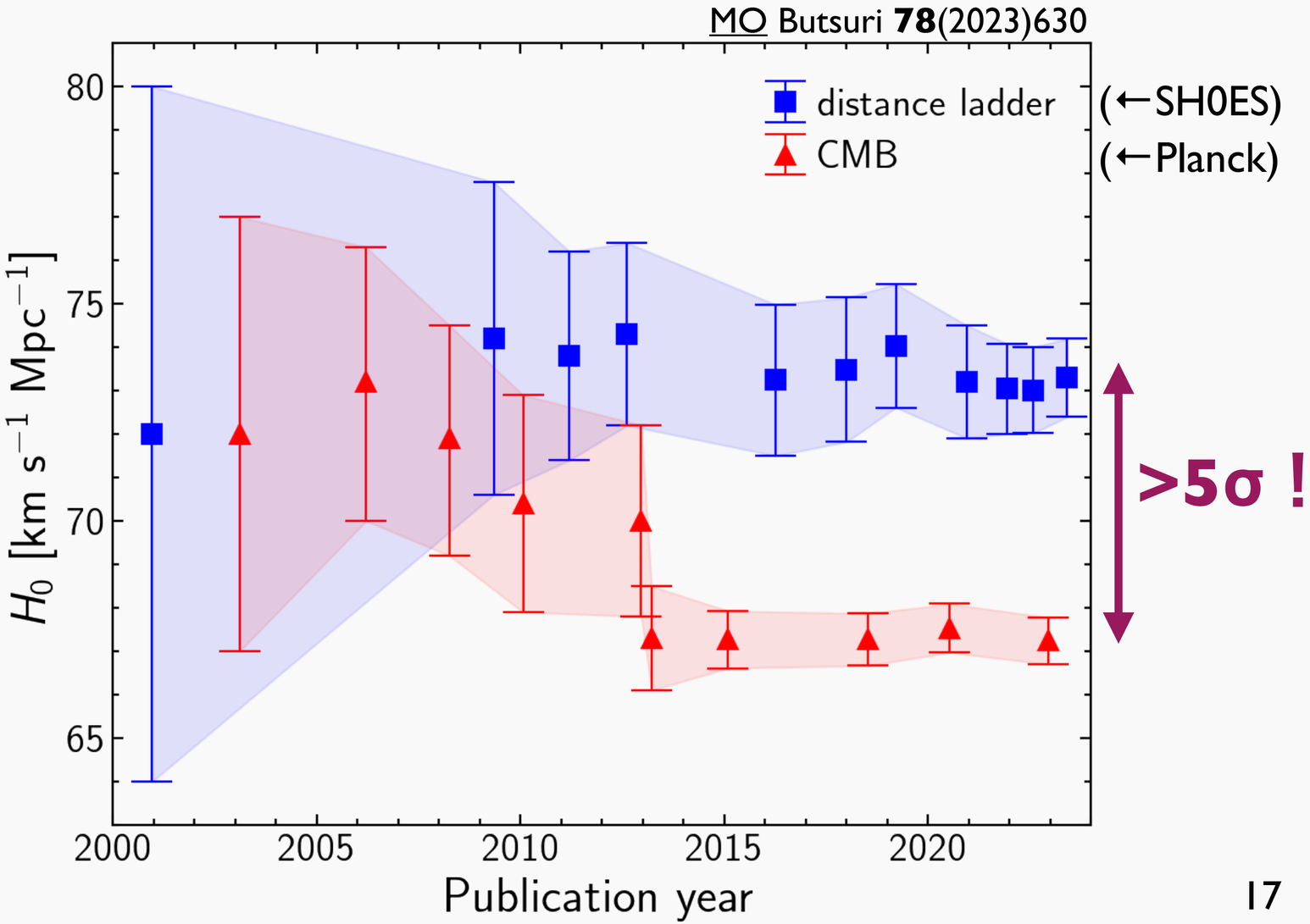

Time delay

- different arrival time between multiple images (months or years)
- can be observed if source is time-variable object such as quasar and supernova

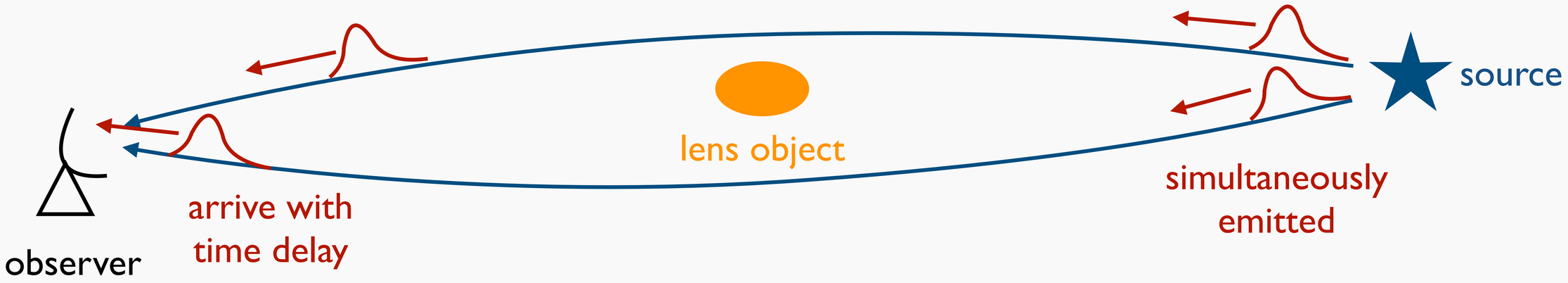

small H_0 → large Universe → large time delay

Time delay in Q0957+561

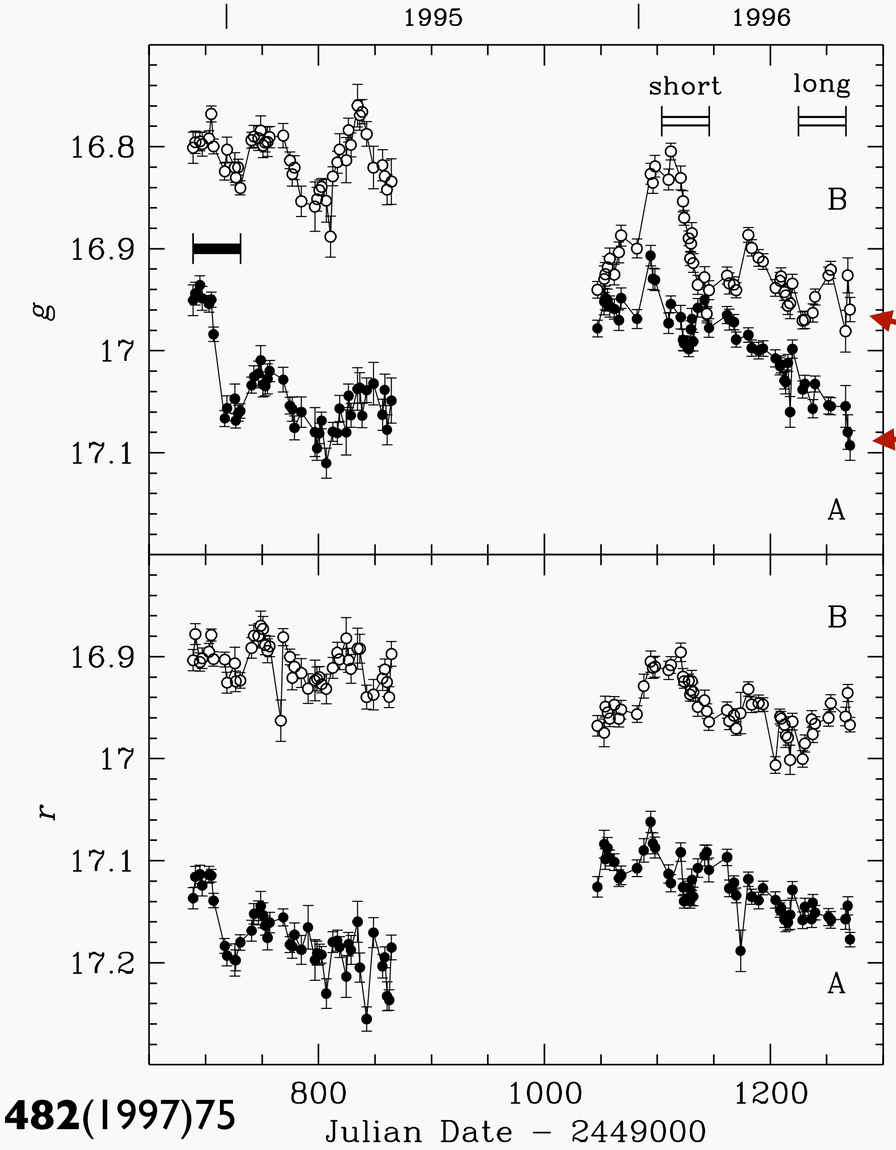

Kundic+ ApJ **482**(1997)75

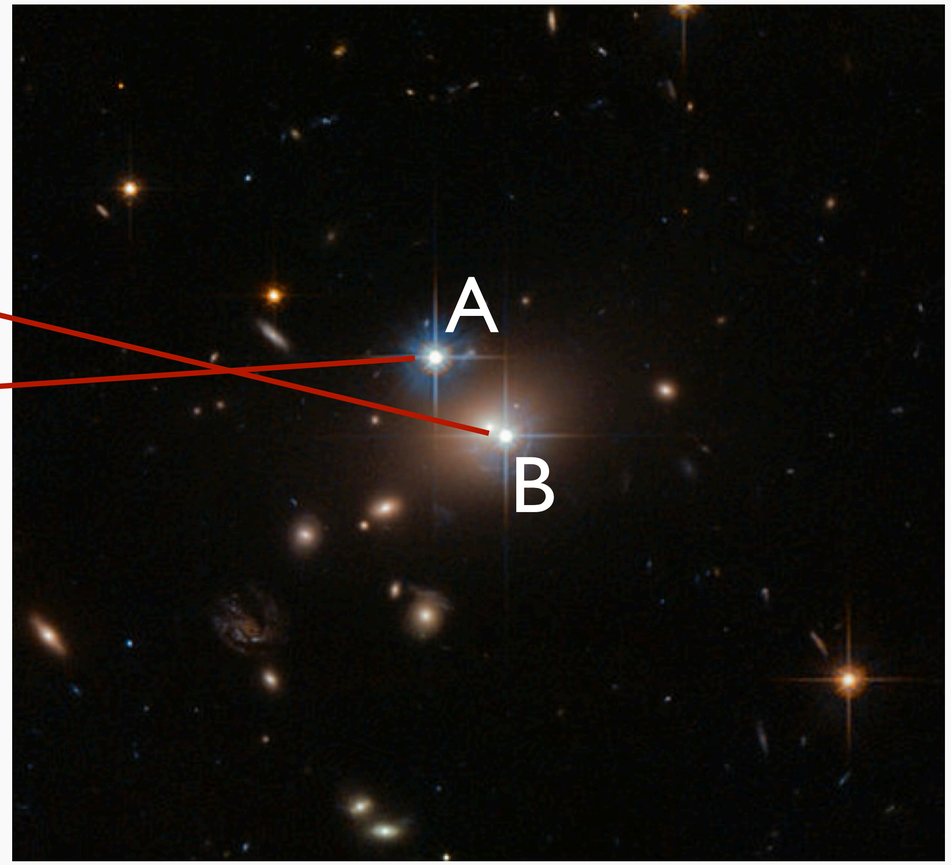

Hubble/ESA/NASA

$$\rightarrow H_0 = 85^{+14}_{-13}\mathrm{km/s/Mpc}$$

Fadely+ ApJ **711**(2010)246

Supernova Refsdal

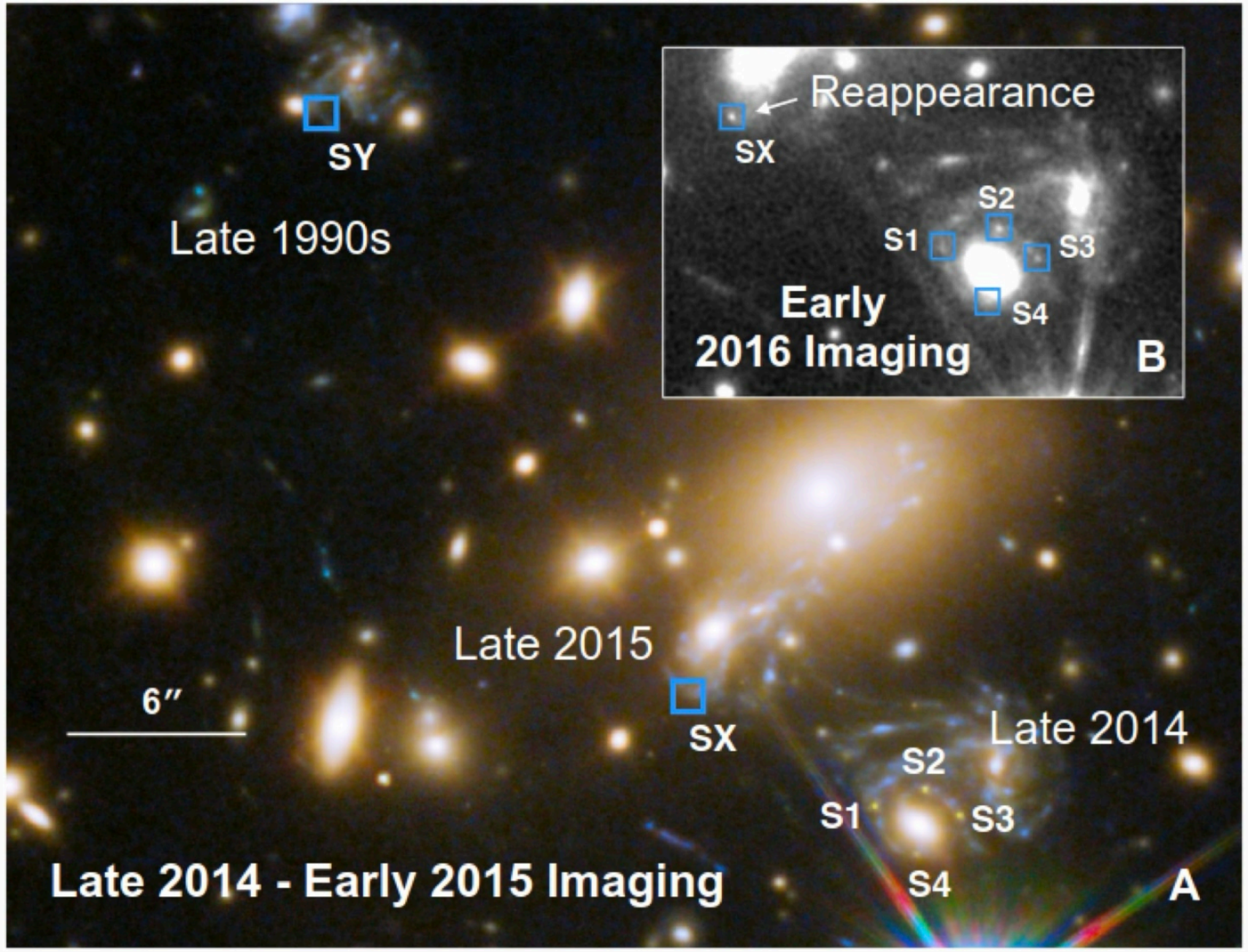

- quadruple images S1-S4 discovered in 2014
- appearance of new image SX in 2015 predicted
- image SX discovered as predicted

Kelly+ (incl. MO) ApJ **948**(2023)93

Hubble constant with Refsdal

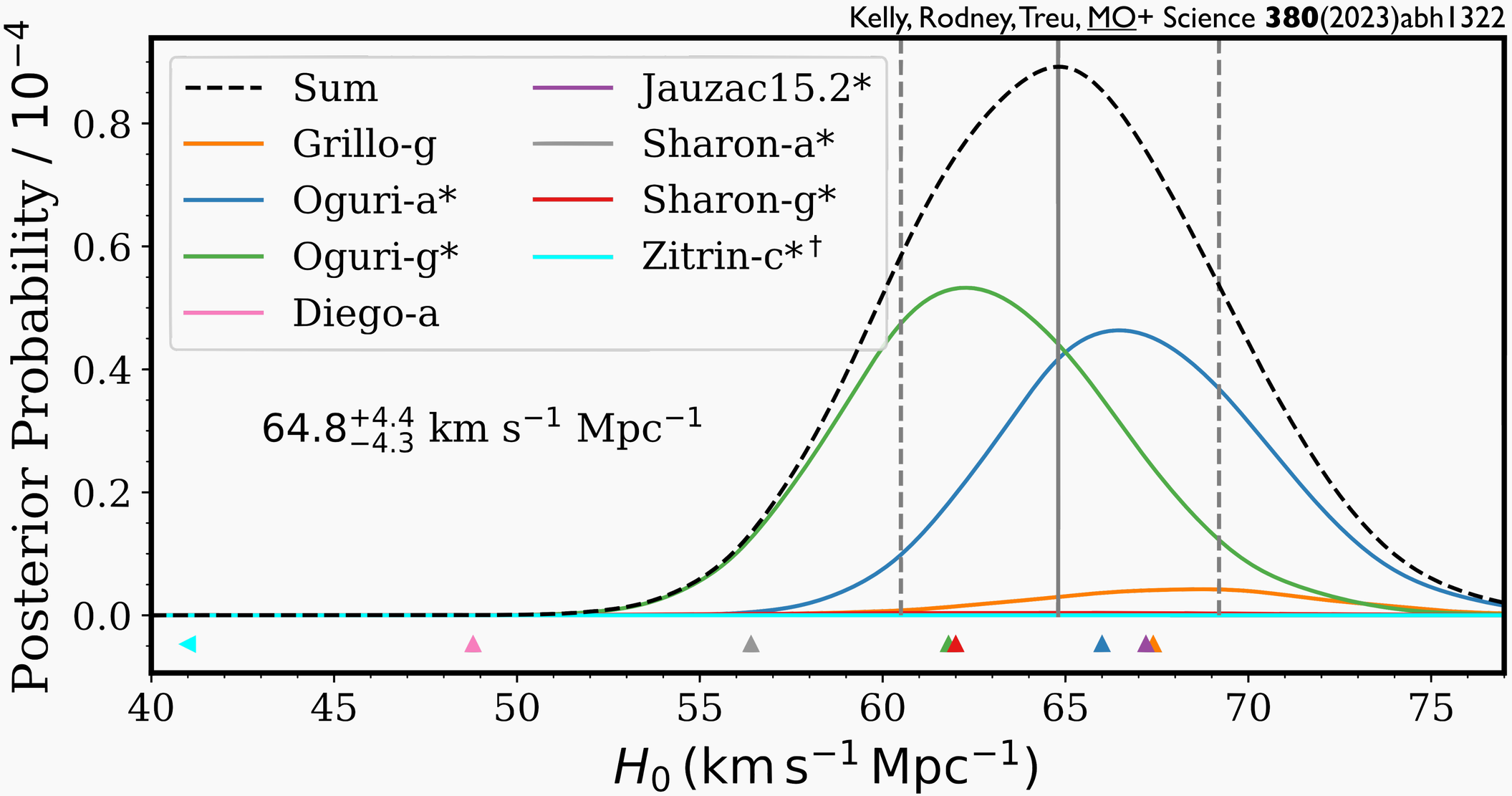

Distant objects with help of magnification

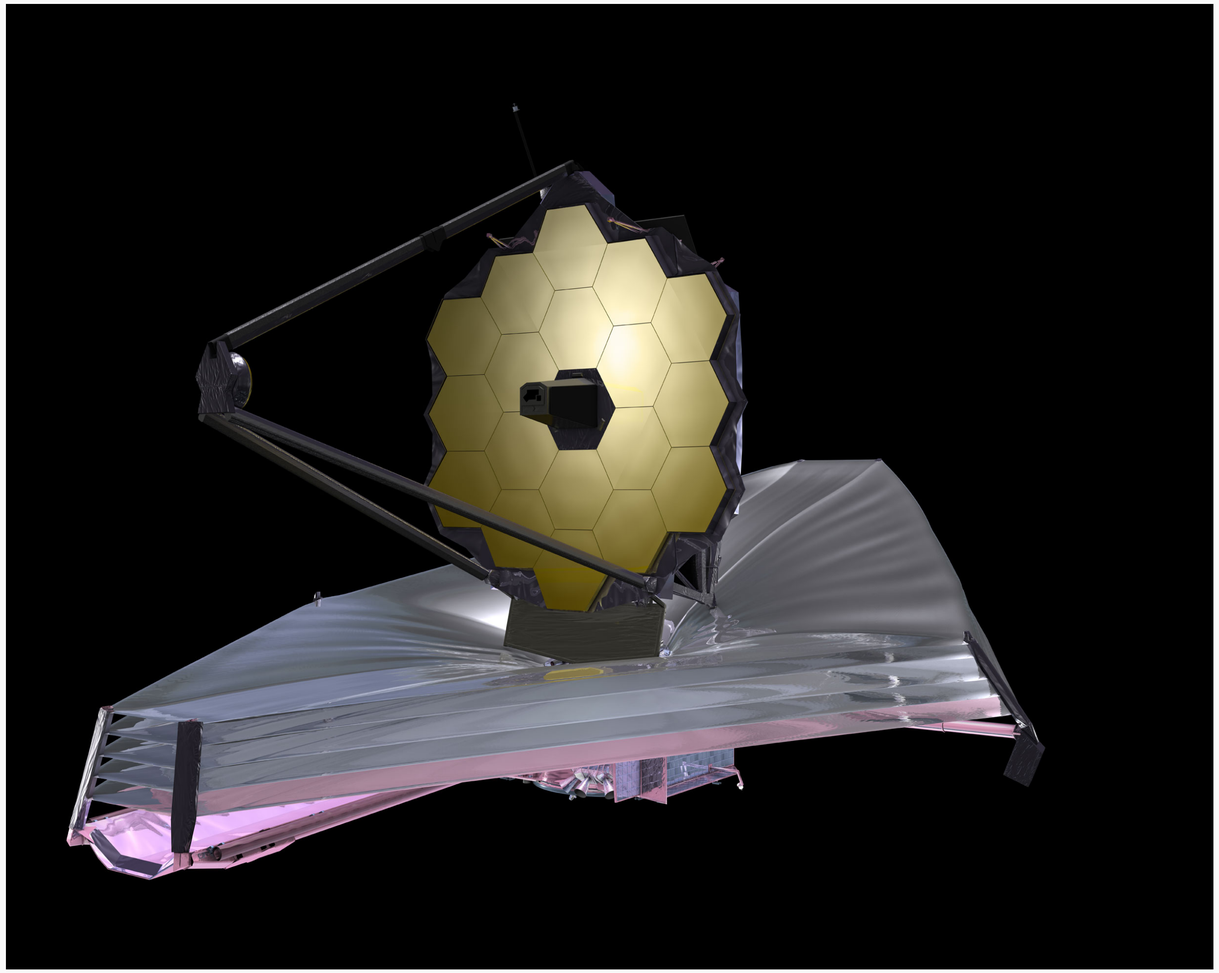

NASA

- huge progress thanks to James Webb Space Telescope (JWST)

Example of magnified distant galaxy

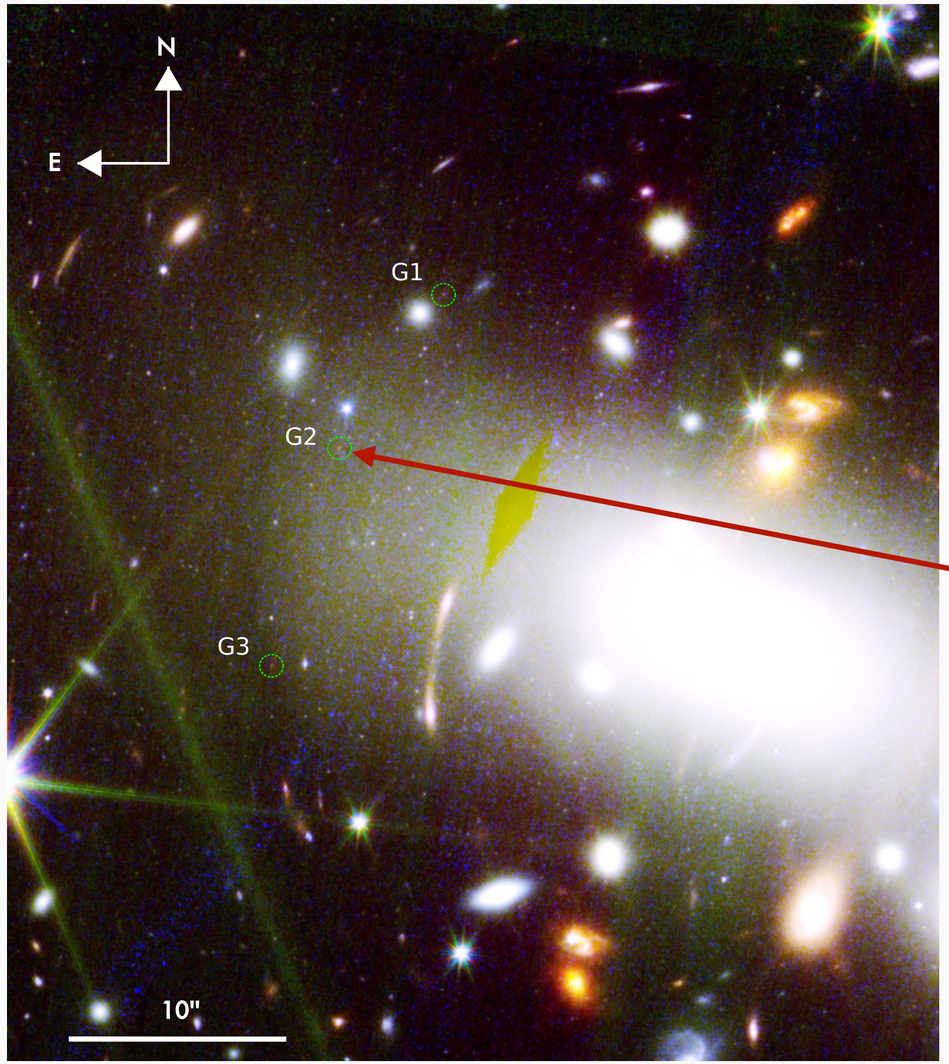

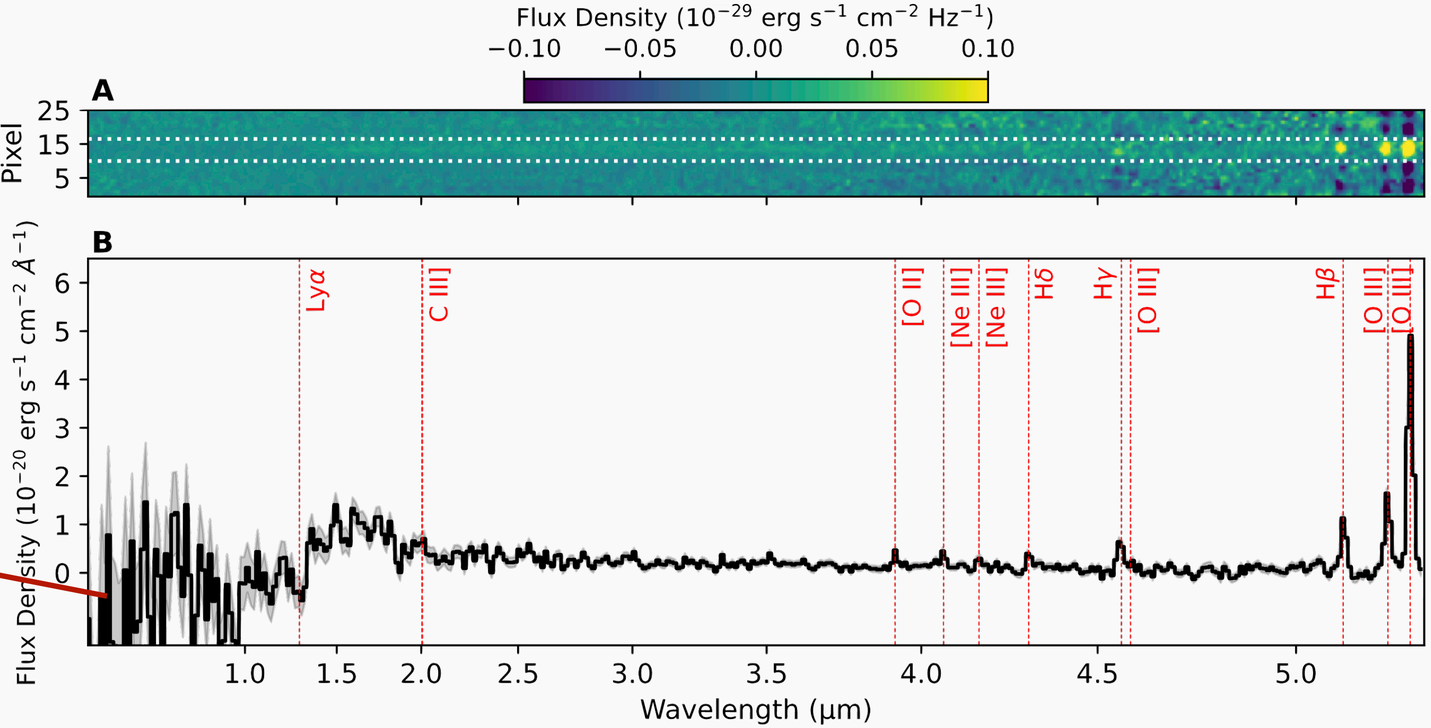

- triple image of galaxy at z=9.51
- spectroscopy thanks to ~20 magnification
- strong O lines, very compact

Williams+ (incl. MO) Sience **380**(2023)416

Internal structure of a distant galaxy

Adamo+ (incl. MO) Nature **632**(2024)513

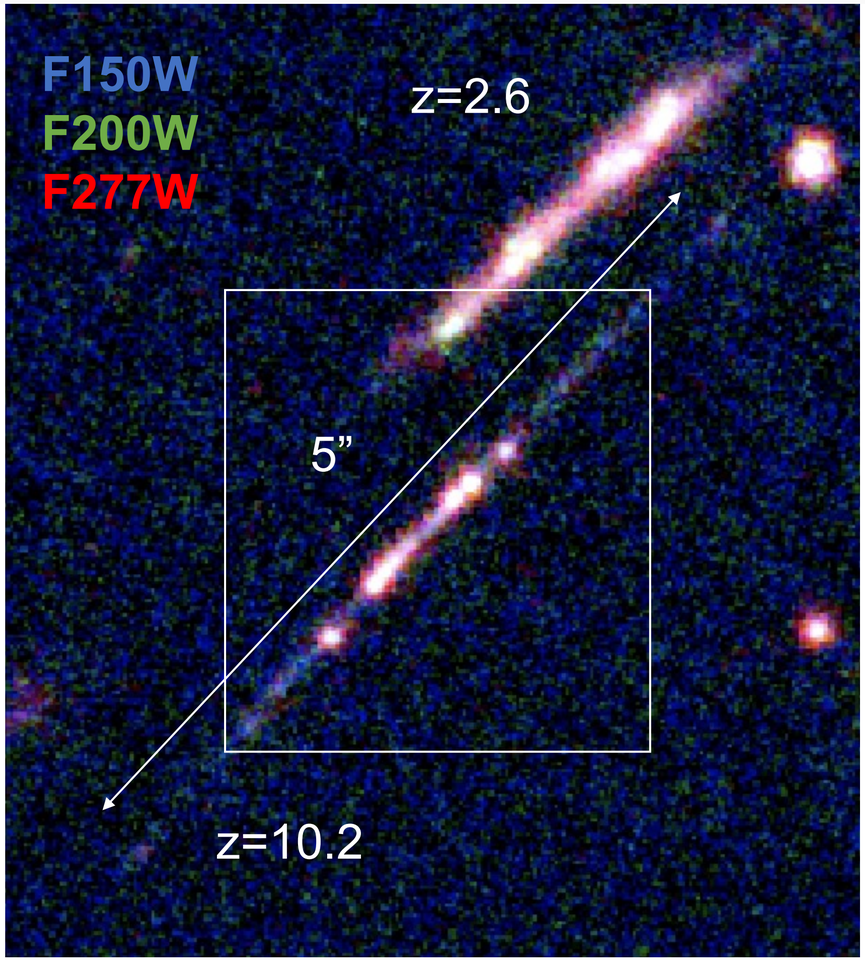

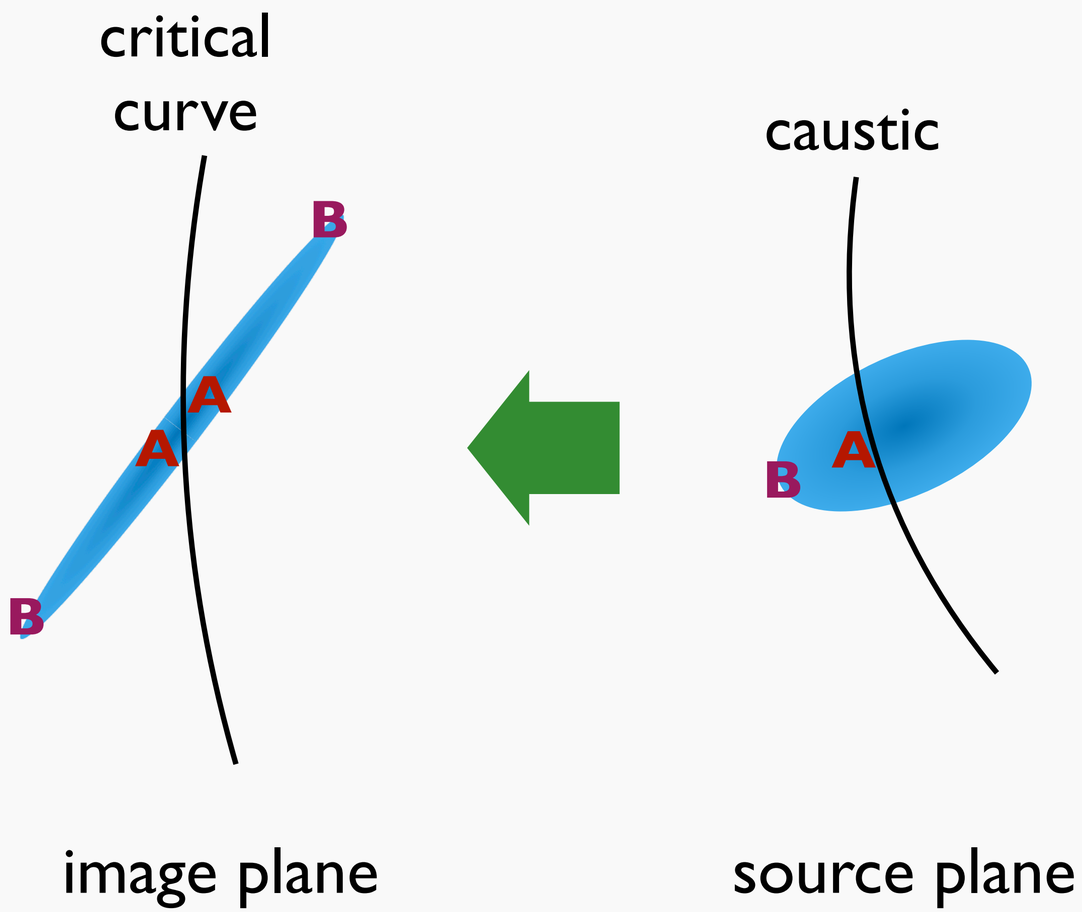

- dominated by star clusters!

Microlensing

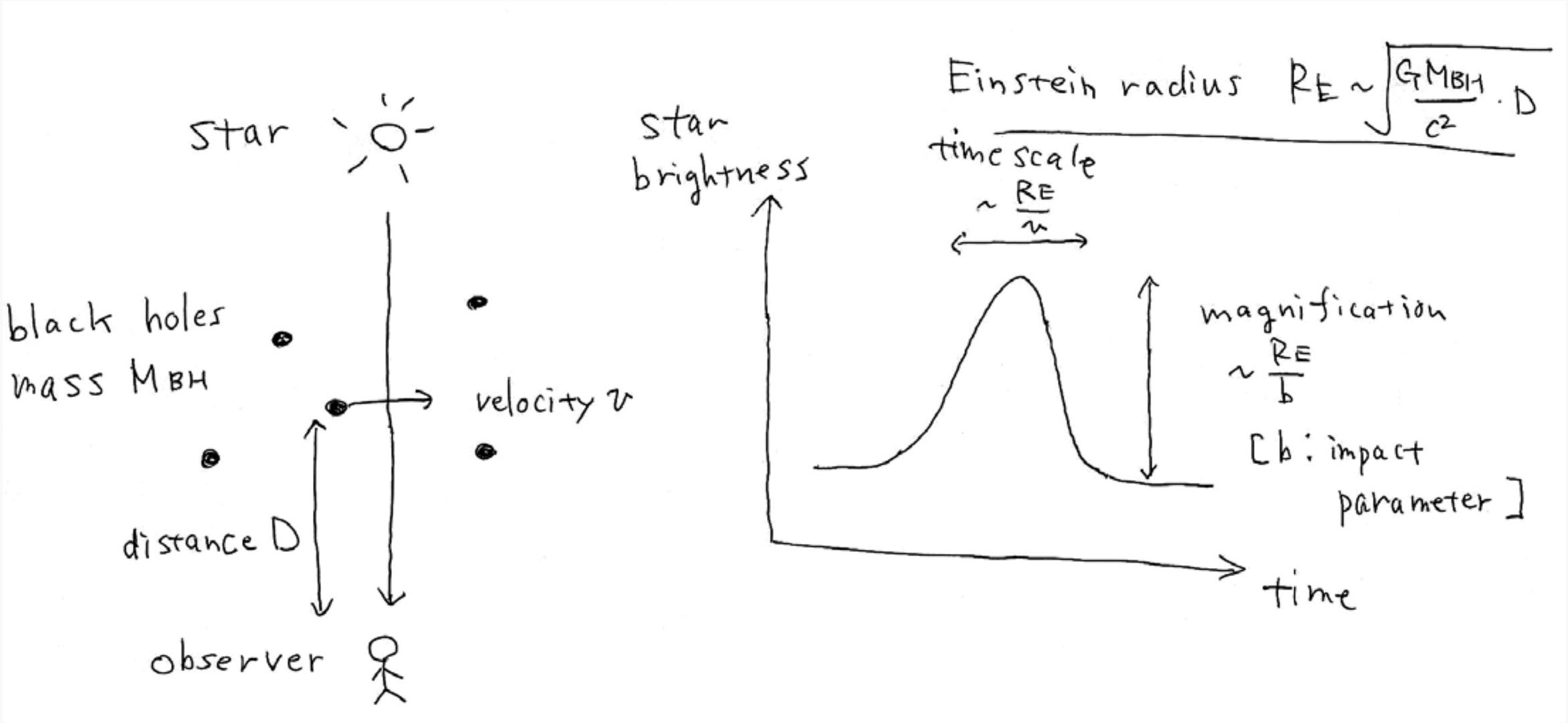

MACHO search

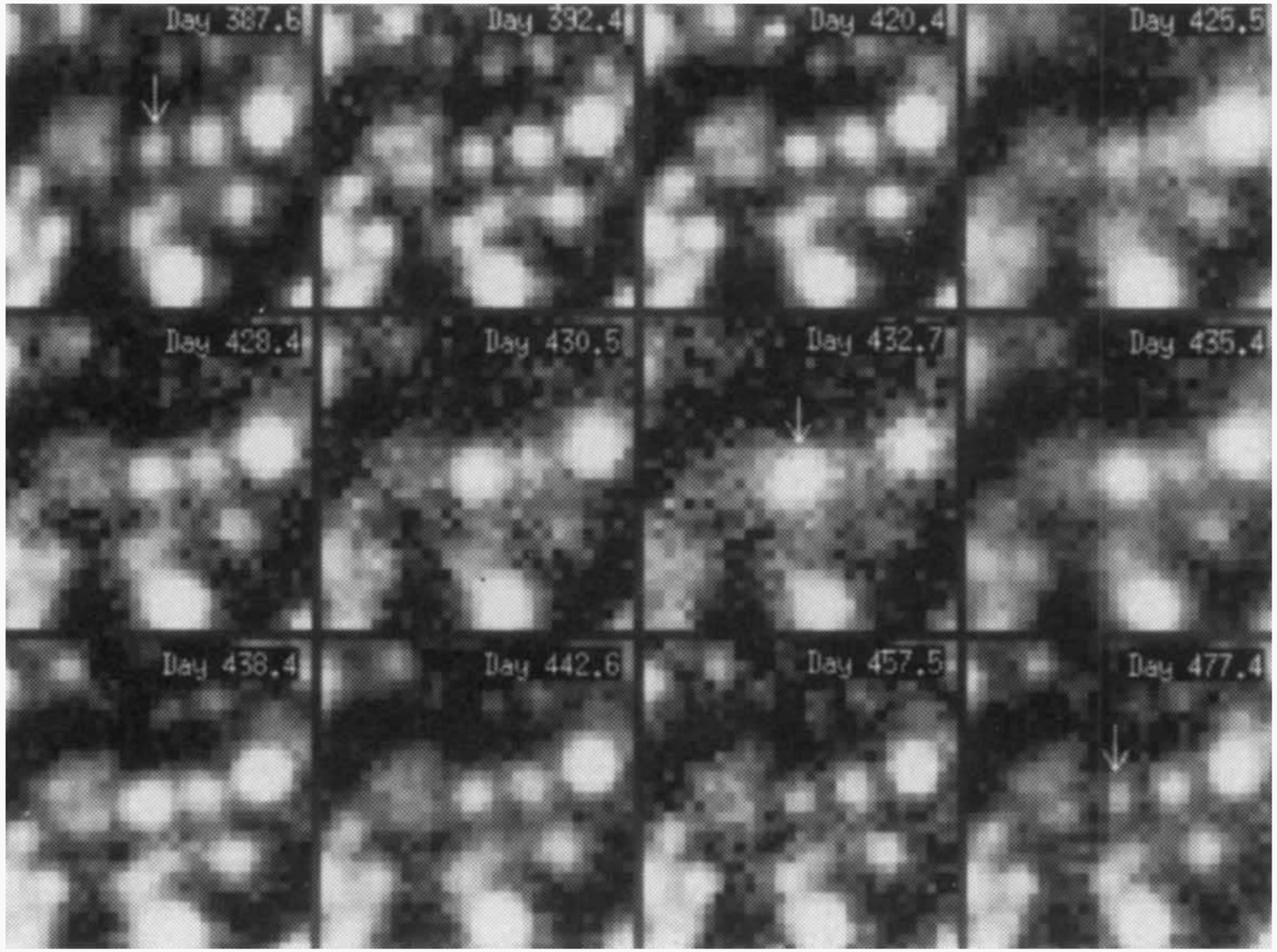

- monitoring of stars in Galactic center and Magellanic cloud
- constrain abundance of primordial black hole (PBH) with mass 10^{-5}-$1M_{\odot}$

Alcock+ Nature **365**(1993)621

MACHO search

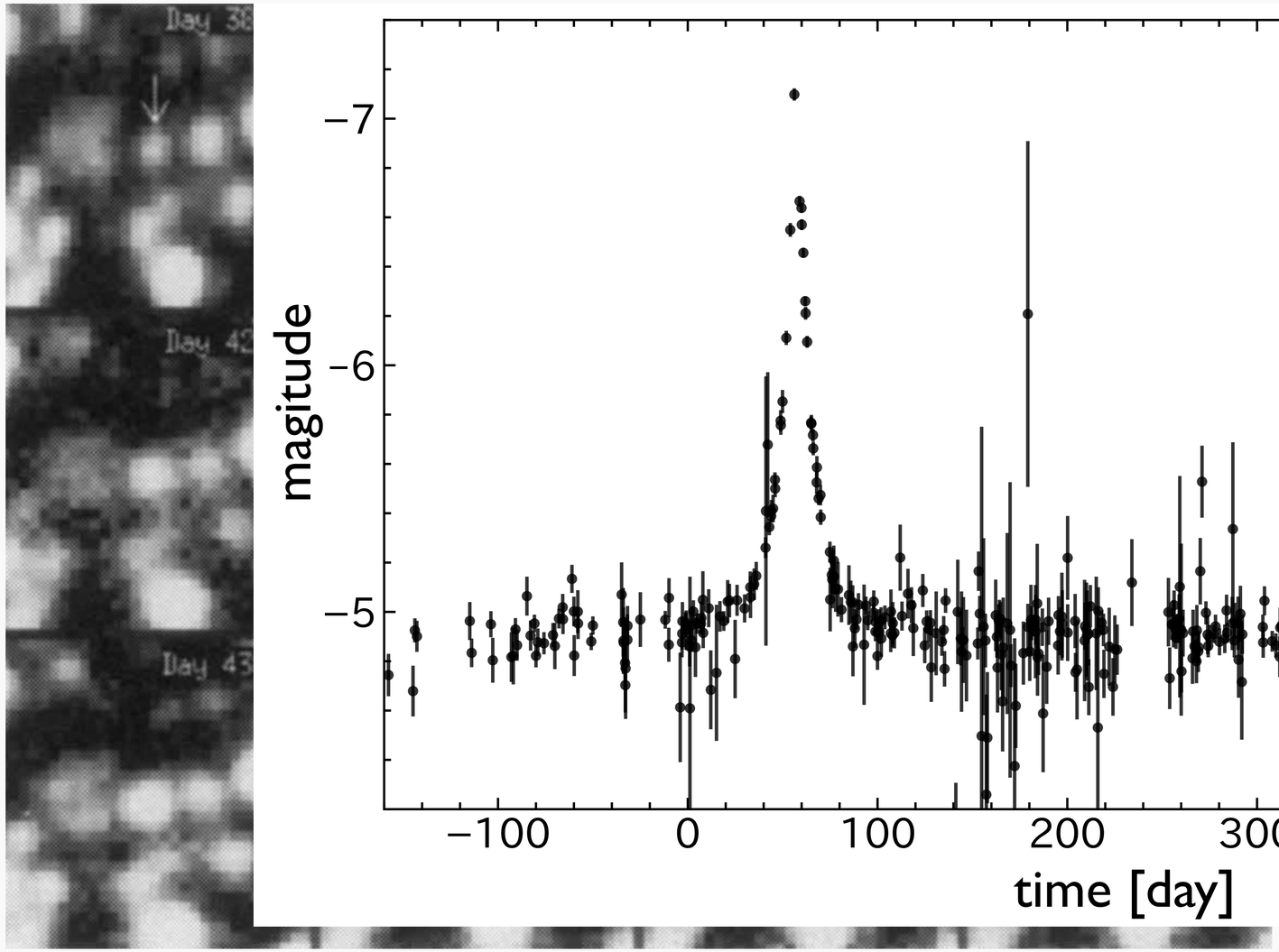

.rs in
nd

nce of
hole (PBH)
$M_\odot$

Alcock+ Nature **365**(1993)621

Subaru HSC microlensing search

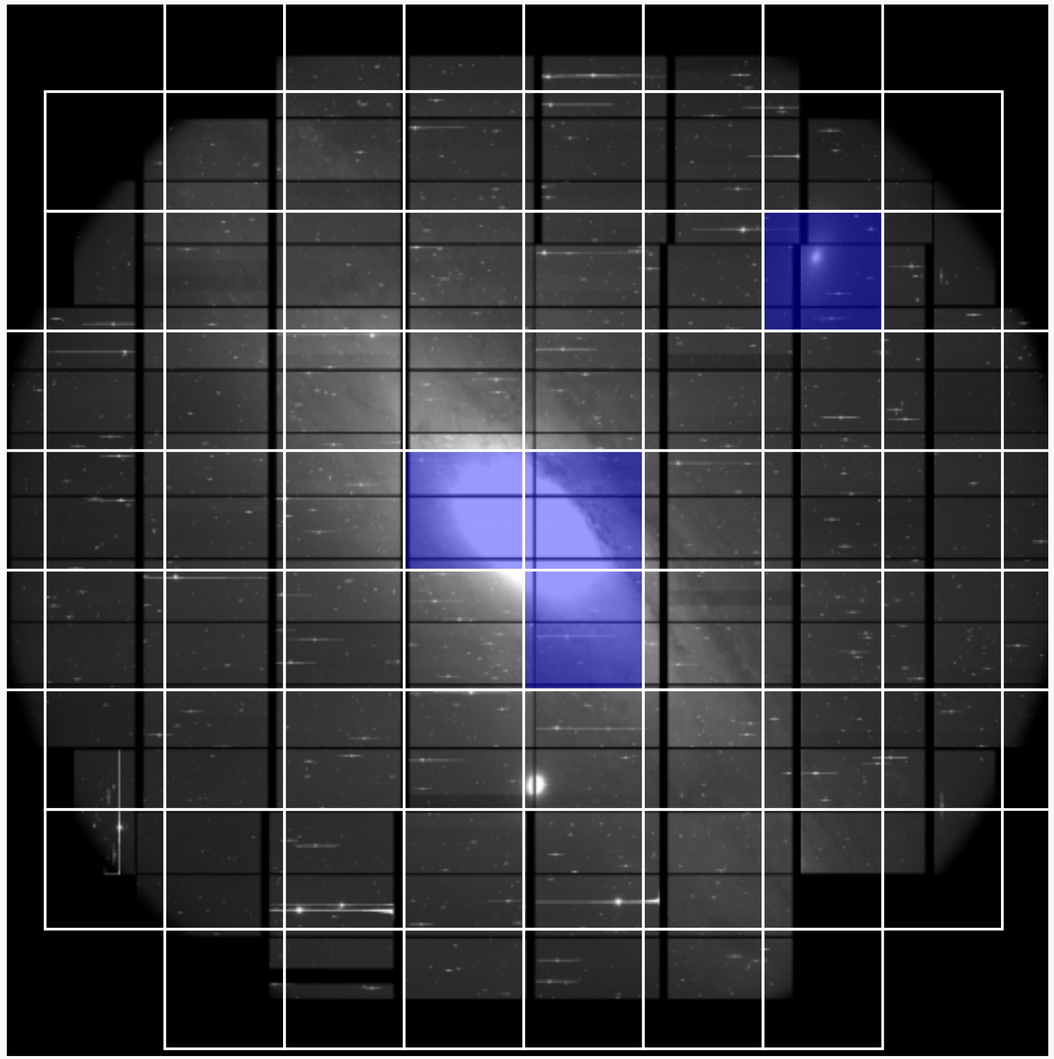

- repeated short exposure observations of M31
- constraint abundance of PBH with mass 10^{-11}-$10^{-6}M_{\odot}$

Niikura, Takada+ (incl. MO) Nat. Ast. **3**(2019)524

Constraints on PBH abundance

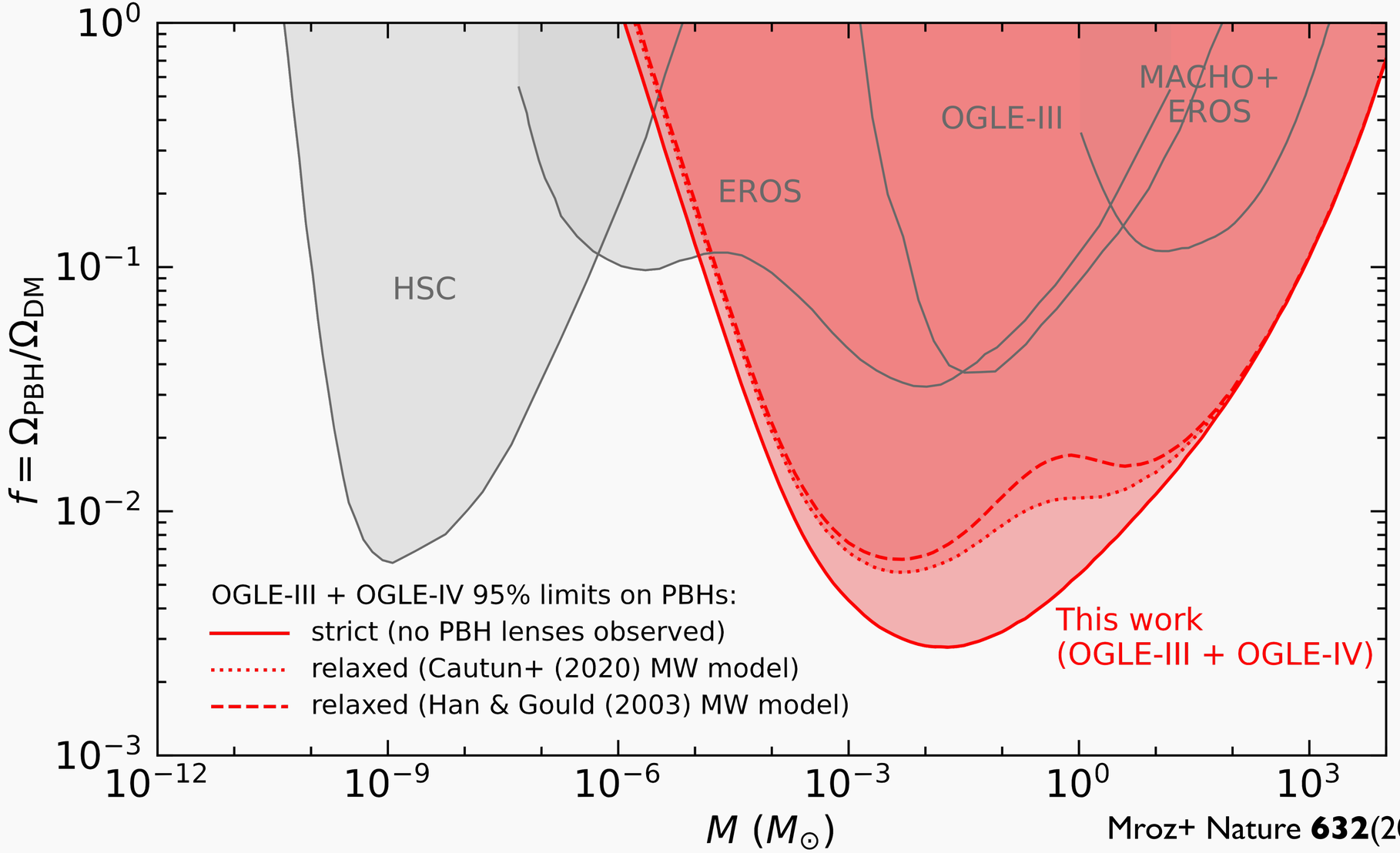

Mroz+ Nature **632**(2024)749

Weak gravitational lensing

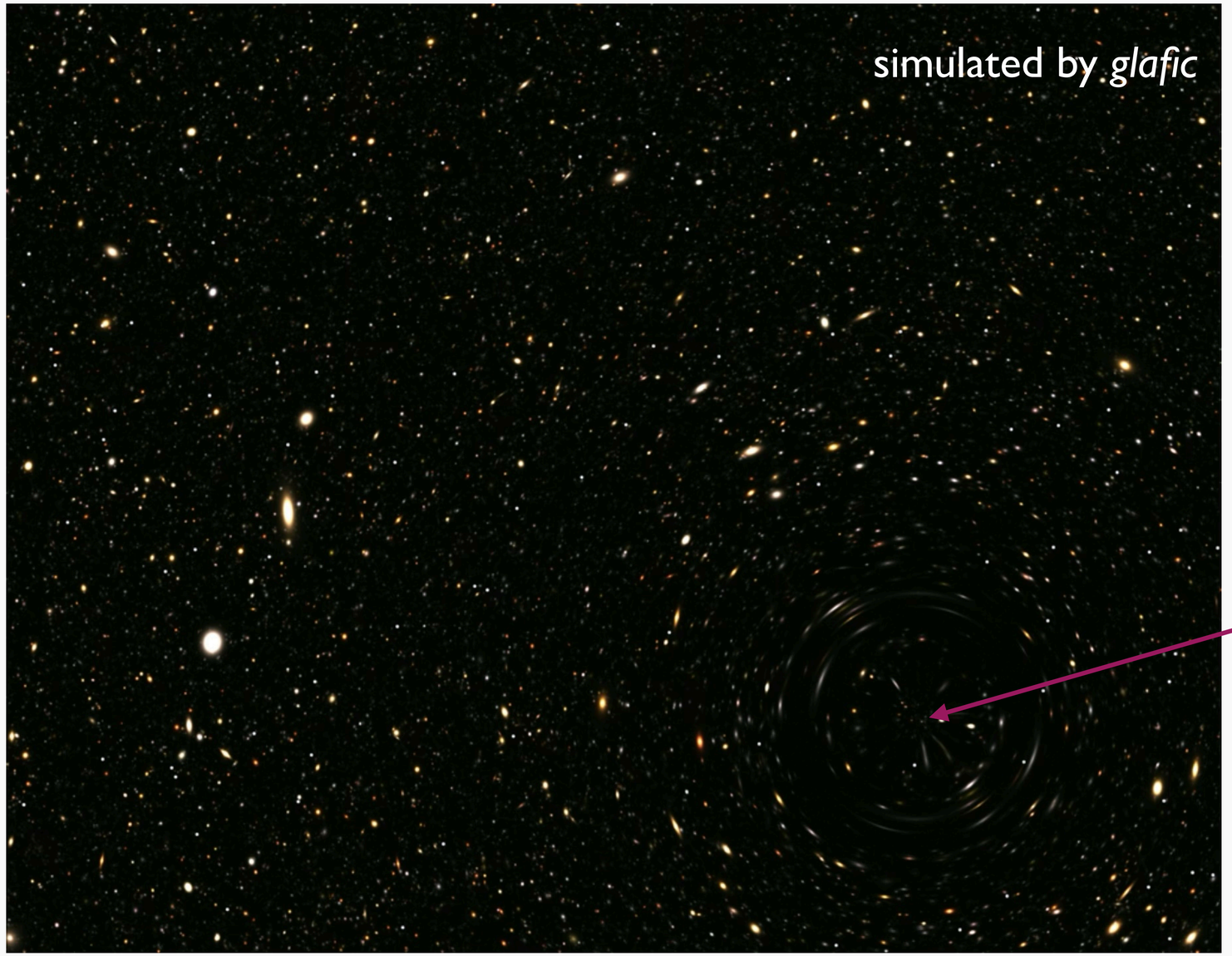

simulation by placing massive object in front of image

Lensing effect on background galaxies

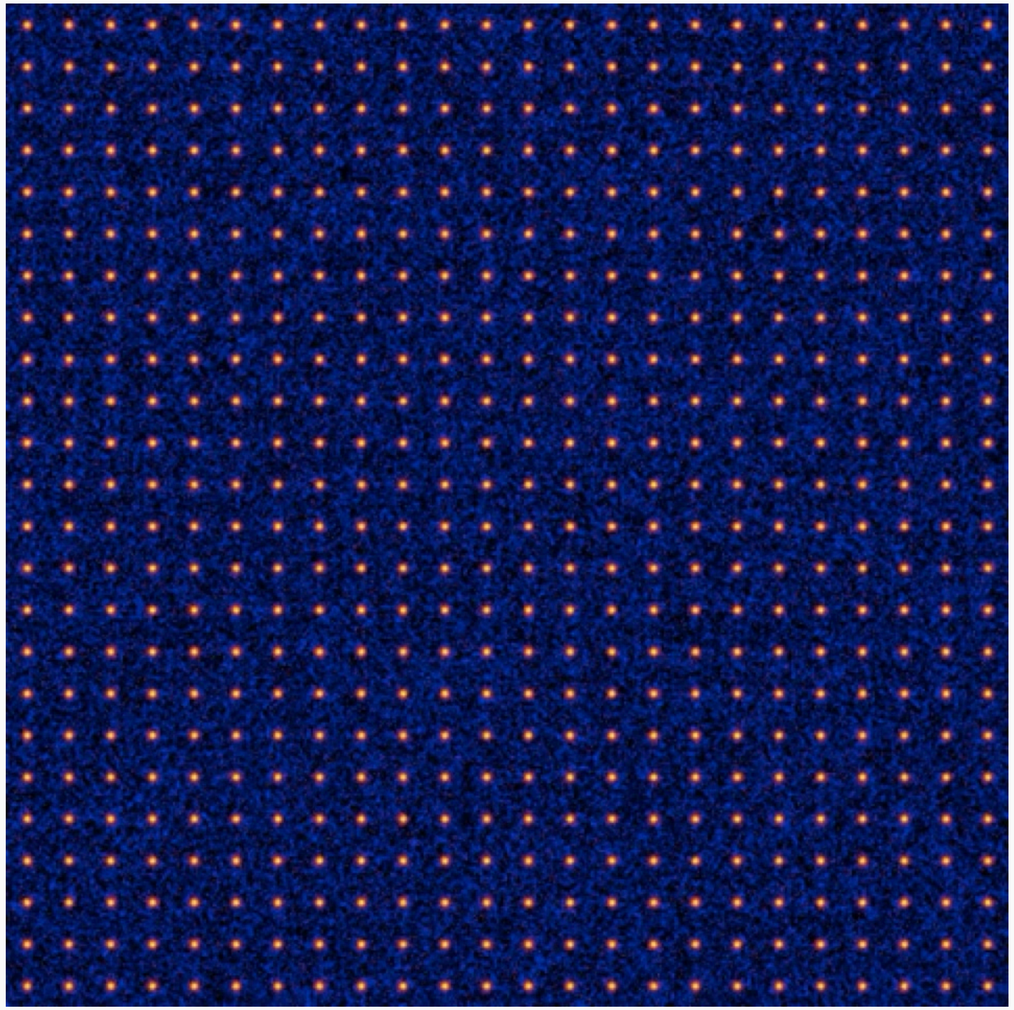

no gravitational lensing

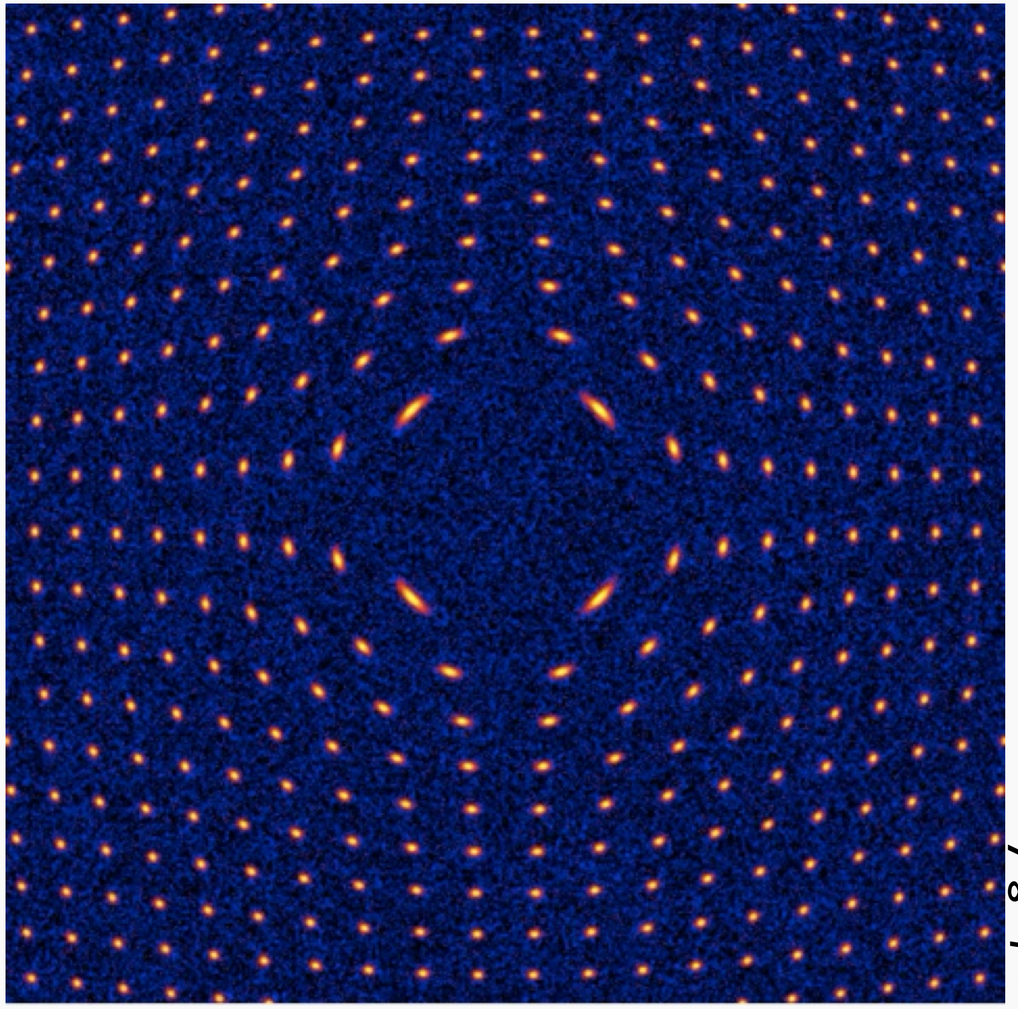

lens object at center

simulated by *glafic*

Reconstruction of mass distribution

MO, Miyazaki+ PASJ **70**(2018)S26

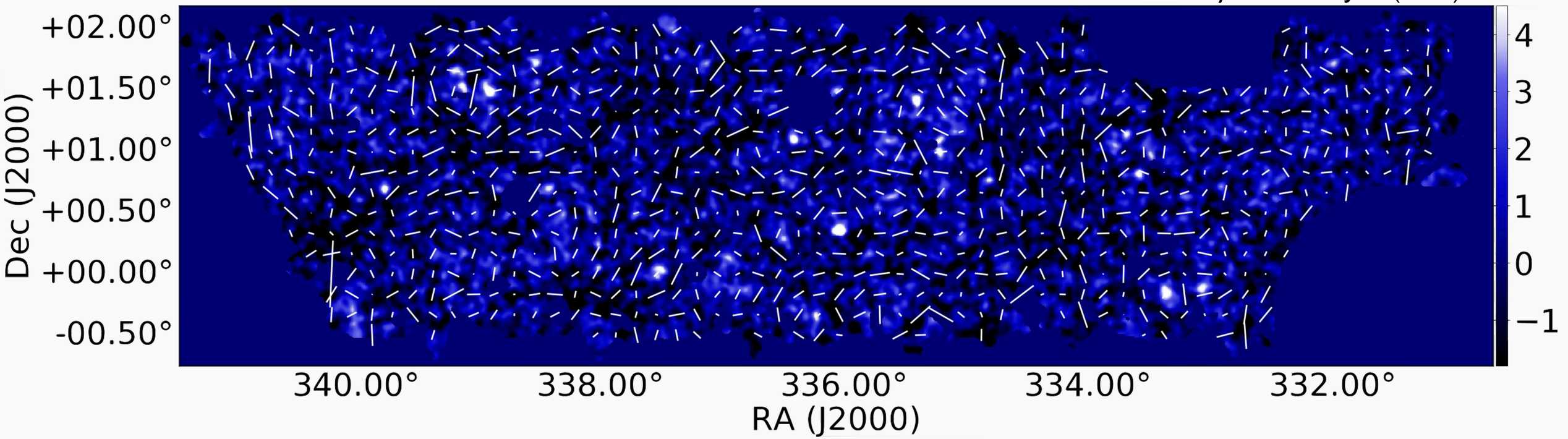

- reconstruction of mass distribution from coherent distortion of galaxy shapes along tangential direction
- searching for clusters based on dark matter density map

Three-dimensional dark matter map

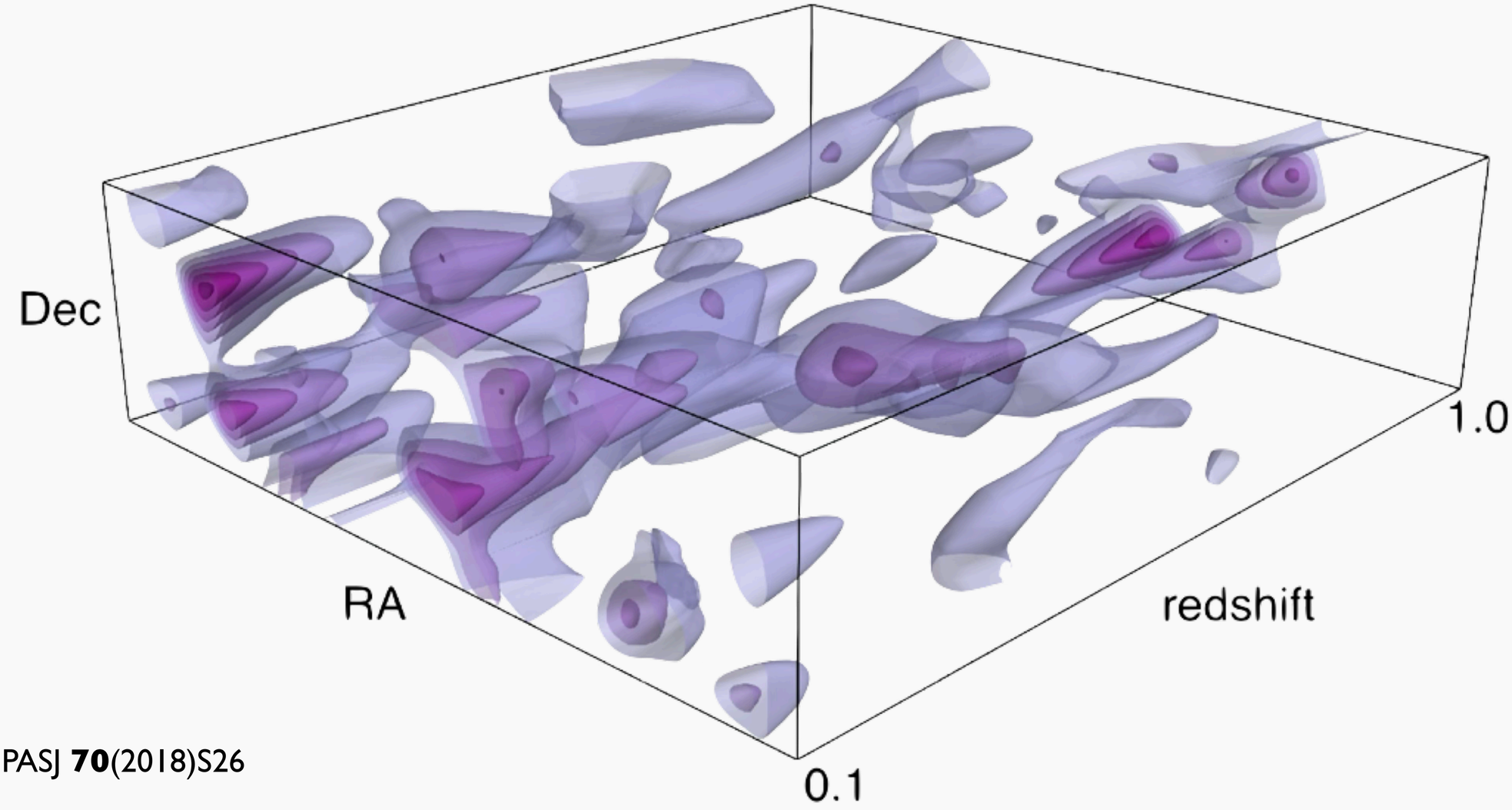

MO, Miyazaki+ PASJ **70**(2018)S26

Summary

- gravitational lensing is essential tool for studying Universe
- wide applications such as Hubble constant measurement and studying dark matter

2. Lens equation

Geodesic equation

- for affine parameter λ, geodesic is defined by parallel transport of tangent vector V^μ to direction of V^μ

$$V^\mu{}_{;\alpha} V^\alpha = 0$$

$$\Rightarrow \left(V^\mu{}_{,\alpha} + \Gamma^\mu{}_{\alpha\beta} V^\beta \right) V^\alpha = 0$$

$$\Rightarrow \frac{d^2 x^\mu}{d\lambda^2} + \Gamma^\mu{}_{\alpha\beta} \frac{dx^\alpha}{d\lambda} \frac{dx^\beta}{d\lambda} = 0$$

geodesic equation

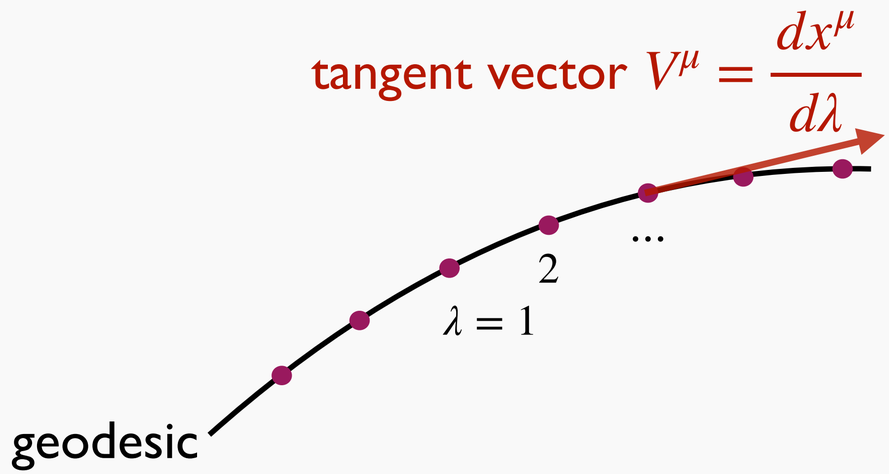

Equivalent form of geodesic equation

$$\left(g_{\mu\nu}V^{\nu}\right)_{;\beta}V^{\beta} = g_{\mu\nu}V^{\nu}{}_{;\beta}V^{\beta} = 0$$

$$\Rightarrow \frac{dx^{\beta}}{d\lambda}\frac{\partial}{\partial x^{\beta}}\left(g_{\mu\nu}\frac{dx^{\nu}}{d\lambda}\right) - \Gamma^{\nu}{}_{\mu\beta}g_{\nu\alpha}\frac{dx^{\alpha}}{d\lambda}\frac{dx^{\beta}}{d\lambda} = 0$$

$$= \frac{d}{d\lambda}\left(g_{\mu\nu}\frac{dx^{\nu}}{d\lambda}\right) - \frac{1}{2}g_{\alpha\beta,\mu}\frac{dx^{\alpha}}{d\lambda}\frac{dx^{\beta}}{d\lambda}$$

$$\Rightarrow \frac{d}{d\lambda}\left(g_{\mu\nu}\frac{dx^{\nu}}{d\lambda}\right) - \frac{1}{2}g_{\alpha\beta,\mu}\frac{dx^{\alpha}}{d\lambda}\frac{dx^{\beta}}{d\lambda} = 0$$

geodesic equation

FLRW Universe

- FLRW metric

$$ds^2 = -c^2dt^2 + a^2\left[d\chi^2 + f_K^2(\chi)\left(d\theta^2 + \sin^2\theta d\phi^2\right)\right]$$

scale factor

$$f_K(\chi) = \begin{cases} \frac{1}{\sqrt{K}}\sin\left(\sqrt{K}\chi\right) & (K > 0) \\ \chi & (K = 0) \\ \frac{1}{\sqrt{-K}}\sinh\left(\sqrt{-K}\chi\right) & (K < 0) \end{cases}$$

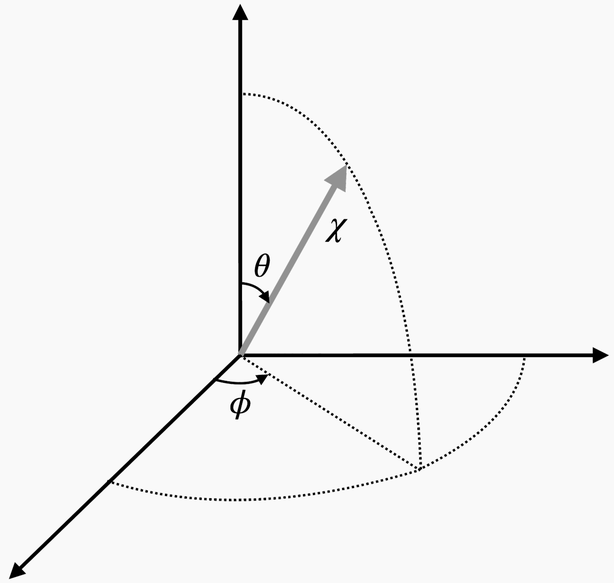

Geodesic in FLRW Universe (I)

- can assume it passes through origin without loss of generality
- $x^3 = \phi$

$$\frac{d}{d\lambda}\left(g_{3\nu}\frac{dx^\nu}{d\lambda}\right) = \frac{1}{2}g_{\alpha\beta,3}\frac{dx^\alpha}{d\lambda}\frac{dx^\beta}{d\lambda} = 0$$

2nd term $= 0$ because $g_{\alpha\beta,\phi} = 0$

$$g_{3\nu}\frac{dx^\nu}{d\lambda} = a^2 f_K^2 \sin^2\theta\frac{d\phi}{d\lambda} = C$$

integral constant
→ $C = 0$ from condition of passing through origin

$$\frac{d\phi}{d\lambda} = 0$$

Geodesic in FLRW Universe (II)

- $x^2 = \theta$

$$\frac{d}{d\lambda}\left(g_{2\nu}\frac{dx^\nu}{d\lambda}\right) = \frac{1}{2}g_{\alpha\beta,2}\frac{dx^\alpha}{d\lambda}\frac{dx^\beta}{d\lambda} = a^2 f_K^2 \sin\theta\cos\theta\left(\frac{d\phi}{d\lambda}\right)^2 = 0$$

2nd term $= 0$ because $d\phi/d\lambda = 0$

$$\Rightarrow \quad \frac{d\theta}{d\lambda} = 0$$

Geodesic in FLRW Universe (III)

- $x^1 = \chi$

$$\frac{d}{d\lambda}\left(g_{1\nu}\frac{dx^\nu}{d\lambda}\right) - \frac{1}{2}g_{\alpha\beta,1}\frac{dx^\alpha}{d\lambda}\frac{dx^\beta}{d\lambda} = 0$$

$$\Rightarrow \quad \frac{d}{d\lambda}\left(g_{1\nu}\frac{dx^\nu}{d\lambda}\right) - a^2 f_K' f_K \underbrace{\left[\left(\frac{d\theta}{d\lambda}\right)^2 + \sin^2\theta\left(\frac{d\phi}{d\lambda}\right)^2\right]}_{=0} = 0$$

$$\Rightarrow \quad a^2\frac{d\chi}{d\lambda} = C$$

integral constant → choose λ so that $C = 1$

$$\Rightarrow \quad \frac{d\chi}{d\lambda} = \frac{1}{a^2}$$

Geodesic in FLRW Universe (IV)

- $x^0 = ct \rightarrow$ use null condition $ds^2 = 0$

$$g_{\mu\nu}\frac{dx^\mu}{d\lambda}\frac{dx^\nu}{d\lambda} = 0 \quad \Rightarrow \quad -\left(\frac{c\,dt}{d\lambda}\right)^2 + \frac{1}{a^2} = 0 \quad \Rightarrow \quad \frac{c\,dt}{d\lambda} = \pm\frac{1}{a}$$

- in summary

$$\frac{c\,dt}{d\lambda} = \pm\frac{1}{a} \qquad \frac{d\chi}{d\lambda} = \frac{1}{a^2}$$

$$\frac{d\theta}{d\lambda} = 0 \qquad \frac{d\phi}{d\lambda} = 0$$

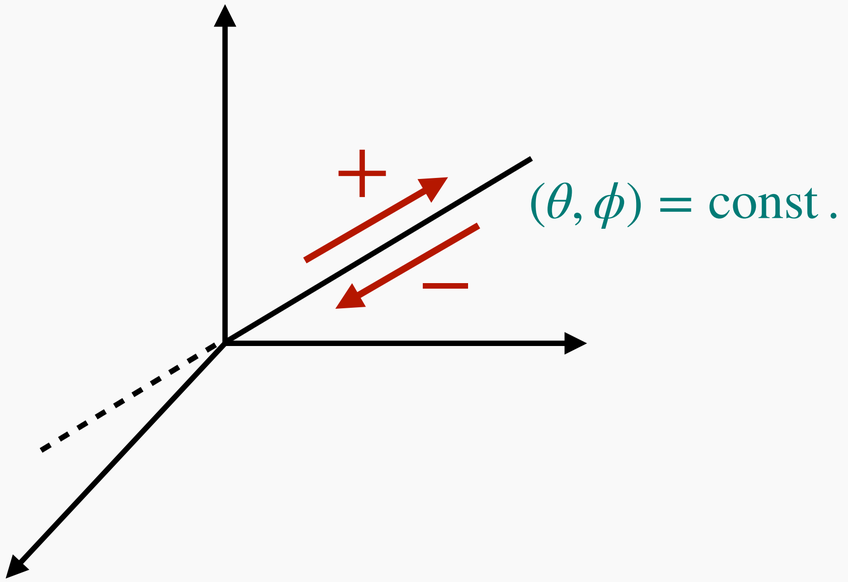

Metric with fluctuations

- metric in Universe with fluctuations (Newton gauge)

$$ds^2 = -\left(1+\frac{2\Phi}{c^2}\right)c^2dt^2 + a^2\left(1-\frac{2\Psi}{c^2}\right)\gamma_{ij}dx^i dx^j$$

gravitational potential　　curvature perturbation

$$\gamma_{ij}dx^i dx^j = d\chi^2 + f_K^2(\chi)\left(d\theta^2 + \sin^2\theta d\phi^2\right)$$

- $\Phi = \Psi$ and Φ, Ψ are small within range of our interest

$$\frac{\Phi}{c^2} \sim \frac{v^2}{c^2} \qquad \left|\frac{\Phi}{c^2}\right| \ll 1$$

→ consider up to linear order of Φ, Ψ

Geodesic in Universe with fluctuations (I)

- observer at origin, separate radial coordinates χ and celestial coordinates θ, ϕ

$$\gamma_{ij} dx^i dx^j = d\chi^2 + f_K^2(\chi)\omega_{ab} dx^a dx^b \qquad i, j, \cdots : \text{from 1 to 3}$$

$$\omega_{ab} dx^a dx^b = d\theta^2 + \sin^2\theta d\phi^2 \qquad a, b, \cdots : \text{from 2 to 3}$$

- solution expected from FLRW Universe case

$$\frac{dx^a}{d\lambda} = \mathcal{O}\left(\frac{\Phi}{c^2}\right) \qquad \frac{d\chi}{d\lambda} = \frac{1}{a^2} + \mathcal{O}\left(\frac{\Phi}{c^2}\right) \qquad \frac{c\,dt}{d\lambda} = -\frac{1}{a} + \mathcal{O}\left(\frac{\Phi}{c^2}\right)$$

Geodesic in Universe with fluctuations (II)

- angular part $\mu = b$ in geodesic equation
- 1st term in left hand side of geodesic equation

2nd order

$$\frac{d}{d\lambda}\left(g_{b\nu}\frac{dx^{\nu}}{d\lambda}\right) = \frac{d}{d\lambda}\left[a^2\left(1-\frac{2\Psi}{c^2}\right)f_K^2\omega_{bc}\frac{dx^c}{d\lambda}\right]$$

$$\simeq \frac{1}{a^2}\frac{d}{d\chi}\left(f_K^2\omega_{bc}\frac{dx^c}{d\chi}\right)$$

$$\simeq \frac{\omega_{bc}}{a^2}\frac{d}{d\chi}\left(f_K^2\frac{dx^c}{d\chi}\right)$$

2nd order

$$\frac{d\chi}{d\lambda} = \frac{1}{a^2} + \mathcal{O}\left(\frac{\Phi}{c^2}\right)$$

Geodesic in Universe with fluctuations (III)

- 2nd term in left hand side of geodesic equation

$$\frac{1}{2} g_{\mu\nu,b} \frac{dx^\mu}{d\lambda} \frac{dx^\nu}{d\lambda} \simeq \frac{1}{2} g_{00,b} \left(\frac{c\,dt}{d\lambda} \right)^2 + \frac{1}{2} g_{11,b} \left(\frac{d\chi}{d\lambda} \right)^2$$

$$\simeq - \frac{\Phi_{,b}}{a^2 c^2} - \frac{\Psi_{,b}}{a^2 c^2}$$

$$\left(\frac{dx^a}{d\chi} \right)^2 \ll 1$$

$$\frac{d\chi}{d\lambda} = \frac{1}{a^2} + \mathcal{O}\left(\frac{\Phi}{c^2} \right), \quad \frac{c\,dt}{d\lambda} = -\frac{1}{a} + \mathcal{O}\left(\frac{\Phi}{c^2} \right)$$

2nd order 2nd order

Geodesic in Universe with fluctuations (IV)

- finally geodesic equation reduces to

$$\frac{d}{d\chi}\left[f_K^2(\chi)\frac{dx^a}{d\chi}\right]+\frac{1}{c^2}\omega^{ab}\left(\Phi_{,b}+\Psi_{,b}\right)=0$$

$$\Phi=\Psi$$

$$\frac{d}{d\chi}\left[f_K^2(\chi)\frac{dx^a}{d\chi}\right]+\frac{2}{c^2}\omega^{ab}\Phi_{,b}=0$$

twice Newtonian case!

equation for light deflection due to gravitational lensing

Deriving lens equation (I)

- integrate equation for light deflection from 0 to χ'

$$f_K^2(\chi')\frac{dx^a}{d\chi'} = -\frac{2}{c^2}\int_0^{\chi'} d\chi\, \omega^{ab}\Phi_{,b}(\chi, \boldsymbol{\theta}(\chi))$$

- divide it by $f_K^2(\chi')$ and integrate over χ' from 0 to χ_s

$$x^a(\chi_\mathrm{s}) - x^a(0) = -\frac{2}{c^2}\int_0^{\chi_\mathrm{s}} d\chi' \frac{1}{f_K^2(\chi')}\int_0^{\chi'} d\chi\, \omega^{ab}\Phi_{,b}(\chi, \boldsymbol{\theta}(\chi))$$

Deriving lens equation (II)

- by switching order of integrals

$$x^a(\chi_s) - x^a(0) = -\frac{2}{c^2}\int_0^{\chi_s} d\chi\, \omega^{ab}\Phi_{,b}(\chi, \boldsymbol{\theta}(\chi)) \int_\chi^{\chi_s} d\chi' \frac{1}{f_K^2(\chi')}$$

$$= \frac{f_K(\chi_s - \chi)}{f_K(\chi) f_K(\chi_s)}$$

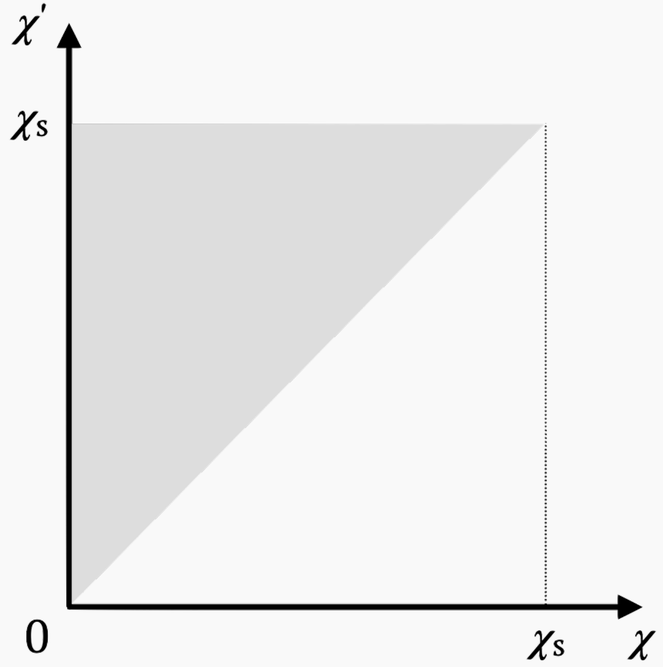

Deriving lens equation (III)

- finally, in vector representation

$$\boldsymbol{\theta}(\chi_\mathrm{s}) = \boldsymbol{\theta}(0) - \frac{2}{c^2}\int_0^{\chi_\mathrm{s}} d\chi \frac{f_K(\chi_\mathrm{s}-\chi)}{f_K(\chi) f_K(\chi_\mathrm{s})} \nabla_{\boldsymbol{\theta}} \Phi(\chi, \boldsymbol{\theta}(\chi))$$

lens equation

(integral equation)

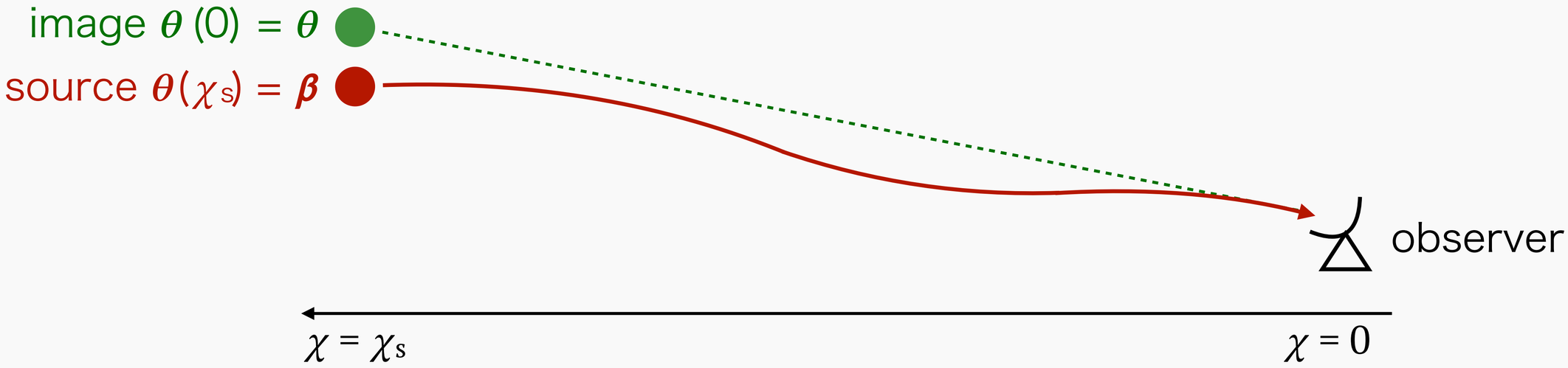

Locally flat coordinates

- change of $\boldsymbol{\theta}(0) - \boldsymbol{\theta}(\chi_s)$ due to gravitational lensing is small

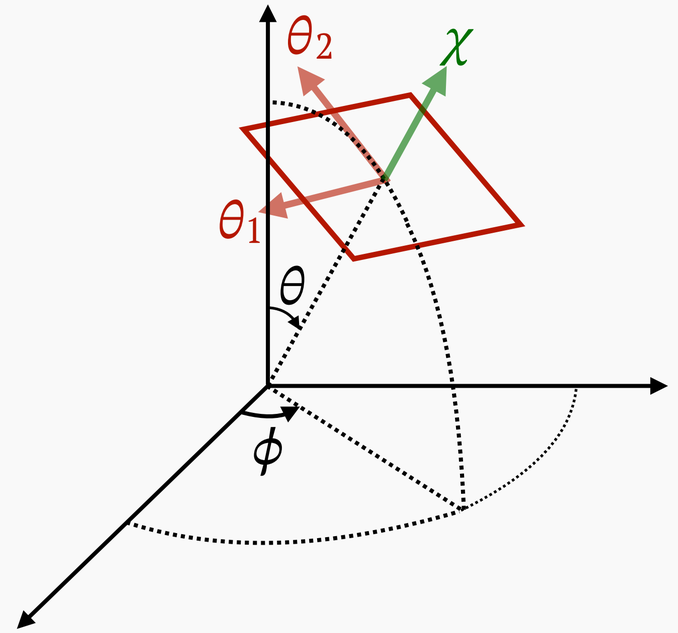

locally flat coordinates

$$\omega_{ab} dx^a dx^b = \tilde{\omega}_{ab} d\tilde{x}^a d\tilde{x}^b = d\theta_1^2 + d\theta_2^2$$

$$\tilde{\omega}_{ab} = \delta_{ab}$$

Born approximation

- lowest order recursive solution of integral equation

$$\boldsymbol{\theta}(\chi_{\rm s}) = \boldsymbol{\theta}(0) - \frac{2}{c^2}\int_0^{\chi_{\rm s}} d\chi \frac{f_K(\chi_{\rm s}-\chi)}{f_K(\chi) f_K(\chi_{\rm s})} \nabla_{\boldsymbol{\theta}} \Phi(\chi, \underline{\boldsymbol{\theta}(0)})$$

$$\boldsymbol{\theta}(\chi) \to \boldsymbol{\theta}(0)$$

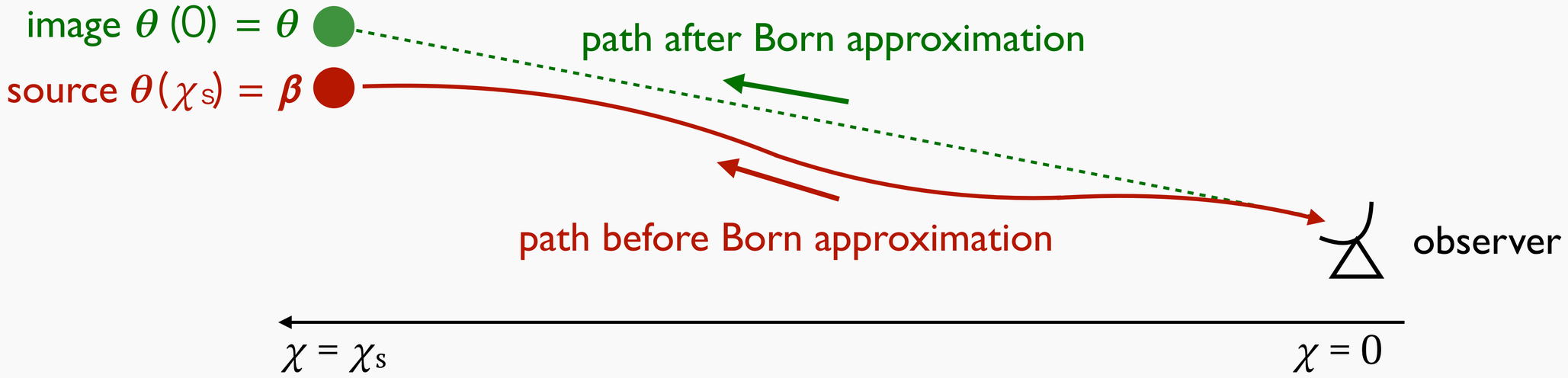

Lens equation

- for source position $\boldsymbol{\beta} = \boldsymbol{\theta}(\chi_{\rm s})$, image position $\boldsymbol{\theta} = \boldsymbol{\theta}(0)$, and under Born approximation

$$\boldsymbol{\beta} = \boldsymbol{\theta} - \boldsymbol{\alpha}(\boldsymbol{\theta}) = \nabla_{\boldsymbol{\theta}}\psi = \nabla_{\boldsymbol{\theta}}\left[\frac{2}{c^2}\int_0^{\chi_{\rm s}} d\chi \frac{f_K(\chi_{\rm s}-\chi)}{f_K(\chi)f_K(\chi_{\rm s})}\Phi(\chi,\boldsymbol{\theta})\right]$$

Lens potential

- mapping from $\boldsymbol{\theta}$ to $\boldsymbol{\beta}$

Thin lens and single plane approximation (I)

- physical coordinates around lens object (scale factor a_l, redshift z_l) perpendicular to line-of-sight direction Z

$$\boldsymbol{X}_\perp = a_\mathrm{l} f_K(\chi_\mathrm{l})\boldsymbol{\theta} \quad \Rightarrow \quad \boldsymbol{X} = (\boldsymbol{X}_\perp, Z)$$

$\chi(z_\mathrm{l})$

- thin lens approximation

$$\rho(\boldsymbol{X}) \simeq \delta^\mathrm{D}(Z)\,\underline{\Sigma(\boldsymbol{X}_\perp)}$$

$$= \int_{-\infty}^{\infty} dZ\,\rho(\boldsymbol{X})$$

surface mass density

Thin lens and single plane approximation (II)

- calculate gravitational potential $\Phi(\boldsymbol{X})$ from $\rho(\boldsymbol{X})$

$$\Phi(\boldsymbol{X}) = -\int d\boldsymbol{X}' \frac{G\rho(\boldsymbol{X}')}{\left|\boldsymbol{X}-\boldsymbol{X}'\right|} = -G\int d\boldsymbol{X}'_{\perp} \frac{1}{\sqrt{\left|\boldsymbol{X}_{\perp}-\boldsymbol{X}'_{\perp}\right|^2 + Z^2}} \Sigma(\boldsymbol{X}'_{\perp})$$

- gradient of gravitational potential

$$\nabla_{\boldsymbol{\theta}}\Phi = Ga_1 f_K(\chi_1) \int d\boldsymbol{X}'_{\perp} \frac{\boldsymbol{X}_{\perp}-\boldsymbol{X}'_{\perp}}{\left\{\left|\boldsymbol{X}_{\perp}-\boldsymbol{X}'_{\perp}\right|^2 + Z^2\right\}^{3/2}} \Sigma(\boldsymbol{X}'_{\perp})$$

Thin lens and single plane approximation (III)

- adopt following approximation

$$\frac{1}{\left\{ \left| \boldsymbol{X}_\perp - \boldsymbol{X}'_\perp \right|^2 + Z^2 \right\}^{3/2}} \simeq \frac{2\delta^{\mathrm{D}}(Z)}{\left| \boldsymbol{X}_\perp - \boldsymbol{X}'_\perp \right|^2} \simeq \frac{2a_1^{-1}\delta^{\mathrm{D}}(\chi - \chi_1)}{\left| \boldsymbol{X}_\perp - \boldsymbol{X}'_\perp \right|^2}$$

- finally gradient of gravitational potential is

$$\nabla_{\boldsymbol{\theta}}\Phi \simeq 2Ga_1 \left\{ f_K(\chi_1) \right\}^2 \delta^{\mathrm{D}}(\chi - \chi_1) \int d\boldsymbol{\theta}' \frac{\boldsymbol{\theta} - \boldsymbol{\theta}'}{\left| \boldsymbol{\theta} - \boldsymbol{\theta}' \right|^2} \Sigma(\boldsymbol{\theta}')$$

Thin lens and single plane approximation (IV)

- plugging into lens equation

$$\boldsymbol{\beta} = \boldsymbol{\theta} - \underbrace{\frac{4G}{c^2}\frac{a_1 f_K(\chi_1) f_K(\chi_s - \chi_1)}{f_K(\chi_s)}}_{=\frac{1}{\pi\Sigma_{cr}}} \int d\boldsymbol{\theta}' \frac{\boldsymbol{\theta} - \boldsymbol{\theta}'}{\left|\boldsymbol{\theta} - \boldsymbol{\theta}'\right|^2} \Sigma(\boldsymbol{\theta}')$$

$$\Sigma_{cr} = \frac{c^2}{4\pi G}\frac{D_{os}}{D_{ol} D_{ls}}$$ critical surface mass density

$$\boldsymbol{\alpha}(\boldsymbol{\theta}) = \nabla_{\boldsymbol{\theta}}\psi = \frac{1}{\pi}\int d\boldsymbol{\theta}' \kappa(\boldsymbol{\theta}') \frac{\boldsymbol{\theta} - \boldsymbol{\theta}'}{\left|\boldsymbol{\theta} - \boldsymbol{\theta}'\right|^2}$$

$$\kappa(\boldsymbol{\theta}) = \frac{\Sigma(\boldsymbol{\theta})}{\Sigma_{cr}}$$ convergence

$$\psi(\boldsymbol{\theta}) = \frac{1}{\pi}\int d\boldsymbol{\theta}' \kappa(\boldsymbol{\theta}') \ln\left|\boldsymbol{\theta} - \boldsymbol{\theta}'\right|$$

Thin lens and single plane approximation (V)

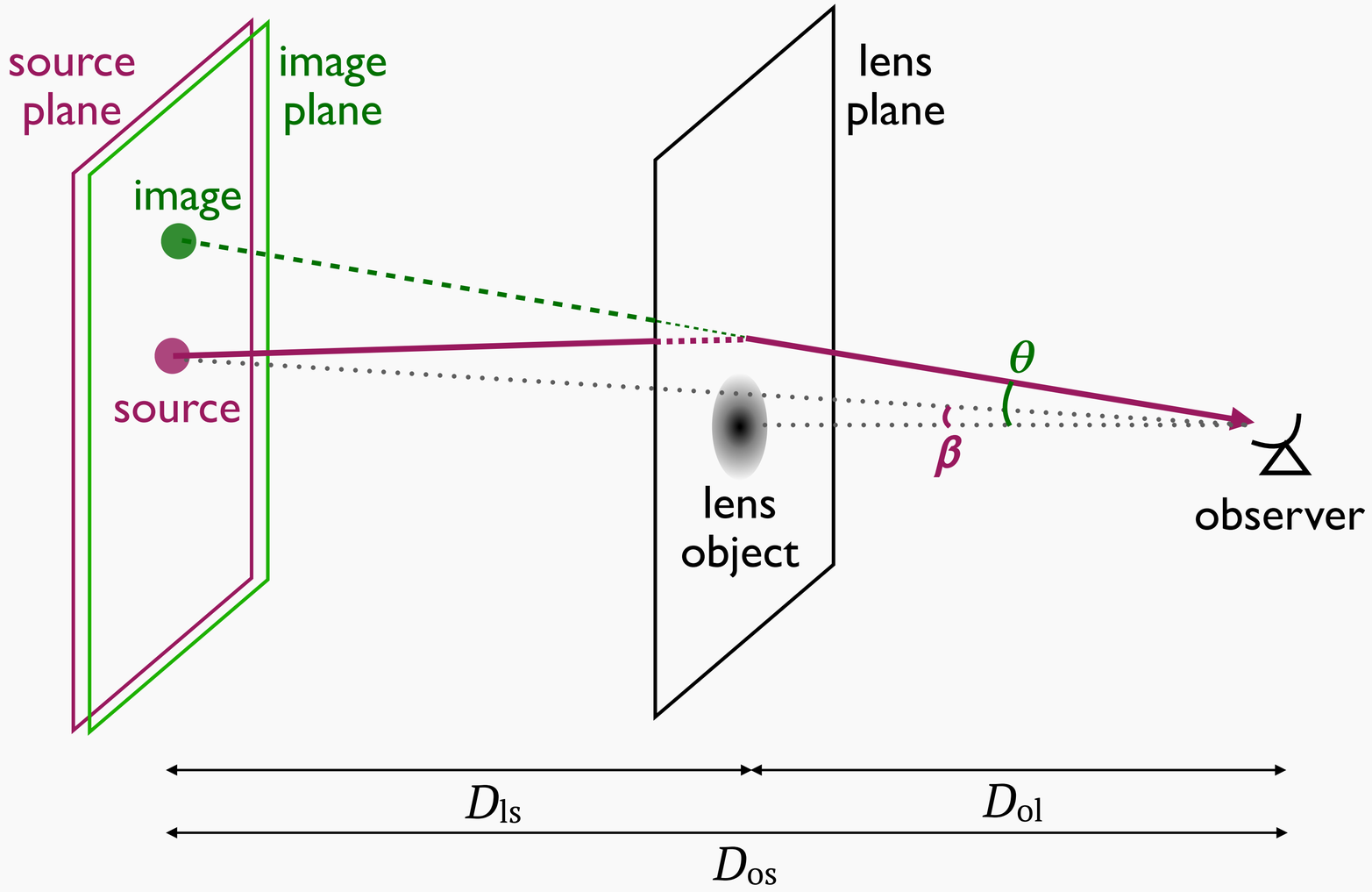

$$\boldsymbol{\beta} = \boldsymbol{\theta} - \boldsymbol{\alpha}(\boldsymbol{\theta})$$

$$\boldsymbol{\alpha}(\boldsymbol{\theta}) = \nabla_{\boldsymbol{\theta}}\psi$$

$$= \frac{1}{\pi}\int d\boldsymbol{\theta}'\kappa(\boldsymbol{\theta}')\frac{\boldsymbol{\theta}-\boldsymbol{\theta}'}{\left|\boldsymbol{\theta}-\boldsymbol{\theta}'\right|^2}$$

$$\kappa(\boldsymbol{\theta}) = \frac{\Sigma(\boldsymbol{\theta})}{\Sigma_{\mathrm{cr}}}$$

Fermat's principle

- light path is determined such that light travel time becomes minimum (stationary point)
- basic principle in geometric optics
- this principle is also the case for gravitational lensing

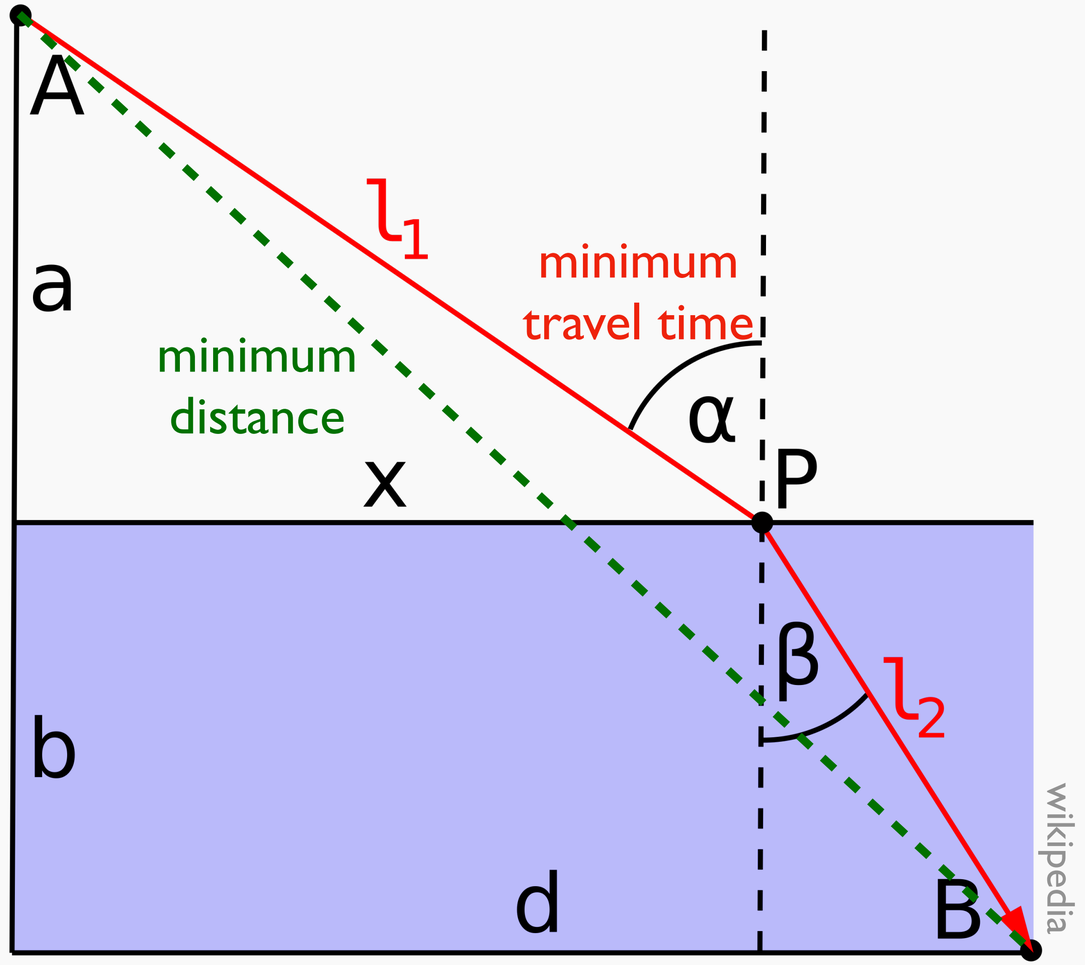

Lens equation from Fermat's principle (I)

- Fermat's principle in expanding Universe is expressed using conformal time $d\eta = dt/a$

$$\delta \int d\eta = 0$$

- from metric and $ds^2 = 0$

$$\frac{c\, d\eta}{d\chi} \simeq - \left[1 - \frac{\Phi}{c^2} - \frac{\Psi}{c^2} + \frac{f_K^2(\chi)}{2} \omega_{ab} \frac{dx^a}{d\chi} \frac{dx^b}{d\chi} \right]$$

Lens equation from Fermat's principle (II)

- plugging into equation of variation

$$\delta \int_0^{\chi_s} d\chi \underbrace{\left[1 - \frac{\Phi}{c^2} - \frac{\Psi}{c^2} + \frac{f_K^2(\chi)}{2} \omega_{ab} \frac{dx^a}{d\chi} \frac{dx^b}{d\chi} \right]}_{= L\left(x^a, \frac{dx^a}{d\chi}, \chi \right)} = 0$$

$$\Rightarrow \quad \frac{d}{d\chi} \left(\frac{\partial L}{\partial (dx^a/d\chi)} \right) - \frac{\partial L}{\partial x^a} = 0$$

Euler-Lagrange equation

$$\Rightarrow \quad \frac{d}{d\chi} \left[f_K^2(\chi) \omega_{ab} \frac{dx^b}{d\chi} \right] + \frac{1}{c^2} \left(\Phi_{,a} + \Psi_{,a} \right) = 0$$

equation for light deflection due to gravitational lensing

Why does Fermat's principle hold?

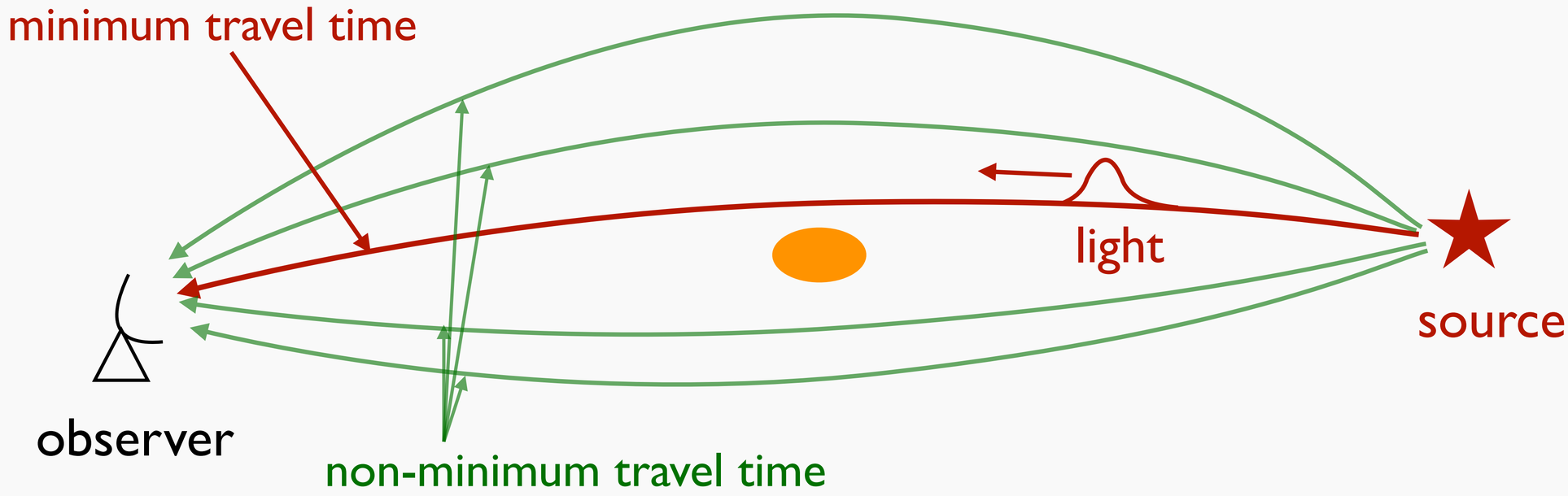

- light travels as if they know "answer" (?)

Wave optics and geometric optics

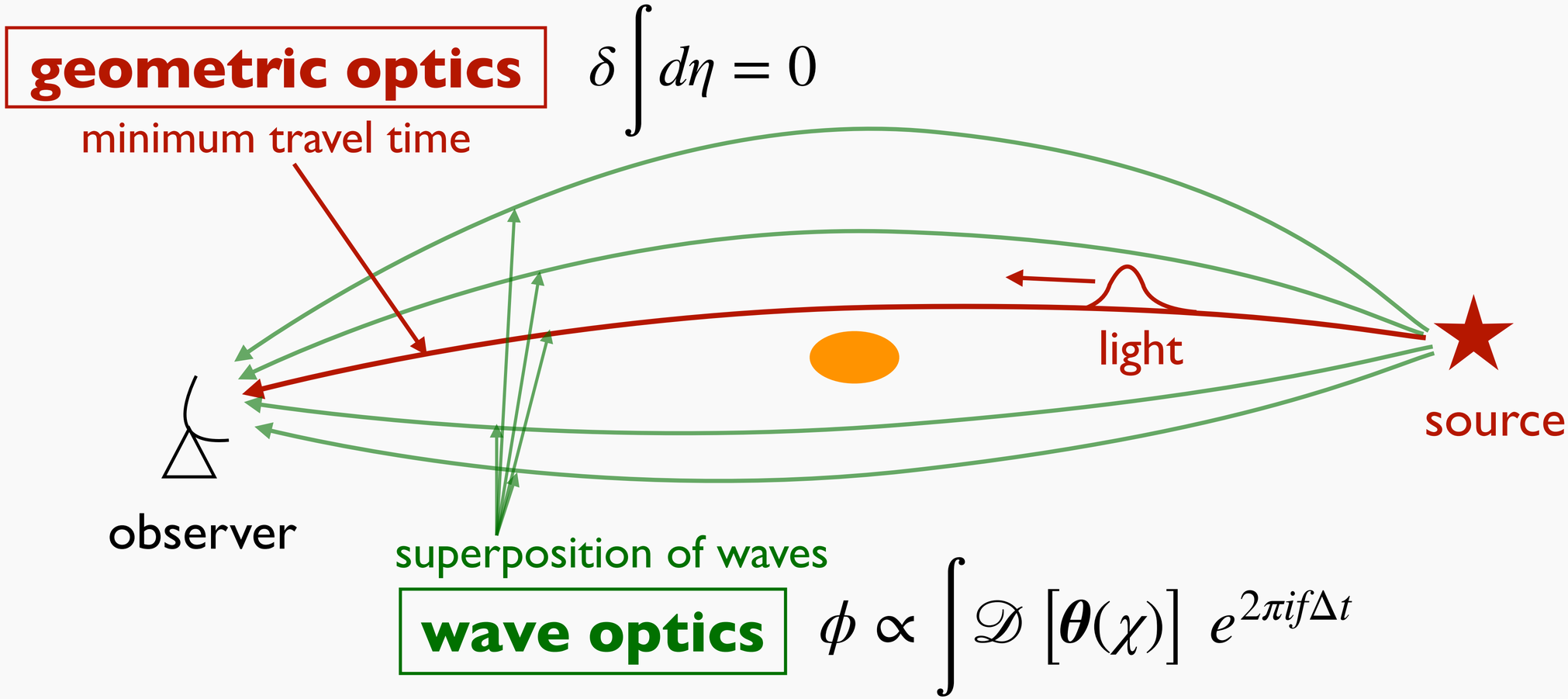

- high frequency limit of **wave optics** → cancellation of integral of oscillating function → **geometric optics**

Analog: least-action principle in mechanics

analytic mechanics $\delta S = 0$

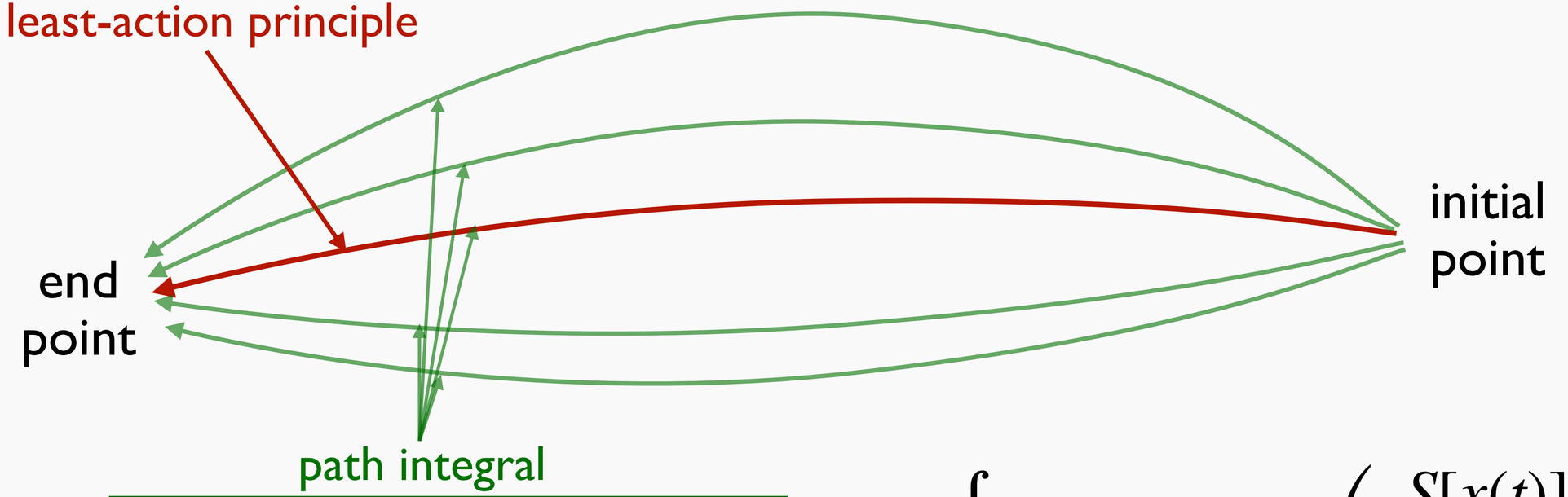

quantum mechanics $\phi \propto \int \mathscr{D}\left[x(t)\right] \exp\left(i\frac{S[x(t)]}{\hbar}\right)$

- $\hbar \to 0$ of **quantum mechanics** → cancellation of integral of oscillating function → **analytic mechanics**

Summary

- lens equation is derived from geodesic equation
- calculation using various approximations such as locally flat coordinates and Born approximation
- lens equation can be derived from Fermat's principle

3. General properties

Summary of lens equation

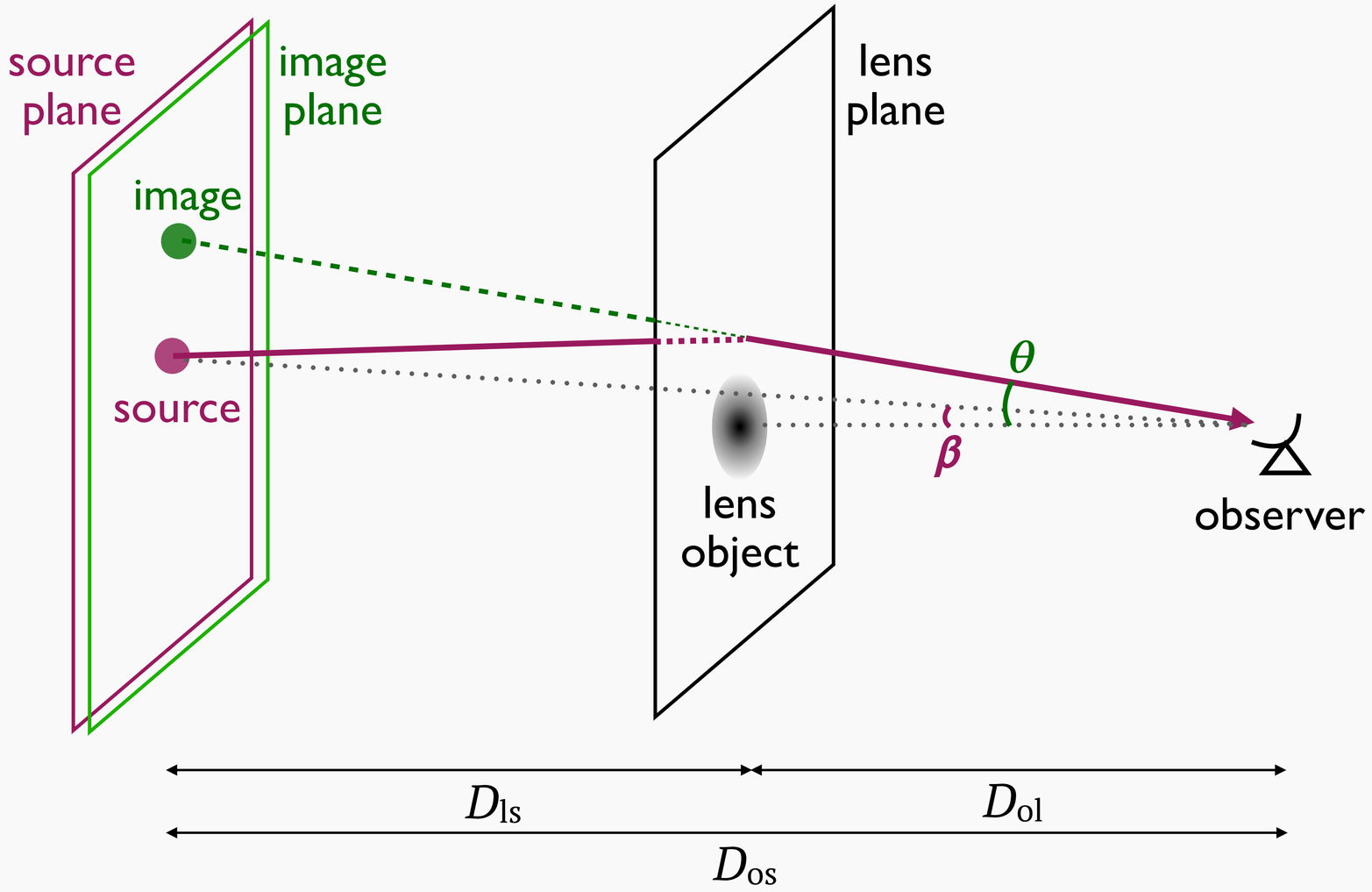

source image deflection angle

$$\boldsymbol{\beta} = \boldsymbol{\theta} - \boldsymbol{\alpha}(\boldsymbol{\theta})$$

$$\boldsymbol{\alpha}(\boldsymbol{\theta}) = \nabla_{\boldsymbol{\theta}}\psi \quad \text{lens potential}$$

$$= \frac{1}{\pi}\int d\boldsymbol{\theta}'\kappa(\boldsymbol{\theta}')\frac{\boldsymbol{\theta}-\boldsymbol{\theta}'}{\left|\boldsymbol{\theta}-\boldsymbol{\theta}'\right|^2}$$

$$\kappa(\boldsymbol{\theta}) = \frac{\Sigma(\boldsymbol{\theta})}{\Sigma_{\mathrm{cr}}}$$

convergence

Relation between ψ and κ

- operate Laplacian to ψ

$$\Delta_{\boldsymbol{\theta}}\psi = \nabla_{\boldsymbol{\theta}}\boldsymbol{\alpha} = \frac{1}{\pi}\int d\boldsymbol{\theta}'\kappa(\boldsymbol{\theta}')\,\nabla_{\boldsymbol{\theta}}\underbrace{\frac{\boldsymbol{\theta}-\boldsymbol{\theta}'}{\left|\boldsymbol{\theta}-\boldsymbol{\theta}'\right|^2}}_{=2\pi\delta^{\mathrm{D}}(\boldsymbol{\theta}-\boldsymbol{\theta}')} = 2\kappa(\boldsymbol{\theta})$$

Gauss' divergence theorem

gravitational lensing version of Poisson equation

Relation between κ and density fluctuation

- without thin lens approximation

$$\psi(\boldsymbol{\theta}) = \frac{2}{c^2}\int_0^{\chi_\mathrm{s}} d\chi \frac{f_K(\chi_\mathrm{s}-\chi)}{f_K(\chi)f_K(\chi_\mathrm{s})}\Phi(\chi,\boldsymbol{\theta})$$

$$\kappa(\boldsymbol{\theta}) = \frac{1}{2}\Delta_{\boldsymbol{\theta}}\psi \simeq \frac{1}{c^2}\int_0^{\chi_\mathrm{s}} d\chi \frac{f_K(\chi_\mathrm{s}-\chi)f_K(\chi)}{f_K(\chi_\mathrm{s})}{}^{(3)}\Delta\Phi$$

$$= \frac{4\pi G}{c^2}\int_0^{\chi_\mathrm{s}} d\chi \frac{f_K(\chi_\mathrm{s}-\chi)f_K(\chi)}{f_K(\chi_\mathrm{s})}\bar{\rho}_\mathrm{m}a^2\delta_\mathrm{m}(\chi,\boldsymbol{\theta})$$

Poisson eq.

integration of density fluctuation along line of sight with weight

Image position and multiple images

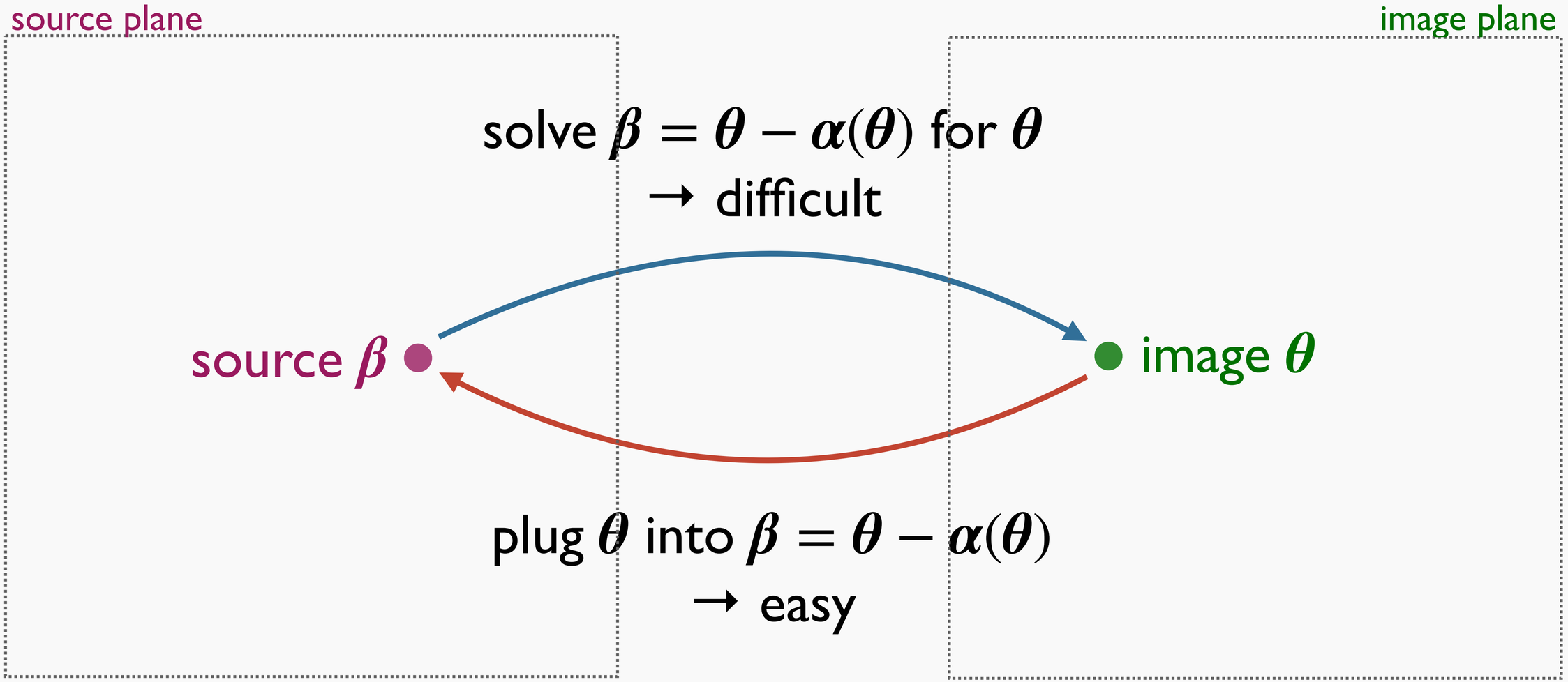

Image position and multiple images

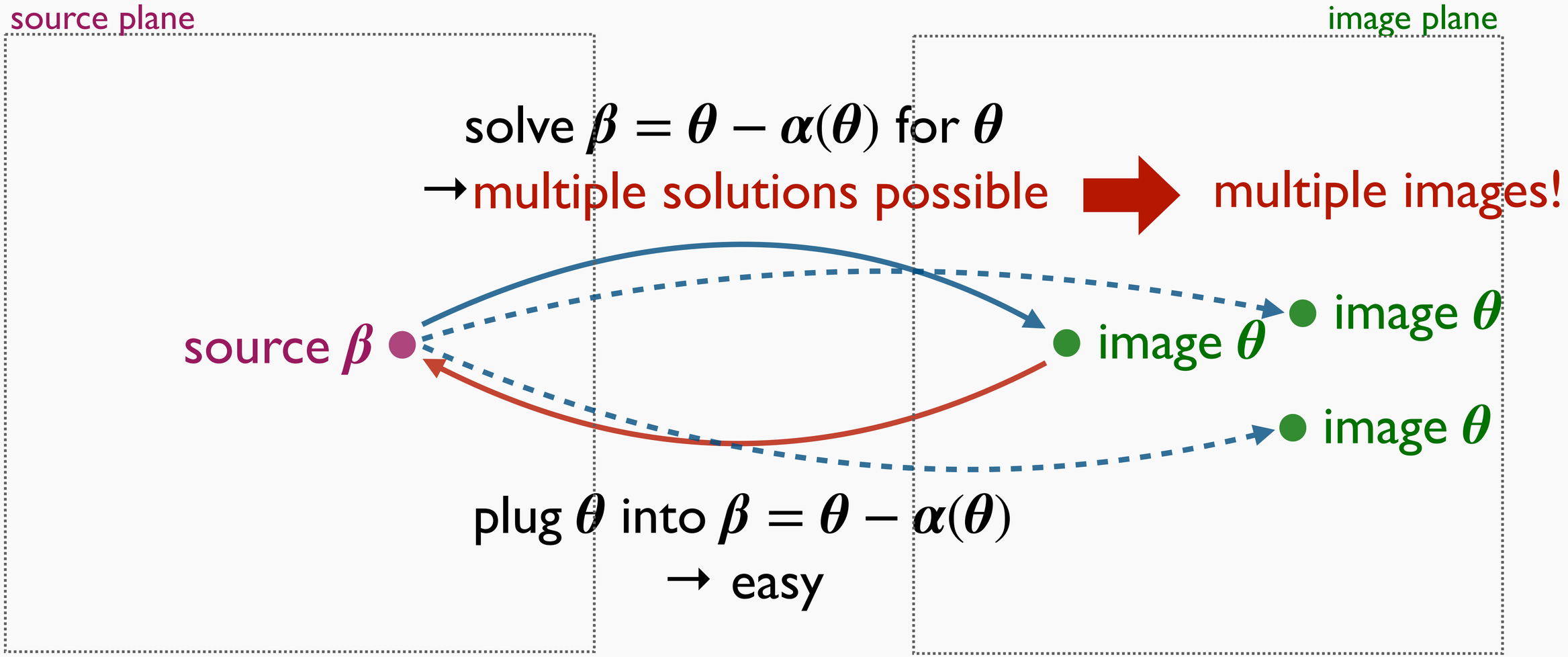

Deformation of image

- relation between infinitesimal vector around source $\delta\boldsymbol{\beta}$ and infinitesimal vector around image position $\delta\boldsymbol{\theta}$

$$\delta\boldsymbol{\beta} = A(\boldsymbol{\theta})\delta\boldsymbol{\theta}$$

$$A(\boldsymbol{\theta}) = \frac{\partial\boldsymbol{\beta}}{\partial\boldsymbol{\theta}} = \begin{pmatrix} \beta_{1,\theta_1} & \beta_{1,\theta_2} \\ \beta_{2,\theta_1} & \beta_{2,\theta_2} \end{pmatrix} = \begin{pmatrix} 1-\psi_{,\theta_1\theta_1} & -\psi_{,\theta_1\theta_2} \\ -\psi_{,\theta_1\theta_2} & 1-\psi_{,\theta_2\theta_2} \end{pmatrix}$$

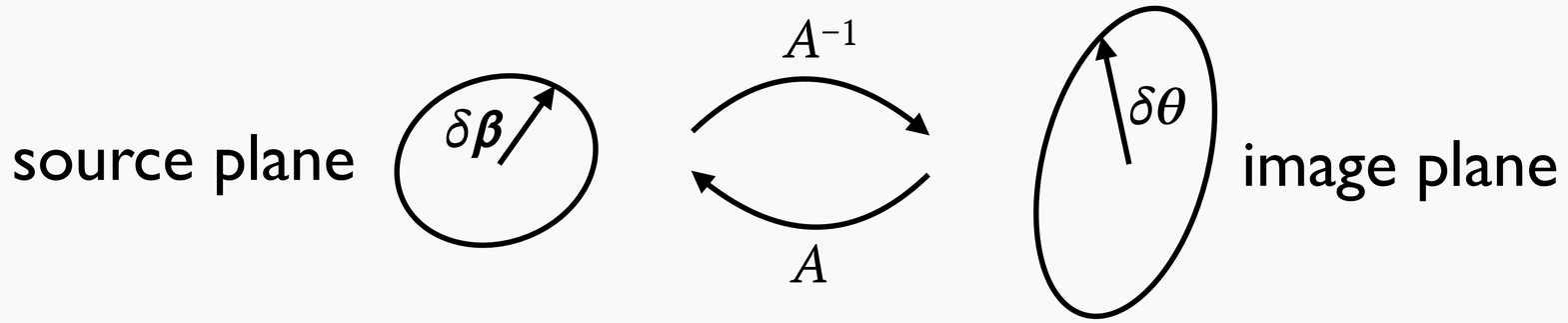

Convergence and shear

- from Poisson equation

$$\mathrm{tr}\,(A) = 2 - \psi_{,\theta_1\theta_1} - \psi_{,\theta_2\theta_2} = 2(1-\kappa)$$

- define shear

$$\gamma_1 = \frac{1}{2}(\psi_{,\theta_1\theta_1} - \psi_{,\theta_2\theta_2})$$

$$\gamma_2 = \psi_{,\theta_1\theta_2}$$

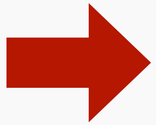

$$A(\boldsymbol{\theta}) = \begin{pmatrix} 1-\kappa-\gamma_1 & -\gamma_2 \\ -\gamma_2 & 1-\kappa+\gamma_1 \end{pmatrix}$$

Deformation of image due to κ and γ

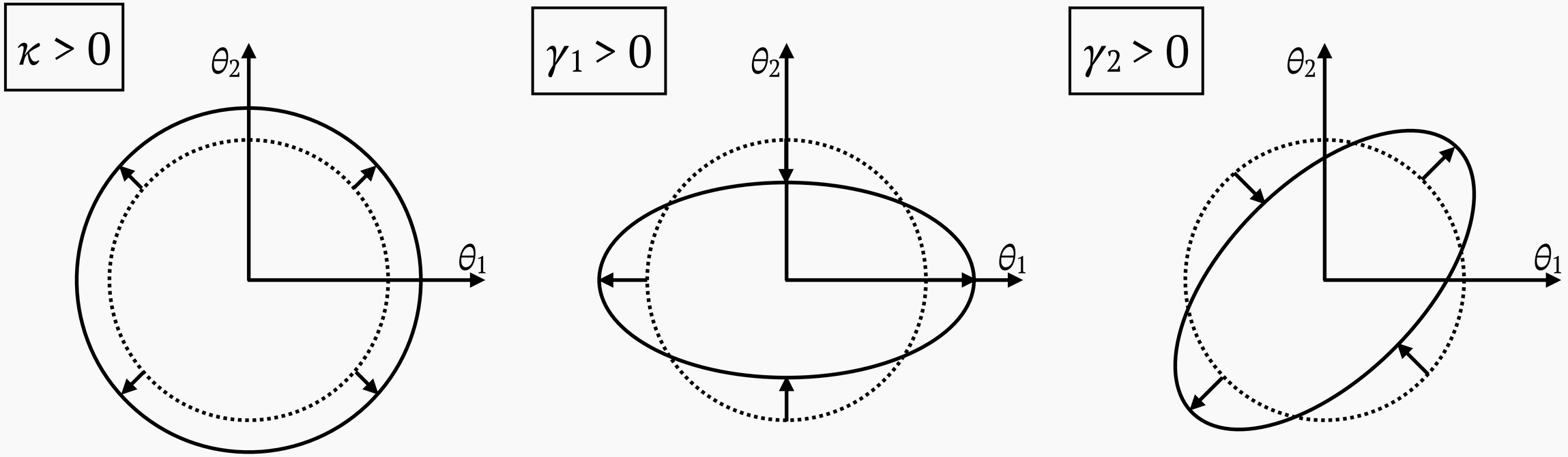

$$\delta\boldsymbol{\theta} = \begin{pmatrix} 1-\kappa-\gamma_1 & -\gamma_2 \\ -\gamma_2 & 1-\kappa+\gamma_1 \end{pmatrix}^{-1} \delta\boldsymbol{\beta}$$

Magnification

- Liouville's theorem indicates that light intensity is conserved during propagation, so magnification μ is given by

$$\mu(\boldsymbol{\theta}) = \frac{1}{\det A(\boldsymbol{\theta})} = \frac{1}{(1-\kappa)^2 - \left|\gamma\right|^2}$$

$$\left|\gamma\right| = \sqrt{\gamma_1^2 + \gamma_2^2}$$

- flux of image is amplified by a factor of $|\mu|$

Parity of image

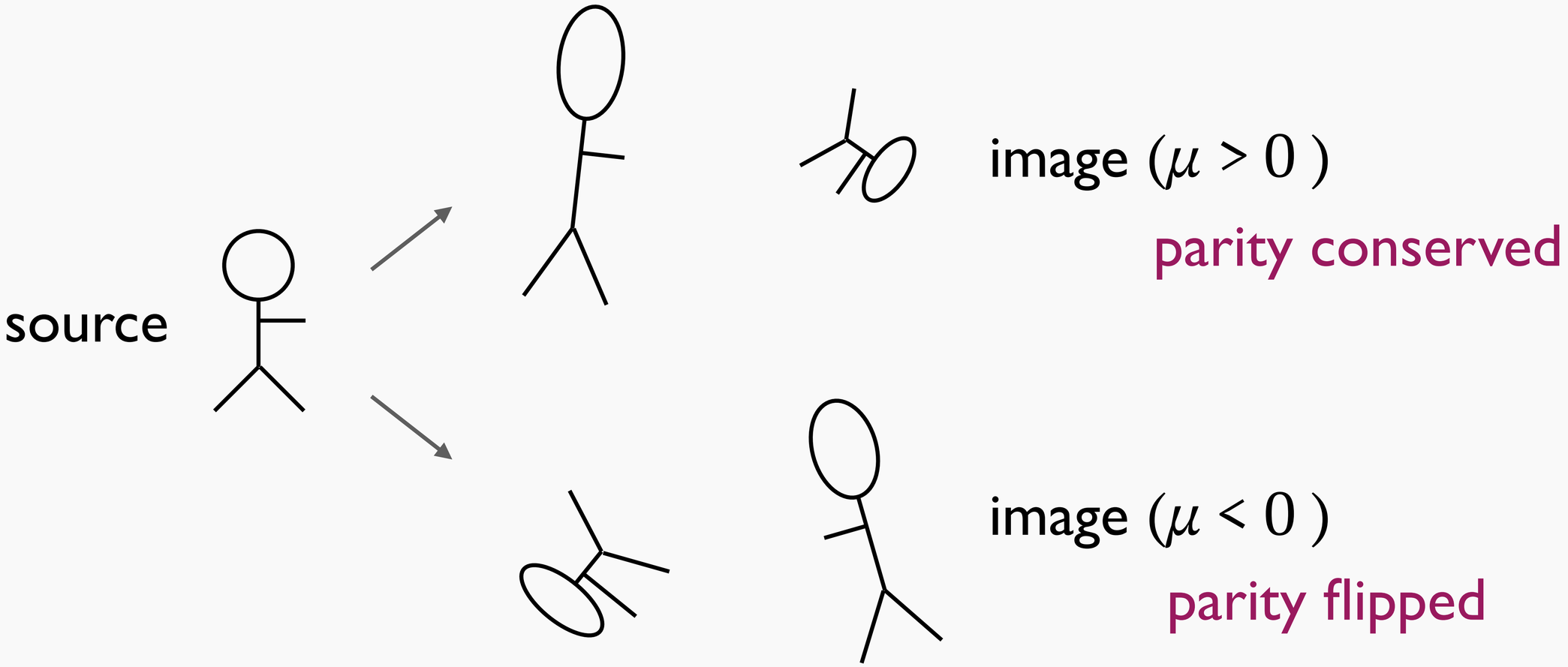

Example

negative parity

positive parity

https://science.nasa.gov/asset/webb/webbs-first-deep-field-nircam-image/

Critical curve and caustic

- critical curve consists of points satisfying $\det A = 0$ ($|\mu| = \infty$) in image plane

$$\left[1 - \kappa(\boldsymbol{\theta}_{\rm c})\right]^2 - \left|\gamma(\boldsymbol{\theta}_{\rm c})\right|^2 = 0$$

- caustic is corresponding curve in source plane

Critical curve and caustic

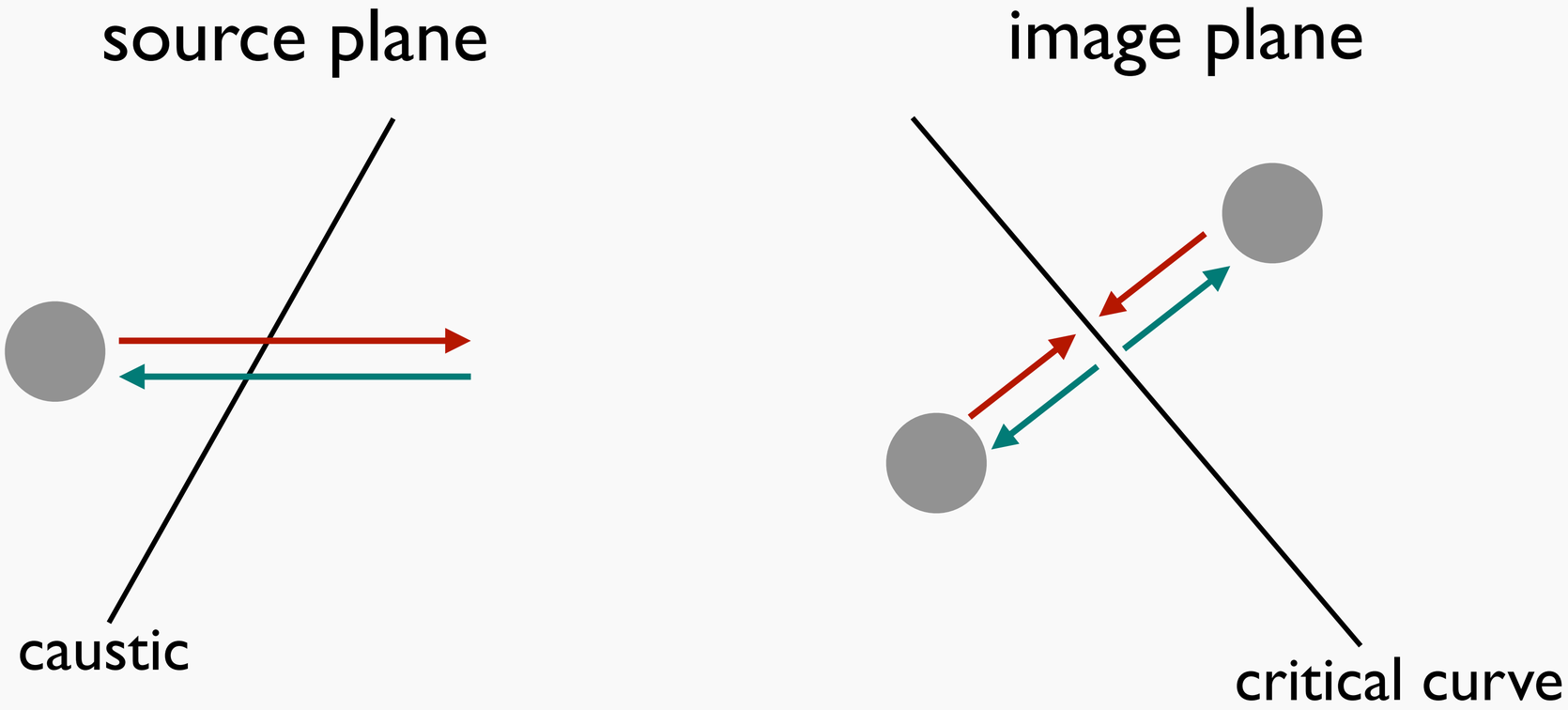

movie file: https://oguri.github.io/for_presen.html

Creation/annihilation of images (point source)

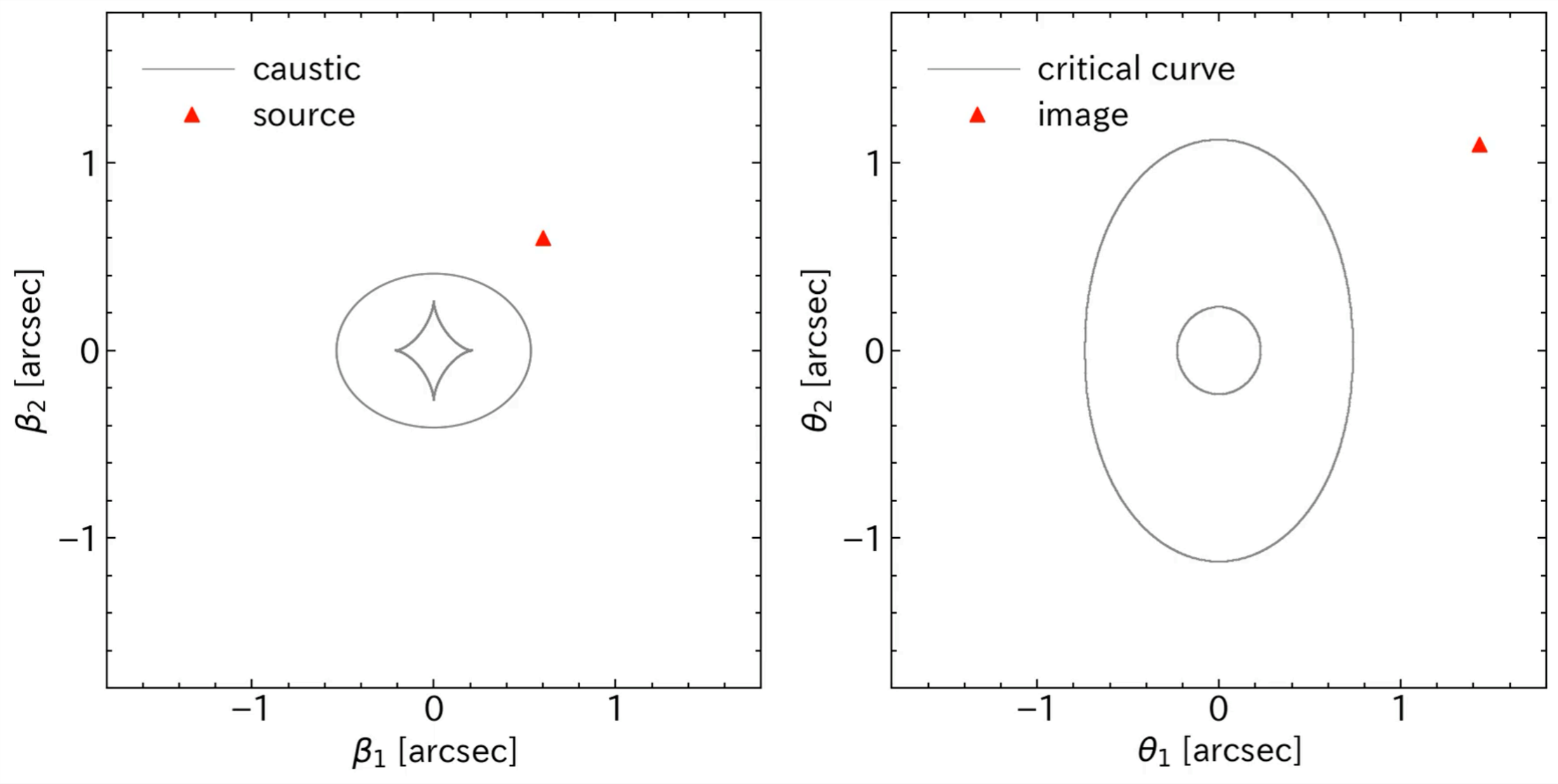

movie file: https://oguri.github.io/for_presen.html

Creation/annihilation of images (extended source)

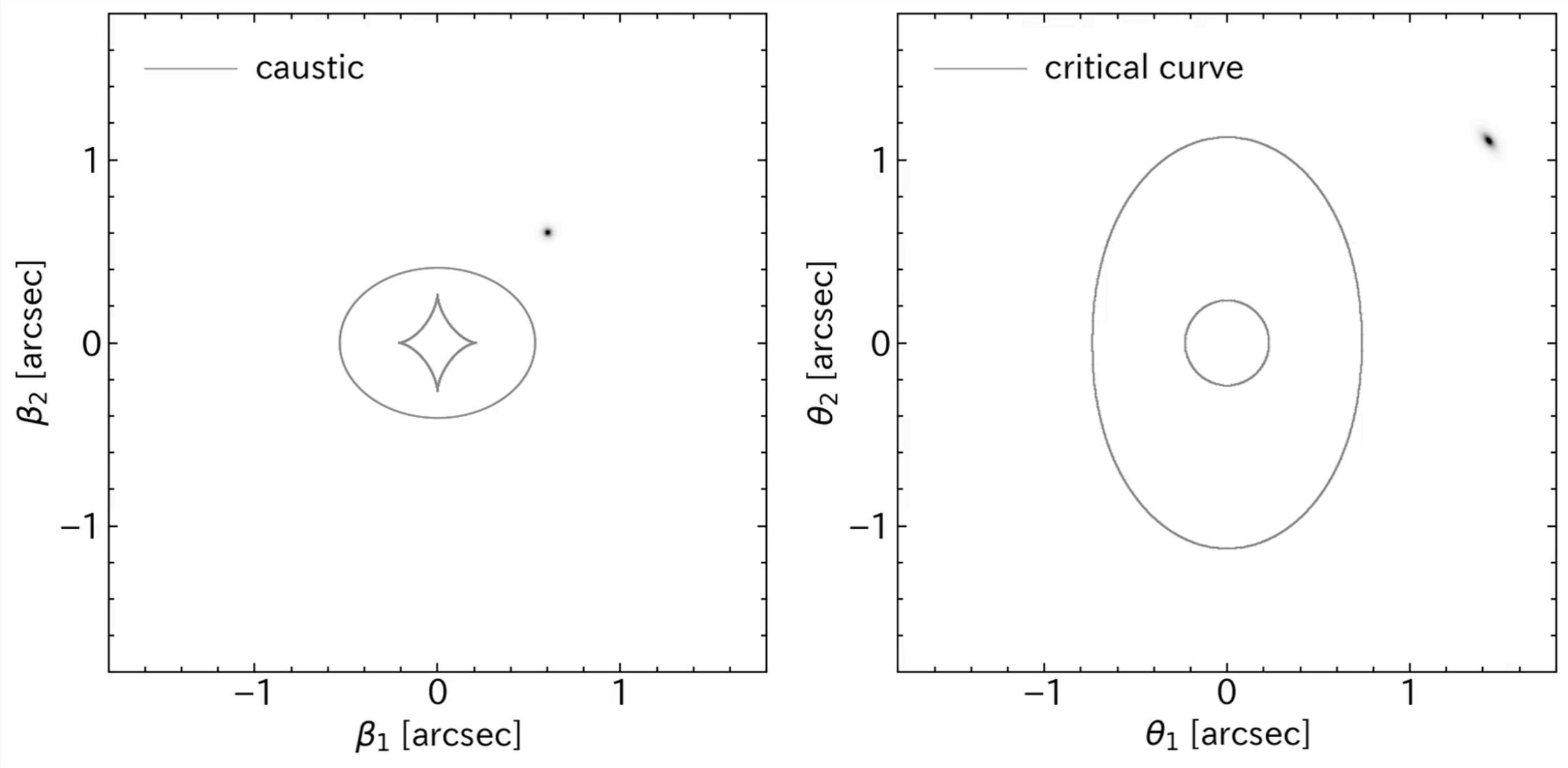

Numerical method to solve lens equation

- solve lens equation numerically for $\boldsymbol{\theta}$

$$\boldsymbol{\beta} = \boldsymbol{\theta} - \boldsymbol{\alpha}(\boldsymbol{\theta})$$

- search wide area in image plane to find all multiple images

Numerical root finding

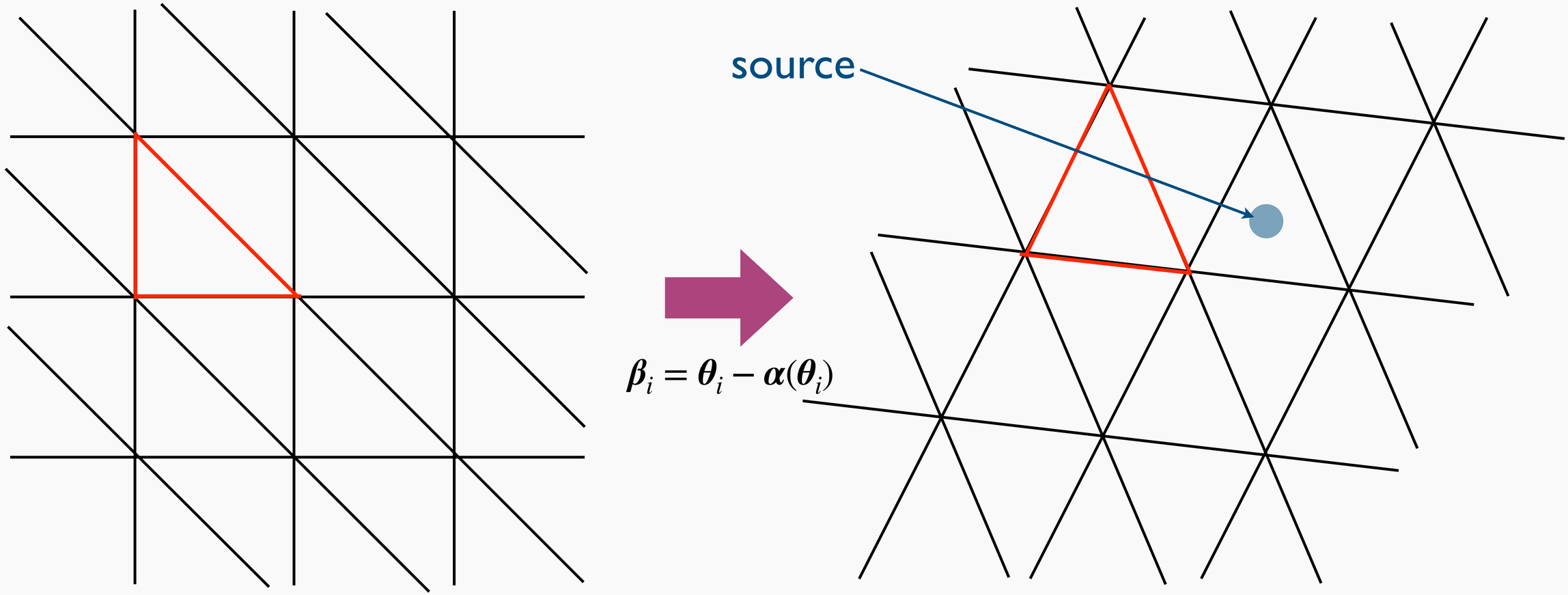

image plane ($\boldsymbol{\theta}_i$)

source plane ($\boldsymbol{\beta}_i$)

Numerical root finding

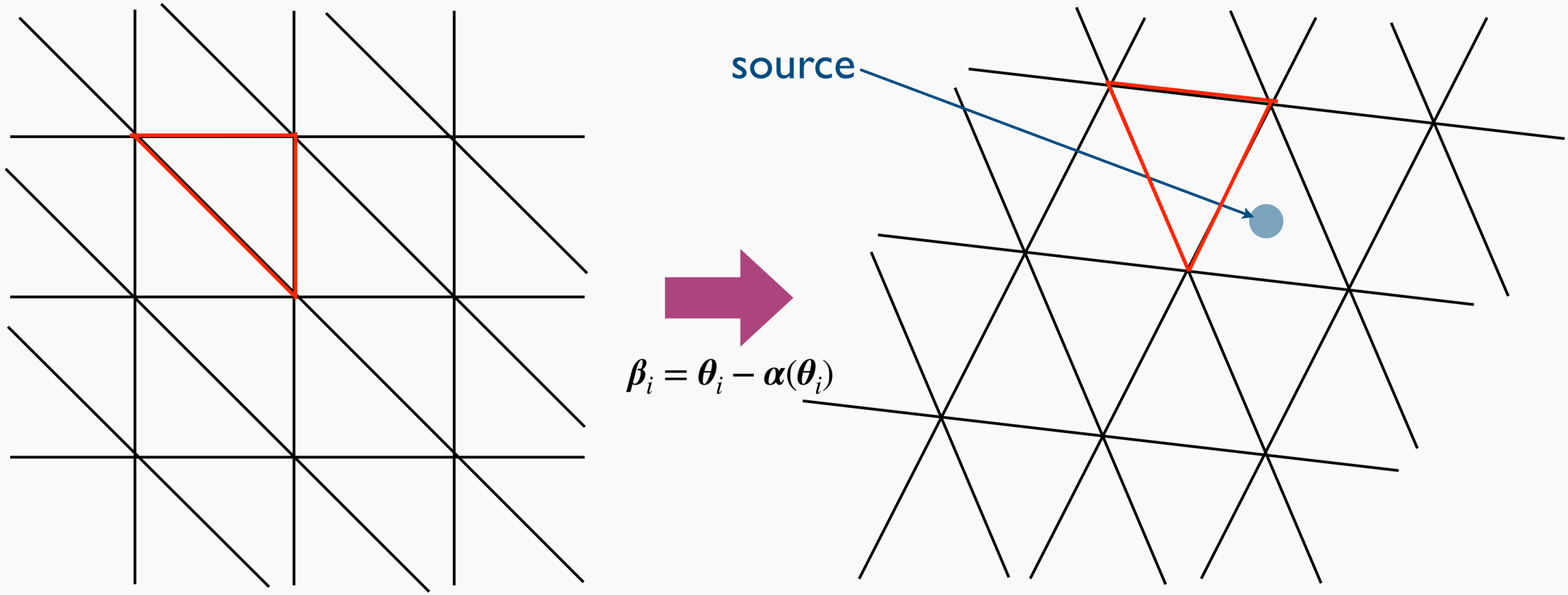

image plane ($\boldsymbol{\theta}_i$)

source plane ($\boldsymbol{\beta}_i$)

Numerical root finding

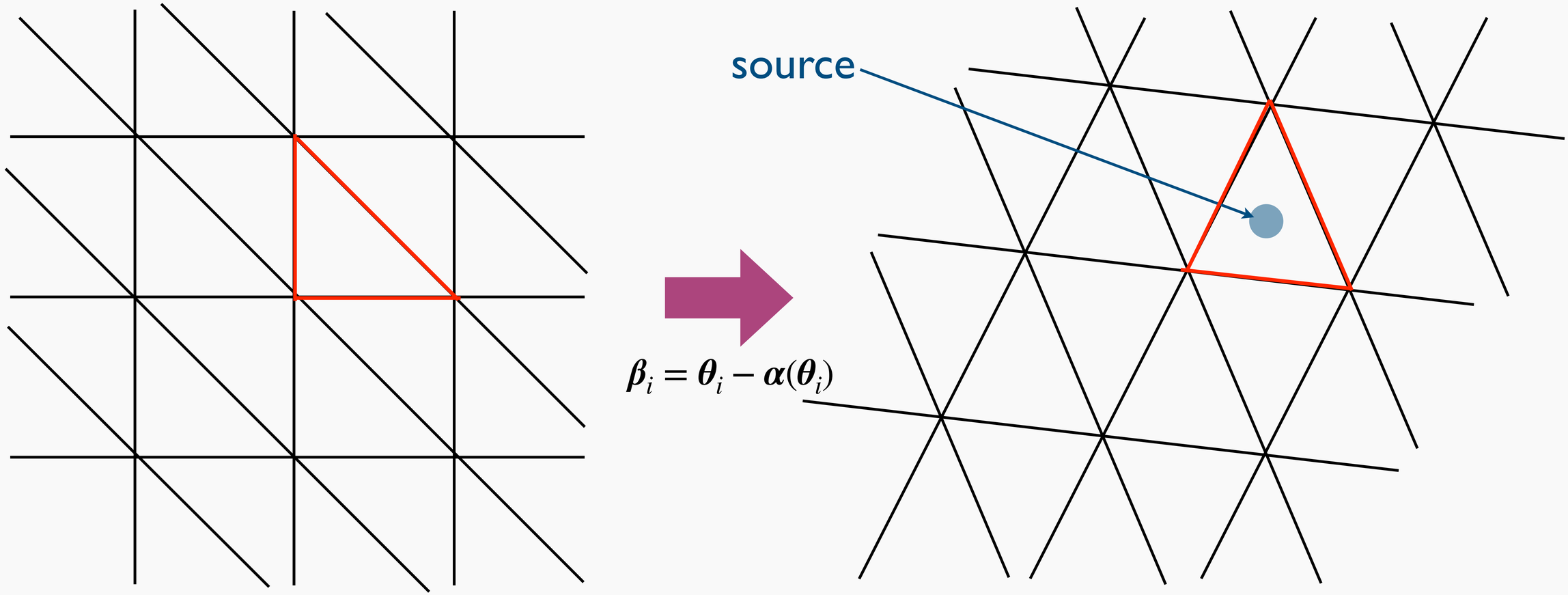

image plane ($\boldsymbol{\theta}_i$)

source plane ($\boldsymbol{\beta}_i$)

Numerical root finding

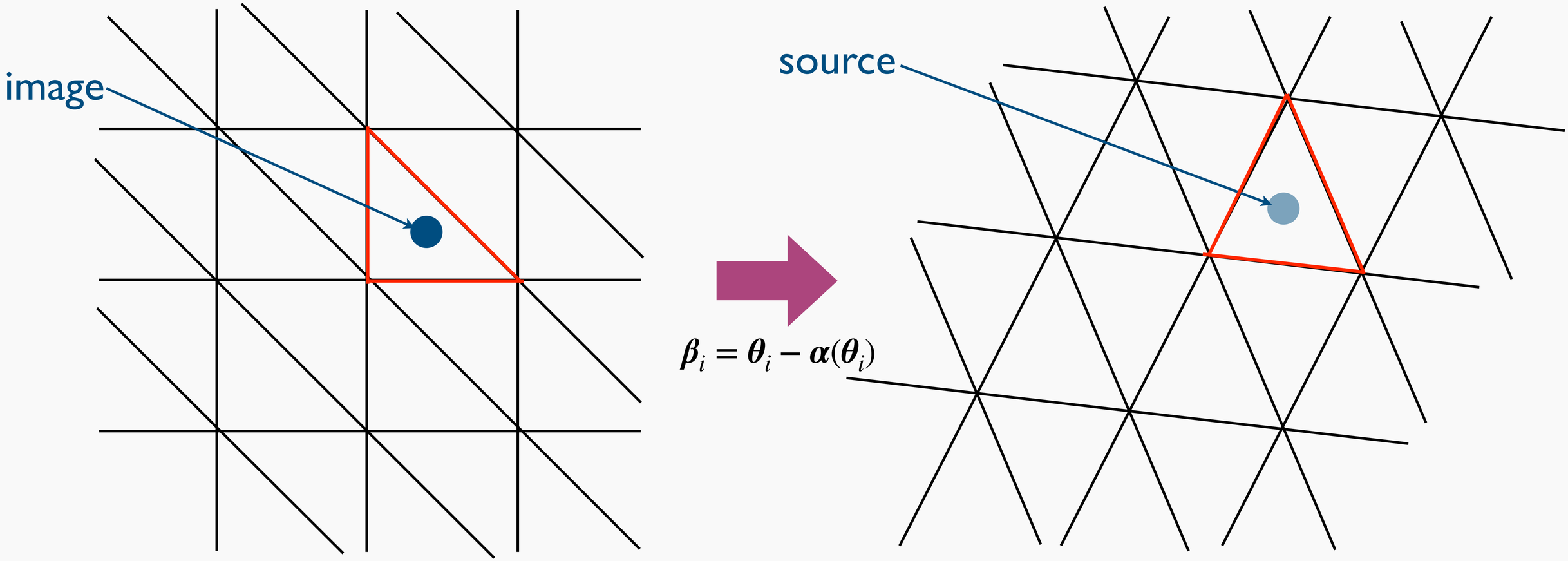

image plane ($\boldsymbol{\theta}_i$)

source plane ($\boldsymbol{\beta}_i$)

Numerical root finding

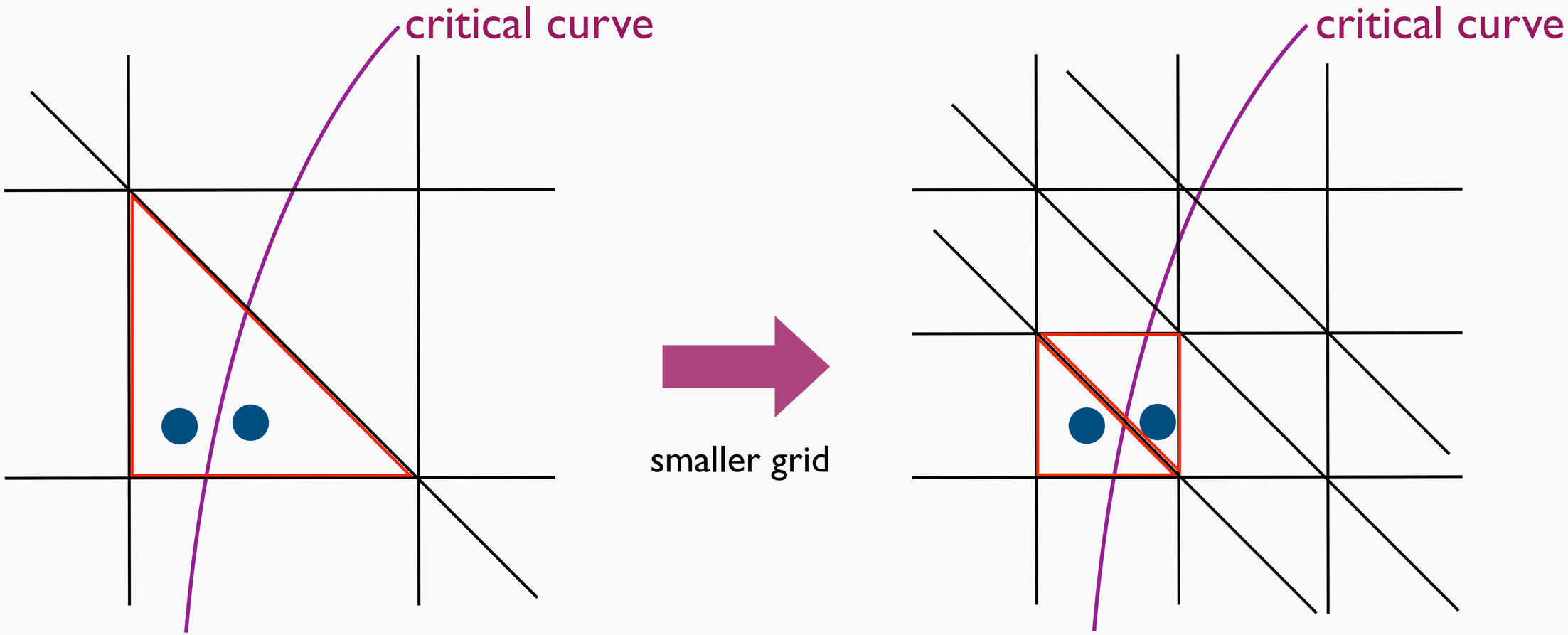

example by *glafic* (MO 2010, https://github.com/oguri/glafic2)

Code to solve lens equation

image plane
(θ_i)

source plane
(β_i)

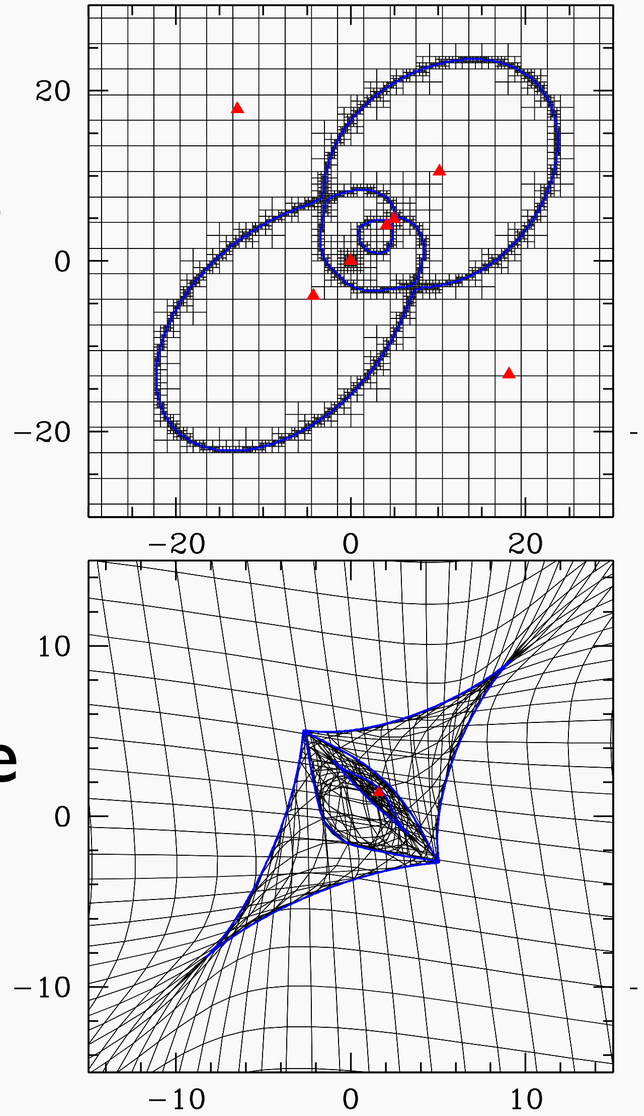

- small grid needed only near critical curve
- efficiently solve lens equation with adaptive grid
- in this example 7 multiple images are successfully found

Time delay

- preparation: cosmological time dilation

$$\chi = \int_{t_1}^{t_0} \frac{c\,dt}{a} = \int_{t_1+\delta t_1}^{t_0+\delta t_0} \frac{c\,dt}{a}$$

$$\delta t_0 = \frac{a(t_0)}{a(t_1)} \delta t_1 = (1+z)\delta t_1$$

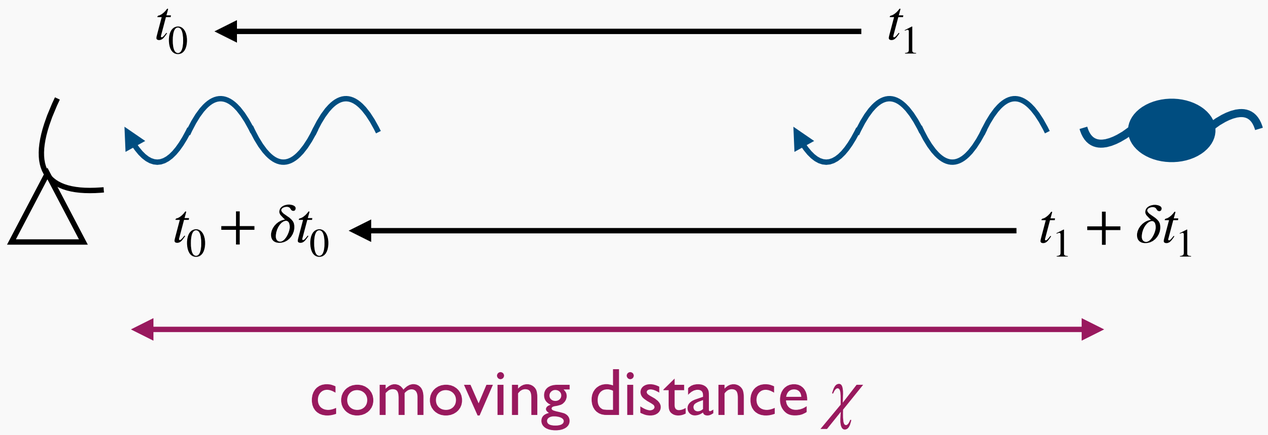

Deriving time delay (I)

- arrival time difference between with and without lensing

$$\Delta t = \int_{\text{w/ lensing}} \frac{dt}{a} - \int_{\text{w/o lensing}} \frac{dt}{a}$$

- from calculation in Fermat's principle

$$\Delta t = \frac{1}{c}\int_0^{\chi_s} d\chi \left[\frac{f_K^2(\chi)}{2} \left| \frac{d\boldsymbol{\theta}}{d\chi} \right|^2 - \frac{2\Phi}{c^2} \right]$$

→ geometrical time delay Δt_{geom} → gravitational time delay Δt_{grav}

Deriving time delay (II)

- calculation of geometrical time delay

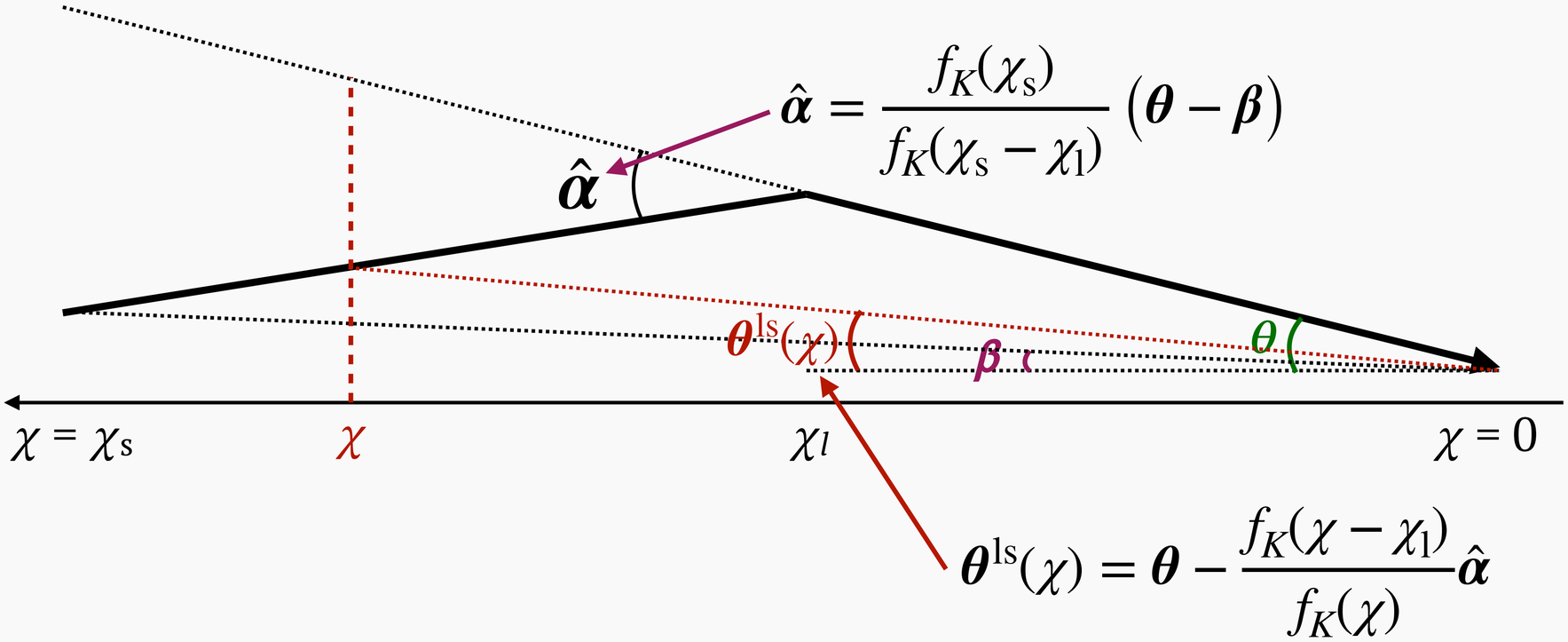

Deriving time delay (III)

- differentiate $\boldsymbol{\theta}^{\mathrm{ls}}$ with respect to χ

$$\frac{d\boldsymbol{\theta}^{\mathrm{ls}}}{d\chi} = \left[\frac{f_K(\chi-\chi_1)f_K'(\chi)}{f_K^2(\chi)} - \frac{f_K'(\chi-\chi_1)}{f_K(\chi)}\right]\hat{\boldsymbol{\alpha}} = -\frac{f_K(\chi_1)}{f_K^2(\chi)}\hat{\boldsymbol{\alpha}}$$

- plug it into Δt_{geom}

$$\Delta t_{\mathrm{geom}} = \frac{1}{c}\int_{\chi_1}^{\chi_{\mathrm{s}}} d\chi \frac{f_K^2(\chi)}{2}\left|\frac{d\boldsymbol{\theta}^{\mathrm{ls}}}{d\chi}\right|^2 = \frac{1}{c}\frac{f_K(\chi_{\mathrm{s}}-\chi_1)f_K(\chi_1)}{f_K(\chi_{\mathrm{s}})}\frac{\left|\hat{\boldsymbol{\alpha}}\right|^2}{2}$$

$$= \frac{1}{c}\frac{f_K(\chi_1)f_K(\chi_{\mathrm{s}})}{f_K(\chi_{\mathrm{s}}-\chi_1)}\frac{\left|\boldsymbol{\theta}-\boldsymbol{\beta}\right|^2}{2}$$

$$\hat{\boldsymbol{\alpha}} = \frac{f_K(\chi_{\mathrm{s}})}{f_K(\chi_{\mathrm{s}}-\chi_1)}(\boldsymbol{\theta}-\boldsymbol{\beta})$$

Deriving time delay (IV)

- gravitational potential in lens plane assuming thin lens

$$\Phi(\boldsymbol{\theta}) \simeq \frac{2G}{1+z_\mathrm{l}} \left\{f_K(\chi_\mathrm{l})\right\}^2 \delta^\mathrm{D}(\chi-\chi_\mathrm{l}) \int d\boldsymbol{\theta}' \Sigma(\boldsymbol{\theta}') \ln \left|\boldsymbol{\theta}_i - \boldsymbol{\theta}'\right|$$
$$= \frac{c^2}{2} \frac{f_K(\chi_\mathrm{l}) f_K(\chi_\mathrm{s})}{f_K(\chi_\mathrm{s}-\chi_\mathrm{l})} \delta^\mathrm{D}(\chi-\chi_\mathrm{l}) \psi(\boldsymbol{\theta})$$

- plug it into Δt_grav

$$\Delta t_\mathrm{grav} = -\frac{1}{c} \frac{f_K(\chi_\mathrm{l}) f_K(\chi_\mathrm{s})}{f_K(\chi_\mathrm{s}-\chi_\mathrm{l})} \psi(\boldsymbol{\theta})$$

Deriving time delay (V)

- finally time delay Δt using angular diameter distances

$$\Delta t = \frac{1+z_\mathrm{l}}{c}\frac{D_\mathrm{ol}D_\mathrm{os}}{D_\mathrm{ls}}\left[\frac{\left|\boldsymbol{\beta}-\boldsymbol{\theta}\right|^2}{2} - \psi(\boldsymbol{\theta})\right]$$

→ geometrical time delay Δt_geom

→ gravitational time delay Δt_grav

Geometrical and gravitational time delays

geometrical time delay

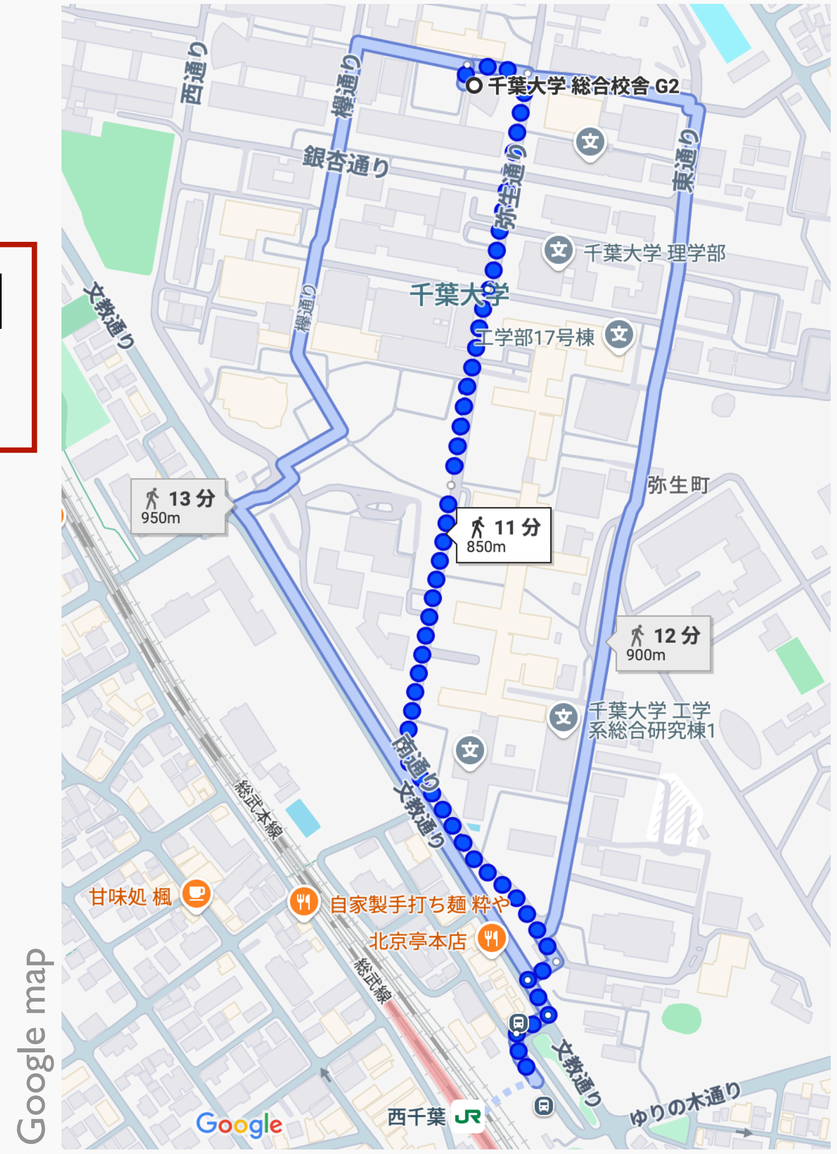

Takamoto+ Nature Photonics **14**(2020)411

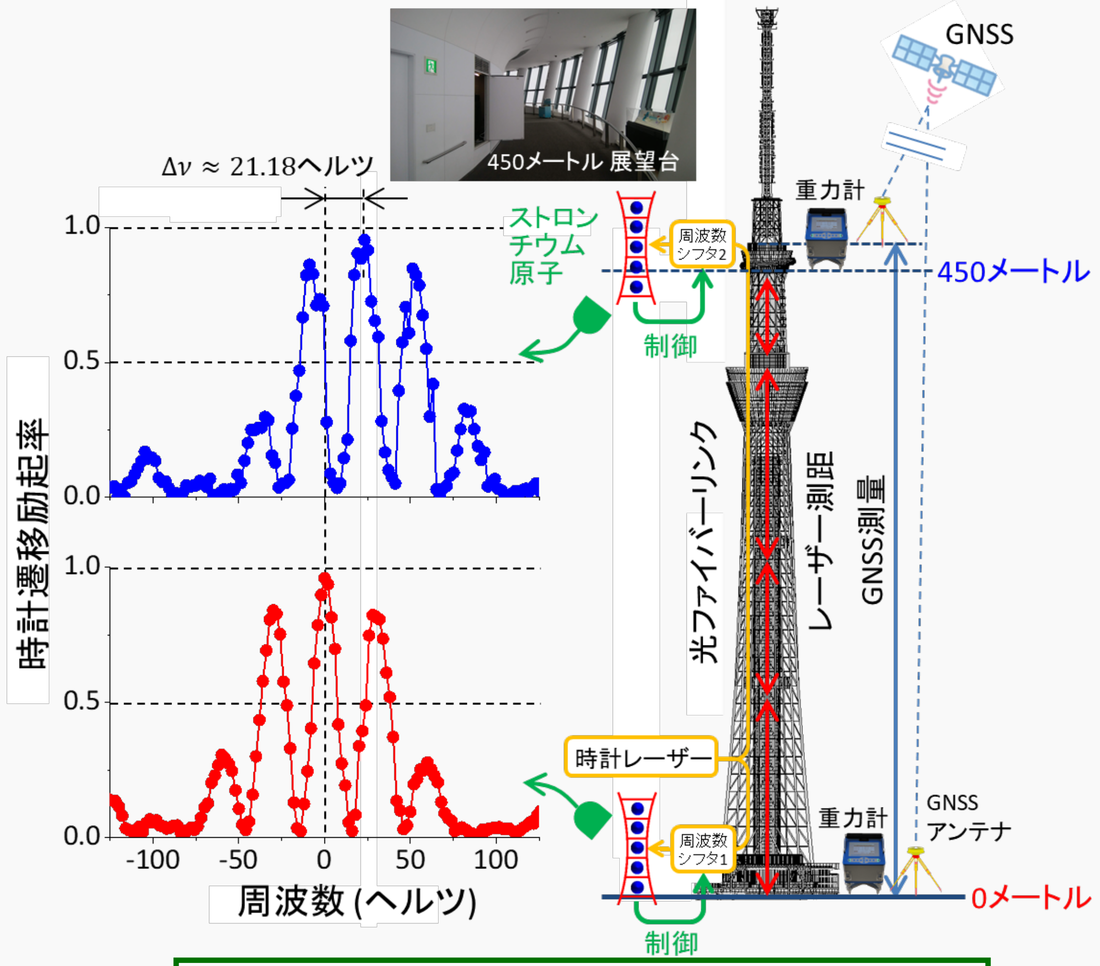

gravitational time delay

Observable time delay

- what we can observe is differential time delay between multiple images

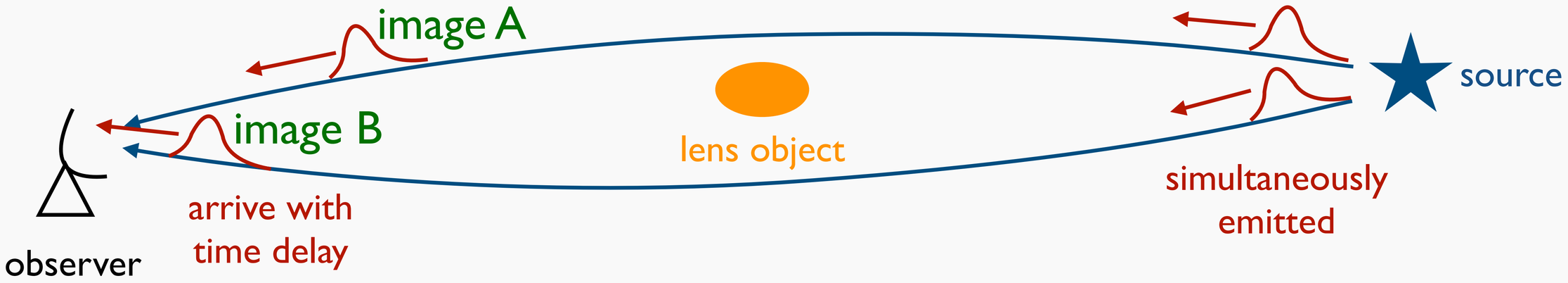

$$\Delta t_{\mathrm{AB}} = \Delta t(\boldsymbol{\theta}_{\mathrm{A}}; \boldsymbol{\beta}) - \Delta t(\boldsymbol{\theta}_{\mathrm{B}}; \boldsymbol{\beta})$$

Connection with Fermat's principle

- derived expression of time delay is correct even for pair of $\boldsymbol{\beta}$, $\boldsymbol{\theta}$ that are not solution of lens equation

$$\Delta t = \frac{1+z_{\rm l}}{c}\frac{D_{\rm ol}D_{\rm os}}{D_{\rm ls}}\left[\frac{\left|\boldsymbol{\beta}-\boldsymbol{\theta}\right|^2}{2}-\psi(\boldsymbol{\theta})\right]$$

- Fermat's principle requires light travel time is stationary

$$\nabla_{\boldsymbol{\theta}}\Delta t = 0 \quad \Rightarrow \quad \boldsymbol{\theta}-\boldsymbol{\beta}-\nabla_{\boldsymbol{\theta}}\psi = 0$$

lens equation is derived

Odd number theorem

- Fermat's principle → images at stationary points of $\Delta t(\boldsymbol{\theta};\boldsymbol{\beta})$
- odd number theorem of number of multiple images from Morse theory

Euler characteristic

$$n_{\min} - n_{\text{sad}} + n_{\max} + 1 = \chi = 2$$

$$n_{\text{tot}} = n_{\min} + n_{\text{sad}} + n_{\max} = \underbrace{1 + 2n_{\text{sad}}}_{\text{odd}}$$

- hold only when lens potential is smooth (e.g., not hold for point mass lens)

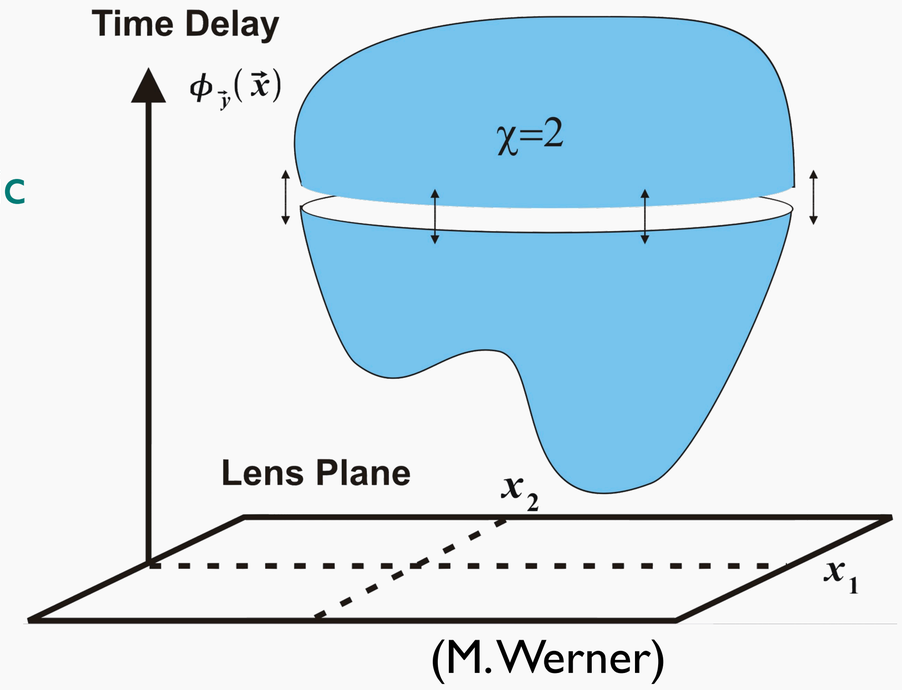

(M. Werner)

Example of odd number theorem

SDSS J1004

5 multiple images of quasar

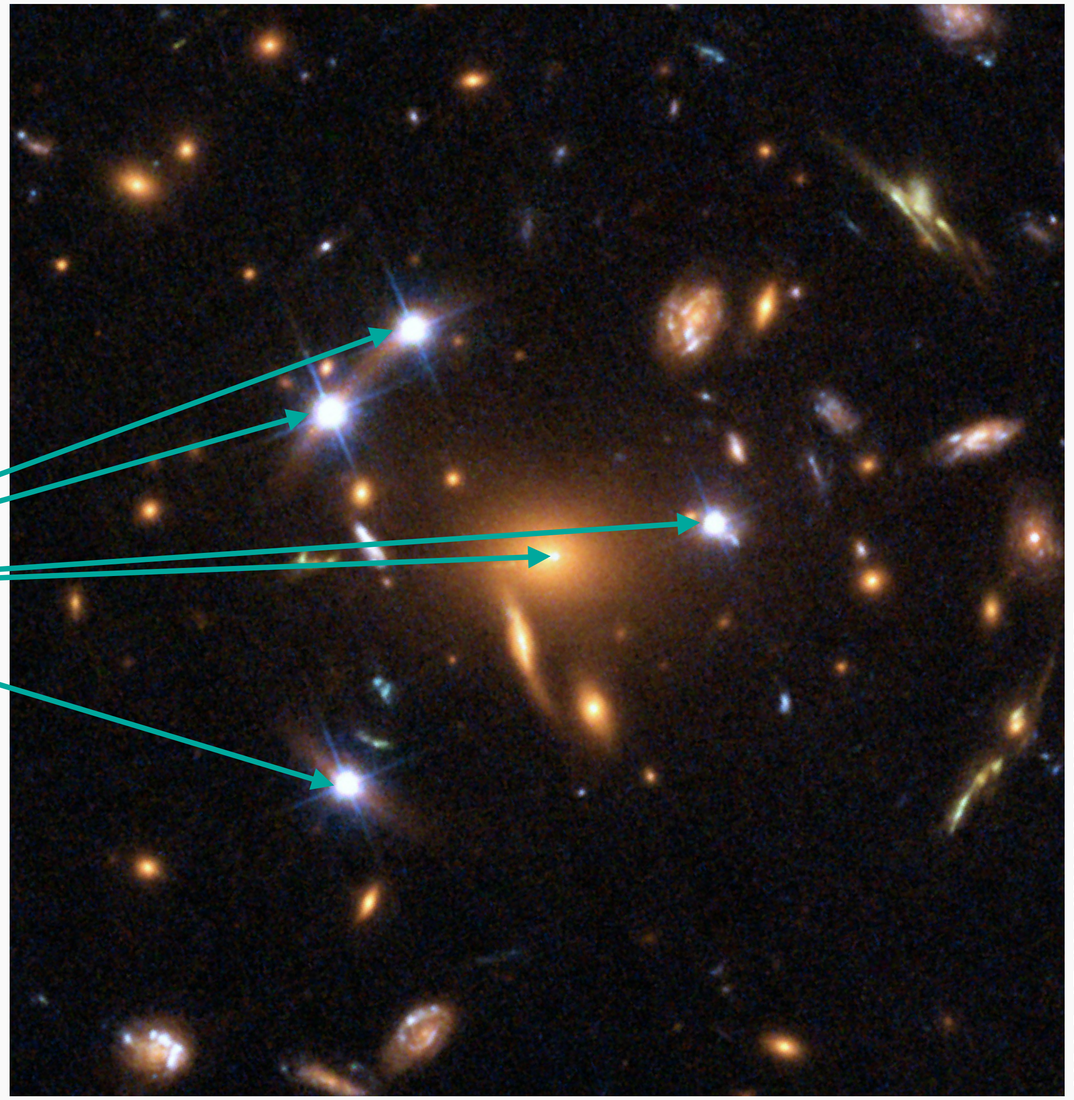

ESA/NASA/K. Sharon/E. Ofek

Summary

- convergence, shear, magnification from derivatives of lens equation
- lens equation is mapping from image to source positions
- lens equation derived also from time delay plus Fermat's principle

4. Examples of solutions of lens equation

Spherically symmetric lens (I)

- setting lens center as origin, convergence of spherically symmetric lens can be written as $\kappa(\theta)$ with $\theta = |\boldsymbol{\theta}|$
- lens potential is

polar coordinates $(\theta_1, \theta_2) = (\theta\cos\varphi, \theta\sin\varphi)$

$$\psi(\boldsymbol{\theta}) = \frac{1}{\pi}\int_0^\infty d\theta' \int_0^{2\pi} d\varphi'\,\theta'\kappa(\theta')\ln\sqrt{\theta^2+\theta'^2-2\theta\theta'\cos\varphi'}$$

$$= 2\int_0^\theta d\theta'\,\theta'\kappa(\theta')\ln\theta + 2\int_\theta^\infty d\theta'\,\theta'\kappa(\theta')\ln\theta'$$

$$\int_0^{2\pi} d\varphi'\,\ln\sqrt{\theta^2+\theta'^2-2\theta\theta'\cos\varphi'} = \pi\ln\left[\frac{1}{2}\left(\theta^2+\theta'^2+\left|\theta^2-\theta'^2\right|\right)\right] = \begin{cases} 2\pi\ln\theta & (\theta \geq \theta') \\ 2\pi\ln\theta' & (\theta < \theta') \end{cases}$$

Spherically symmetric lens (II)

- add constant term to lens potential

$$\psi(\boldsymbol{\theta}) - 2\int_0^\infty d\theta'\,\theta'\kappa(\theta')\ln\theta' \rightarrow \psi(\boldsymbol{\theta})$$

$$\psi(\theta) = 2\int_0^\theta d\theta'\,\theta'\kappa(\theta')\ln\left(\frac{\theta}{\theta'}\right)$$

function of only $\theta = |\boldsymbol{\theta}|$

Spherically symmetric lens (III)

- deflection angle $\boldsymbol{\alpha}(\boldsymbol{\theta})$ is

$$\boldsymbol{\alpha}(\boldsymbol{\theta}) = \nabla_{\boldsymbol{\theta}}\psi(\theta) = \left[\frac{2}{\theta^2}\int_0^{\theta} d\theta'\,\theta'\kappa(\theta')\right]\boldsymbol{\theta} = \bar{\kappa}(<\theta)\boldsymbol{\theta}$$

$\boldsymbol{\alpha} \parallel \boldsymbol{\theta}$
$\rightarrow \boldsymbol{\beta} \parallel \boldsymbol{\theta}$

- average convergence $\bar{\kappa}(<\theta)$

$$\bar{\kappa}(<\theta) = \frac{2}{\theta^2}\int_0^{\theta} d\theta'\,\theta'\kappa(\theta')$$

- setting $\beta = |\boldsymbol{\beta}|$, lens equation is one-dimensional

$$\boxed{\beta = \theta - \alpha(\theta) = \left[1 - \bar{\kappa}(<\theta)\right]\theta}$$

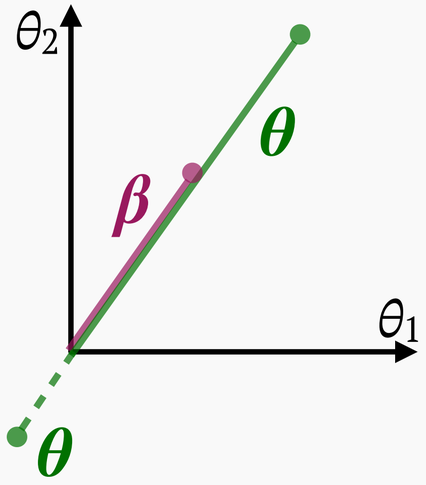

Spherically symmetric lens (IV)

- calculate shear γ_1, γ_2

$$\gamma_1 = \frac{1}{2}\left[\frac{\partial(\bar{\kappa}\theta_1)}{\partial\theta_1} - \frac{\partial(\bar{\kappa}\theta_2)}{\partial\theta_2}\right] = -(\bar{\kappa} - \kappa)\frac{\theta_1^2 - \theta_2^2}{\theta^2}$$

$$\gamma_2 = \frac{\partial(\bar{\kappa}\theta_1)}{\partial\theta_2} = -(\bar{\kappa} - \kappa)\frac{2\theta_1\theta_2}{\theta^2}$$

- for $\bar{\kappa}(<\theta) > \kappa(\theta)$, $|\kappa| \ll 1$, image is distorted along tangential direction around lens center

$$\gamma_+(\theta) = \bar{\kappa}(<\theta) - \kappa(\theta)$$ tangential shear

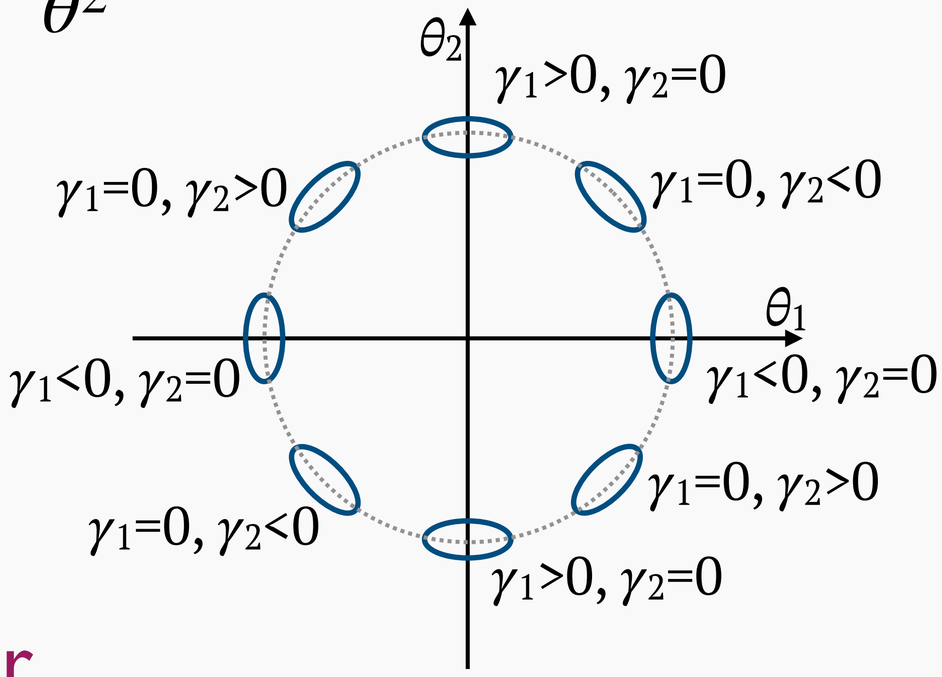

Einstein radius

- when $\beta = 0$ image is circle, obvious from symmetry
- $|\mu| = \infty$, ring for finite source size (Einstein ring)
- from lens equation, radius of ring $\theta_{\rm Ein}$ is

$$\bar{\kappa}(< \theta_{\rm Ein}) = 1$$

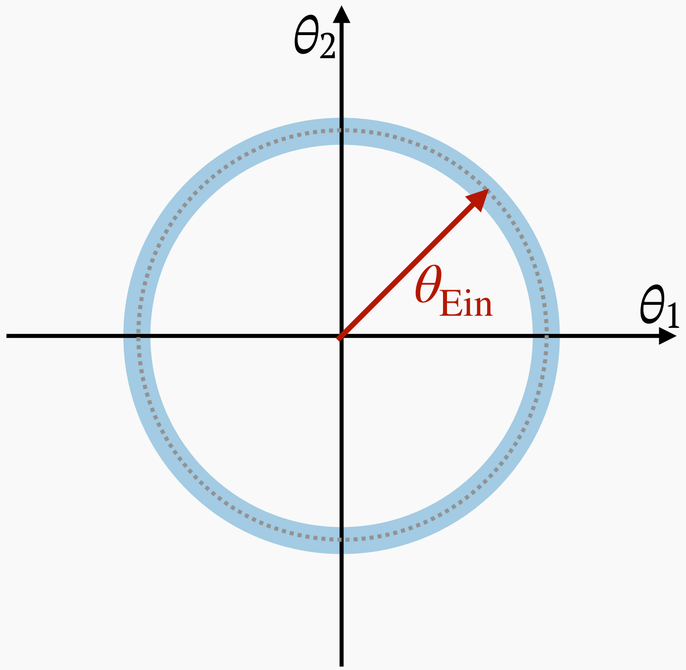

Total mass within Einstein radius

- mass within radius θ in lens plane projected along line-of-sight

$$M(<\theta) = D_{\rm ol}^2 \int_0^\theta d\theta' 2\pi\theta' \Sigma(\theta')$$

- observation of Einstein radius provides

$$M(<\theta_{\rm Ein}) = \pi D_{\rm ol}^2 \theta_{\rm Ein}^2 \Sigma_{\rm cr}$$

general relation that holds for any density profile of lens

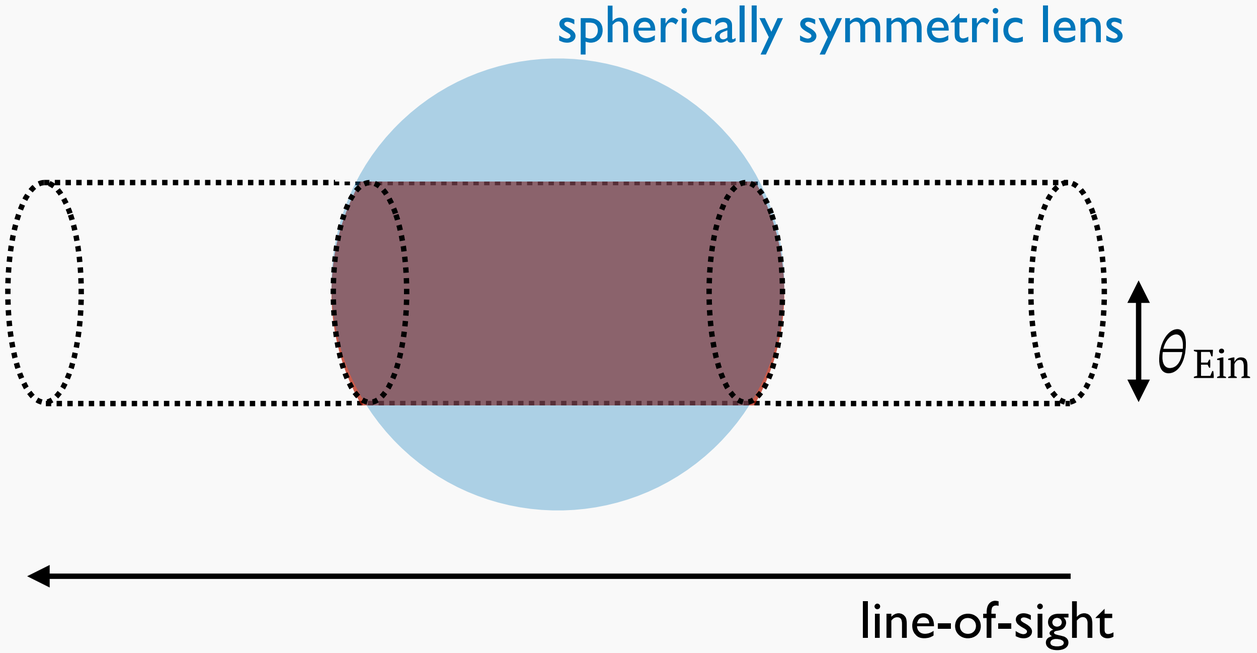

Multiple images for spherically symmetric lens

- one-dimensional lens equation

$$\beta = \theta - \alpha(\theta) = \left[1 - \bar{\kappa}(<\theta)\right]\theta$$

- extend to $\theta < 0$

$$\boldsymbol{\alpha}(-\boldsymbol{\theta}) = -\bar{\kappa}(<\theta)\boldsymbol{\theta} \quad \Rightarrow \quad \alpha(-\theta) = -\alpha(\theta)$$
$$\psi(-\theta) = \psi(\theta)$$

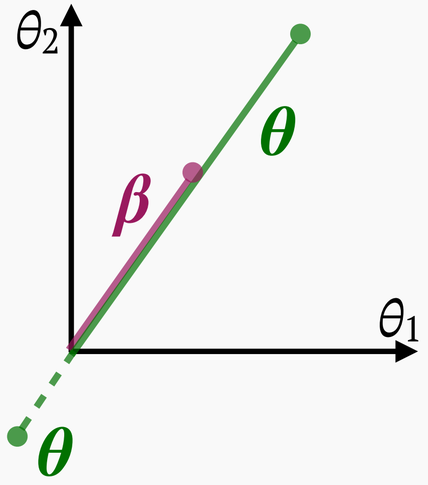

- diagrammatic approach

$$\begin{cases} Y = \theta - \beta \\ Y = \alpha(\theta) \end{cases}$$

their intersections are solutions of lens equation

Diagrammatic approach

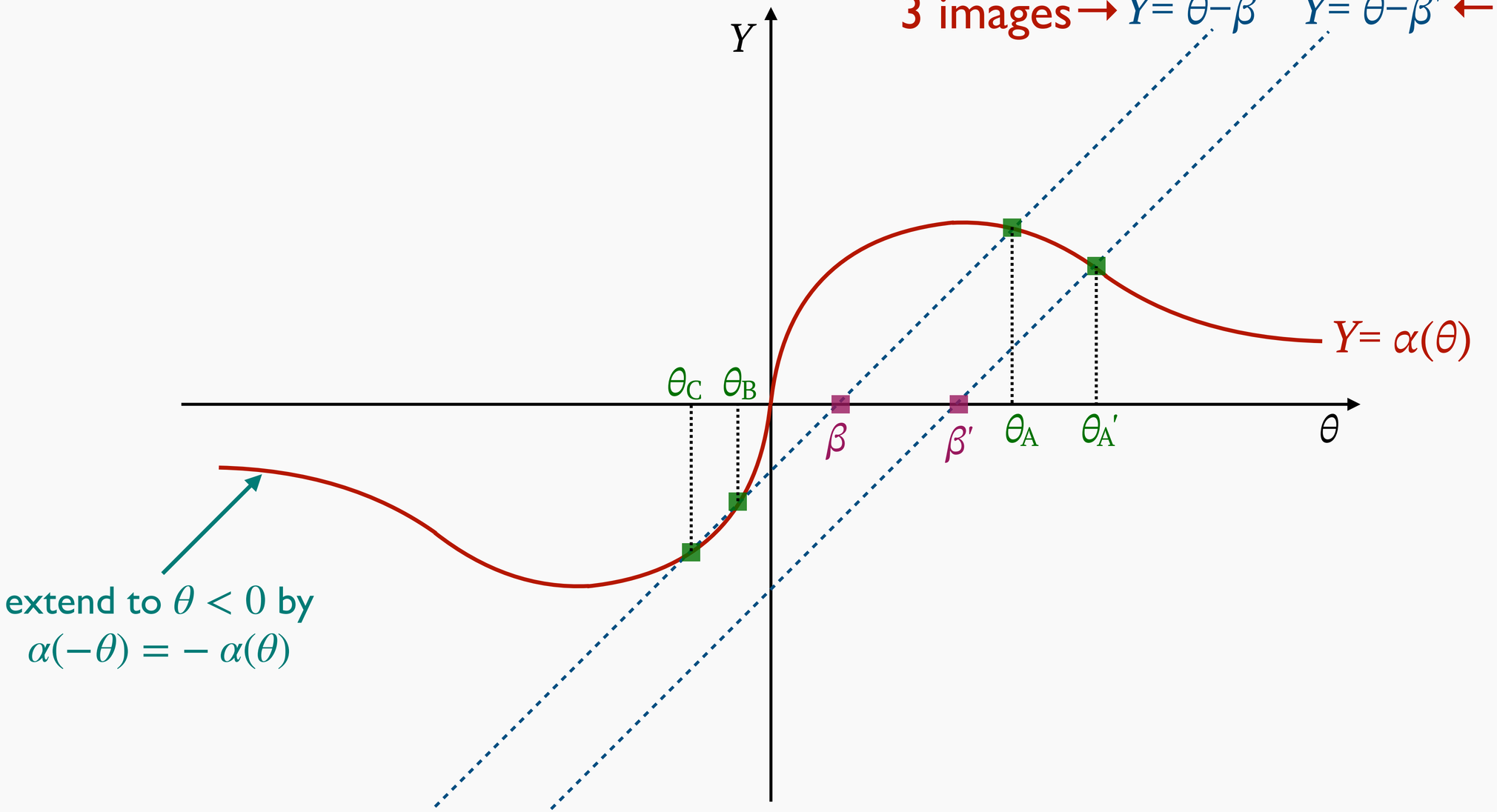

Multiple images for point source

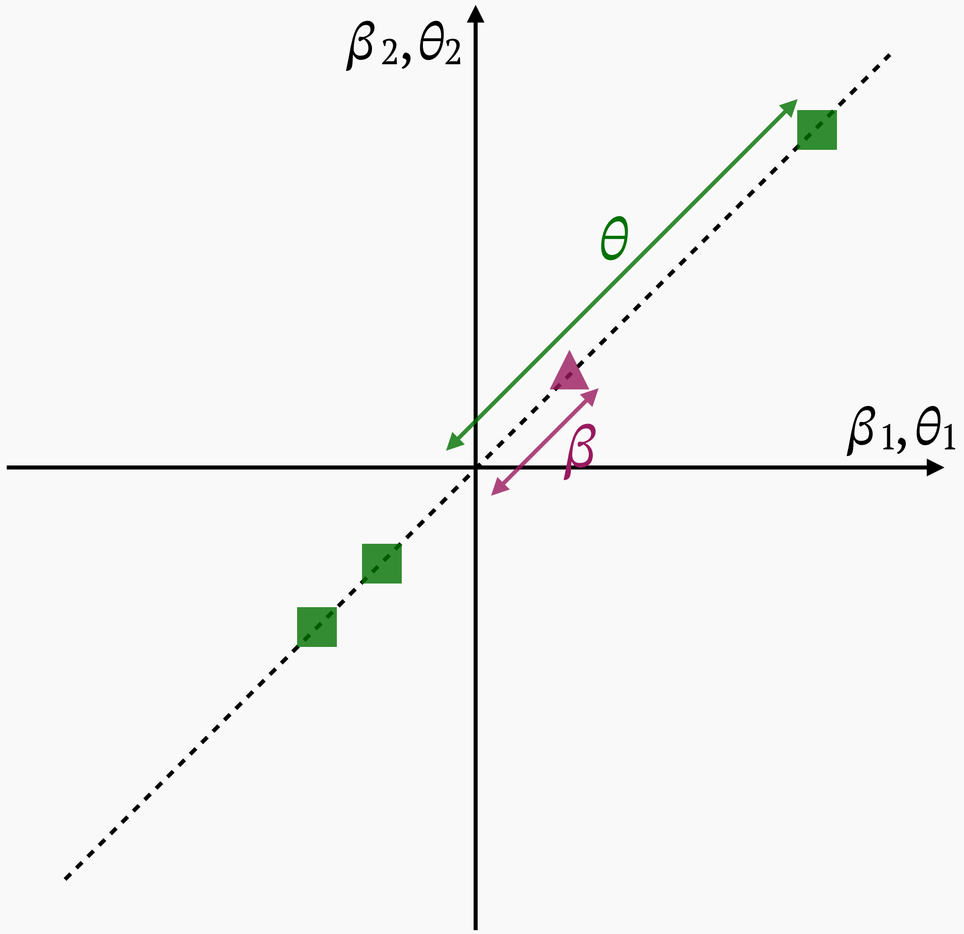

3 images

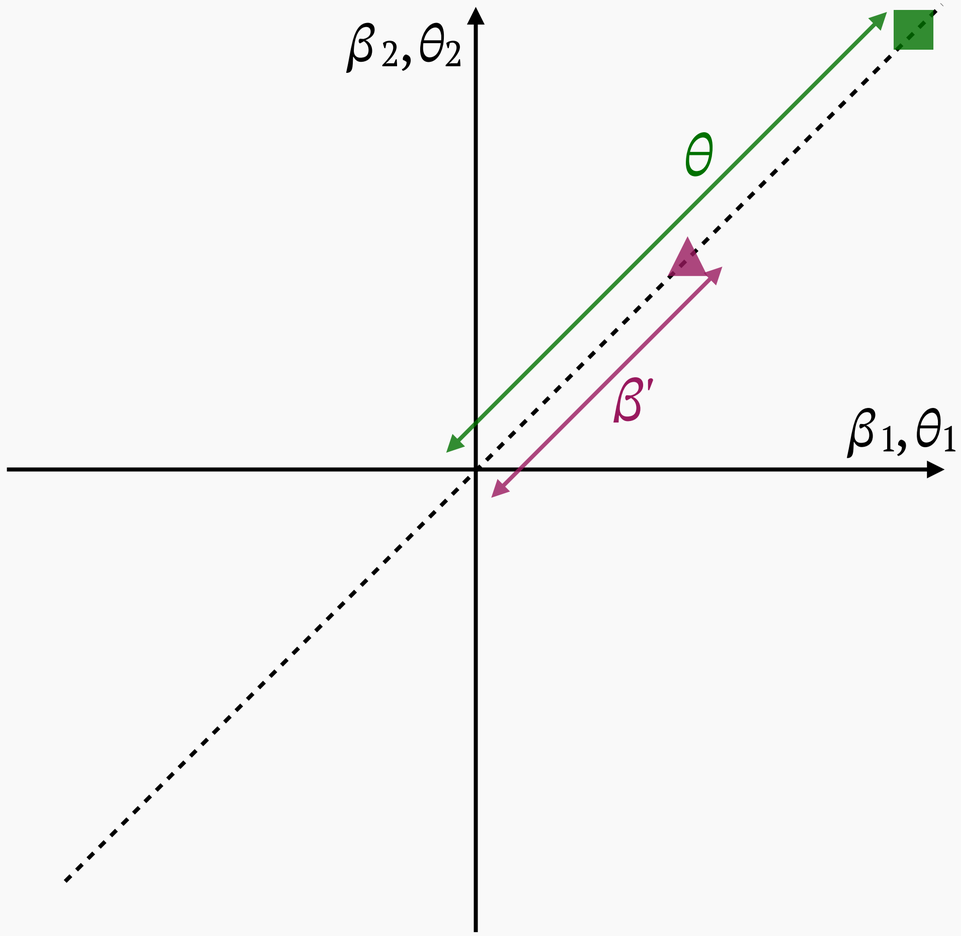

1 image

Multiple images for extended source

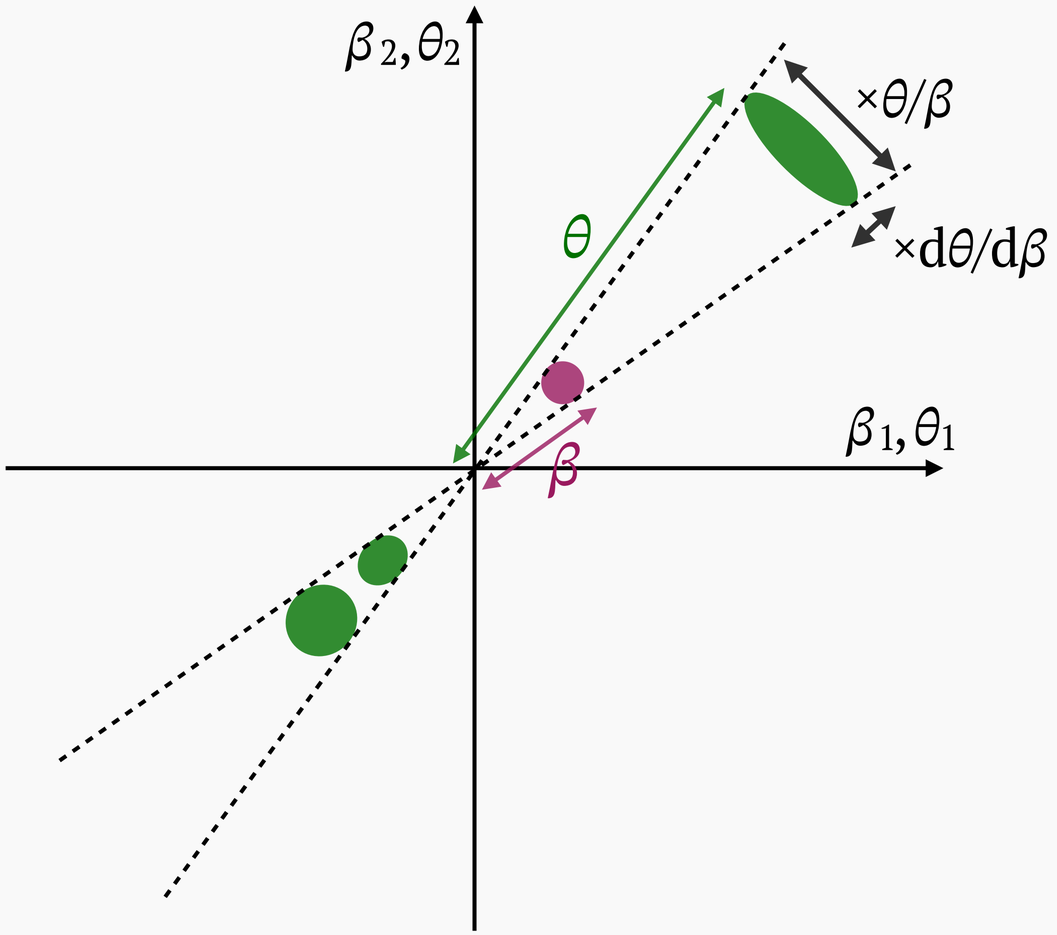

- tangential magnification

$$\mu_t = \frac{\theta}{\beta} = \frac{1}{1-\bar{\kappa}}$$

- radial magnification

$$\mu_r = \frac{d\theta}{d\beta} = \frac{1}{1-2\kappa+\bar{\kappa}}$$

- agree with μ from definition

$$\mu = \mu_t \mu_r = \frac{1}{(1-\bar{\kappa})(1-2\kappa+\bar{\kappa})}$$

Example: point mass lens (I)

- mass model for star and black hole

$$\rho(\boldsymbol{r}) = M\delta^{\mathrm{D}}(\boldsymbol{r})$$

$$\Rightarrow \quad \kappa(\boldsymbol{\theta}) = \frac{4\pi GM}{c^2}\frac{D_{\mathrm{ls}}}{D_{\mathrm{ol}}D_{\mathrm{os}}}\delta^{\mathrm{D}}(\boldsymbol{\theta})$$

$$\Rightarrow \quad \bar{\kappa}(<\theta) = \frac{1}{\pi\theta^2}\int_{|\boldsymbol{\theta}'|<\theta} d\boldsymbol{\theta}'\,\kappa(\boldsymbol{\theta}') = \frac{4GM}{c^2}\frac{D_{\mathrm{ls}}}{D_{\mathrm{ol}}D_{\mathrm{os}}}\frac{1}{\theta^2}$$

- Einstein radius is derived from $\bar{\kappa}(<\theta_{\mathrm{Ein}}) = 1$ as

$$\theta_{\mathrm{Ein}} = \sqrt{\frac{4GM}{c^2}\frac{D_{\mathrm{ls}}}{D_{\mathrm{ol}}D_{\mathrm{os}}}} \quad \Rightarrow \quad \bar{\kappa}(<\theta) = \frac{\theta_{\mathrm{Ein}}^2}{\theta^2}$$

Example: point mass lens (II)

- lens equation

$$\beta = \theta - \frac{\theta_{\rm Ein}^2}{\theta}$$

- lens potential

$$\psi(\theta) = \theta_{\rm Ein}^2 \ln \theta$$

- always 2 images

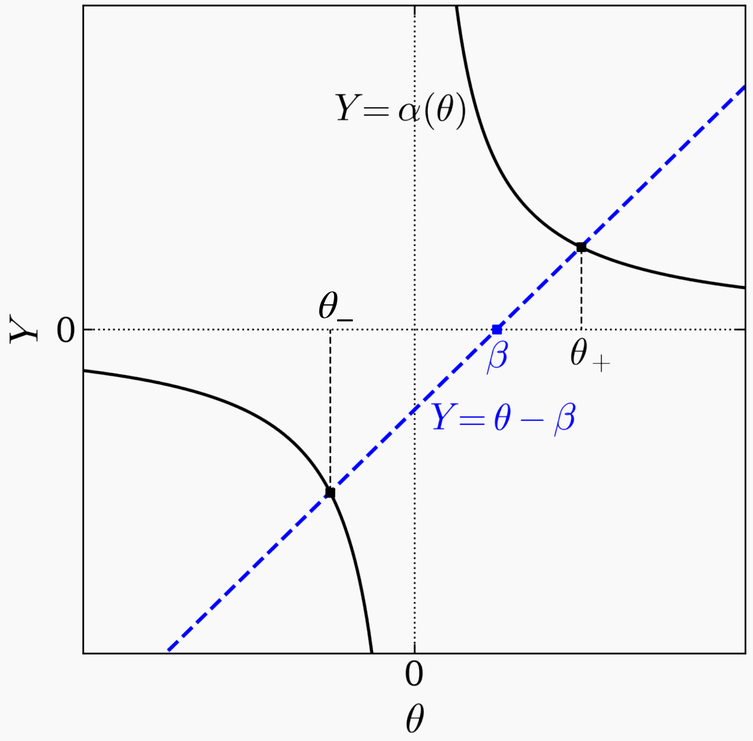

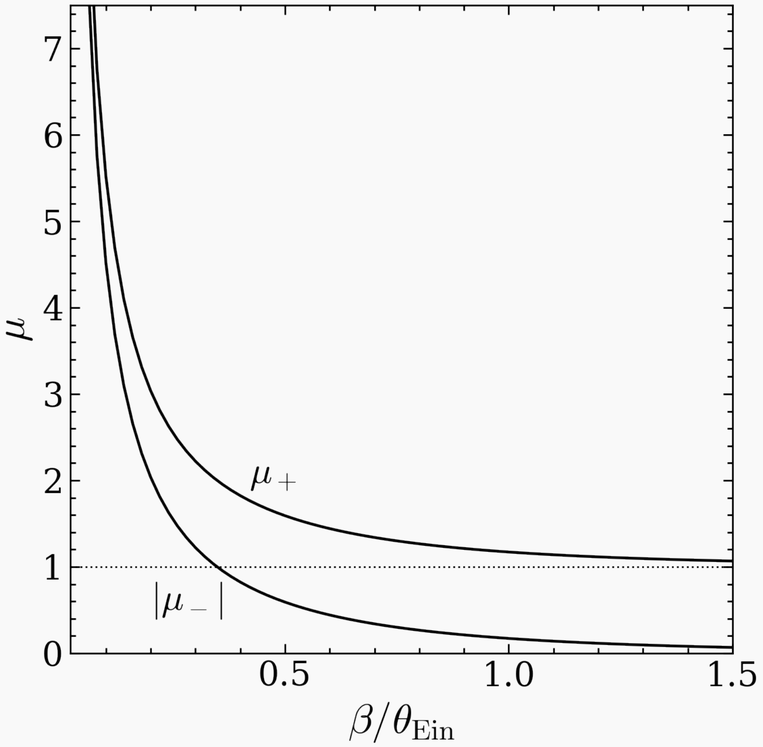

Example: point mass lens (III)

- setting normalized source position as $y = \beta/\theta_{\rm Ein}$

$$\frac{\theta_\pm}{\theta_{\rm Ein}} = \frac{y \pm \sqrt{y^2+4}}{2}$$

$y \to 0 \quad \theta_+ \to \theta_{\rm Ein} \quad \theta_- \to -\theta_{\rm Ein}$

$y \to \infty \quad \theta_+ \to \beta \quad \theta_- \to 0$

$$\mu_\pm = \left[1 - \left(\frac{\theta_{\rm Ein}}{\theta_\pm}\right)^4\right]^{-1} = \frac{1}{2} \pm \frac{y^2+2}{2y\sqrt{y^2+4}}$$

$y \to 0 \quad \mu_+ \to +\infty \quad \mu_- \to -\infty$

$y \to \infty \quad \mu_+ \to 1 \quad \mu_- \to 0$

$$\mu_{\rm tot} = \left|\mu_+\right| + \left|\mu_-\right| = \frac{y^2+2}{y\sqrt{y^2+4}}$$

Example: point mass lens (IV)

- time delay

$$\Delta t(\theta_{\pm};\,\beta) = \frac{1+z_{\rm l}}{c}\frac{D_{\rm ol}D_{\rm os}}{D_{\rm ls}}\theta_{\rm Ein}^2\left(\frac{\theta_{\rm Ein}^2}{2\theta_{\pm}^2} - \ln\left|\theta_{\pm}\right|\right) = \frac{4GM(1+z_{\rm l})}{c^3}\left(\frac{\theta_{\rm Ein}^2}{2\theta_{\pm}^2} - \ln\left|\theta_{\pm}\right|\right)$$

~Schwarzschild radius / c

- observable time delay

$$\Delta t(\theta_{-};\,\beta) - \Delta t(\theta_{+};\,\beta) = \frac{4GM(1+z_{\rm l})}{c^3}\left[\frac{y\sqrt{y^2+4}}{2} + \ln\left(\frac{\sqrt{y^2+4}+y}{\sqrt{y^2+4}-y}\right)\right]$$

arrive θ_+ first, then θ_-

increasing function of y

Example: point mass lens (V)

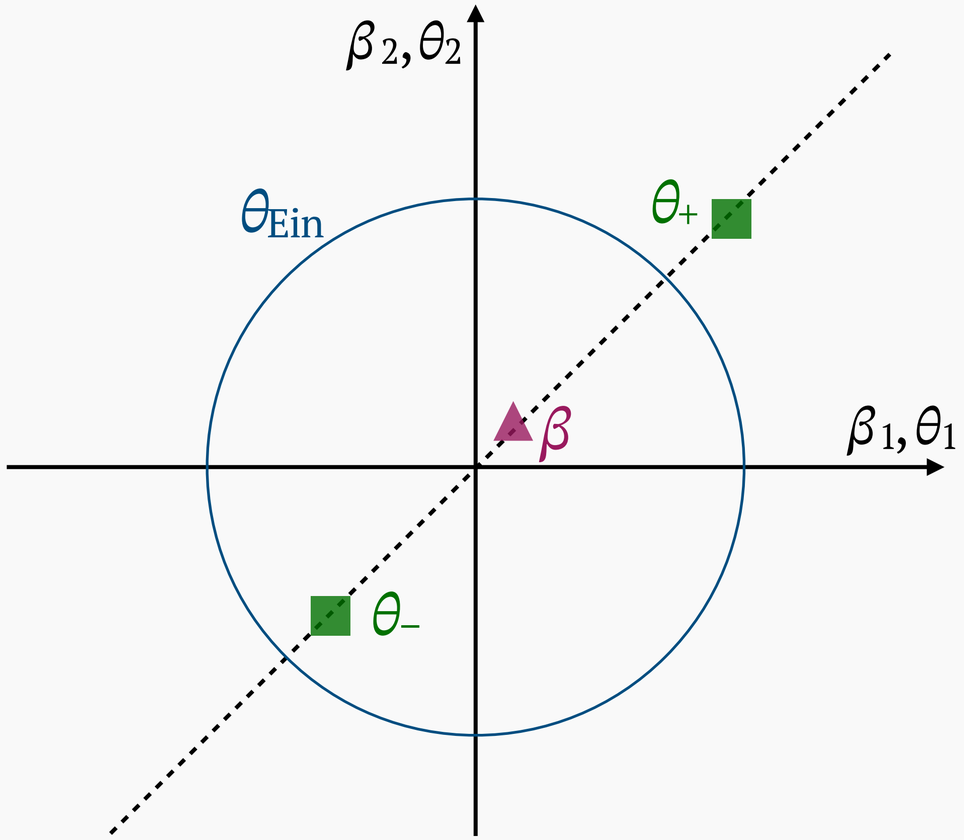

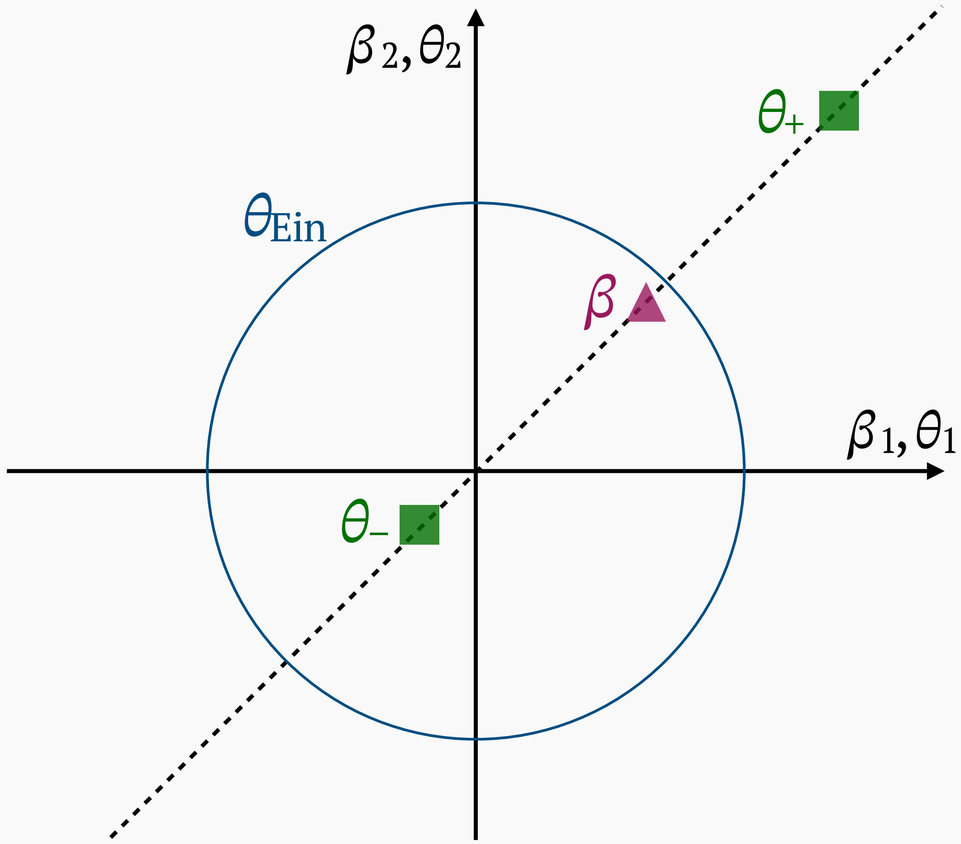

$y = \beta/\theta_{\rm Ein}$ small $\rightarrow \Delta t$ small, $\mu_+ \simeq |\mu_-| \gg 1$

$y = \beta/\theta_{\rm Ein}$ large $\rightarrow \Delta t$ large, $\mu_+ \simeq 1, |\mu_-| \ll 1$

similar qualitative behavior in other lens models

Example: singular isothermal sphere (I)

(SIS)

- mass model for galaxy (and cluster)

$$\rho(r) = \frac{\sigma^2}{2\pi G r^2}$$

σ : velocity dispersion

$$\kappa(\theta) = \frac{2\sigma^2}{c^2}\frac{D_{\rm ol}D_{\rm ls}}{D_{\rm os}}\int_{-\infty}^{\infty} dZ \frac{1}{Z^2 + D_{\rm ol}^2\theta^2} = \frac{2\pi\sigma^2}{c^2}\frac{D_{\rm ls}}{D_{\rm os}}\frac{1}{\theta} = \frac{\theta_{\rm Ein}}{2\theta}$$

$$\bar{\kappa}(<\theta) = \frac{4\pi\sigma^2}{c^2}\frac{D_{\rm ls}}{D_{\rm os}}\frac{1}{\theta} = \frac{\theta_{\rm Ein}}{\theta}$$

$$\theta_{\rm Ein} = \frac{4\pi\sigma^2}{c^2}\frac{D_{\rm ls}}{D_{\rm os}}$$

Example: singular isothermal sphere (II)

(SIS)

- lens potential, deflection angle

$$\psi(\theta) = \theta_{\rm Ein}\theta$$

$$\alpha(\theta) = \theta_{\rm Ein}$$

- extend to $\theta < 0$

$$\beta = \theta - \theta_{\rm Ein}\frac{\theta}{|\theta|}$$

- 2 images for $\beta < \theta_{\rm Ein}$,
  1 image for $\beta > \theta_{\rm Ein}$

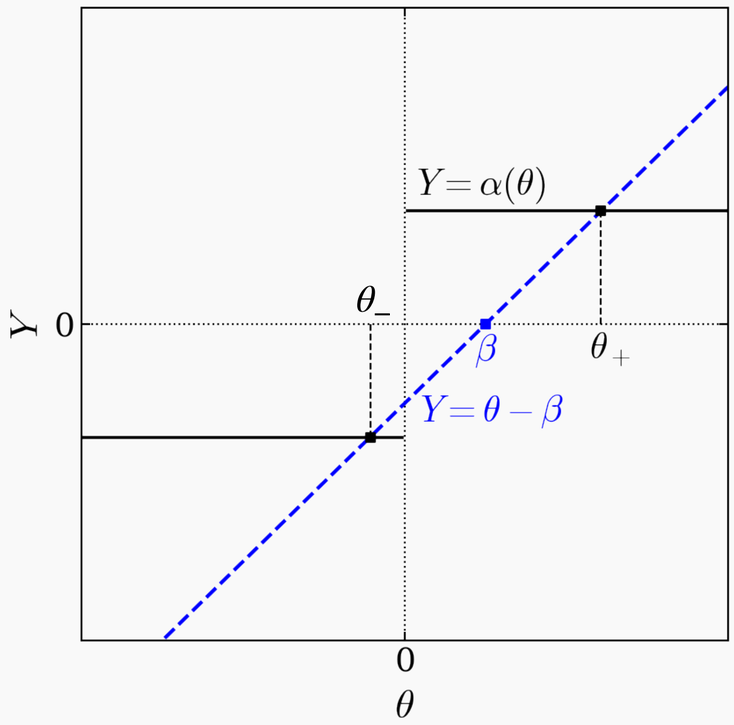

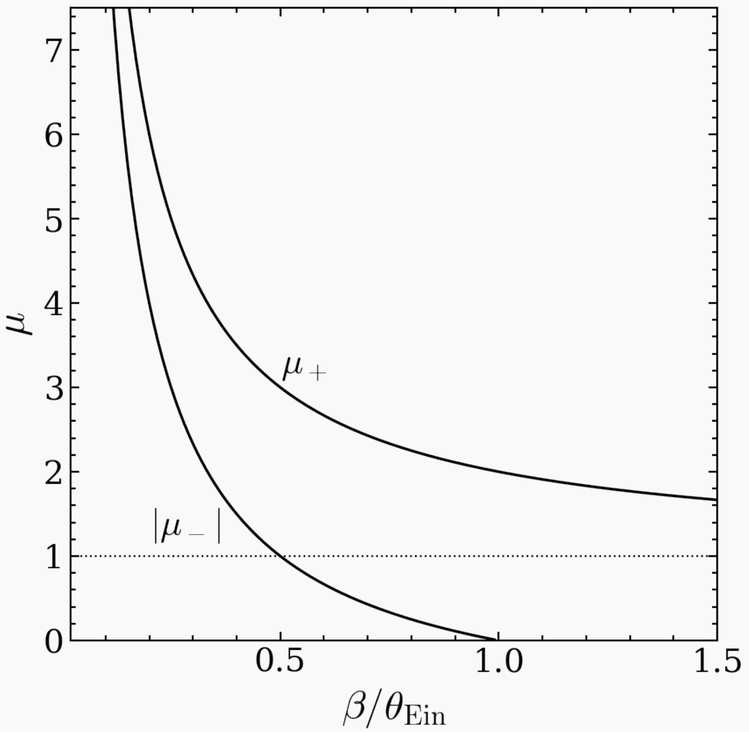

Example: singular isothermal sphere (III)

(SIS)

- setting normalized source position as $y = \beta/\theta_{\mathrm{Ein}}$

$$\frac{\theta_{\pm}}{\theta_{\mathrm{Ein}}} = y \pm 1$$

$y \to 0 \quad \theta_{+} \to \theta_{\mathrm{Ein}} \quad \theta_{-} \to -\theta_{\mathrm{Ein}}$

$y \to 1 \quad \theta_{+} \to 2\theta_{\mathrm{Ein}} \quad \theta_{-} \to 0$

$$\mu_{\pm} = \left(1 - \frac{\theta_{\mathrm{Ein}}}{|\theta_{\pm}|}\right)^{-1} = 1 \pm \frac{1}{y}$$

$y \to 0 \quad \mu_{+} \to +\infty \quad \mu_{-} \to -\infty$

$y \to 1 \quad \mu_{+} \to 2 \quad \mu_{-} \to 0$

$$\mu_{\mathrm{tot}} = |\mu_{+}| + |\mu_{-}| = \frac{2}{y}$$

- $\theta_{+} - \theta_{-} = 2\theta_{\mathrm{Ein}} \rightarrow$ measure θ_{Ein} from multiple image positions

Example: singular isothermal sphere (IV)

(SIS)

- time delay

$$\Delta t(\theta_{\pm};\,\beta) = \frac{1+z_{\rm l}}{c}\frac{D_{\rm ol}D_{\rm os}}{D_{\rm ls}}\theta_{\rm Ein}^2\left(\frac{1}{2}-\frac{|\theta_{\pm}|}{\theta_{\rm Ein}}\right)$$

- observable time delay

$$\Delta t(\theta_{-};\,\beta) - \Delta t(\theta_{+};\,\beta) = 2\frac{1+z_{\rm l}}{c}\frac{D_{\rm ol}D_{\rm os}}{D_{\rm ls}}\theta_{\rm Ein}^2 y = 2\frac{1+z_{\rm l}}{c}\frac{D_{\rm ol}D_{\rm ls}}{D_{\rm os}}\left(\frac{4\pi\sigma^2}{c^2}\right)^2 y$$

arrive θ_+ first, then θ_-

increasing function of y

$$= \frac{1+z_{\rm l}}{c}\frac{D_{\rm ol}D_{\rm os}}{D_{\rm ls}}\frac{\theta_+^2-\theta_-^2}{2}$$

expression with $\theta_{\pm}$

Example: cored isothermal sphere (I)

- mass model removing central singularity of SIS

$$\rho(r) = \frac{\sigma^2}{2\pi G}\frac{1}{r^2 + r_{\rm c}^2}$$

σ : velocity dispersion

$$\theta_0 = \frac{4\pi\sigma^2}{c^2}\frac{D_{\rm ls}}{D_{\rm os}} \qquad \theta_{\rm c} = \frac{r_{\rm c}}{D_{\rm ol}}$$

$$\kappa(\theta) = \frac{2\sigma^2}{c^2}\frac{D_{\rm ol}D_{\rm ls}}{D_{\rm os}}\int_{-\infty}^{\infty} dZ \frac{1}{Z^2 + D_{\rm ol}^2(\theta^2 + \theta_{\rm c}^2)} = \frac{\theta_0}{2\sqrt{\theta^2 + \theta_{\rm c}^2}}$$

$$\bar{\kappa}(<\theta) = \frac{\theta_0}{\theta^2}\left(\sqrt{\theta^2 + \theta_{\rm c}^2} - \theta_{\rm c}\right)$$

$$\psi(\theta) = \theta_0\left[\sqrt{\theta^2 + \theta_{\rm c}^2} - \theta_{\rm c}\ln\left(\theta_{\rm c} + \sqrt{\theta^2 + \theta_{\rm c}^2}\right)\right]$$

Example: cored isothermal sphere (II)

- lens equation

$$\beta = \theta - \frac{\theta_0}{\theta}\left(\sqrt{\theta^2 + \theta_c^2} - \theta_c\right)$$

- 3 or 1 multiple images

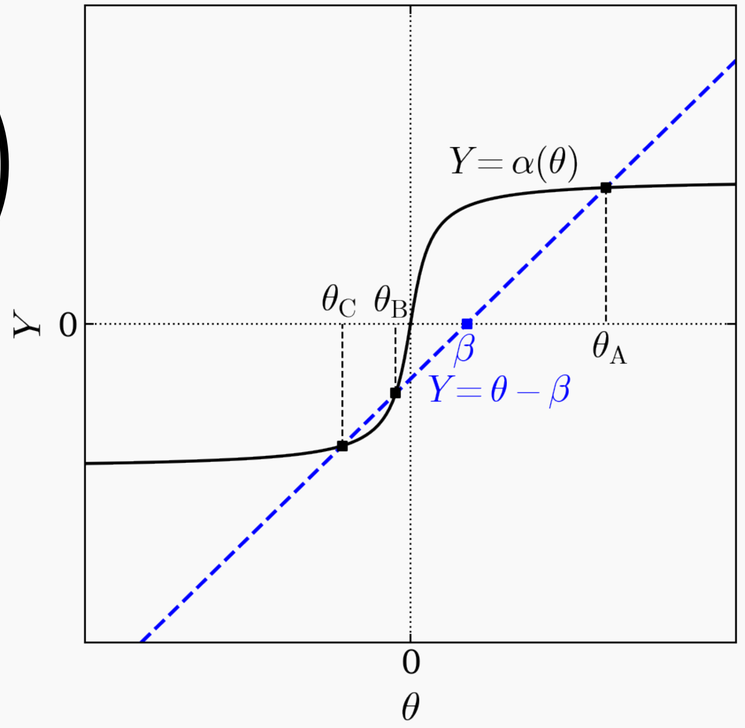

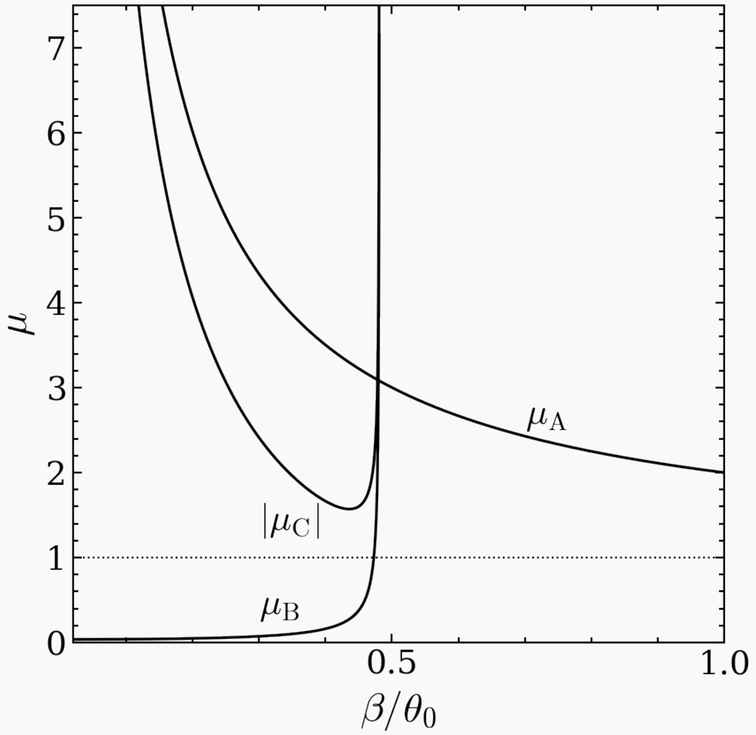

Example: NFW profile (I)

- mass model of dark matter halo

$$\rho(r) = \frac{\rho_{\rm s}}{(r/r_{\rm s})(1 + r/r_{\rm s})^2}$$

- deflection angle etc. can be computed analytically

Bartelmann A&A **313**(1996)697, Wright & Brainerd ApJ **534**(2000)34

Example: NFW profile (II)

- 3 or 1 multiple images, magnification relatively high

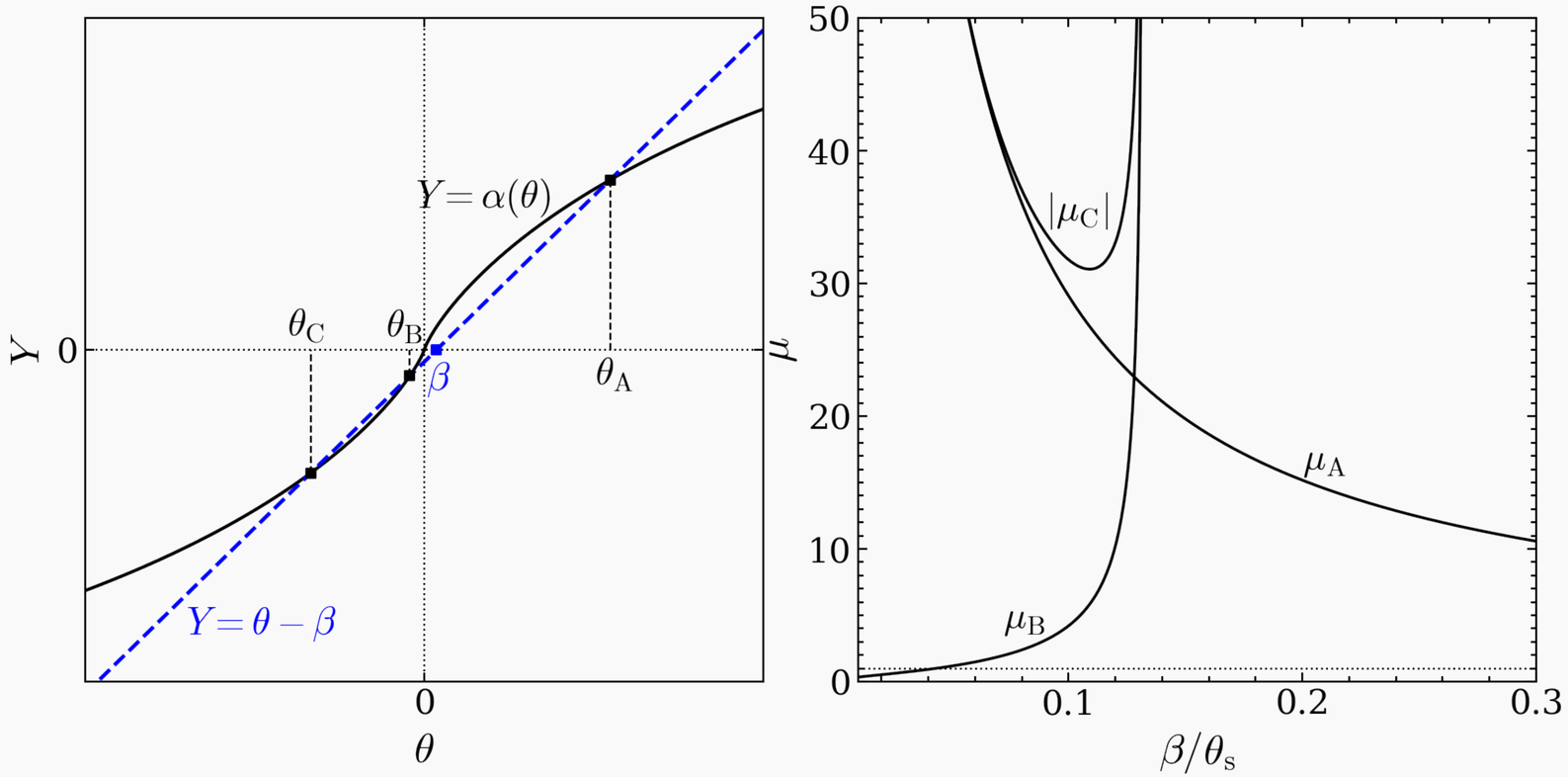

Example: power-law lens (I)

- useful for investigating radial profile dependence

$$\rho(r) \propto r^{-\eta}$$

$$\Rightarrow \bar{\kappa}(<\theta) = \left(\frac{\theta}{\theta_{\rm Ein}}\right)^{1-\eta}$$

$$\Rightarrow \alpha(\theta) = \theta_{\rm Ein}\left(\frac{\theta}{\theta_{\rm Ein}}\right)^{2-\eta}$$

$$\Rightarrow \kappa(\theta) = \frac{3-\eta}{2}\left(\frac{\theta}{\theta_{\rm Ein}}\right)^{1-\eta}$$

$$\Rightarrow \psi(\theta) = \frac{\theta_{\rm Ein}^2}{3-\eta}\left(\frac{\theta}{\theta_{\rm Ein}}\right)^{3-\eta}$$

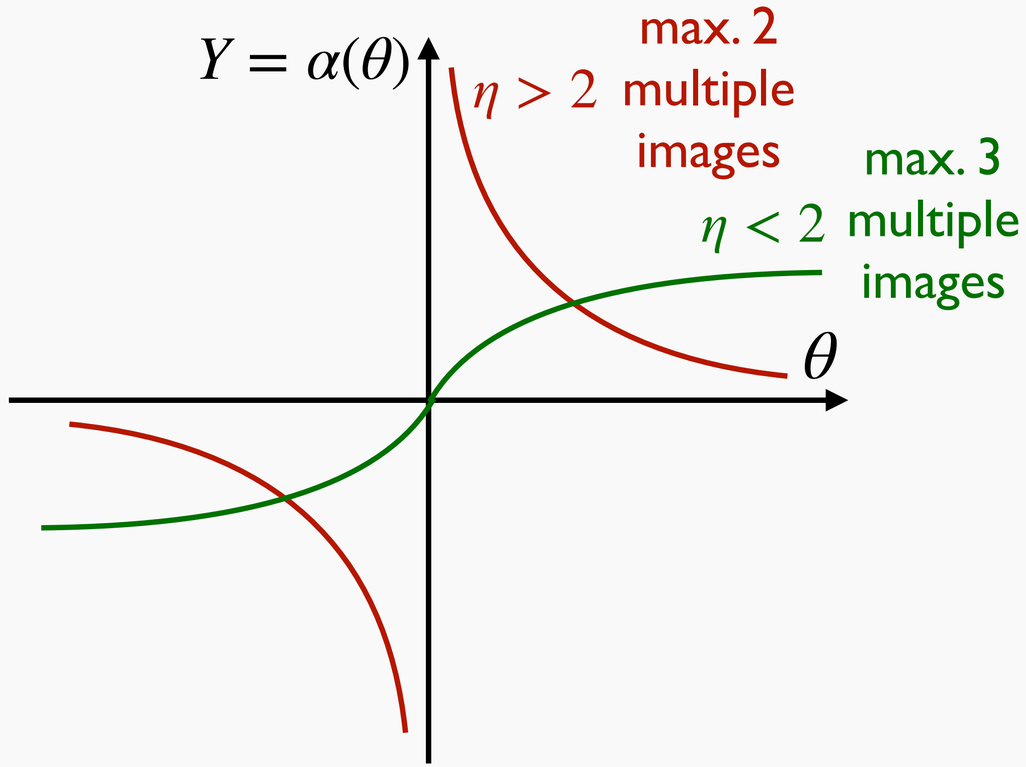

Example: power-law lens (II)

- radial magnification at Einstein radius

$$\mu_{\mathrm{r}}(\theta_{\mathrm{Ein}}) = \frac{1}{2\left[1-\kappa(\theta_{\mathrm{Ein}})\right]} = \frac{1}{\eta - 1}$$

- μ_{r} large for small η (shallow radial profile)

  ➡ relatively large magnification of NFW profile

External perturbation

- one of causes of non-sphericity
- perturbation by external object with lens potential ψ_{X}

$$\psi_{\mathrm{ext}}(\boldsymbol{\theta}) = \psi_{\mathrm{X}}(\boldsymbol{\theta} - \boldsymbol{\theta}_0)$$

external perturbation to lens

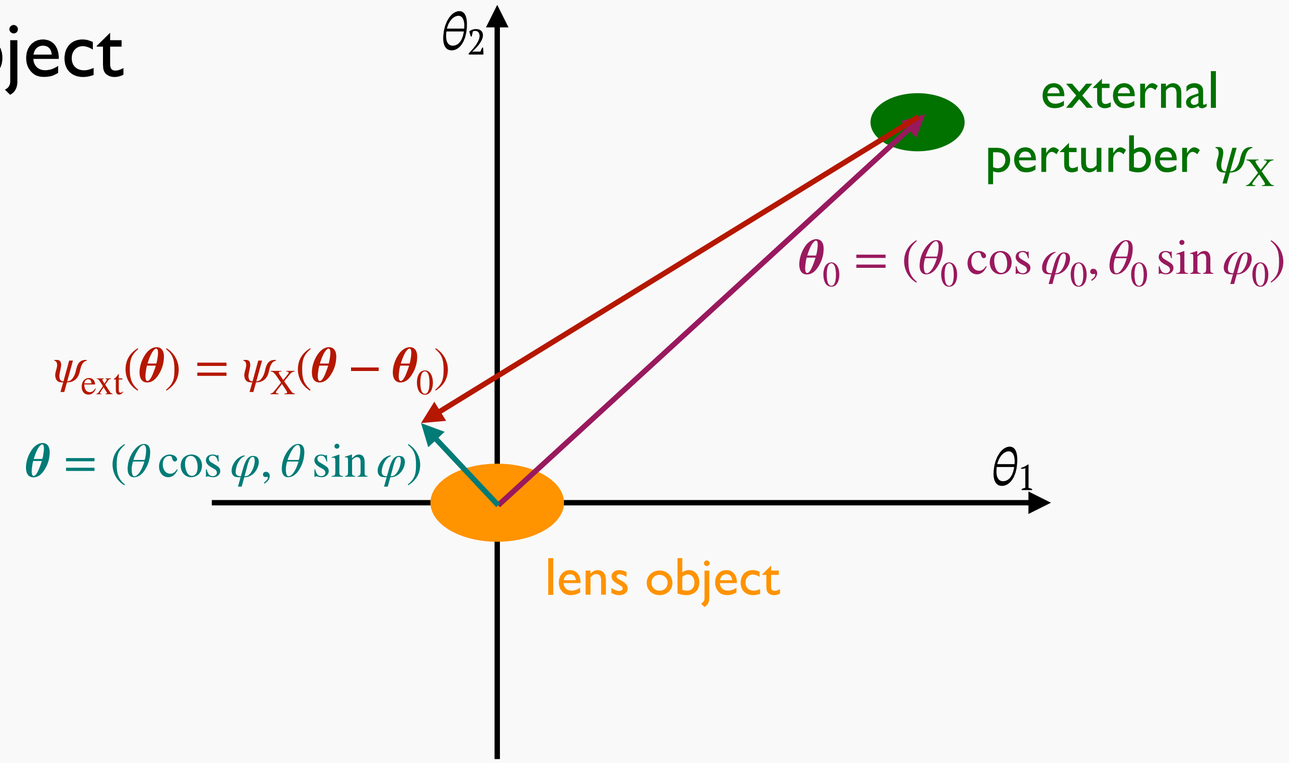

External convergence and shear

- Taylor expand

$$\psi_{\rm ext}(\boldsymbol{\theta}) = \psi_{\rm X}(-\boldsymbol{\theta}_0) + \boldsymbol{\theta}\cdot\left.\frac{\partial\psi_{\rm X}}{\partial\boldsymbol{\theta}}\right|_{-\boldsymbol{\theta}_0} + \frac{1}{2}\boldsymbol{\theta}\cdot H\left(\psi_{\rm X}(-\boldsymbol{\theta}_0)\right)\boldsymbol{\theta} + \cdots$$

constant → ignored

constant deflection → degenerate with $\boldsymbol{\beta}$

lower order term that is meaningful

$$\kappa_{\rm X}(-\boldsymbol{\theta}_0) = \kappa_{\rm ext}$$
$$\gamma_{\rm X1}(-\boldsymbol{\theta}_0) = -\gamma_{\rm ext}\cos 2\varphi_0$$
$$\gamma_{\rm X2}(-\boldsymbol{\theta}_0) = -\gamma_{\rm ext}\sin 2\varphi_0$$

$$\Rightarrow\quad \psi_{\rm ext}(\boldsymbol{\theta}) \simeq \frac{\theta^2}{2}\left[\kappa_{\rm ext} - \gamma_{\rm ext}\cos 2(\varphi-\varphi_0)\right]$$

external convergence

external shear

Example: SIS plus external shear (I)

- $\varphi_0 = \pi/2$ without loss of generality

$$\psi(\boldsymbol{\theta}) = \theta_{\mathrm{Ein}}\theta + \frac{\gamma_{\mathrm{ext}}}{2}\theta^2 \cos 2\varphi = \theta_{\mathrm{Ein}}\sqrt{\theta_1^2 + \theta_2^2} + \frac{\gamma_{\mathrm{ext}}}{2}\left(\theta_1^2 - \theta_2^2\right)$$

- lens equation

$$\beta_1 = \left[\left(1 - \gamma_{\mathrm{ext}}\right)\theta - \theta_{\mathrm{Ein}}\right]\cos\varphi = \left(1 - \gamma_{\mathrm{ext}}\right)\theta_1 - \frac{\theta_{\mathrm{Ein}}\theta_1}{\sqrt{\theta_1^2 + \theta_2^2}}$$

$$\beta_2 = \left[\left(1 + \gamma_{\mathrm{ext}}\right)\theta - \theta_{\mathrm{Ein}}\right]\sin\varphi = \left(1 + \gamma_{\mathrm{ext}}\right)\theta_2 - \frac{\theta_{\mathrm{Ein}}\theta_2}{\sqrt{\theta_1^2 + \theta_2^2}}$$

Example: SIS plus external shear (II)

- calculate inverse magnification

$$\mu^{-1} = 1 - \gamma_{\rm ext}^2 - \frac{\theta_{\rm Ein}}{\theta}\left(1 - \gamma_{\rm ext}\cos 2\varphi\right)$$

- critical curve in parametric representation

$$\theta(\varphi) = \frac{1 - \gamma_{\rm ext}\cos 2\varphi}{1 - \gamma_{\rm ext}^2}\theta_{\rm Ein}$$

caustic

$$\beta_1(\varphi) = -\frac{2\gamma_{\rm ext}}{1 + \gamma_{\rm ext}}\theta_{\rm Ein}\cos^3\varphi$$

$$\beta_2(\varphi) = \frac{2\gamma_{\rm ext}}{1 - \gamma_{\rm ext}}\theta_{\rm Ein}\sin^3\varphi$$

astroid

movie file: https://oguri.github.io/for_presen.html

Example: SIS plus external shear (III)

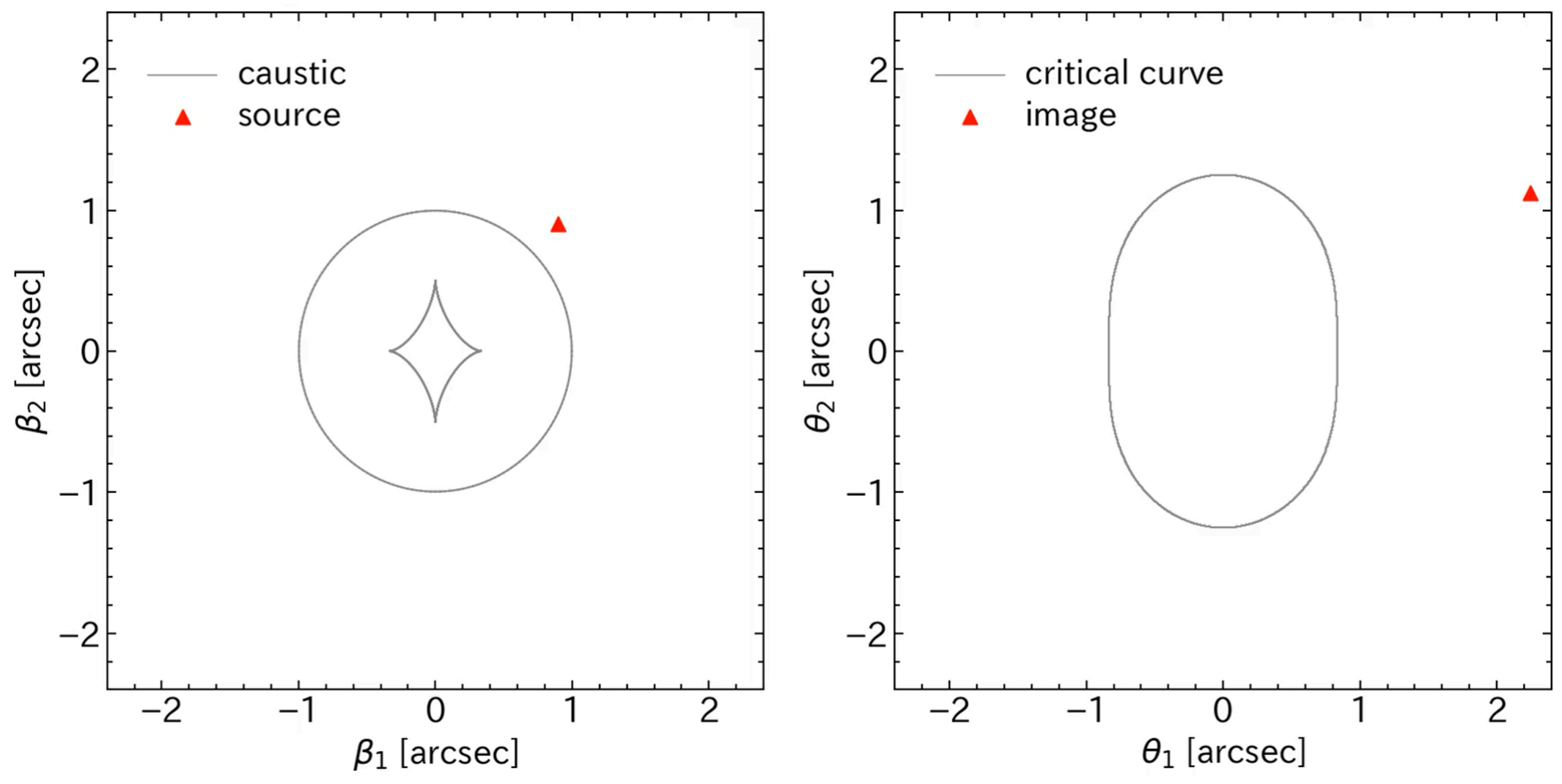

Mass-sheet degeneracy

- consider effect of external convergence

$$\psi_{\rm ext}(\boldsymbol{\theta}) \simeq \frac{\theta^2}{2}\left[\kappa_{\rm ext} - \gamma_{\rm ext}\cos 2(\varphi - \varphi_0)\right]$$

- lens equation with external convergence

$$\boldsymbol{\beta} = \boldsymbol{\theta} - \boldsymbol{\alpha}(\boldsymbol{\theta}) - \kappa_{\rm ext}\boldsymbol{\theta}$$

$$(1-\kappa_{\rm ext})^{-1}\boldsymbol{\beta} = \boldsymbol{\theta} - (1-\kappa_{\rm ext})^{-1}\boldsymbol{\alpha}(\boldsymbol{\theta})$$

transform unobservable image position

transform unobservable deflection angle

image position θ unchanged

Mass-sheet transform

- observed image positions unchanged by following transform

$$\psi(\boldsymbol{\theta}) \rightarrow (1-\kappa_{\rm ext})\psi(\boldsymbol{\theta}) + \kappa_{\rm ext}\frac{\left|\boldsymbol{\theta}\right|^2}{2}$$

$$\boldsymbol{\beta} \rightarrow (1-\kappa_{\rm ext})\boldsymbol{\beta}$$

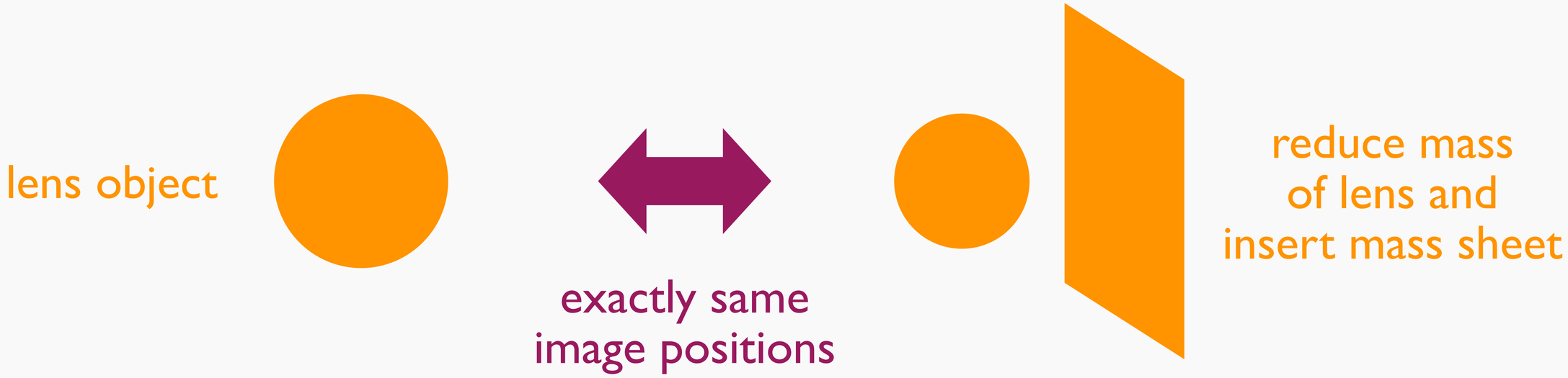

Magnification and time delay

- magnification changed by mass-sheet transform, ratio not changed

$$\mu \rightarrow (1-\kappa_{\rm ext})^{-2}\mu \quad \Rightarrow \quad \frac{\mu_i}{\mu_j} \rightarrow \frac{\mu_i}{\mu_j}$$

usually cannot be observed

observable from flux ratio of multiple images

- time delay changed by facto fo $(1-\kappa_{\rm ext})$

$$\frac{\left|\boldsymbol{\theta}-\boldsymbol{\beta}\right|^2}{2}-\psi(\boldsymbol{\theta}) \rightarrow (1-\kappa_{\rm ext})\left[\frac{\left|\boldsymbol{\theta}-\boldsymbol{\beta}\right|^2}{2}-\psi(\boldsymbol{\theta})\right] - \kappa_{\rm ext}(1-\kappa_{\rm ext})\frac{\left|\boldsymbol{\beta}\right|^2}{2}$$

not contribute to observable time delay

⇒ systematic error in H_0 measurement

Elliptical mass density distribution

- about convergence of spherically symmetric lens $\kappa(\theta)$

$$\theta \rightarrow v = \sqrt{\frac{\theta_1^2}{(1-e)} + (1-e)\theta_2^2}$$

- lensing properties analytically computed only for some lens models, for other models numerical integrations needed

Summary

- in the case of spherically symmetric lens, lens equation reduces to one dimensional equation
- number of images and configuration easily understood with diagrammatic approach
- number of images and their configuration becomes complicated for non-spherically symmetric lens

5. Strong lensing

Strong lensing analysis

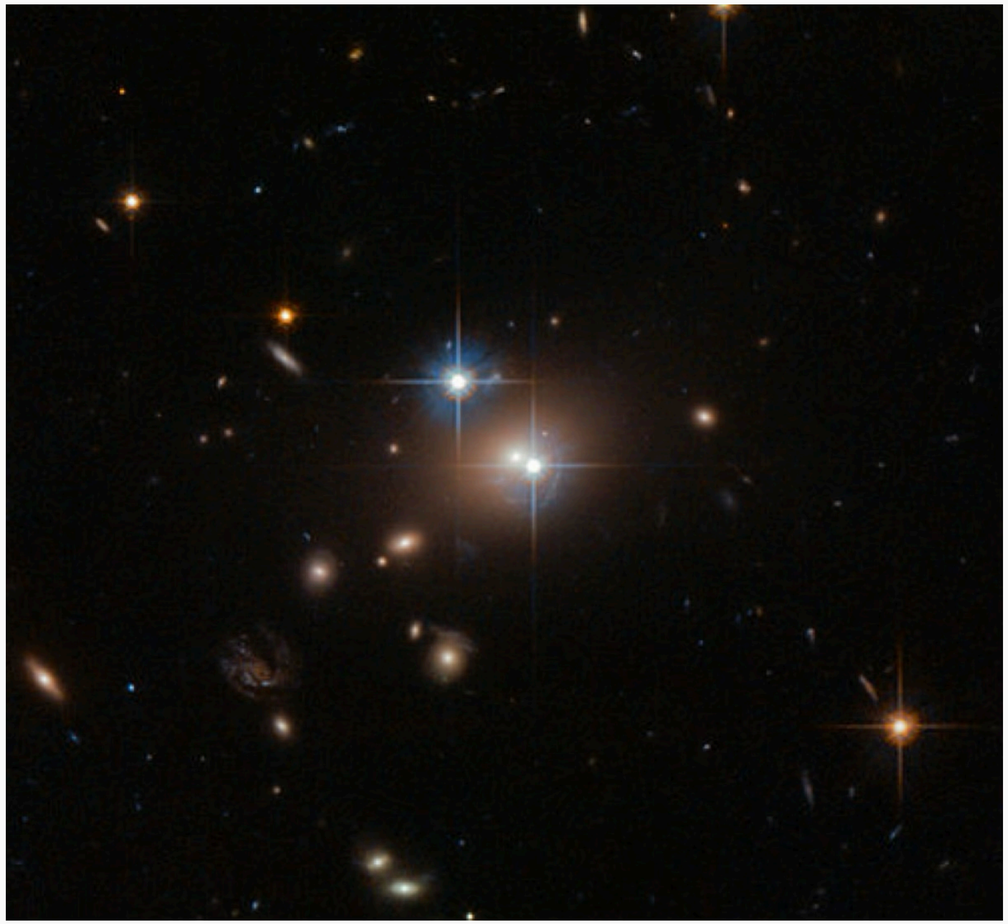

Hubble/ESA/NASA

NASA/ESA/CSA/STScI

- observables: multiple image positions, flux ratios, multiple image shapes (galaxies), time delays (quasar, supernovae, etc.)

Strong lensing analysis

- multiple image positions

  common source position β $\rightarrow$ $\underline{\boldsymbol{\theta}_j - \boldsymbol{\alpha}(\boldsymbol{\theta}_j) = \boldsymbol{\theta}_k - \boldsymbol{\alpha}(\boldsymbol{\theta}_k)}$

  constraint on mass distribution

- parameters determined by minimizing chi-square

number of sources N_i, number of multiple images for each source i N_{ij}

$$\chi^2_{\rm pos} = \sum_{i=1}^{N_i} \sum_{j=1}^{N_{ij}} \frac{\left| \boldsymbol{\theta}_{ij}^{\rm obs} - \boldsymbol{\theta}_{ij}(\boldsymbol{\beta}_i; \boldsymbol{p}_{\rm model}) \right|^2}{\sigma_{ij}^2}$$

σ_{ij}: error of image position

Evaluating chi-square in source plane

- need to solve lens equation in evaluating chi-square

$$\chi^2_{\rm pos} = \sum_{i=1}^{N_i} \sum_{j=1}^{N_{ij}} \frac{\left| \boldsymbol{\theta}_{ij}^{\rm obs} - \boldsymbol{\theta}_{ij}(\boldsymbol{\beta}_i; \boldsymbol{p}_{\rm model}) \right|^2}{\sigma_{ij}^2}$$

lens equation
→ multiple image position for source i

- avoid solving lens equation using approximation

$$\chi^2_{\rm pos} \simeq \sum_{i=1}^{N_i} \sum_{j=1}^{N_{ij}} \frac{\left| \left[A(\boldsymbol{\theta}_{ij}^{\rm obs}; \boldsymbol{p}_{\rm model}) \right]^{-1} \left[\boldsymbol{\beta}_{ij}^{\rm obs}(\boldsymbol{p}_{\rm model}) - \boldsymbol{\beta}_i \right] \right|^2}{\sigma_{ij}^2}$$

fast evaluation possible

Flux ratio and time delay

- flux ratio

$$\chi^2_{\rm flux} = \sum_{i=1}^{N_i} \sum_{j=1}^{N_{ij}} \frac{\left[f_{ij}^{\rm obs} - \left| \mu_{ij}(\boldsymbol{\beta}_i; \boldsymbol{p}_{\rm model}) \right| f_{{\rm src},i} \right]^2}{\sigma^2_{f,ij}}$$

- time delay

$$\chi^2_{\rm td} = \sum_{i=1}^{N_i} \sum_{j=1}^{N_{ij}} \frac{\left[\Delta t_{ij}^{\rm obs} - \Delta t_{ij}(\boldsymbol{\beta}_i; \boldsymbol{p}_{\rm model}) - \Delta t_i \right]^2}{\sigma^2_{\Delta t,ij}}$$

Example: quasar lensing

- quadruple quasar lens WFI2033−4723
  z_s=1.662, z_l=0.661, maximum image separation 2.53 arcsec

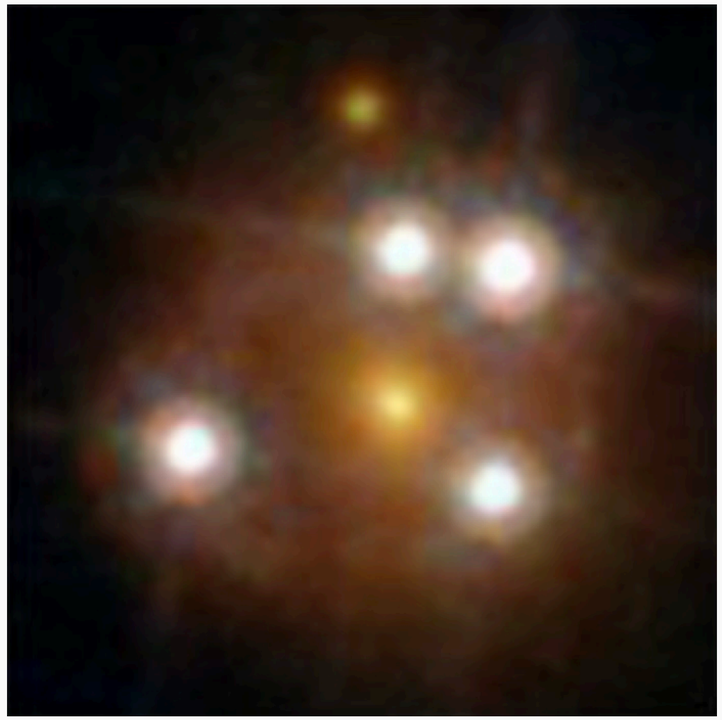

Suyu+ MNRAS **468**(2017)2590

Bonvin+ A&A **629**(2019)A97

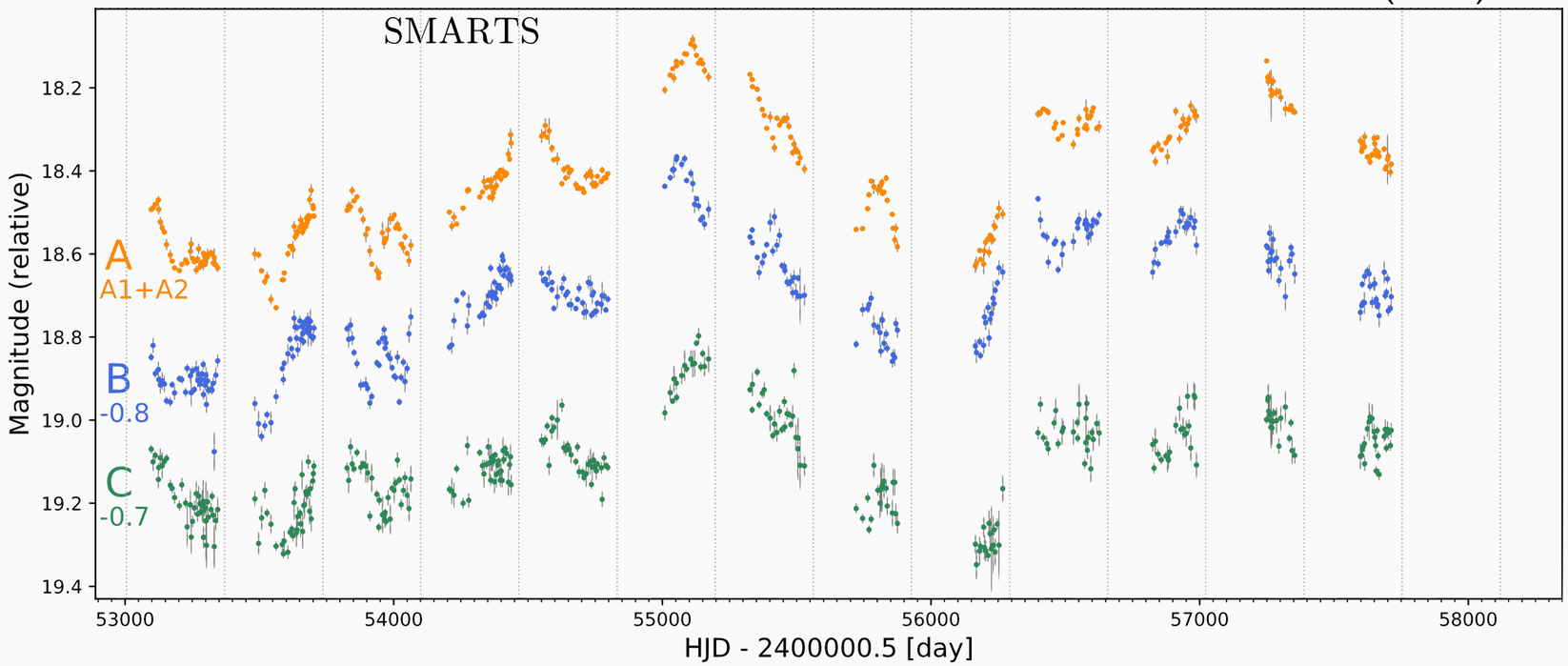

time delays from ~13 year monitoring (max. ~60 days)

Mass modeling

- mass modeling of WFI2033−4723

observational constraints: image+lens position, flux ratio, time delay

$$N_{\mathrm{const}} = 15$$

assumed model: singular isothermal ellipsoid+external shear
+higher order perturbation (+source position, H_0)

$$N_{\mathrm{param}} = 12$$

degree of freedom (dof) $15 - 12 = 3$

Result of mass modeling

- observed image positions etc well reproduced $\chi^2/\mathrm{dof} = 4.3/3$

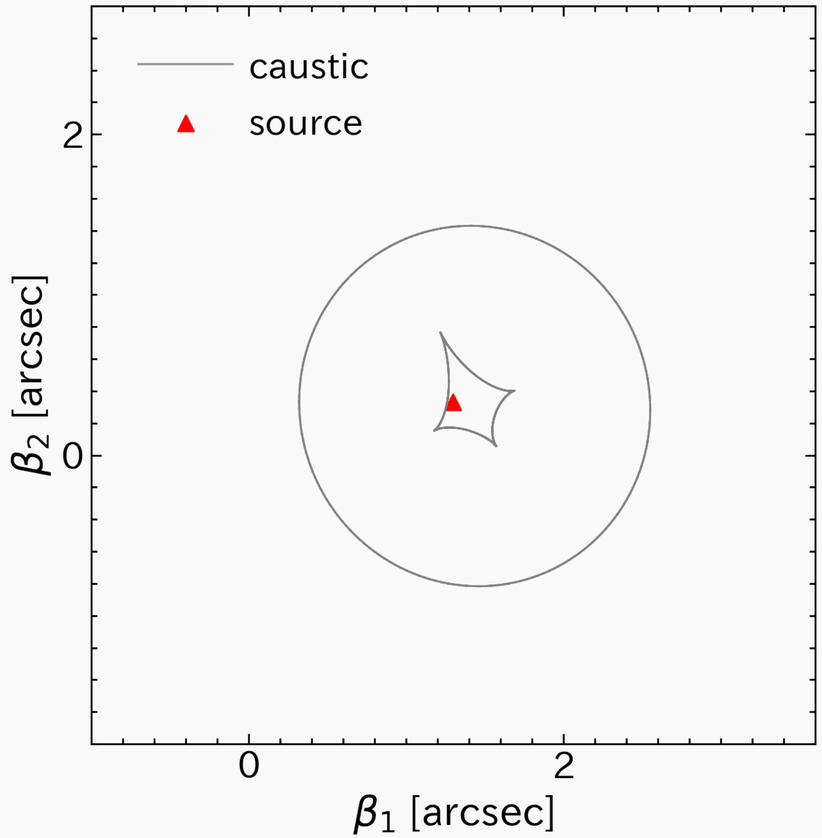

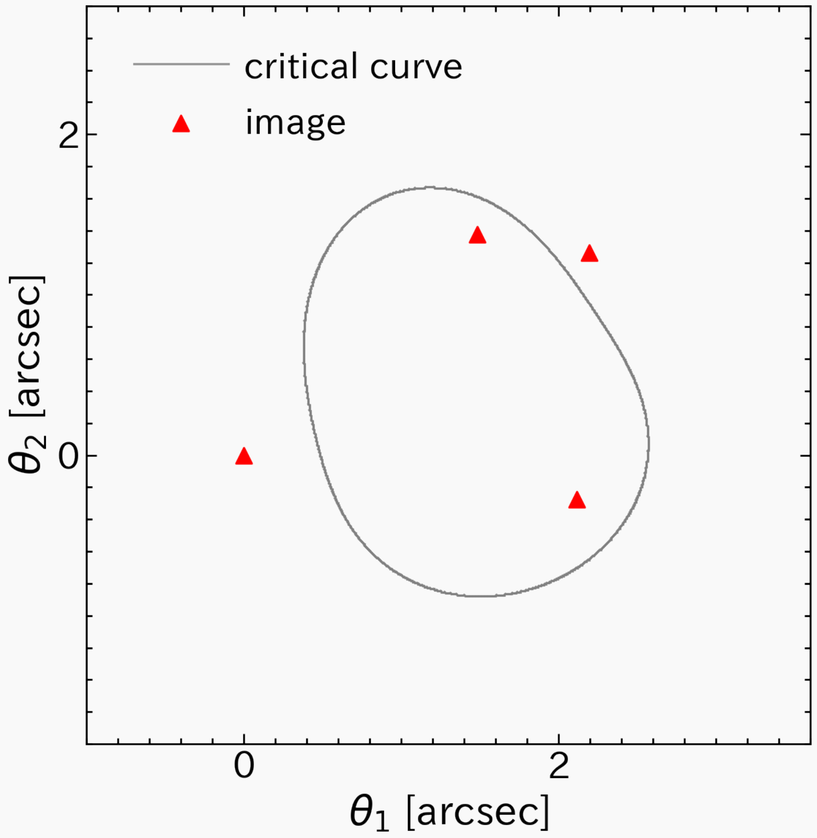

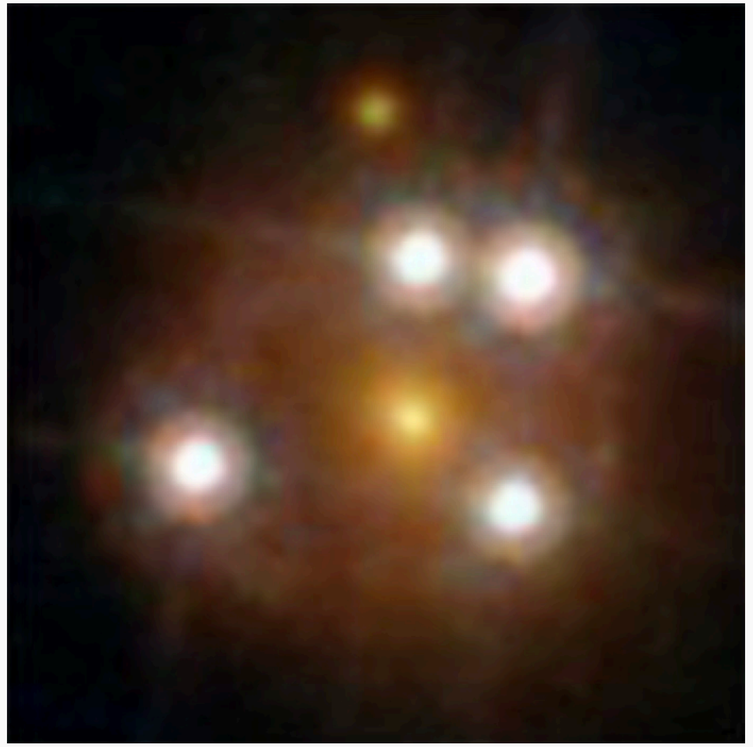

Extending to power-law ellipsoid

- constraint on slope is relatively weak

$$\rho(r) \propto r^{-\eta}$$

- mass within Einstein radius is robustly constrained

$$\bar{\kappa}(<\theta_{\rm Ein}) = 1$$

$$\theta_{\rm max} \simeq 2\theta_{\rm Ein}$$

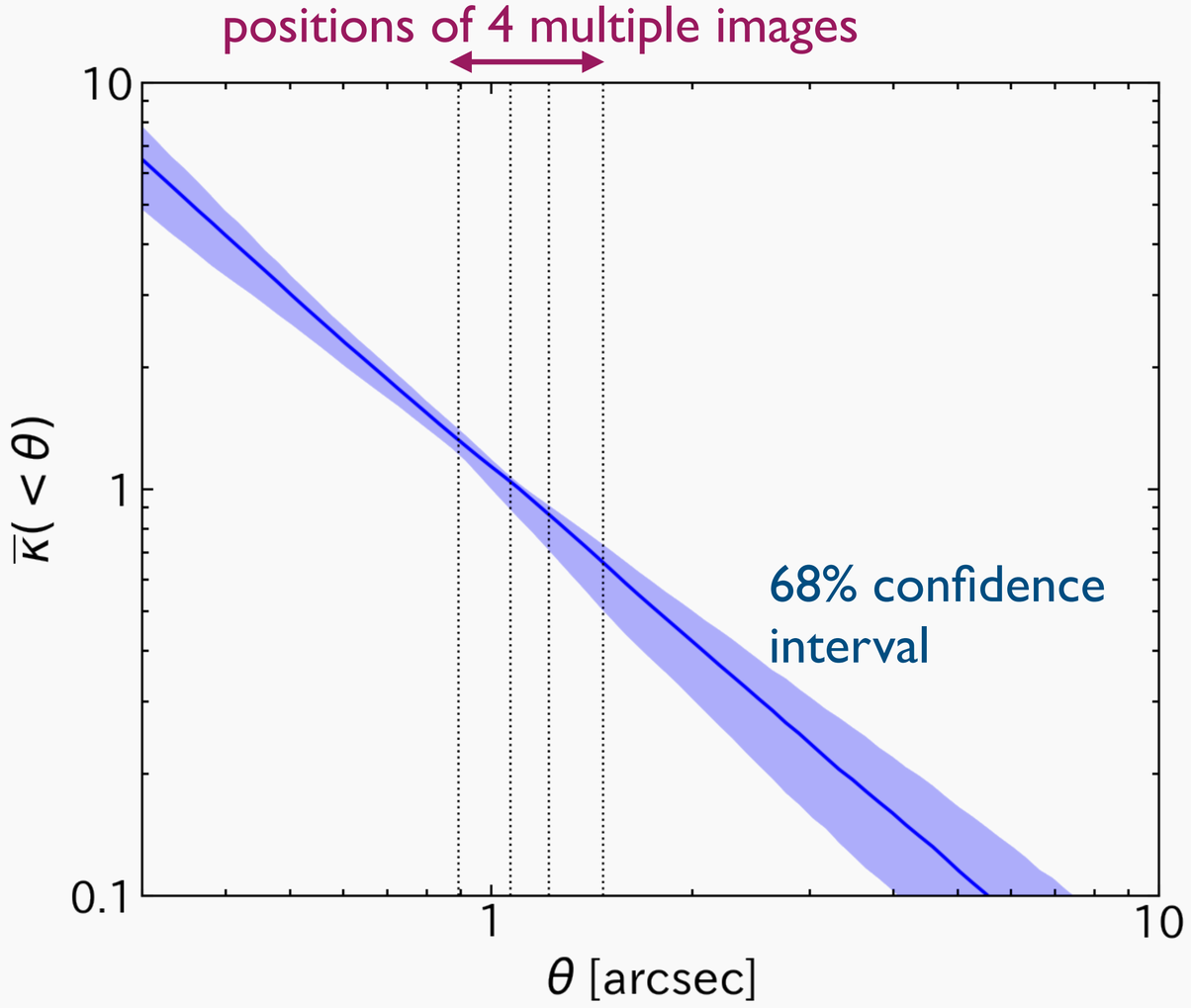

Constraint on Hubble constant H_0

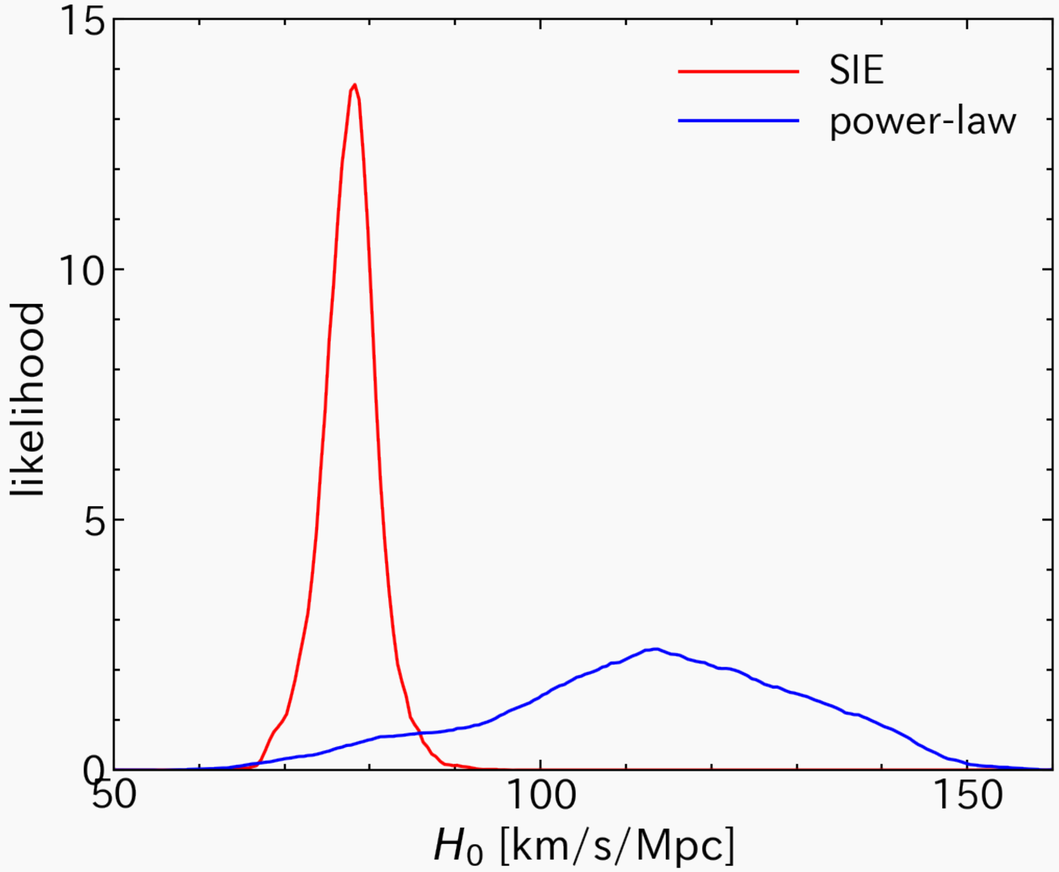

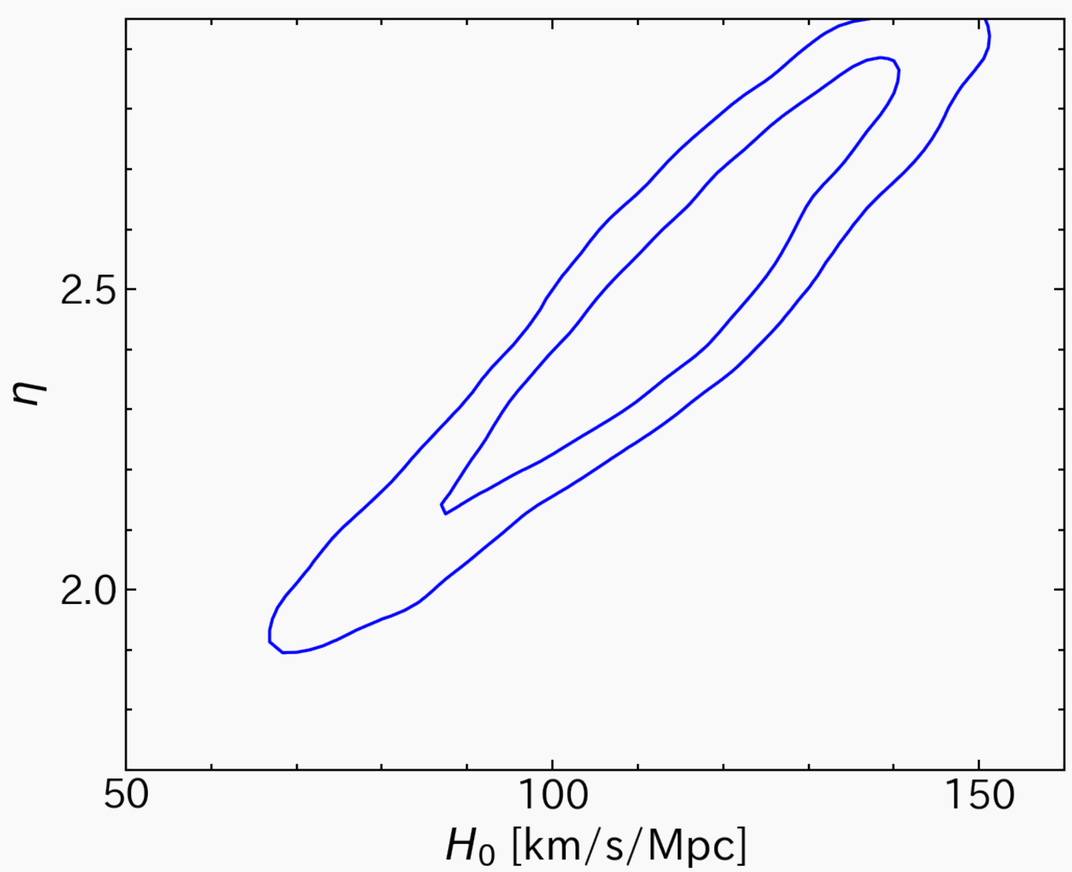

- constraint weak for power-law
- degeneracy between H_0 and slope (≃mass-sheet degeneracy)

Improving constraint on H_0

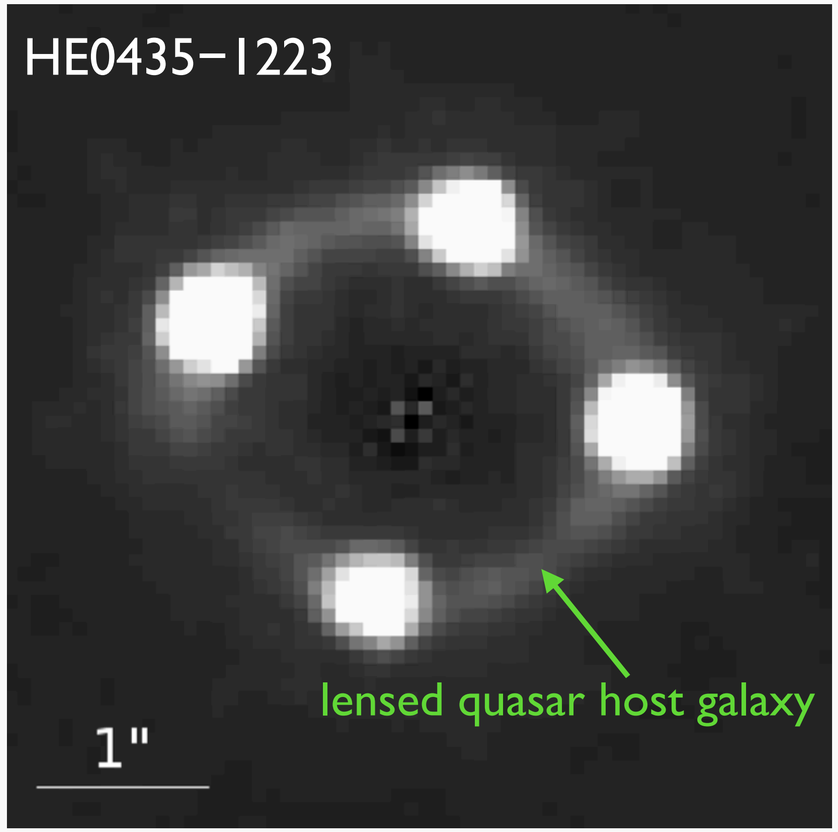

Suyu+ MNRAS **468**(2017)2590

mass model constraint from lensed quasar host galaxy shape

Wong+ MNRAS **465**(2017)4895

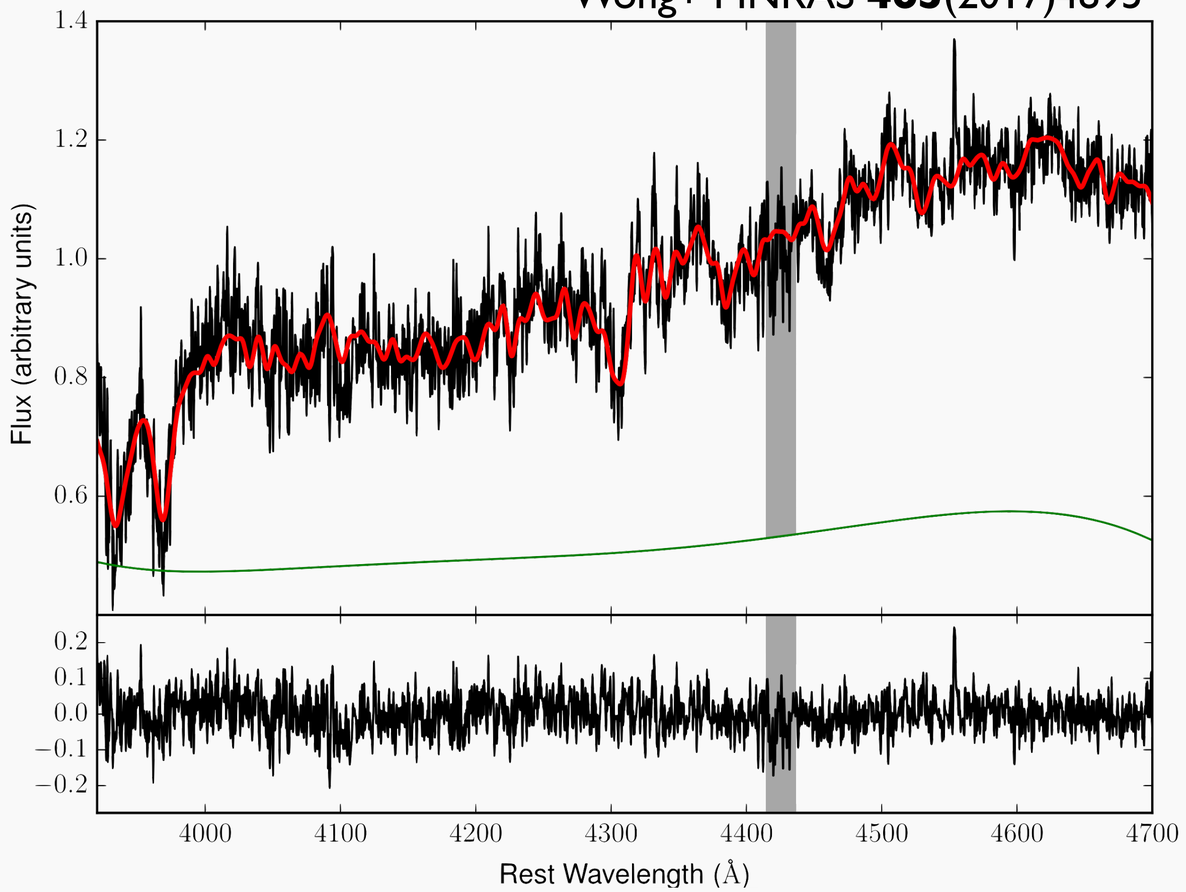

mass model constraint from velocity dispersion of lens galaxy

Example: cluster lensing

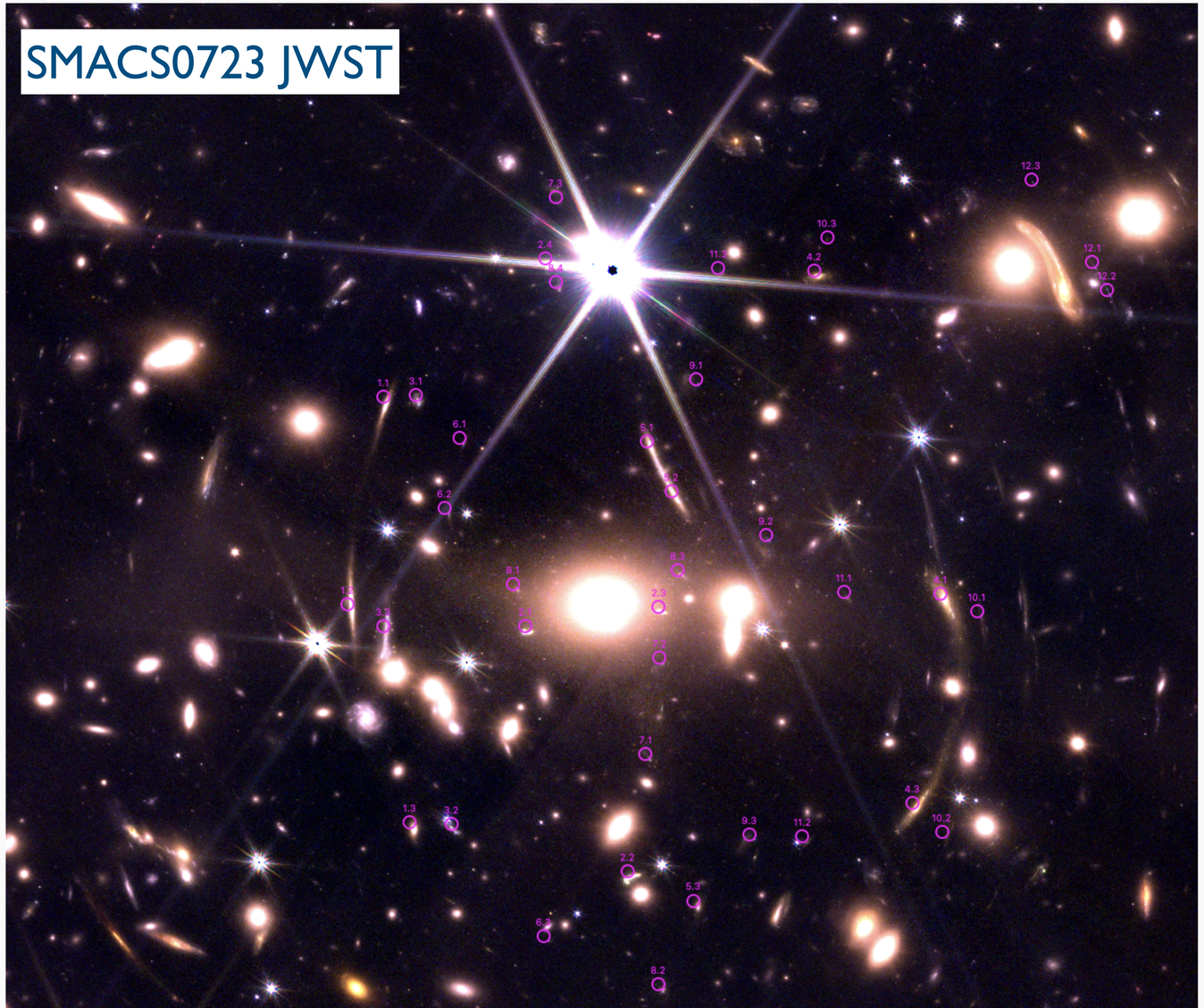

- one of first targets of James Webb Space Telescope (JWST)
- 43 multiple images from 14 background source galaxies

Derived mass model

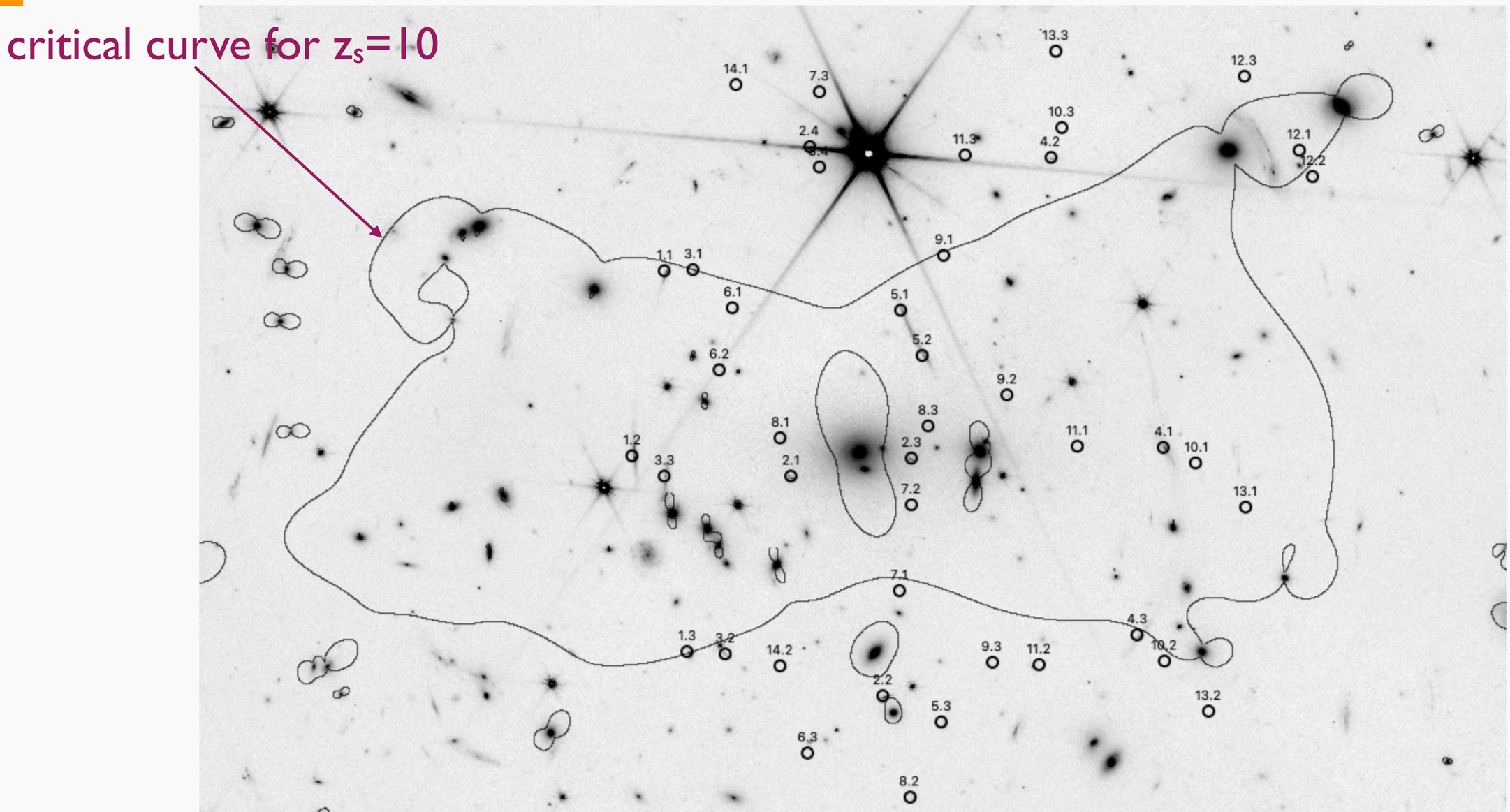

Average convergence

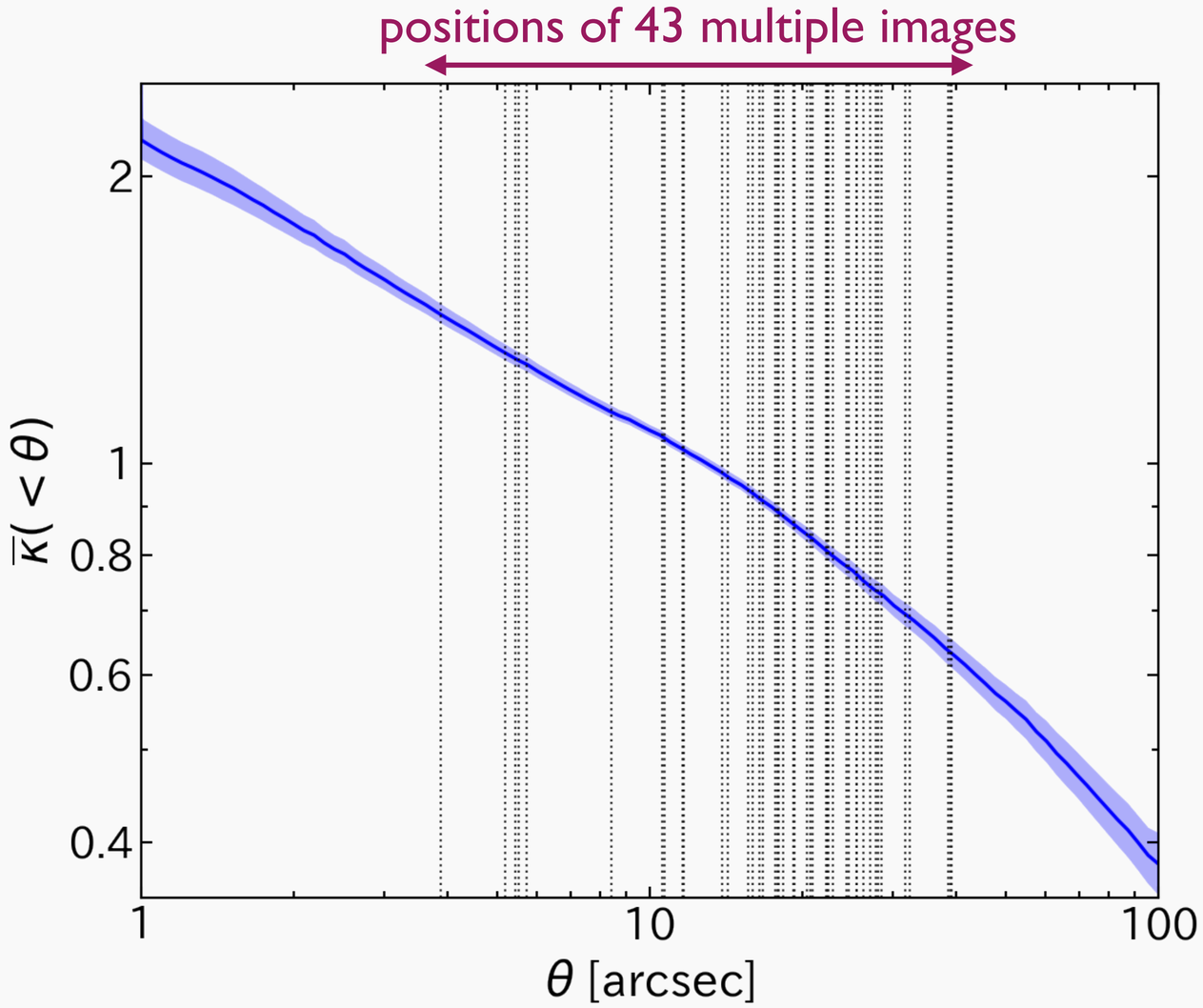

multiple images for a wide range of radii

density profile well constrained including slope

Source redshift dependence

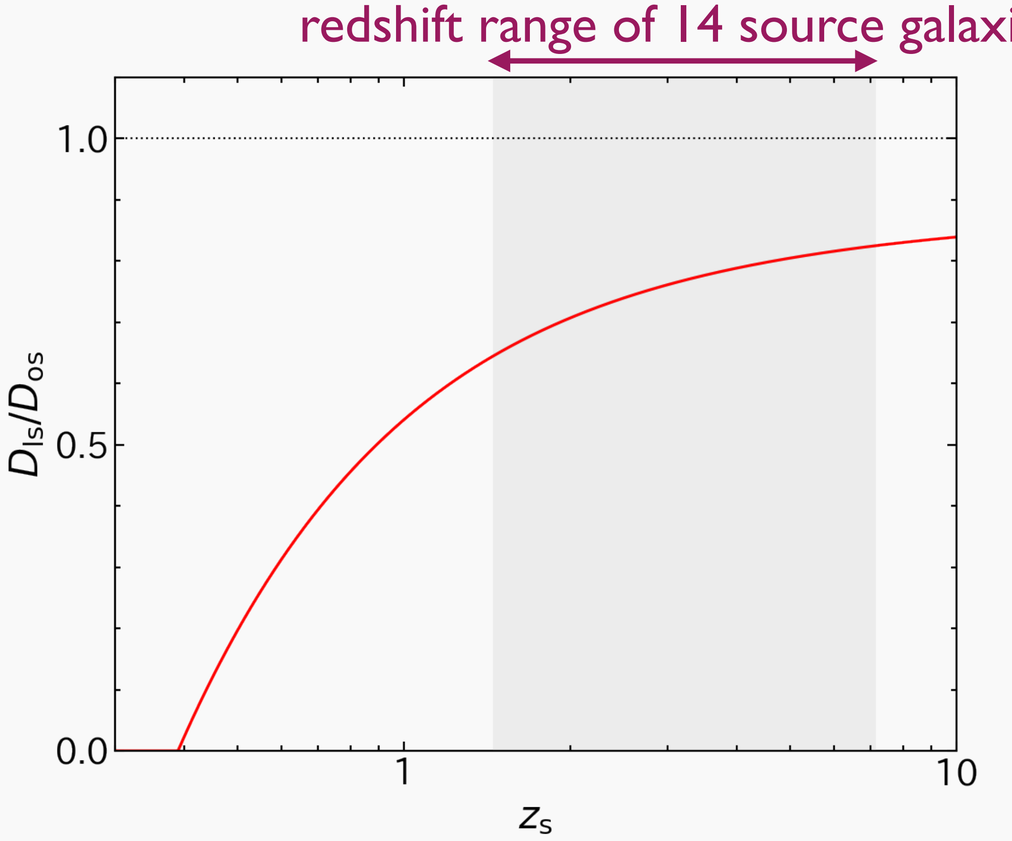

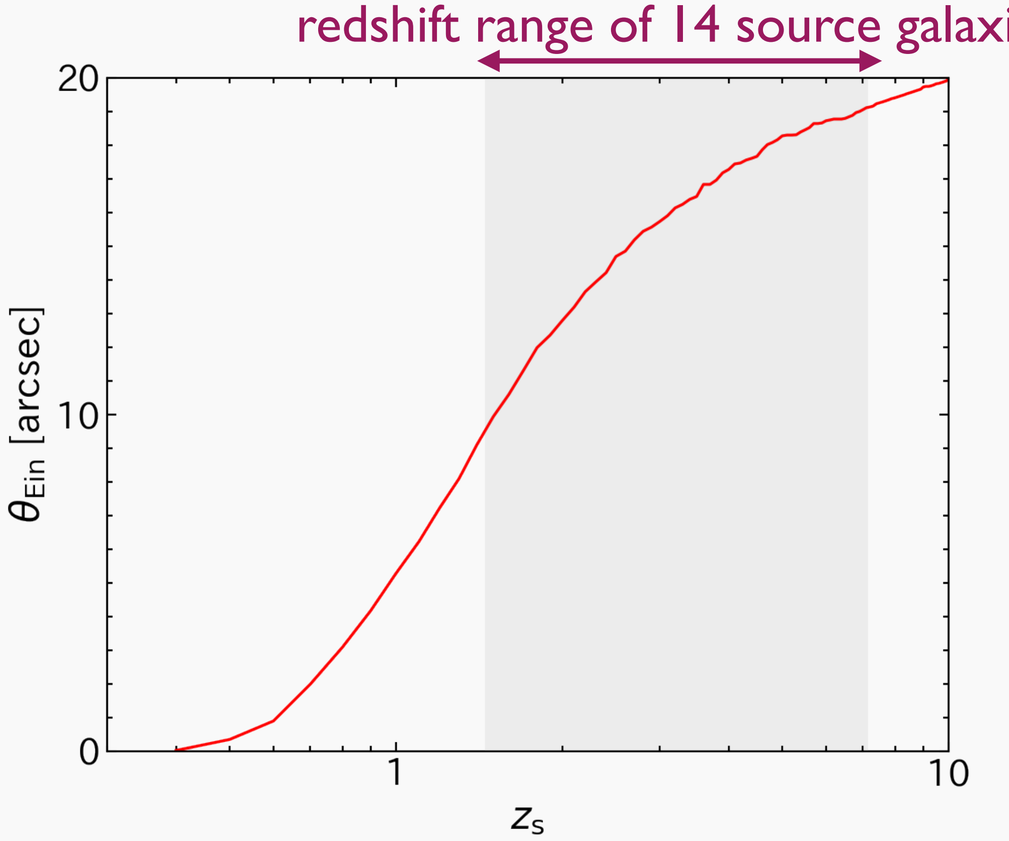

$$\Sigma_{cr}^{-1} \propto \frac{D_{ls}}{D_{os}}$$ ➡ θ_{Ein} depend on source redshift ➡ constraint of $\bar{\kappa}(<\theta_{Ein}) = 1$ at multiple radii

Issue of cluster lensing

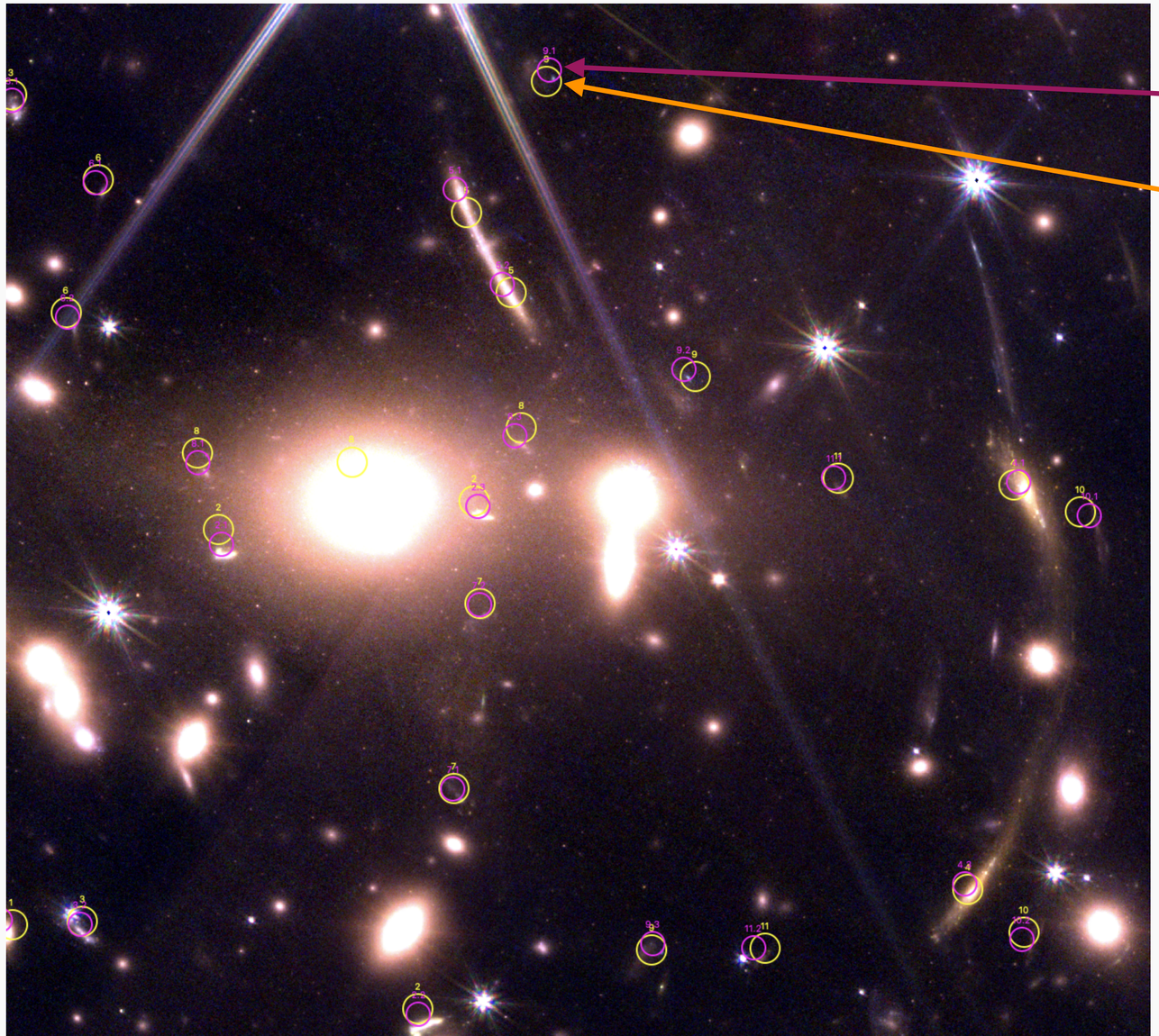

observed image position

image position predicted by mass model

- significant difference of image positions
- originate from complicated mass distribution in real cluster

https://github.com/oguri/glafic2

Issue of cluster lensing

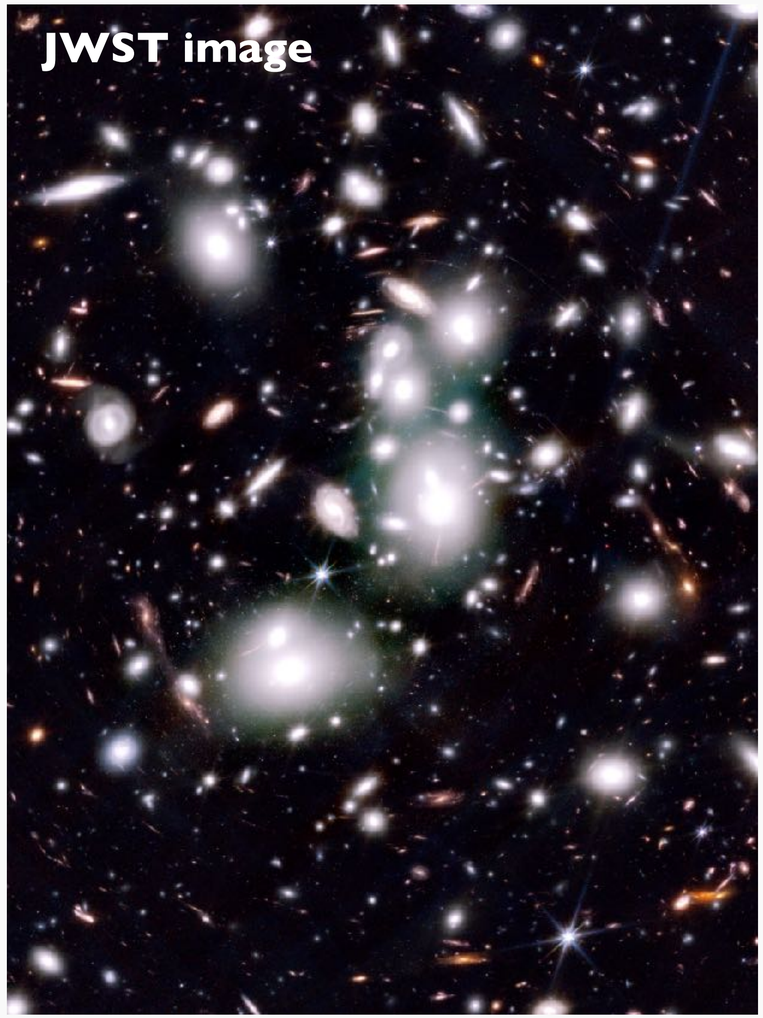

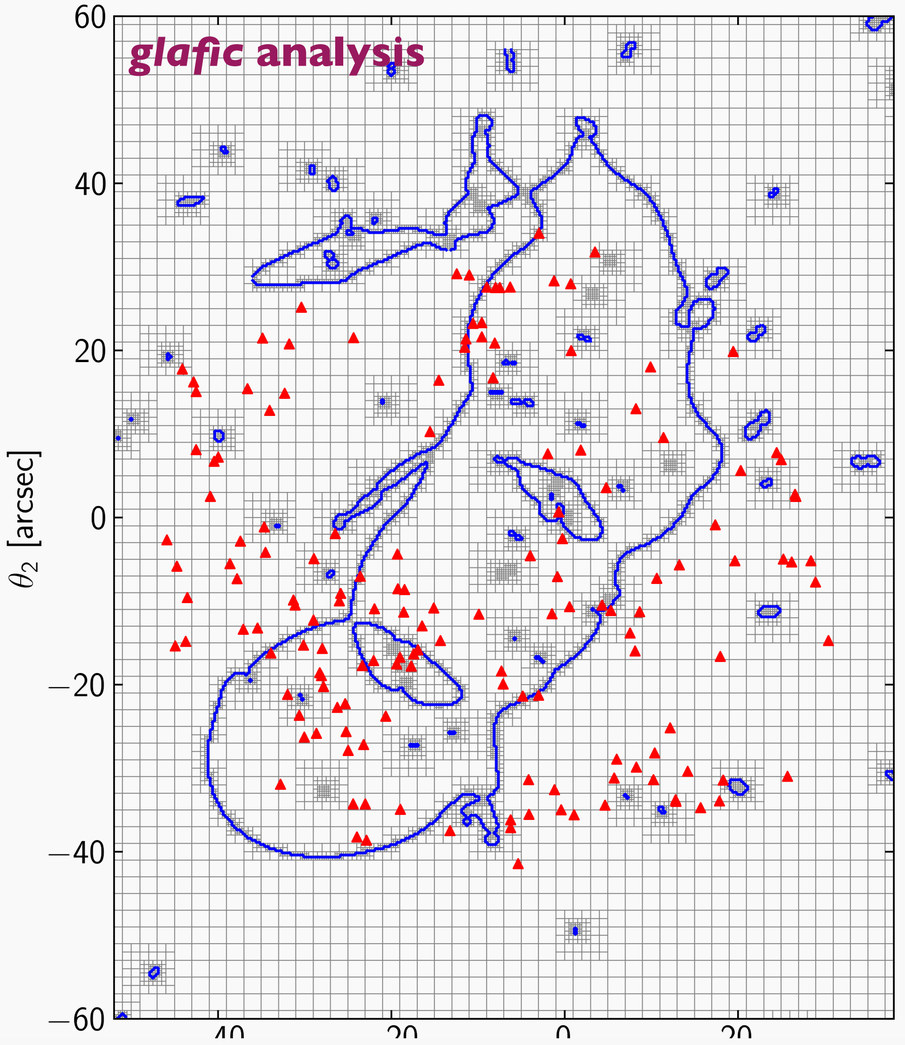

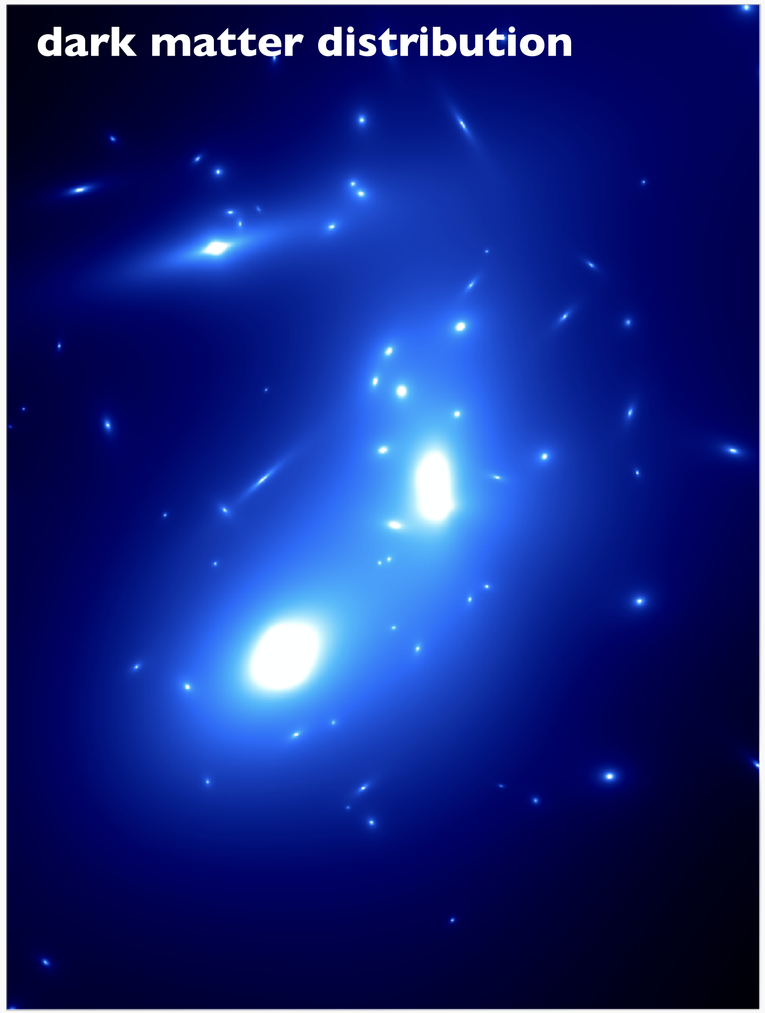

- detailed mass modeling using >100 multiple images

Example: extended source

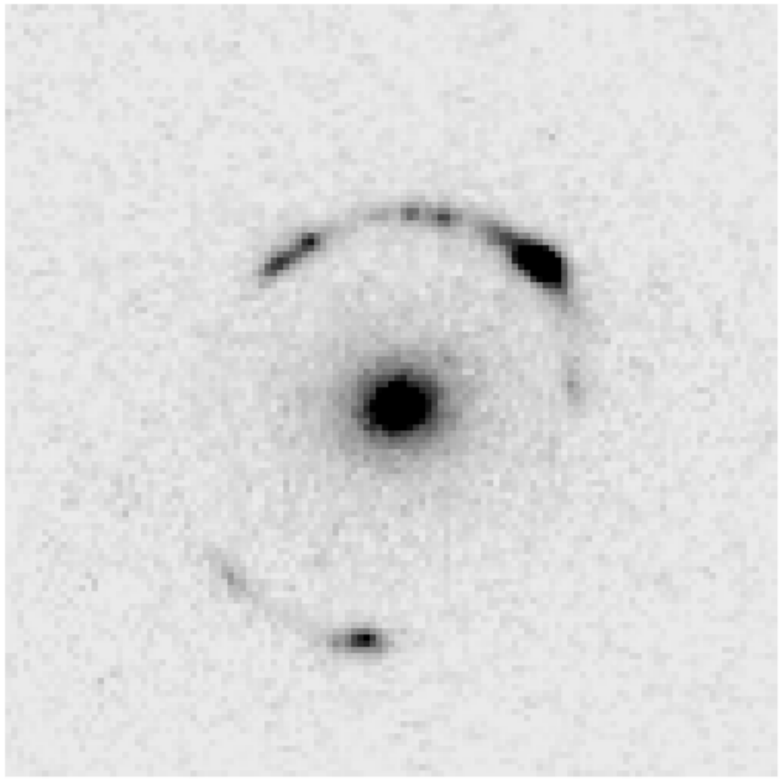

SDSSJ002927.38+254401.7

Shu+ ApJ **824**(2016)86

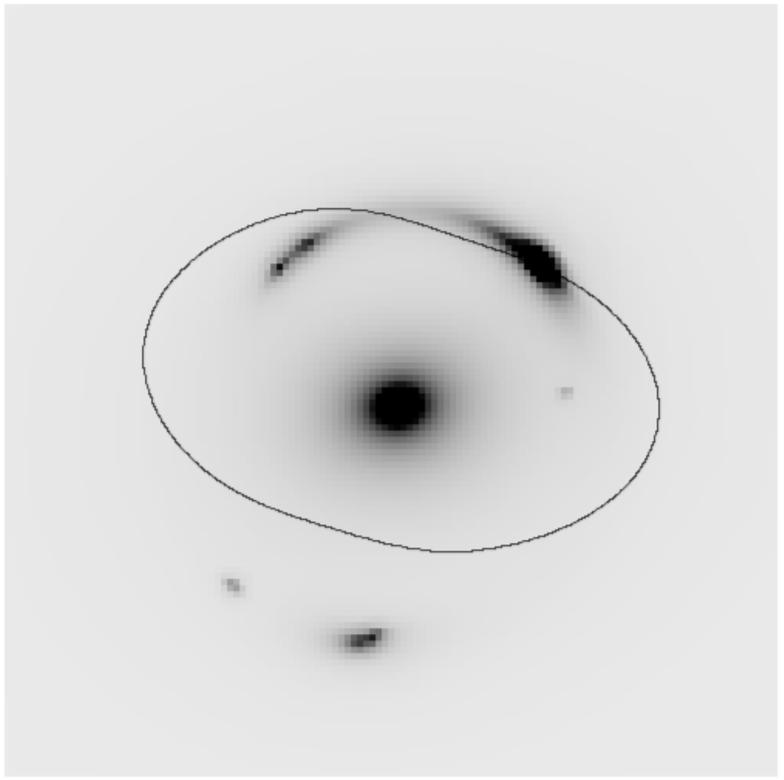

result of mass modeling

- fitting all pixels

$$\chi^2_{\rm ext} = \sum_{i_x=1}^{N_x} \sum_{i_y=1}^{N_y} \frac{\left[f^{\rm obs}(i_x, i_y) - f(i_x, i_y; \boldsymbol{p}_{\rm source}, \boldsymbol{p}_{\rm model}) \right]^2}{\sigma^2(i_x, i_y)}$$

challenge:

- computational cost
- complex source morphology
- complex mass distribution
- …

Small scale dark matter distribution

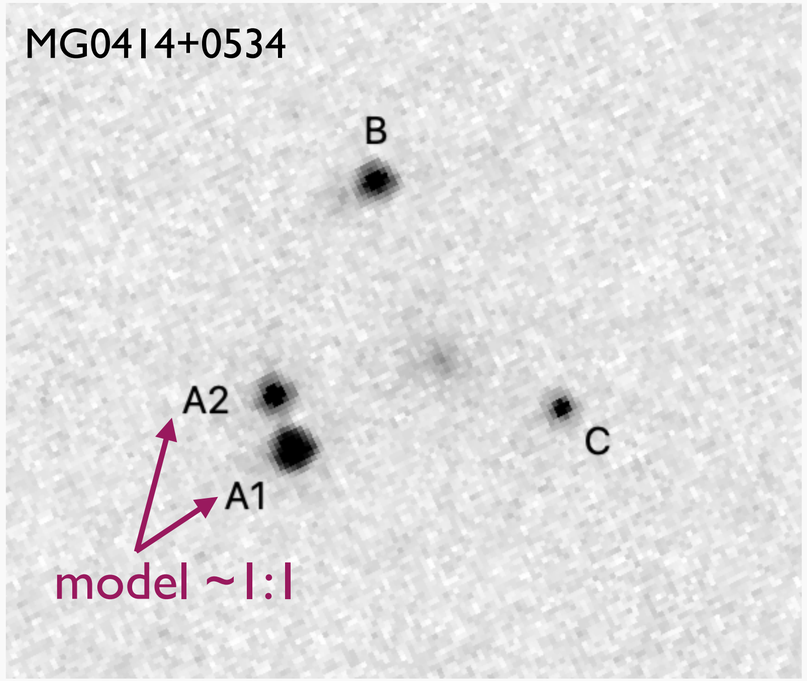

flux ratio of multiple images of point source

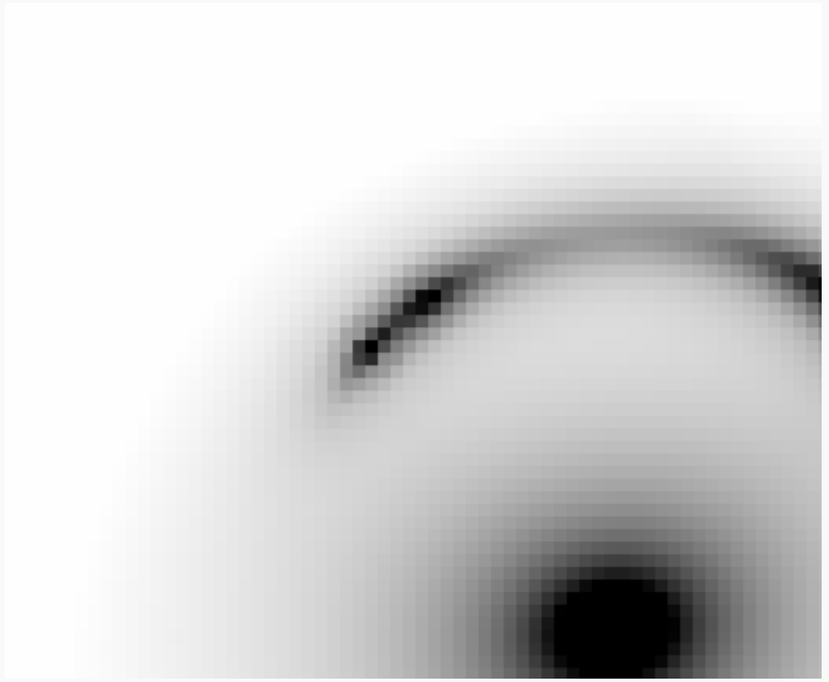

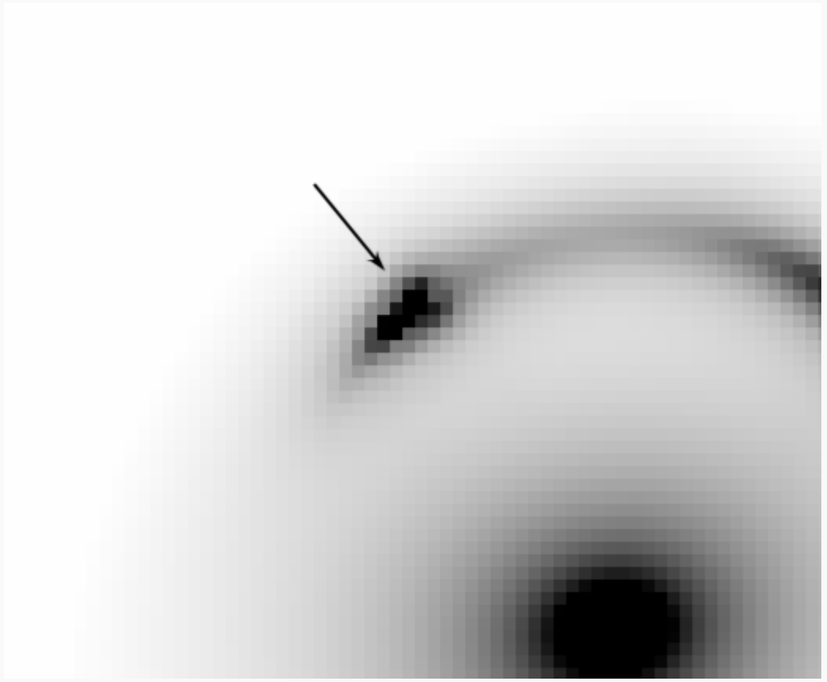

change of shape of lensed extended source

Small $10^6 M_\odot$ object detected in B1938+666

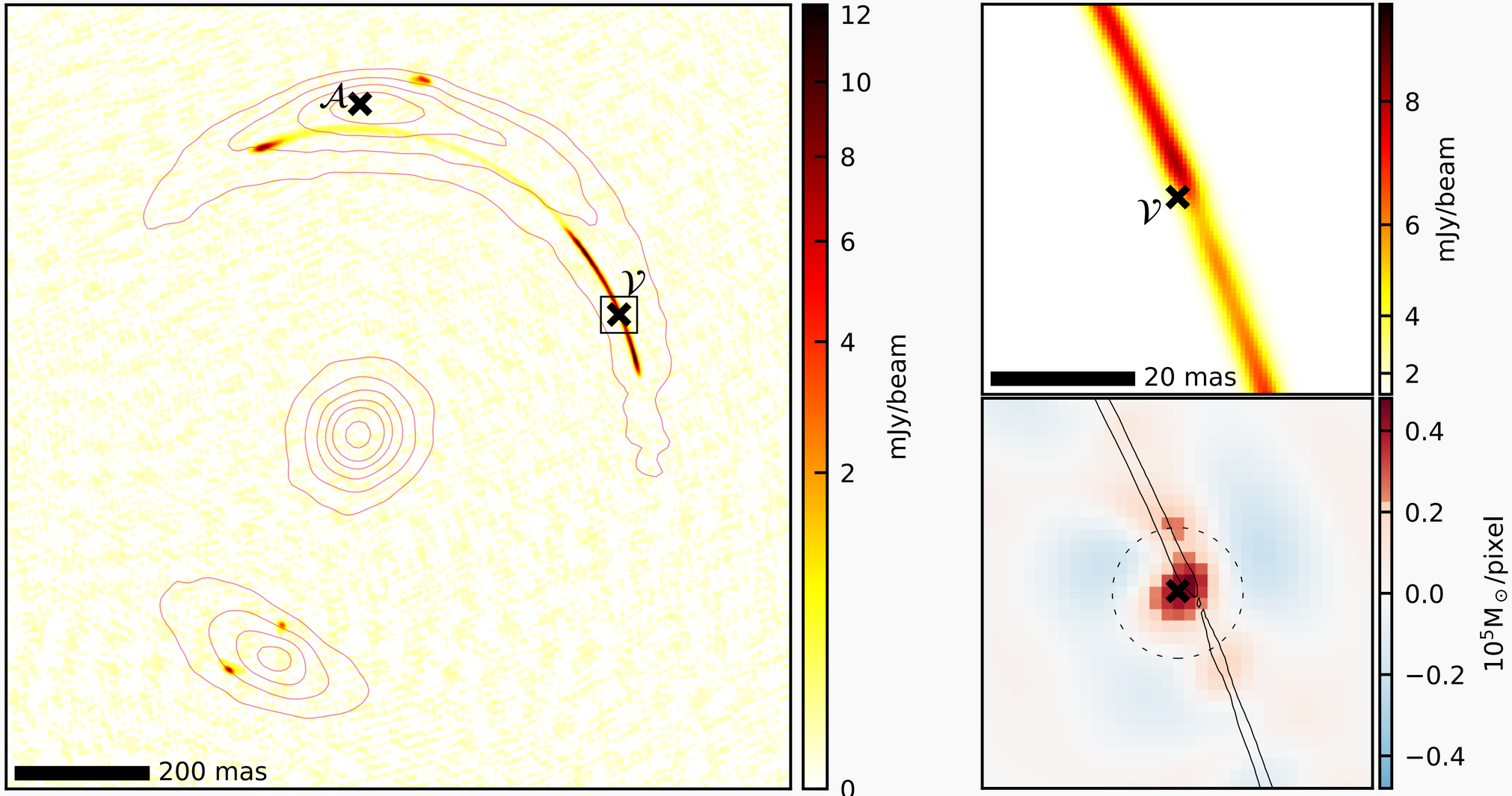

Powell+ Nat. Ast. **9**(2025)1714

Strong lensing probability

- strong lensing produced only when lens object is located along line-of-sight of source → strong lensing probability

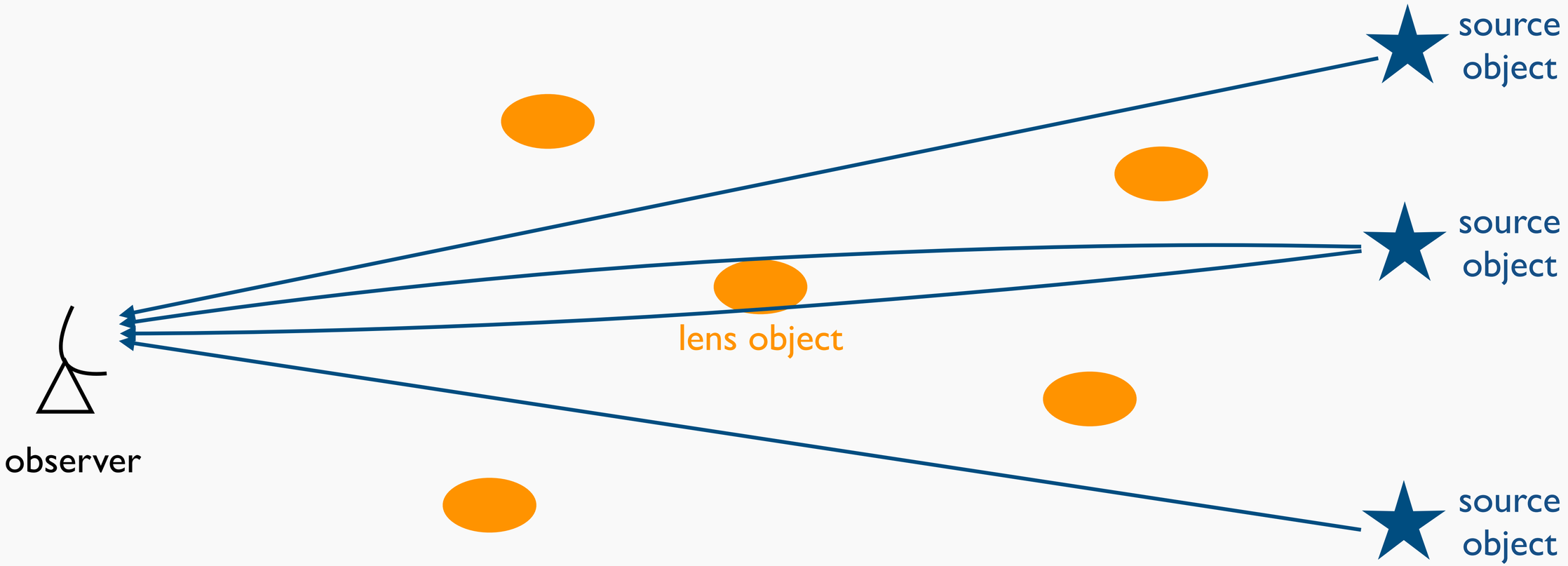

Lensing cross section

- area (solid angle) $\sigma_{\rm sl}$ on sky within which background source is strongly lensed for a lens

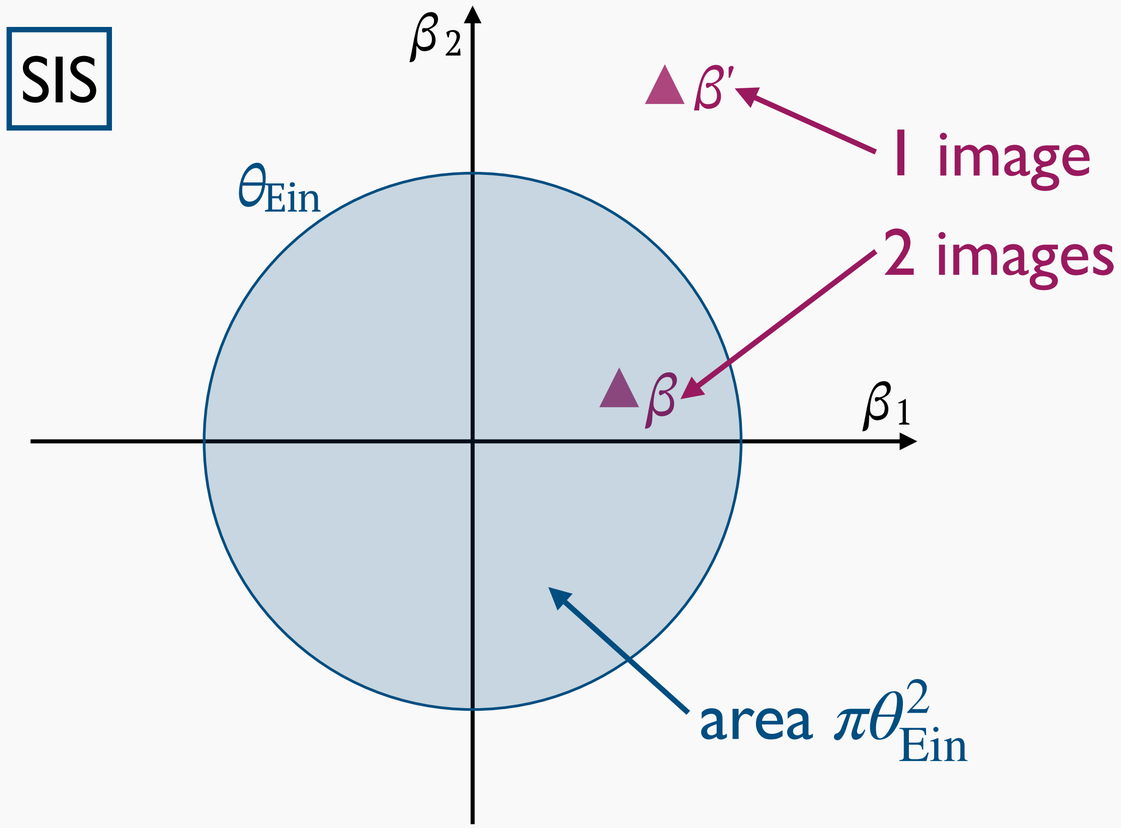

$\sigma_{\rm sl} = \pi\theta^2_{\rm Ein}$ when strong lensing is defined by forming multiple images

(only for SIS, different for different mass model)

Calculating strong lensing probability

- strong lensing probability for source at z_s

$$P_{sl}(z_s) = \int_0^{z_s} dz_l \frac{d^2V}{dz_l d\Omega} \int_0^{\infty} dM \frac{dn}{dM} \sigma_{sl}(M;\, z_l, z_s)$$

comoving volume element $\frac{d^2V}{dz_l d\Omega} = f_K^2(\chi(z_l)) \frac{c}{H(z_l)}$ mass function of lens lensing cross section

- for SIS, velocity dispersion σ corresponds to mass

$$P_{sl}(z_s) = \int_0^{z_s} dz_l \frac{d^2V}{dz_l d\Omega} \int_0^{\infty} d\sigma \frac{dn}{d\sigma} \sigma_{sl}(\sigma;\, z_l, z_s)$$

velocity dispersion function

Calculating strong lensing probability

- observed velocity dispersion function

$$\frac{dn}{d\sigma} \propto \sigma^{-\alpha} \exp\left[-\left(\frac{\sigma}{\sigma_*}\right)^{\beta}\right]$$

$$\alpha \simeq 1, \beta \simeq 2, \sigma_* \simeq 200\,\mathrm{km/s}$$

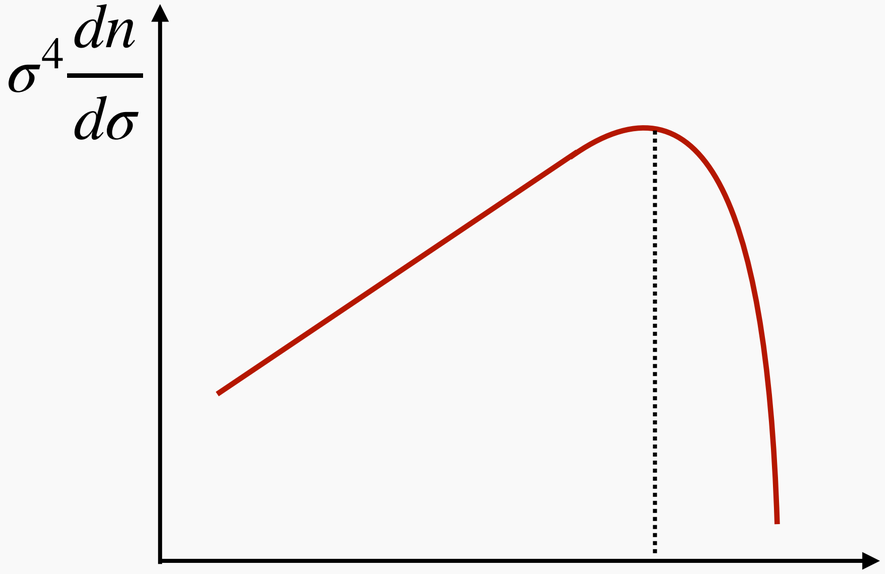

lens galaxy is typically
massive galaxy (elliptical galaxy)

Source redshift dependence

- for $z_s \ll 1$

$$\frac{d^2V}{dz_l d\Omega} \propto z_l^2$$

$$P_{sl}(z_s) \propto z_s^3$$

- increasing function of z_s

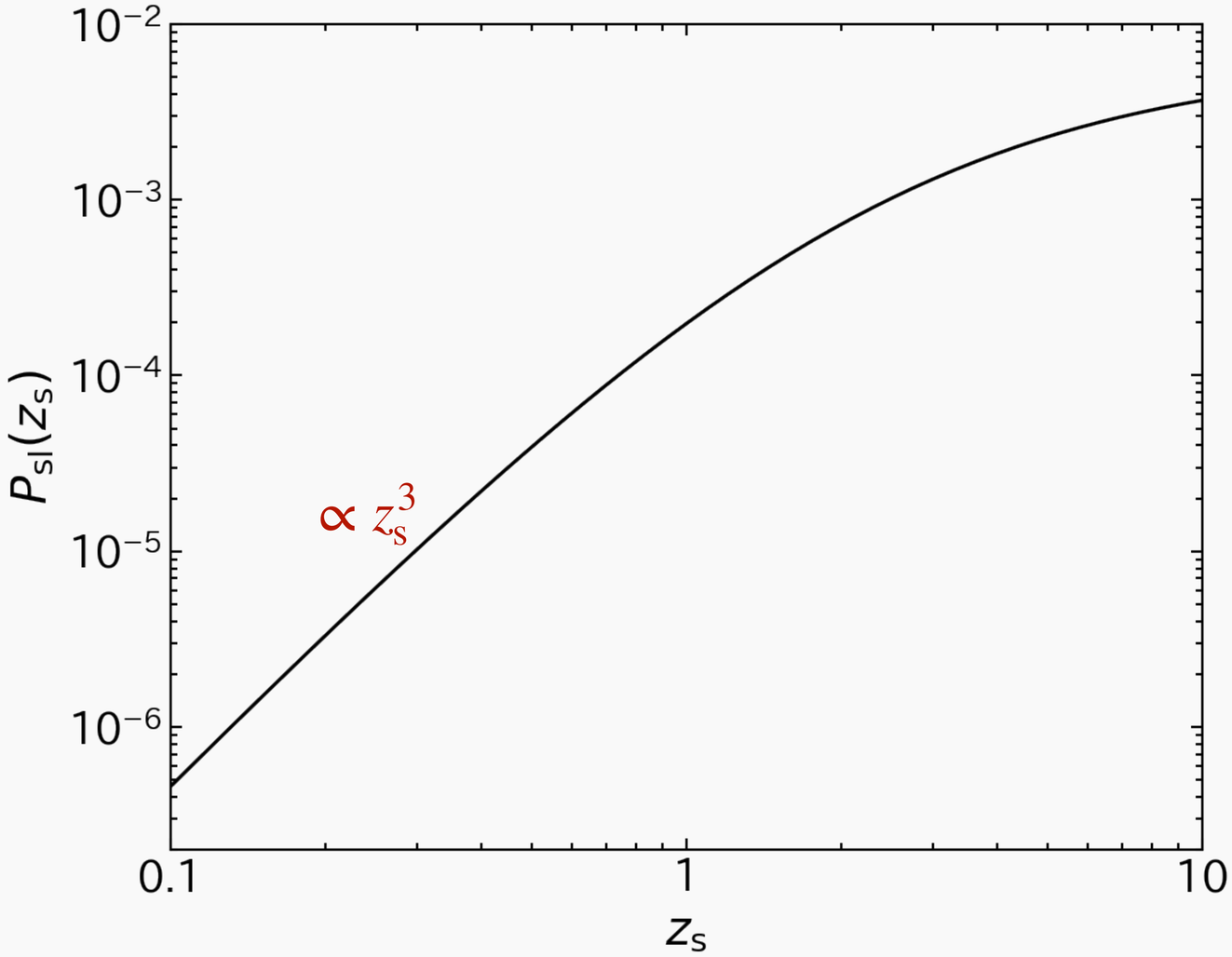

Contribution of cluster

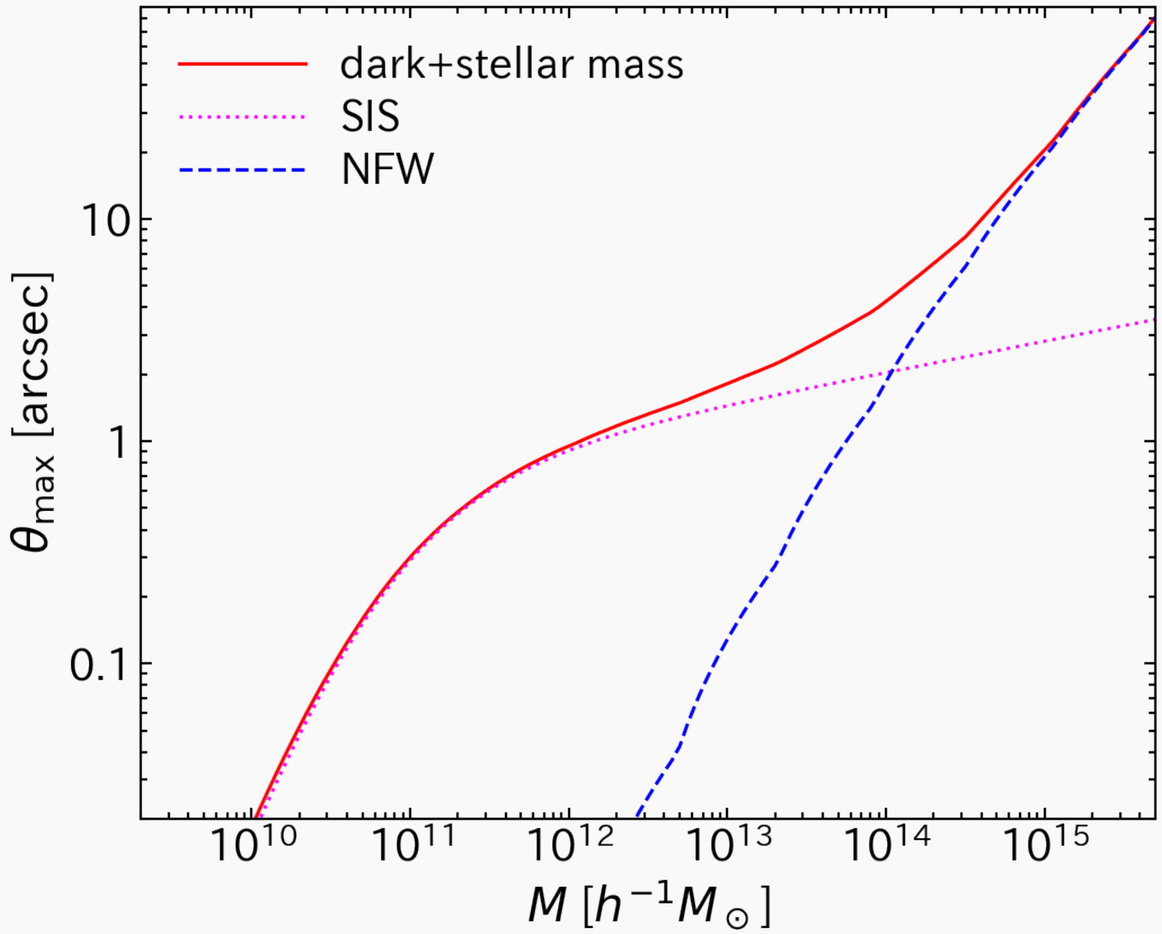

density profile of cluster is NFW-like

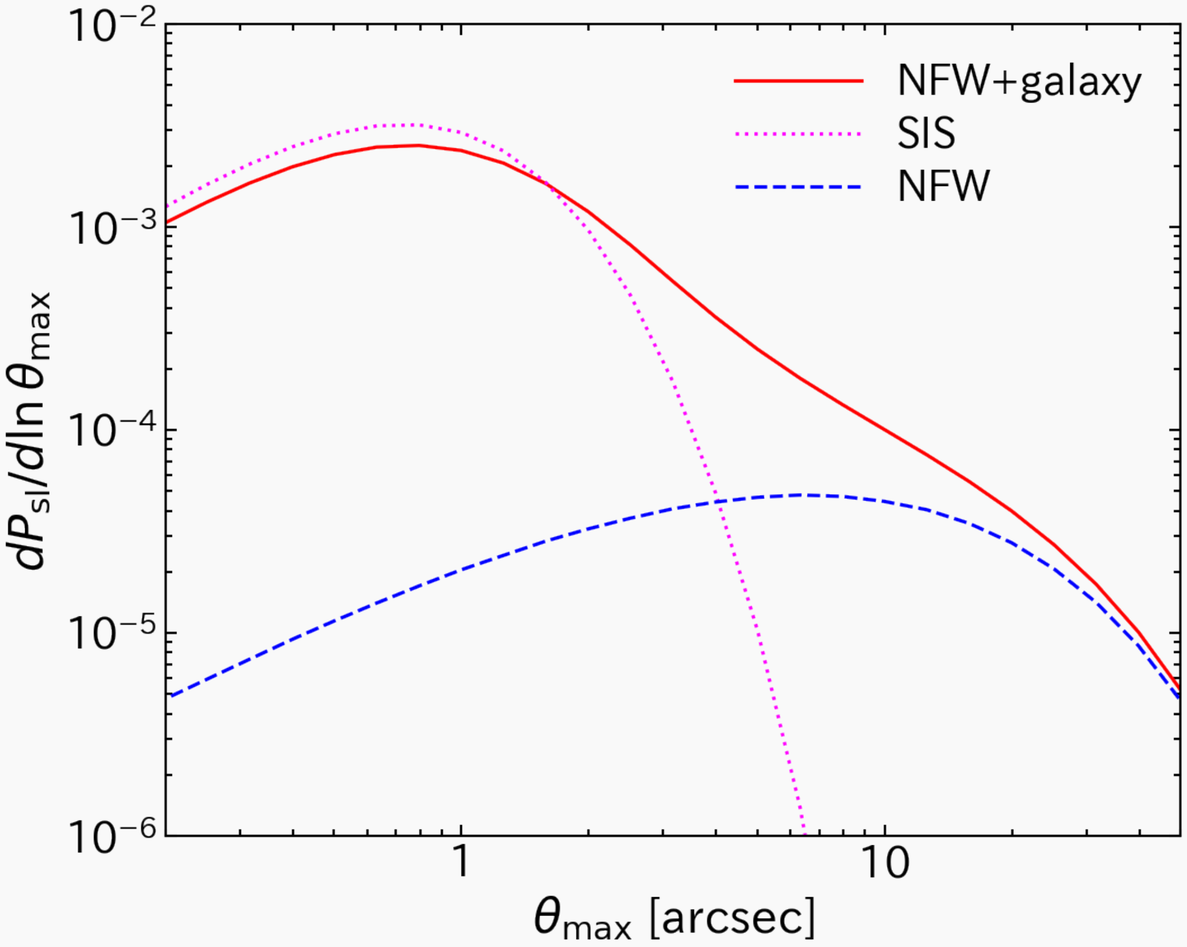

cluster contribution to total lensing probability is minor

Mock catalog of strong gravitational lenses

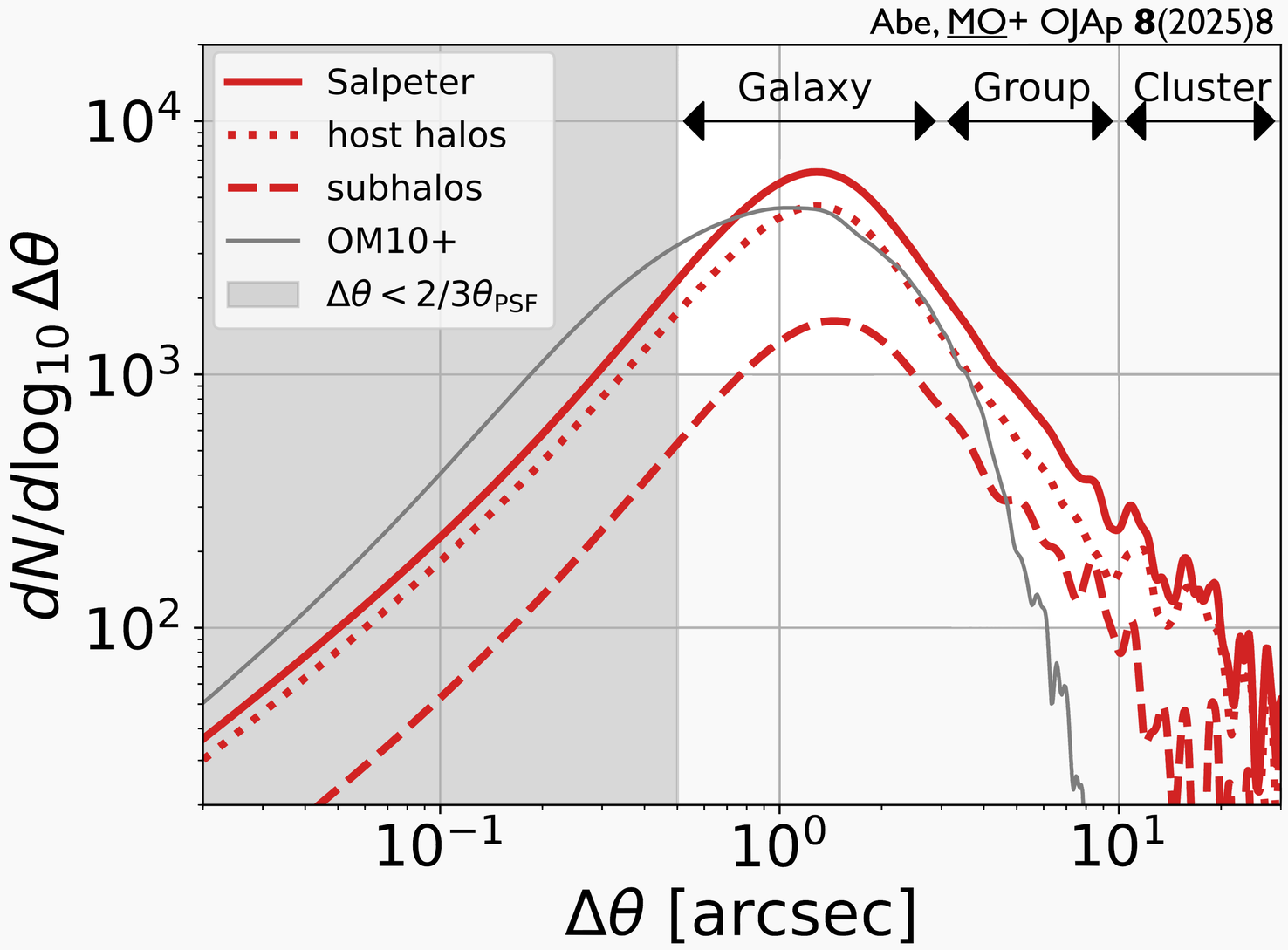

- halo model approach with halos, subhalos, and galaxies
- NFW for halos/subhalos and Hernquist for galaxies
- naturally predict transition from galaxy- to cluster-scale lenses

New sources

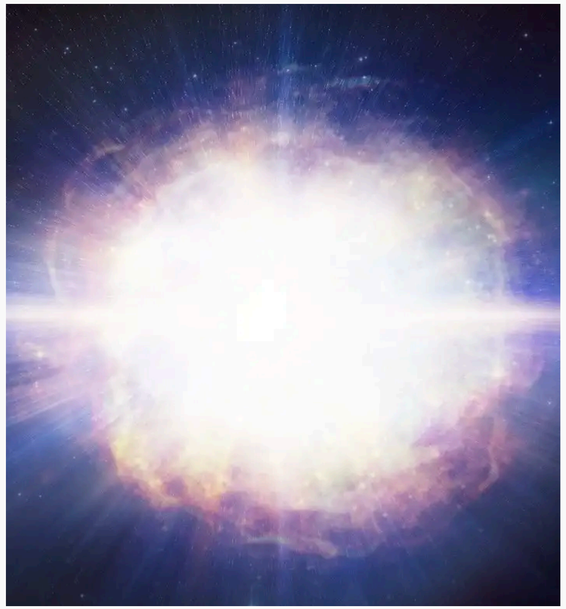

M. Weiss

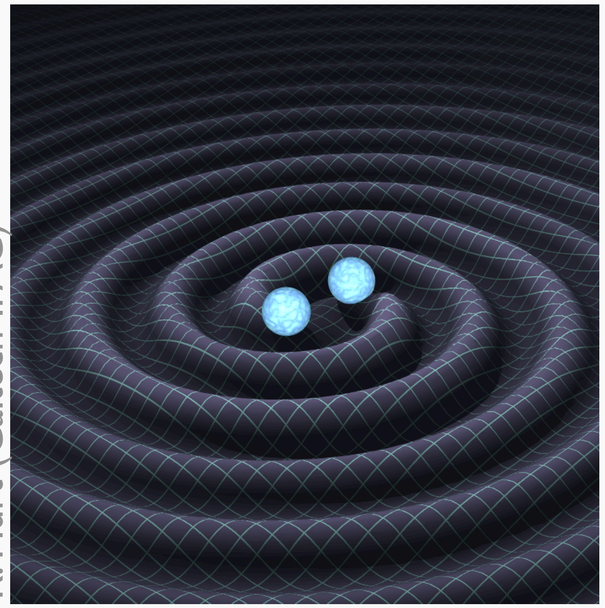

R. Hurt (Caltech-IPAC)

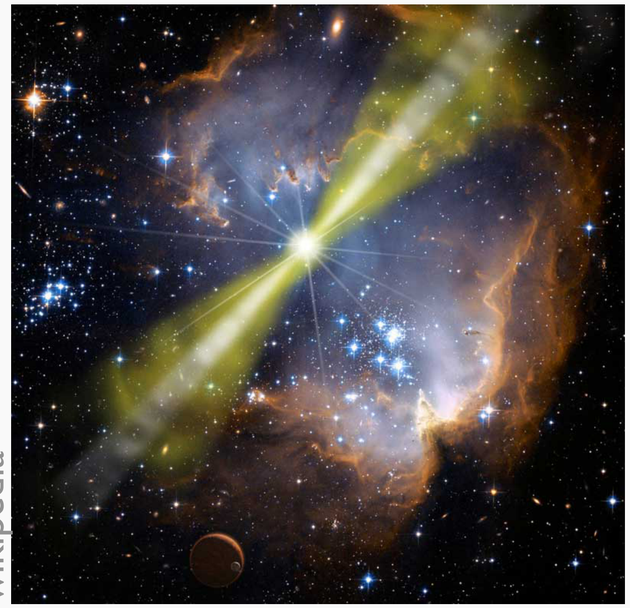

wikipedia

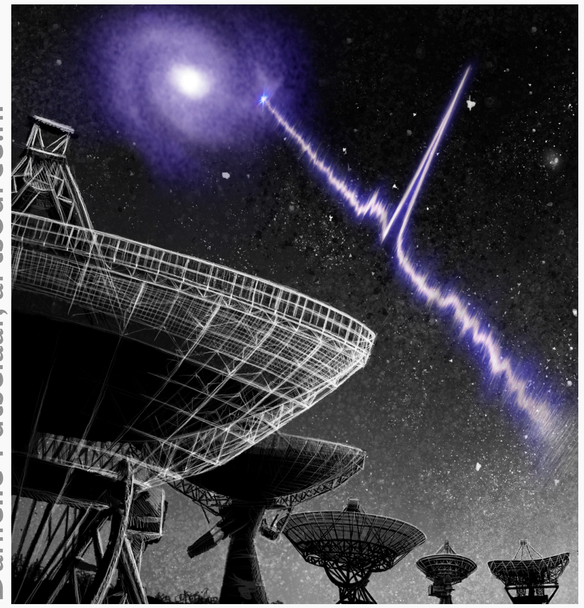

Danielle Futselaar, artsource.nl

supernova

gravitational waves

gamma-ray burst

fast radio burst

see MO Rep. Prog. Phys. **82**(2019)126901

Summary

- mass distribution determined so as to reproduce observed multiple image positions
- degeneracy between Hubble constant and lens mass distribution when measuring Hubble constant from observed time delay
- strong lensing probability is increasing function of source redshift

6. Microlensing

Point mass lens

- play central role in microlensing

$$\theta_{\rm Ein} = \sqrt{\frac{4GM}{c^2}\frac{D_{\rm ls}}{D_{\rm ol}D_{\rm os}}}$$

$$y = \frac{\beta}{\theta_{\rm Ein}}$$

$$\mu_{\rm tot}(y) = \frac{y^2+2}{y\sqrt{y^2+4}}$$

Magnification curve

- ignore acceleration, assume constant velocity

$$y(t) = \sqrt{y_0^2 + \left(\frac{t - t_0}{t_{\rm Ein}}\right)^2}$$

time at $y = y_0$

impact parameter

$$t_{\rm Ein} = \frac{(1 + z_{\rm l}) D_{\rm ol} \theta_{\rm Ein}}{v_\perp}$$

Einstein time

$$\mu(t) = \mu_{\rm tot}(y(t)) = \frac{\{y(t)\}^2 + 2}{y(t)\sqrt{\{y(t)\}^2 + 4}}$$

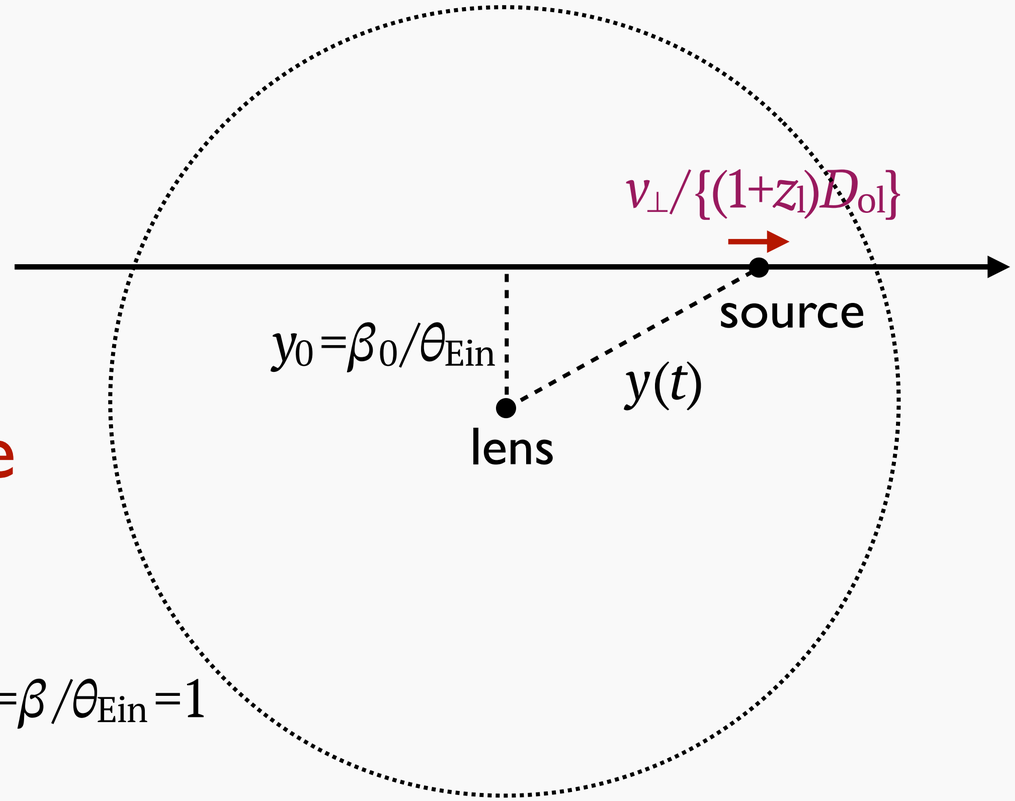

movie file: https://oguri.github.io/for_presen.html

Microlensing animation

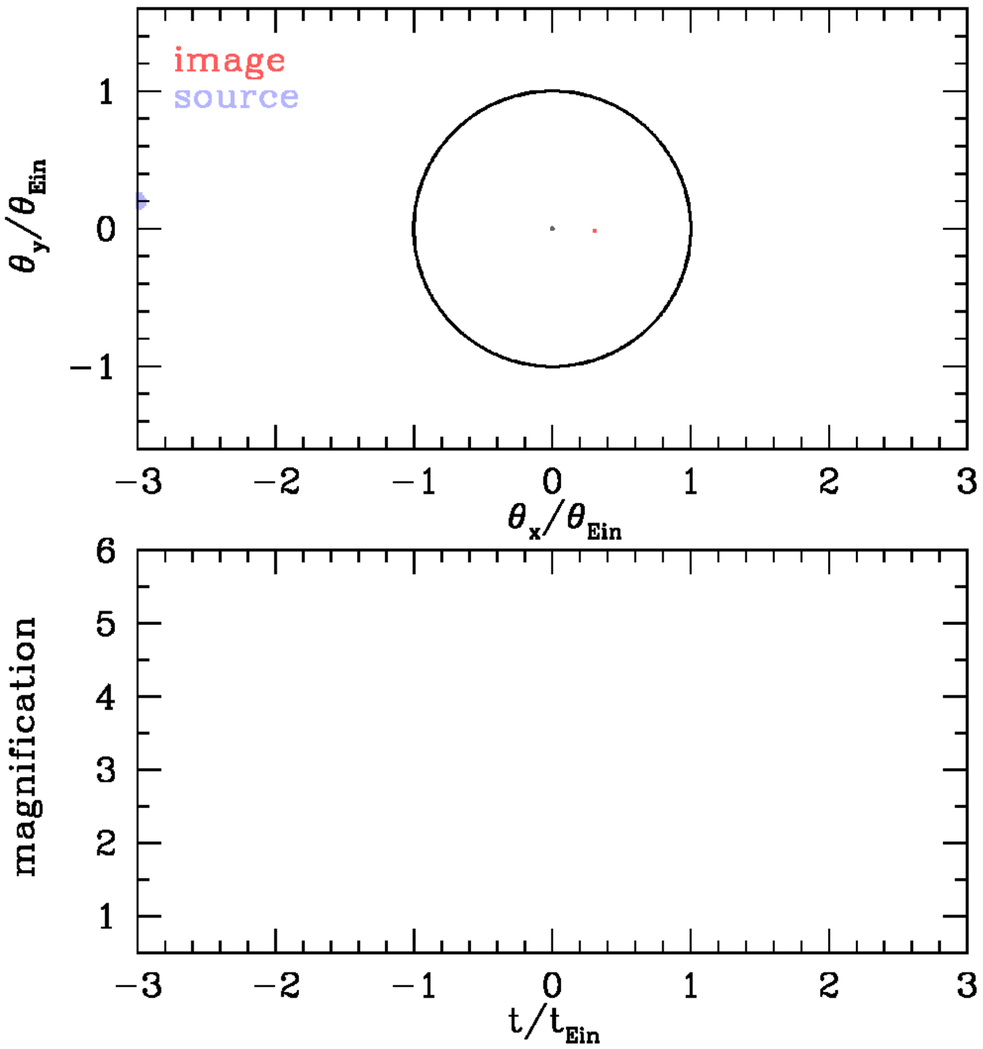

Magnification curve for point mass lens

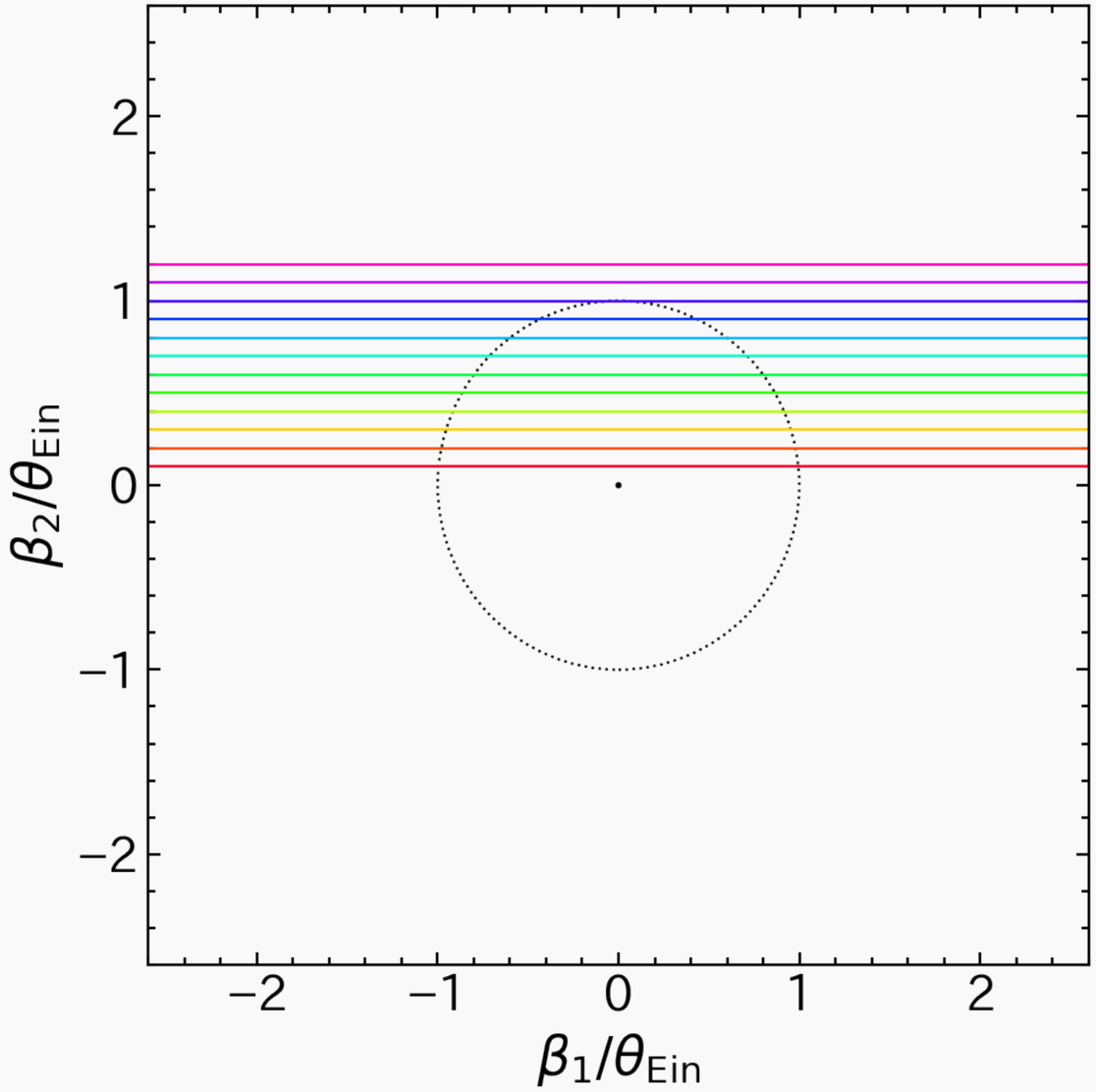

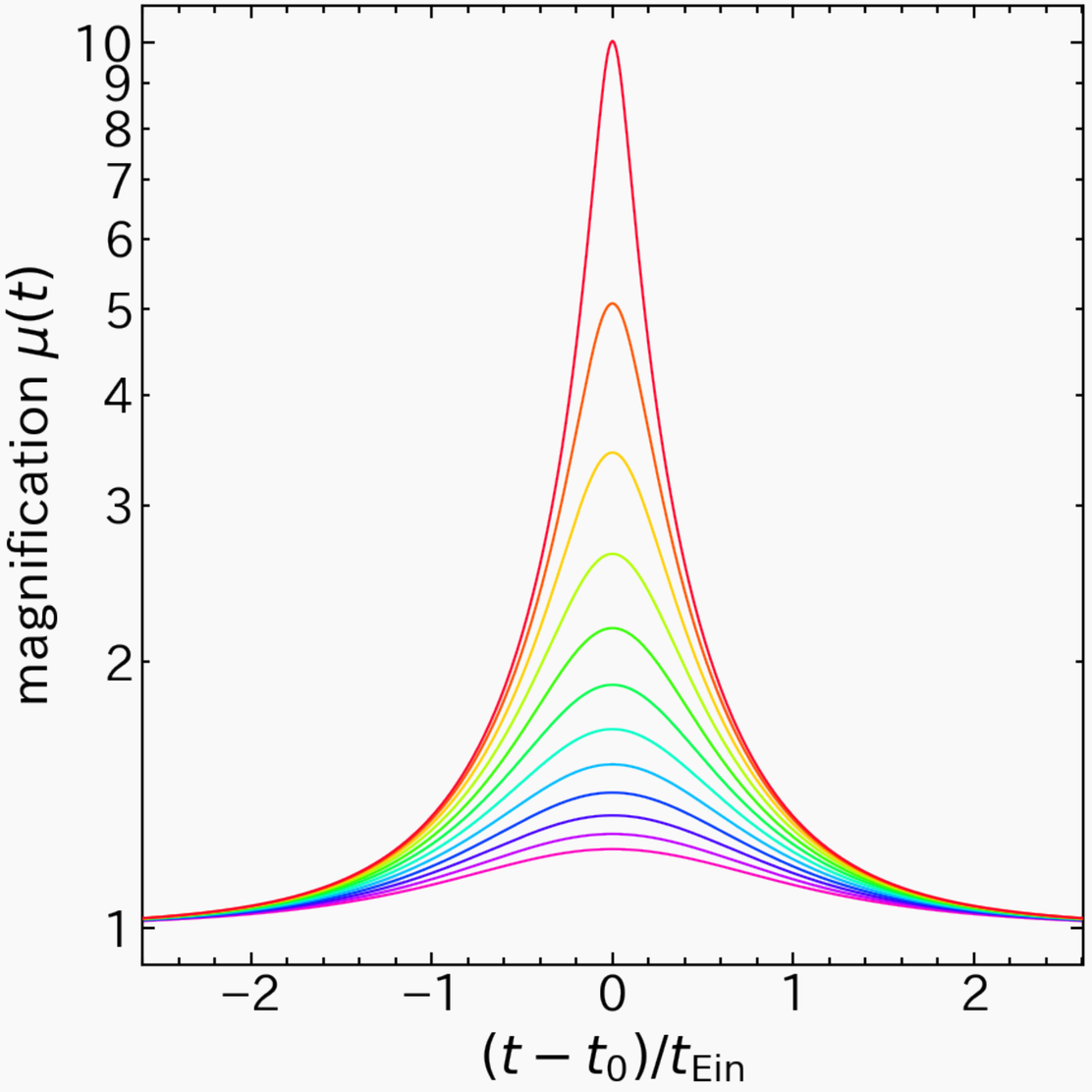

Physical quantities from magnification curve

- physical quantities obtained from magnification curve are

$$y_0 = \frac{\beta_0}{\theta_{\rm Ein}}$$

$$t_{\rm Ein} = \frac{(1+z_{\rm l})D_{\rm ol}\theta_{\rm Ein}}{v_\perp}$$

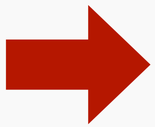

degeneracy between mass M, velocity $v_\perp$, distance D

- need other observables to break degeneracy

Effect of finite source size

- source is not point-like but has finite radius

$$\rho_* = \frac{\beta_*}{\theta_{\rm Ein}}$$ normalized radius of source

$$\mu(t, \rho_*) = \frac{1}{\pi\rho_*^2} \int_0^{2\pi} d\varphi \int_0^{\rho_*} d\rho\, \rho \mu_{\rm tot} \left(\sqrt{\left\{ y(t) + \rho\cos\varphi \right\}^2 + \left\{ \rho \sin\varphi \right\}^2} \right)$$

assume uniform brightness

$\theta_{\rm Ein}$ can be inferred if β_* is estimated with some methods

Magnification curve for finite source size

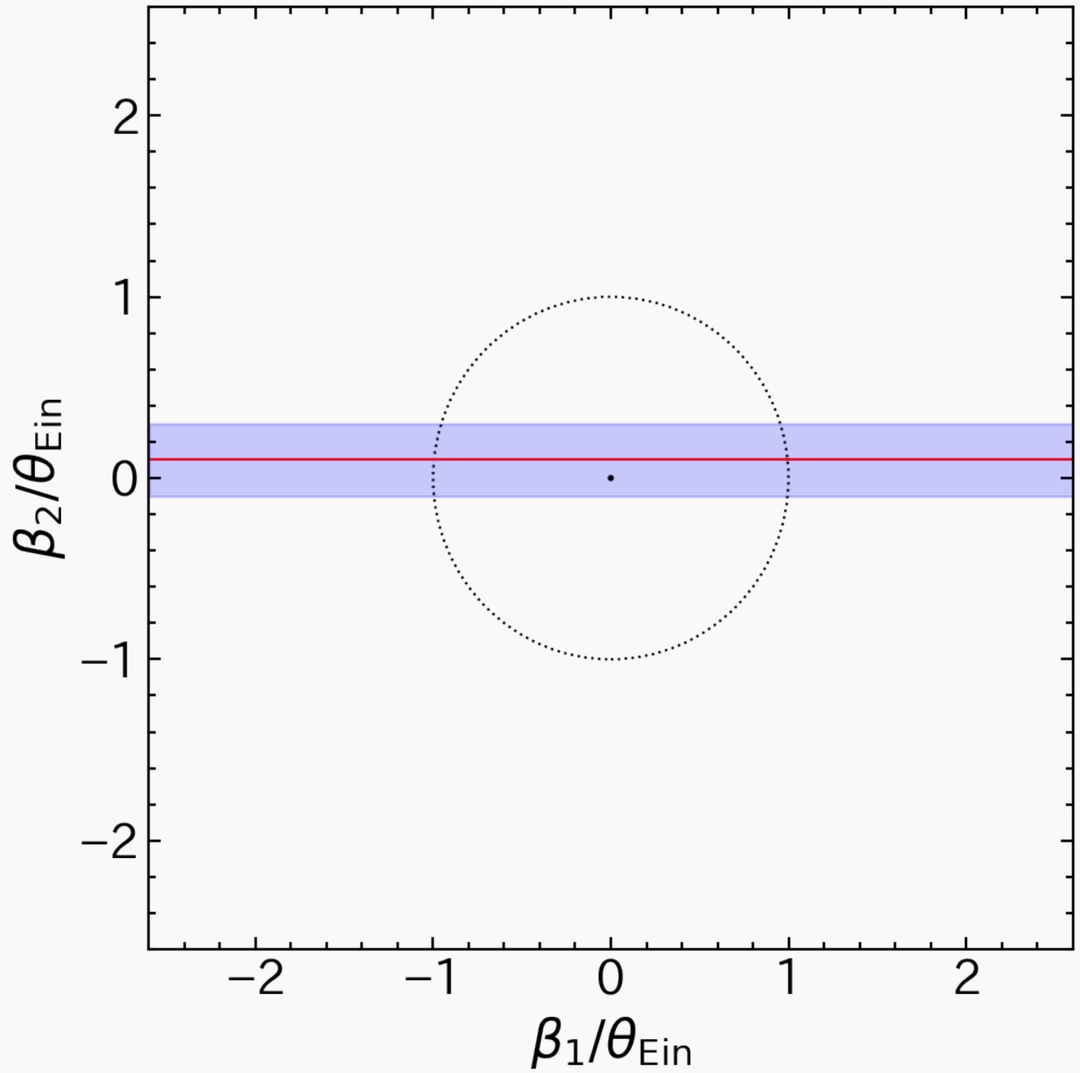

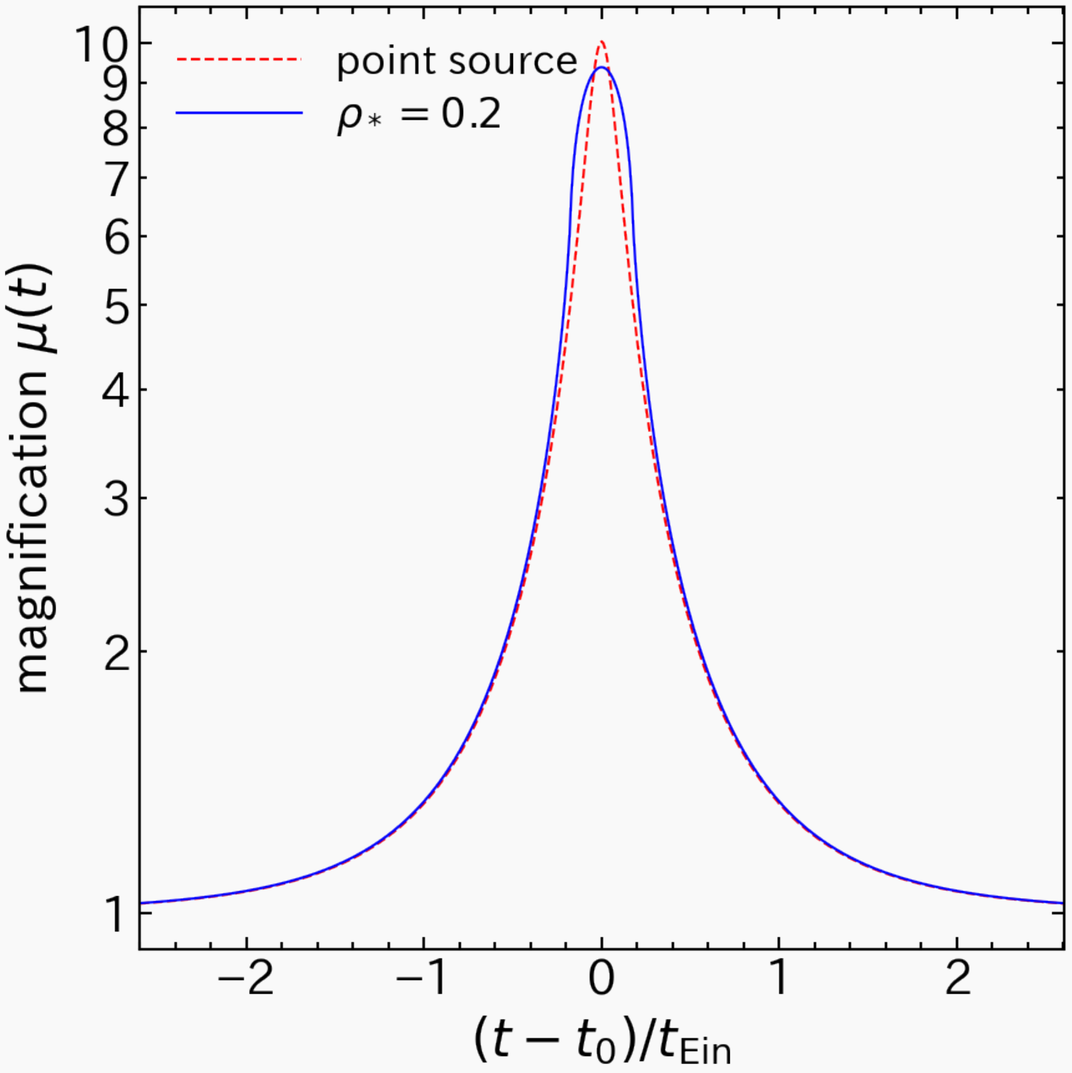

Microlensing parallax

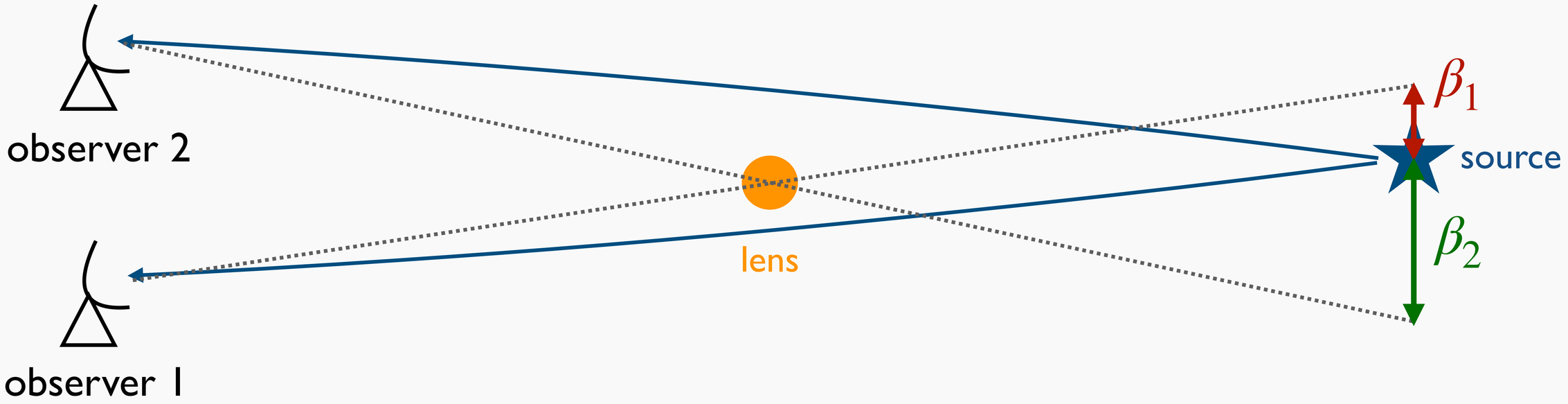

- observers at different positions → different source positions → different magnifications
- distance between observers known → $\sim D\theta_{\mathrm{Ein}}$ can be measured

Various parallax

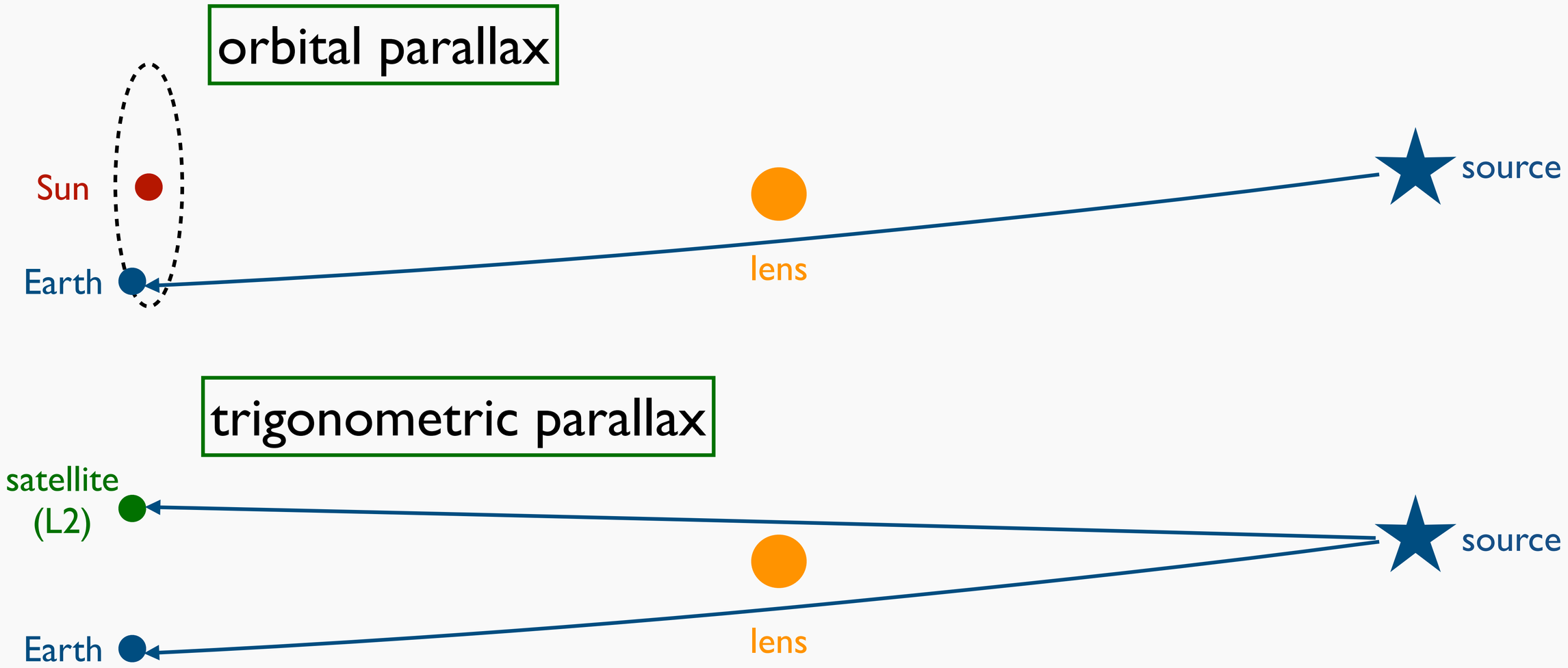

Orbital parallax

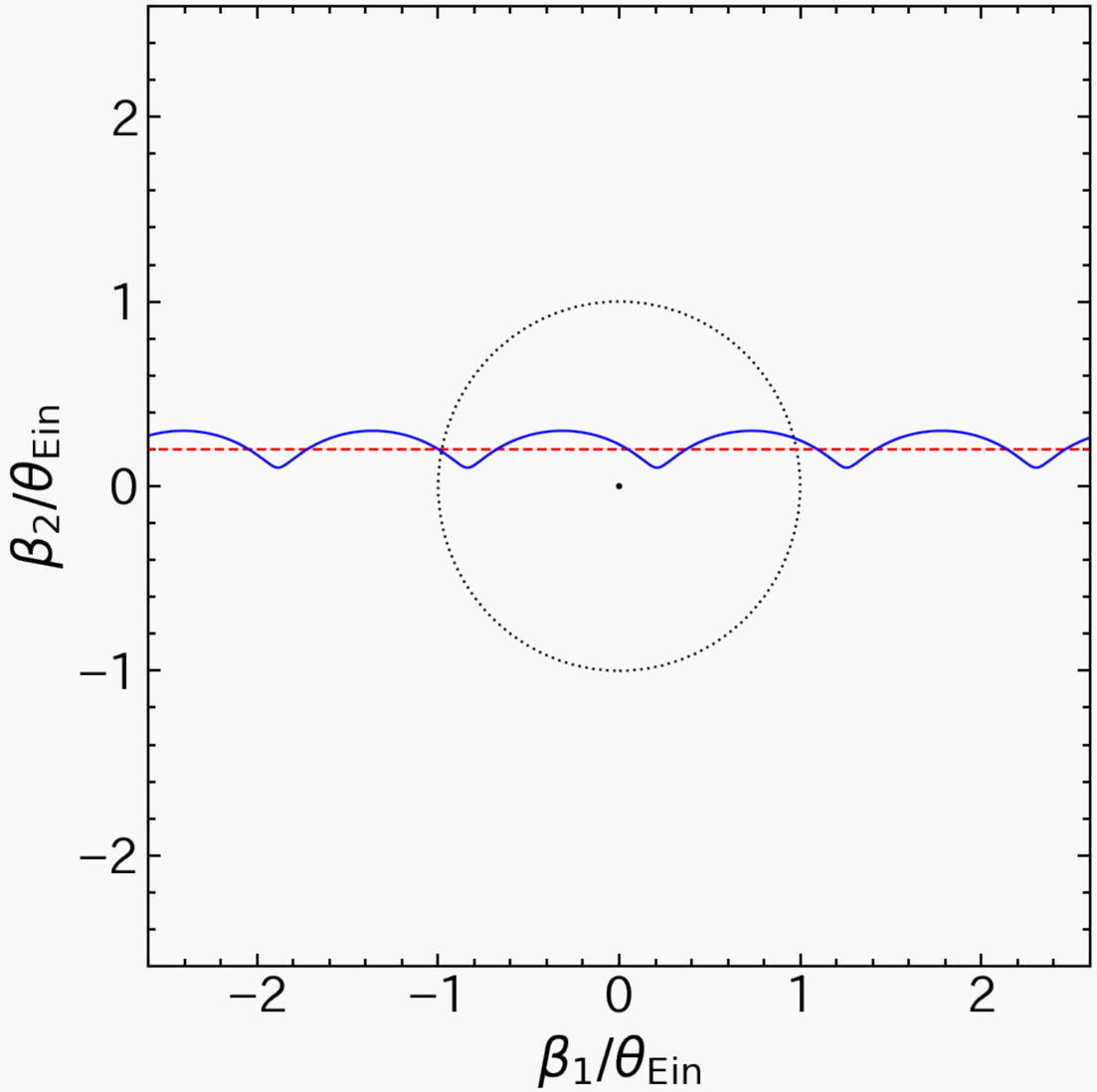

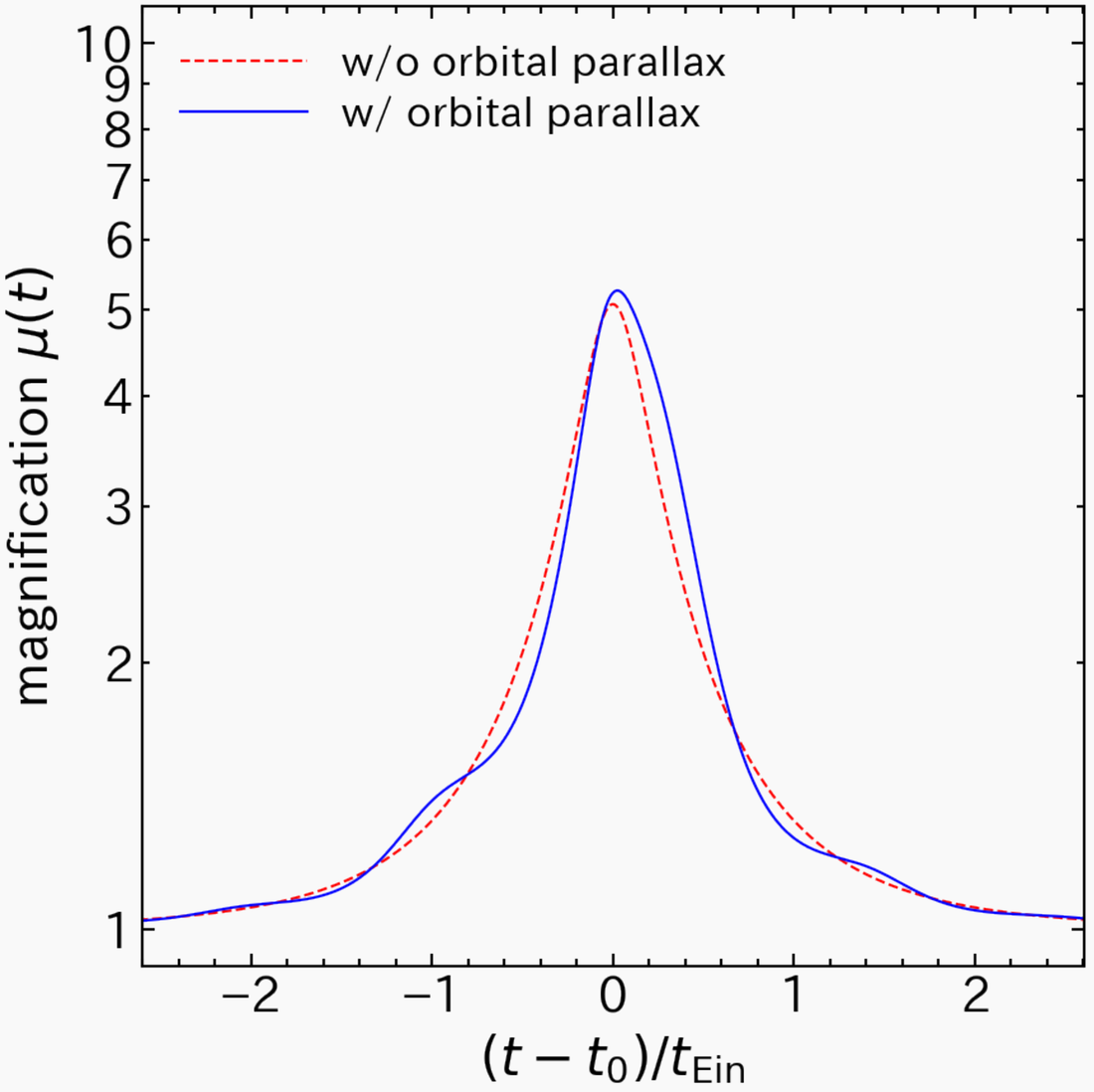

Trigonometric parallax

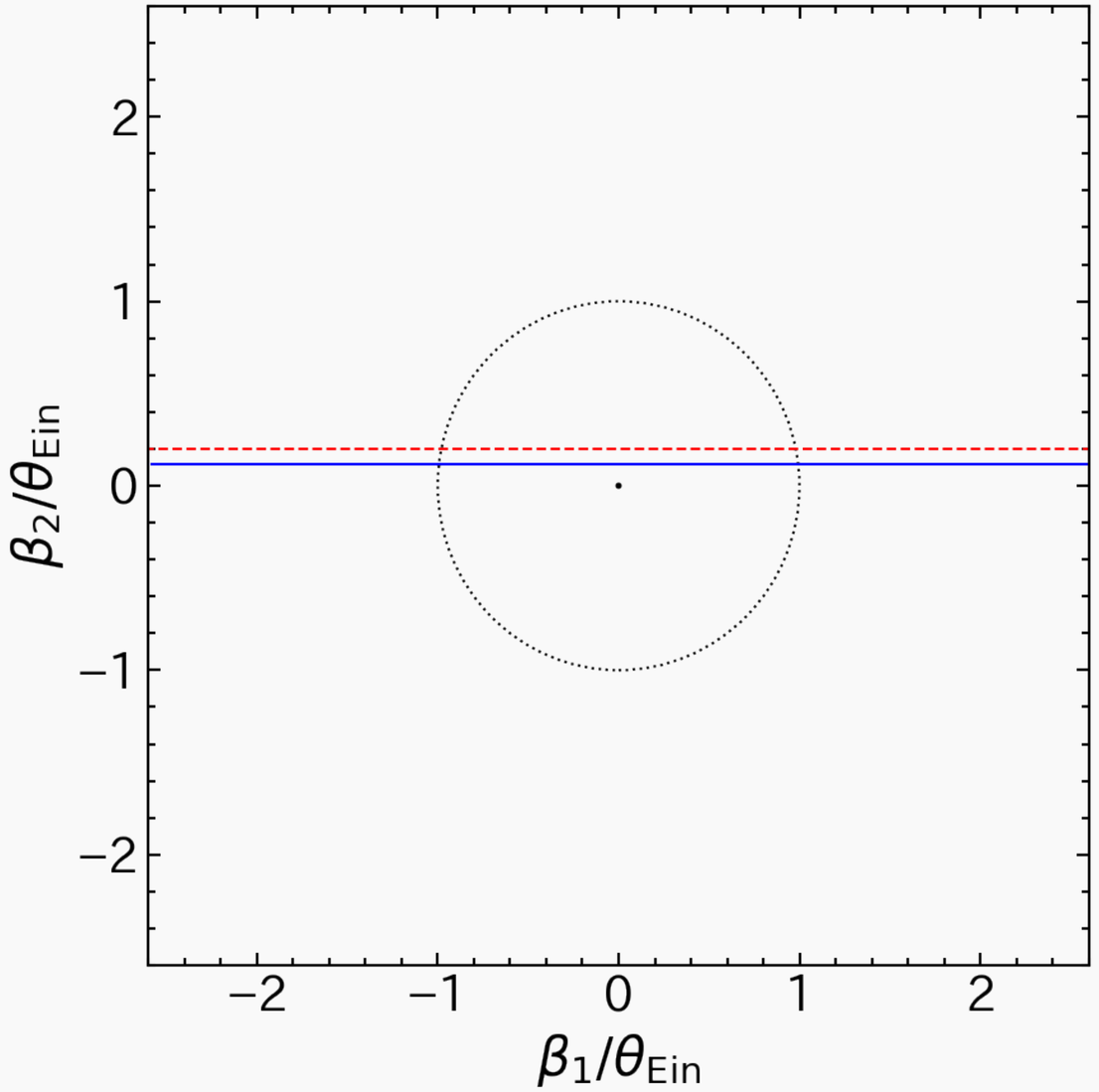

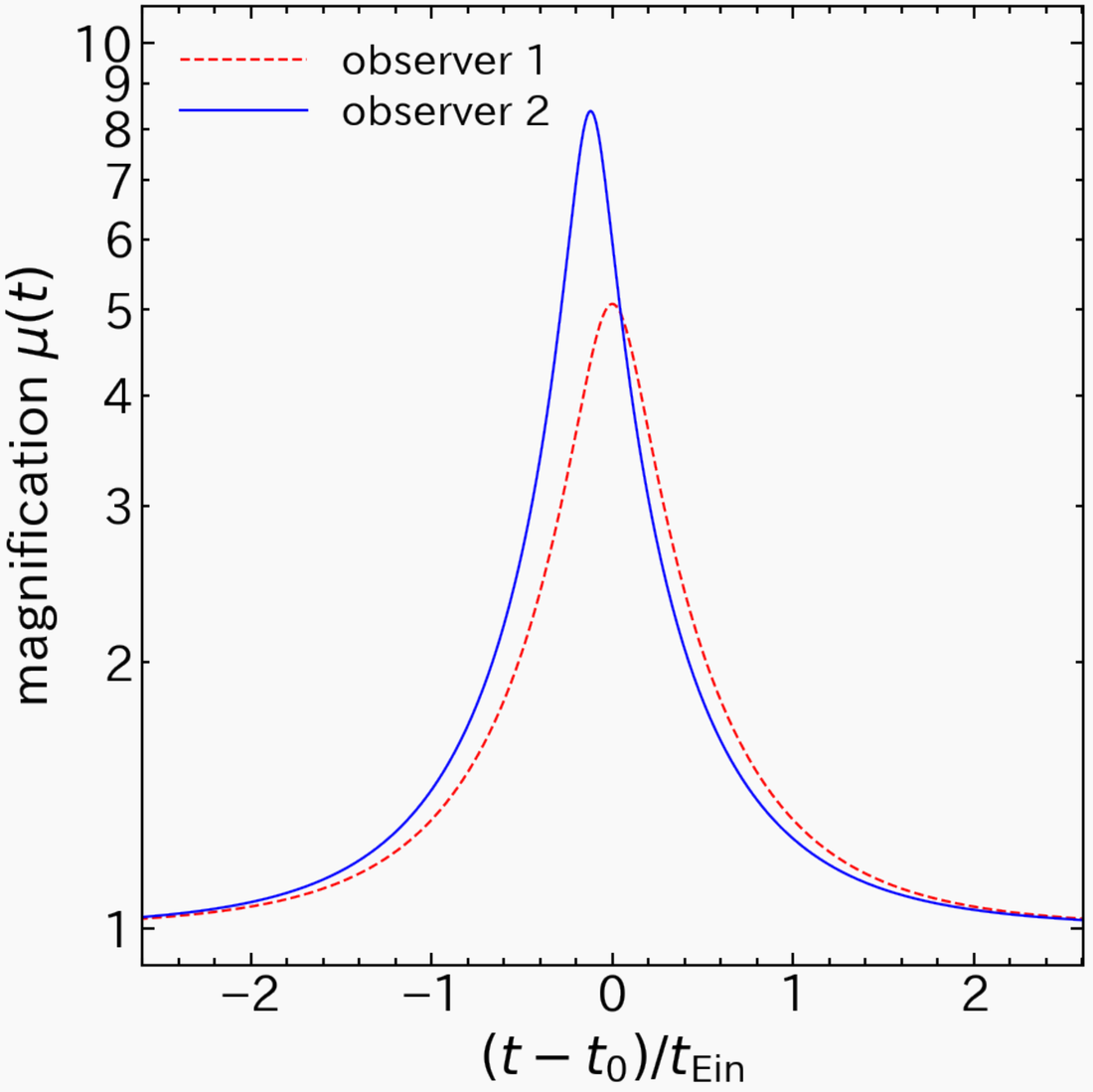

Examples of parallax observations

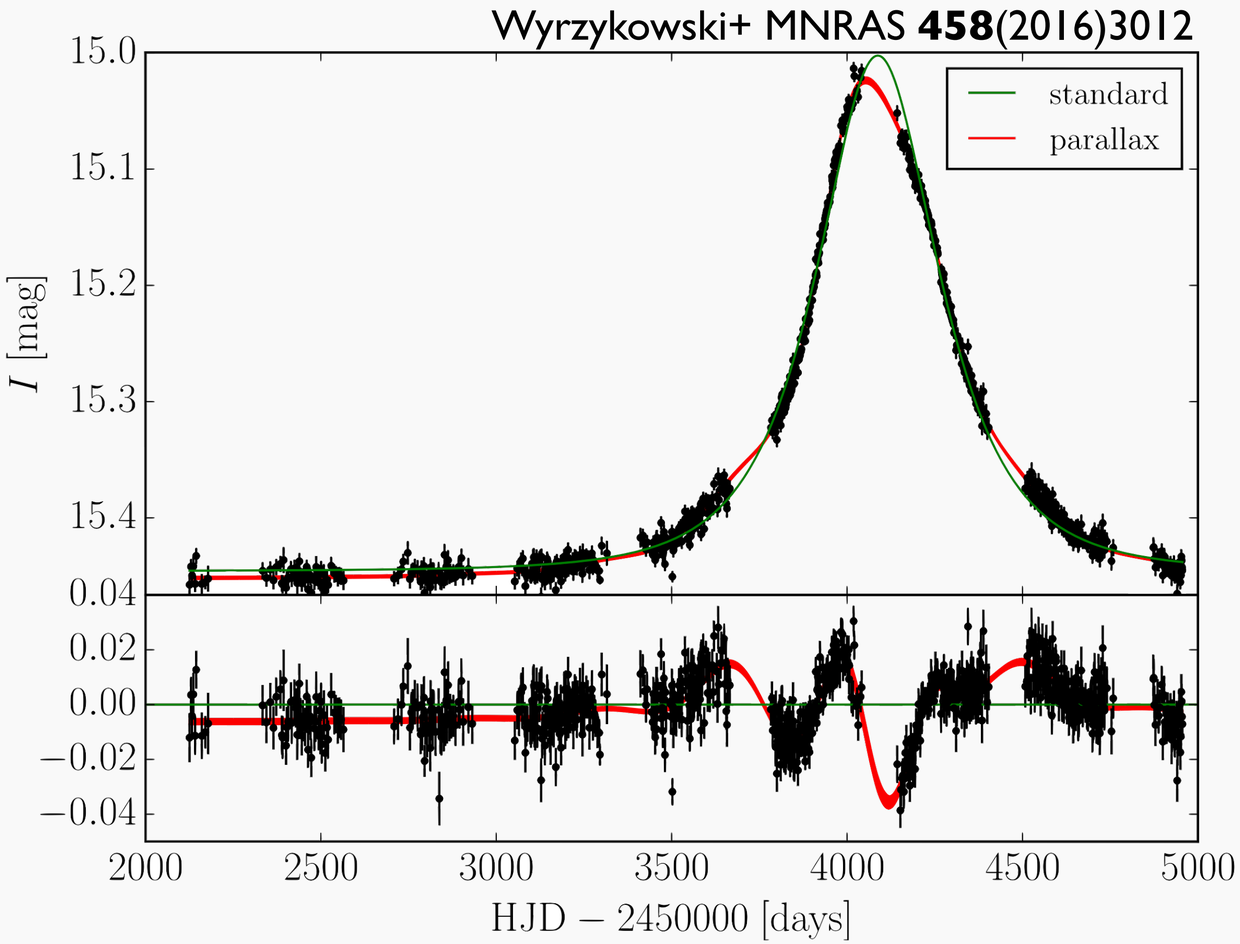

orbital parallax
(OGLE3-ULENS-PAR-02)

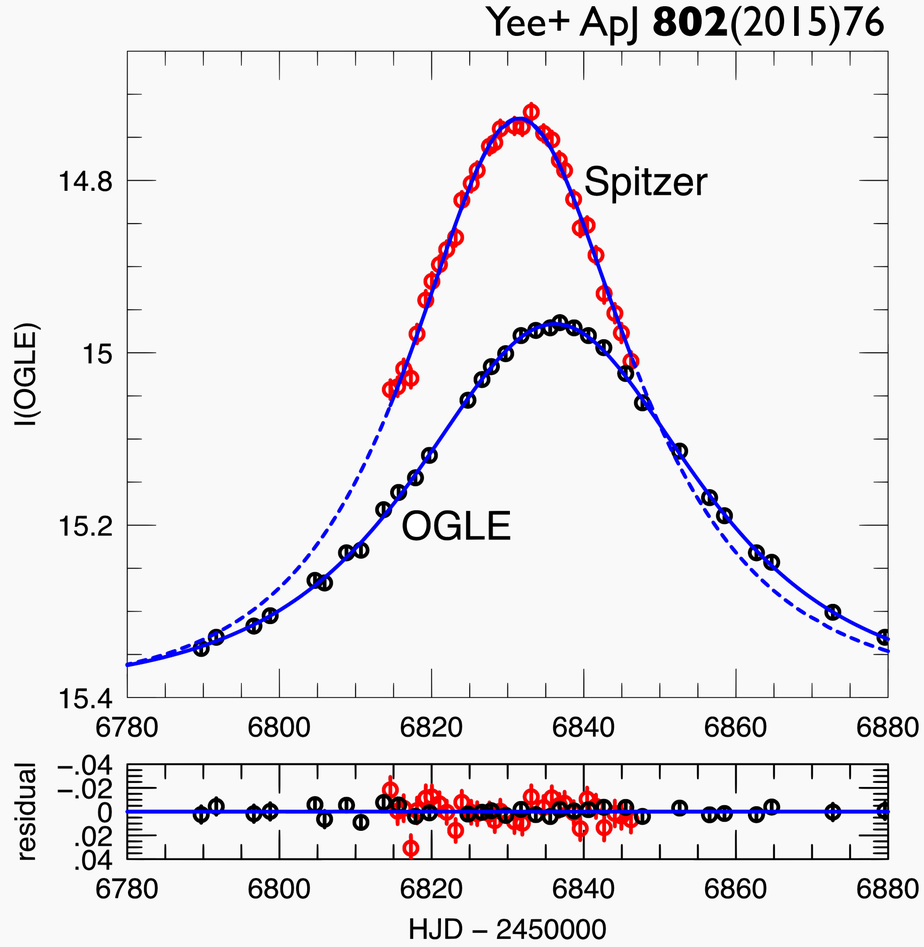

trigonometric parallax
(OGLE-2014-BLG-0939)

Microlensing probability

- calculation similar to strong lensing probability

$$P_{\rm ml}(z_{\rm s};\,>\mu_{\rm th}) = \int_0^{z_{\rm s}} dz_{\rm l} \frac{d^2V}{dz_{\rm l}d\Omega} \int_0^{\infty} dM \frac{dn}{dM} \sigma_{\rm ml}(M;\,z_{\rm l}, z_{\rm s},\,>\mu_{\rm th})$$

- microlensing cross section

Einstein radius of point mass lens

$$\sigma_{\rm ml}(M;\,z_{\rm l}, z_{\rm s},\,>\mu_{\rm th}) = \pi\theta_{\rm Ein}^2 y_{0,\,\rm max}^2(\mu_{\rm th})$$

$$= \frac{4\pi GM}{c^2} \frac{D_{\rm ls}}{D_{\rm ol}D_{\rm os}} y_{0,\,\rm max}^2(\mu_{\rm th})$$

calculate from $\mu_{\rm tot}(y)$ of point mass lens

$$y_{0,\,\rm max}^2(\mu_{\rm th}) = \frac{2}{\mu_{\rm th}\sqrt{\mu_{\rm th}^2 - 1} + \mu_{\rm th}^2 - 1}$$

Microlensing probability

- probability is proportional to mean mass density of lens

$$\int_0^\infty dMM\frac{dn}{dM} = \rho$$

- does not depend on mass M!

Microlensing rate

- probability that microlensing happens within a unit time

$$\Gamma_{\rm ml}(z_{\rm s};>\mu_{\rm th}) = \int_0^{z_{\rm s}} dz_{\rm l} \frac{d^2V}{dz_{\rm l}d\Omega} \int_0^{\infty} dM \frac{dn}{dM} \frac{d\sigma_{\rm ml}}{dt}$$

$$\frac{d\sigma_{\rm ml}}{dt} = \frac{2\theta_{\rm Ein}^2 y_{0,\,\rm max}}{t_{\rm Ein}}$$

$\Gamma_{\rm ml} \sim \frac{P_{\rm ml}}{t_{\rm Ein}}$, depends on lens mass M through $t_{\rm Ein}$

Dark matter search with microlensing

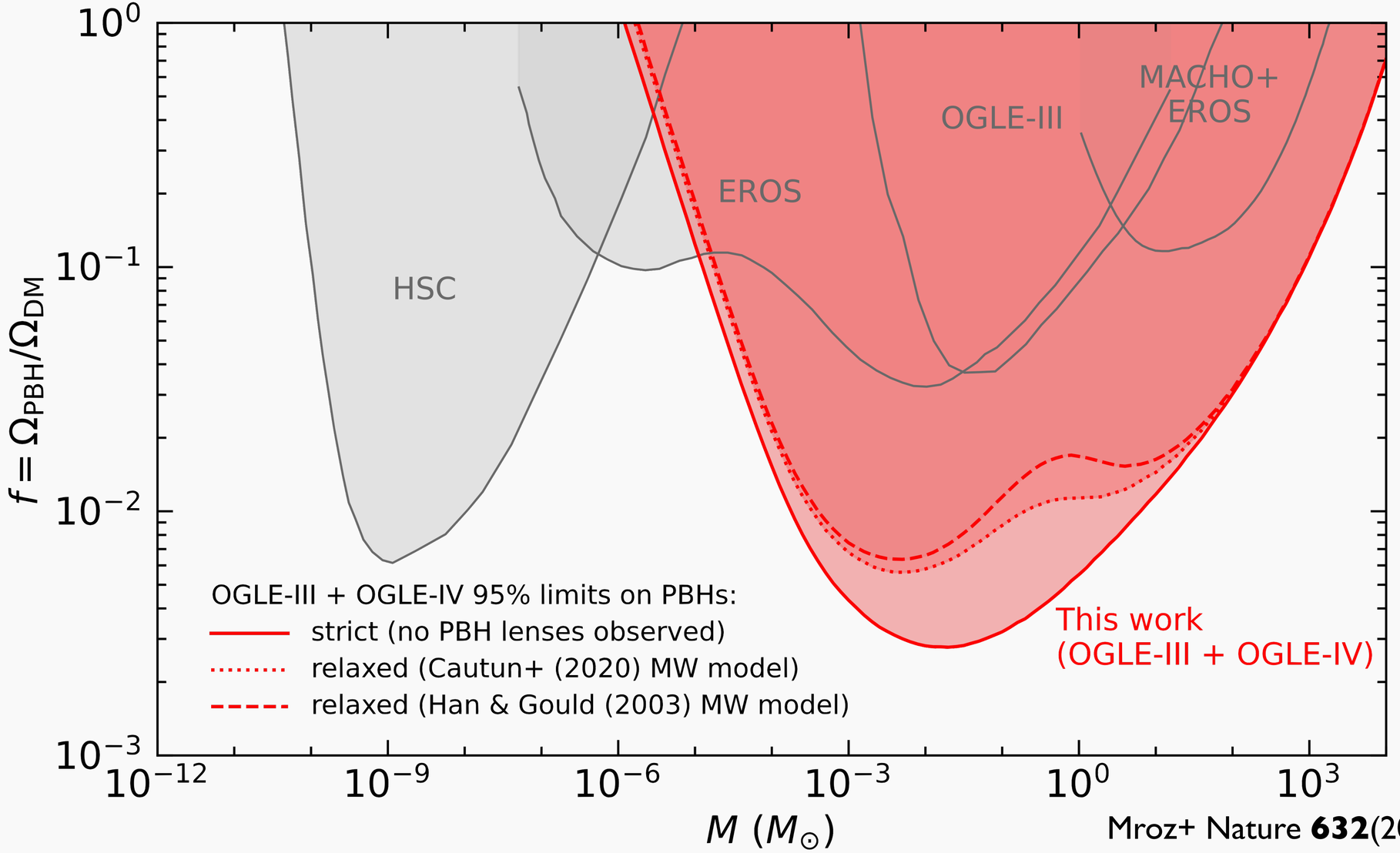

Mroz+ Nature **632**(2024)749

movie file: https://oguri.github.io/for_presen.html

Non-spherically sym. lens: caustic crossing

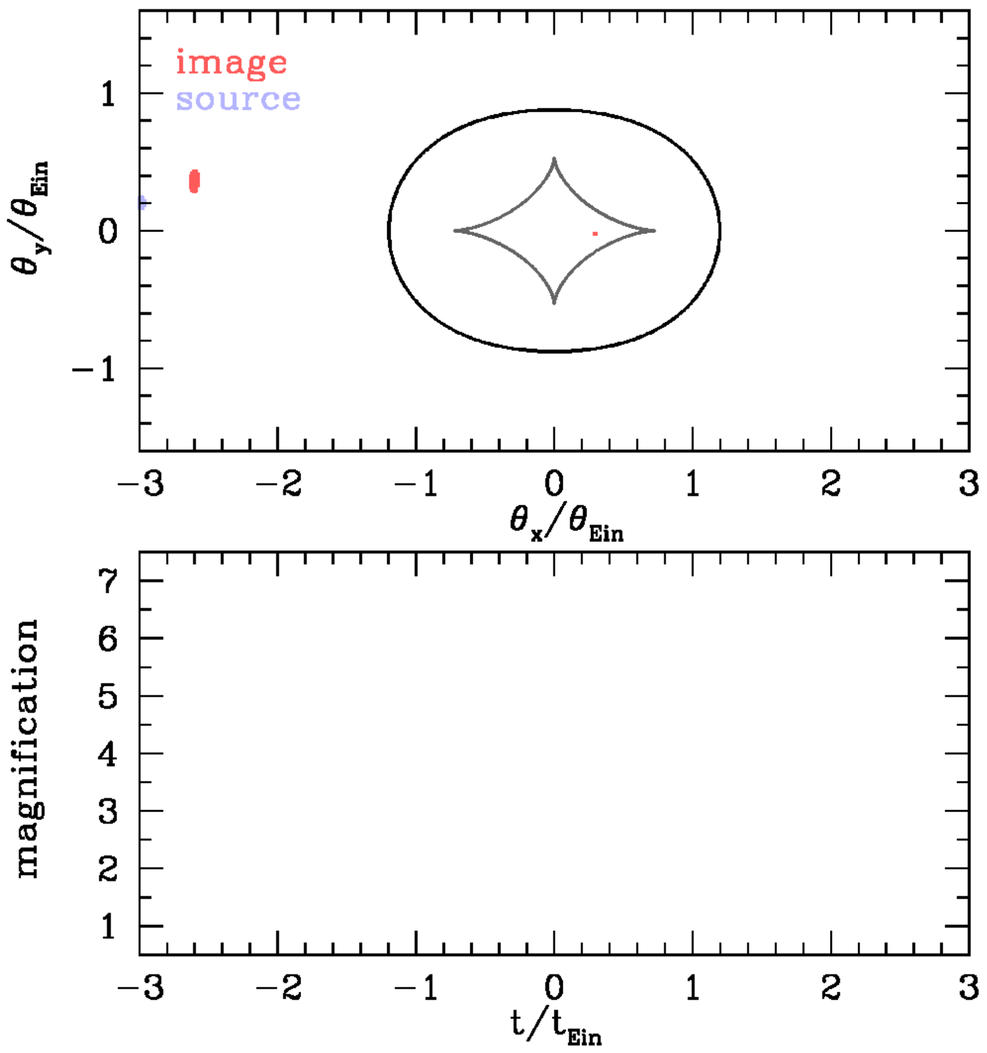

Microlensing by binary lens

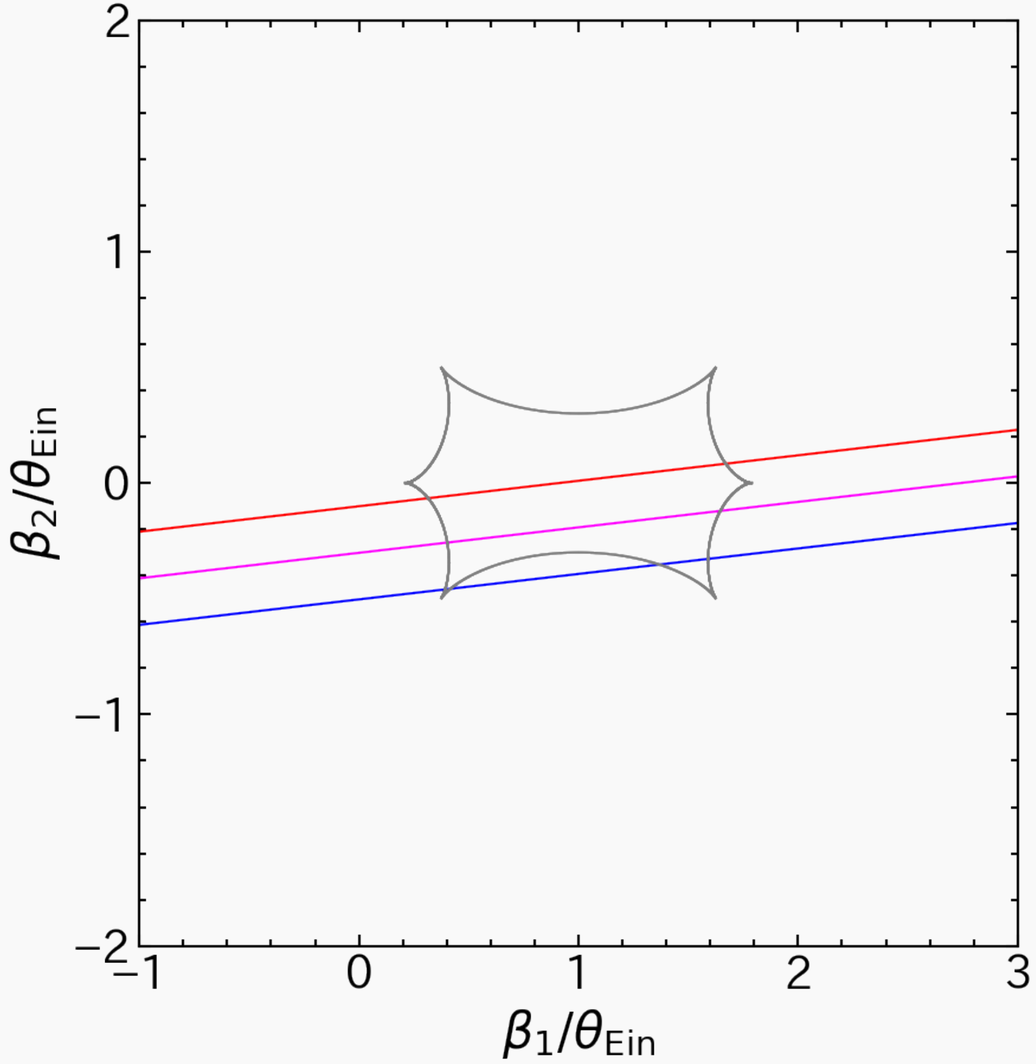

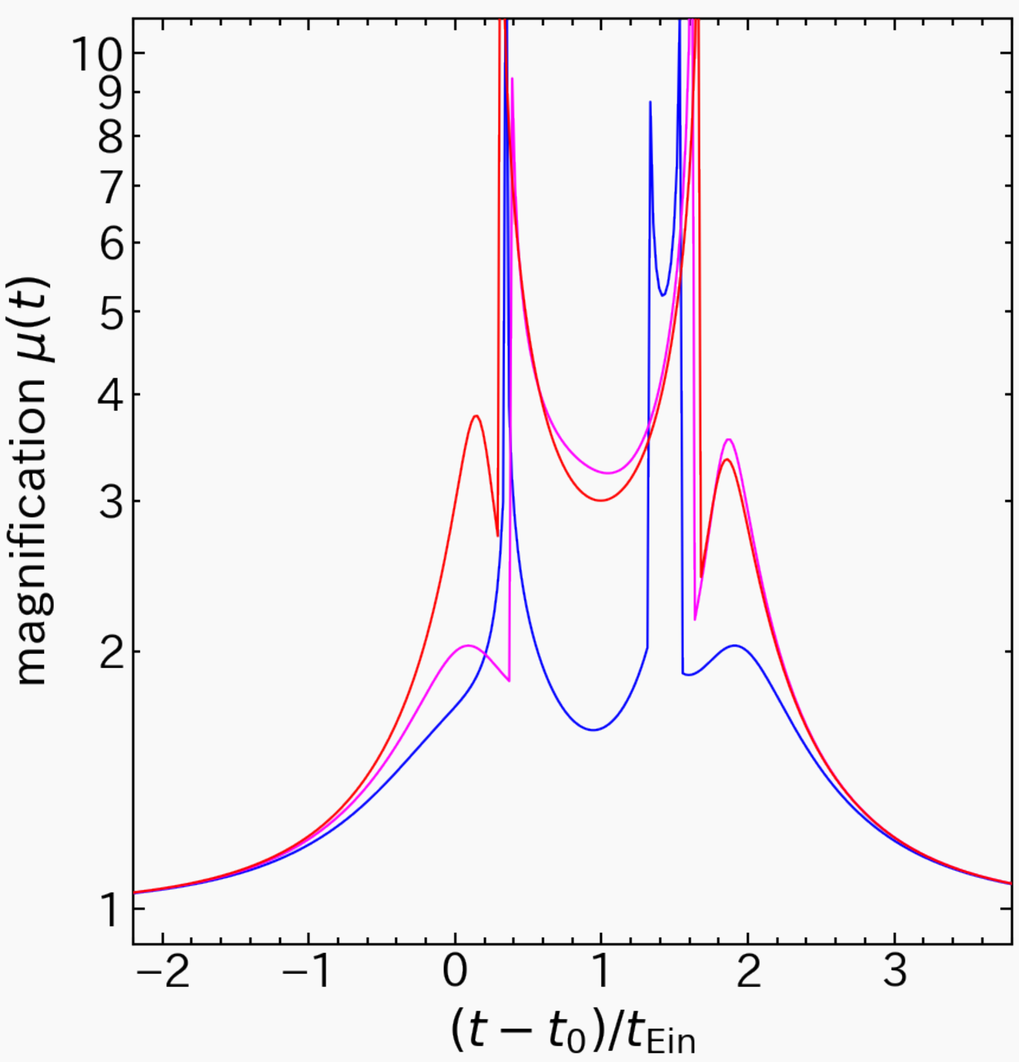

Microlensing search of exoplanet

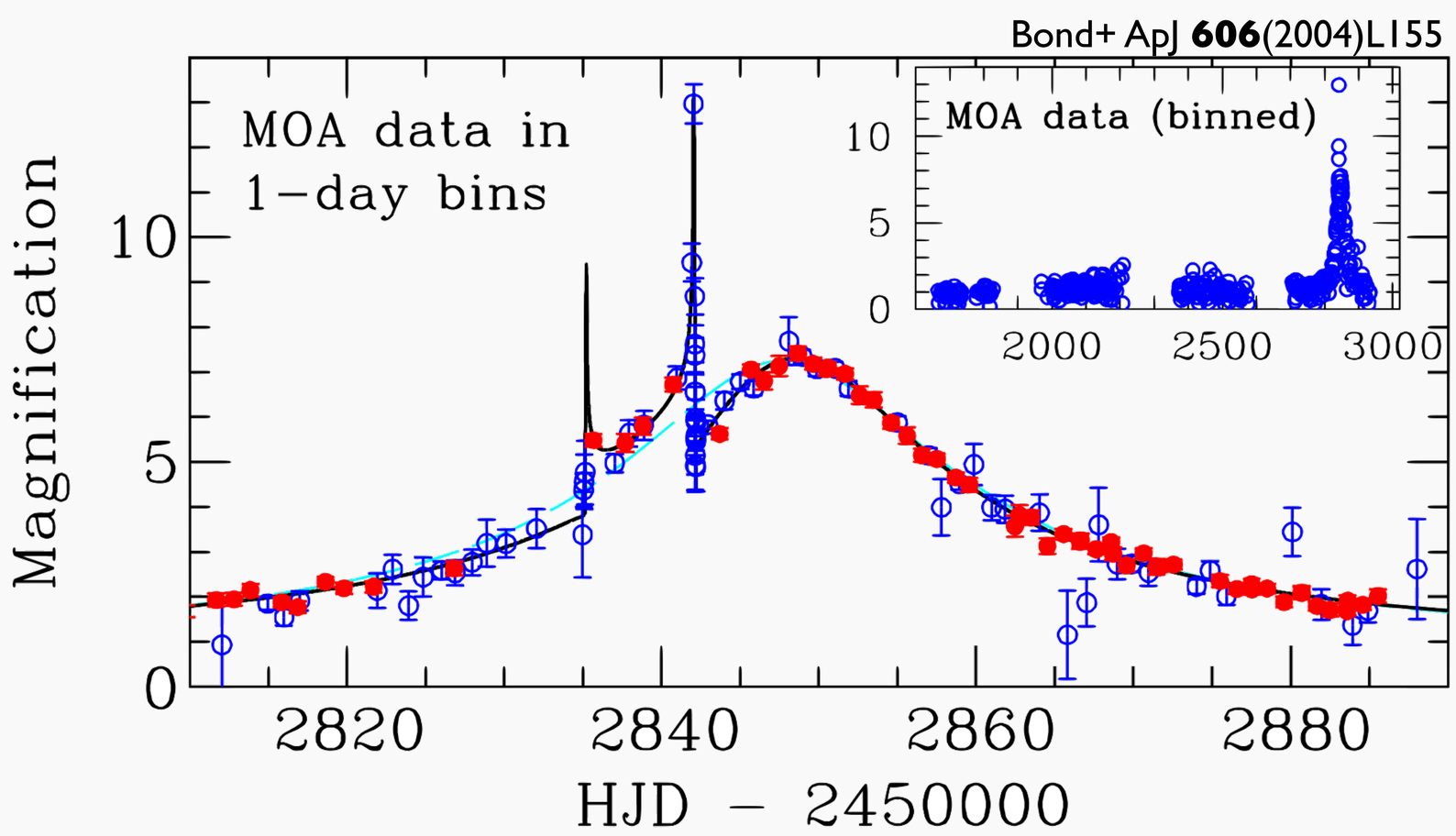

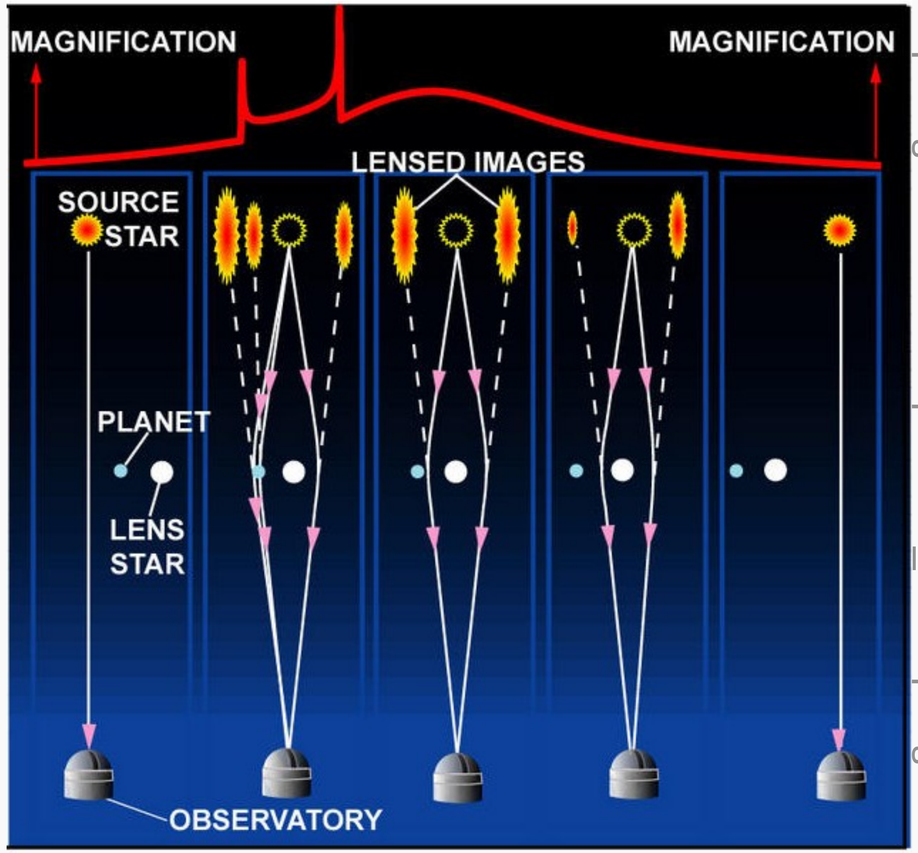

https://ogle.astrouw.edu.pl/cont/4_main/epl/blg235/

Microlensing at cosmological distances

Fudamoto+ (incl. MO) Nat. Ast. **9**(2025)428

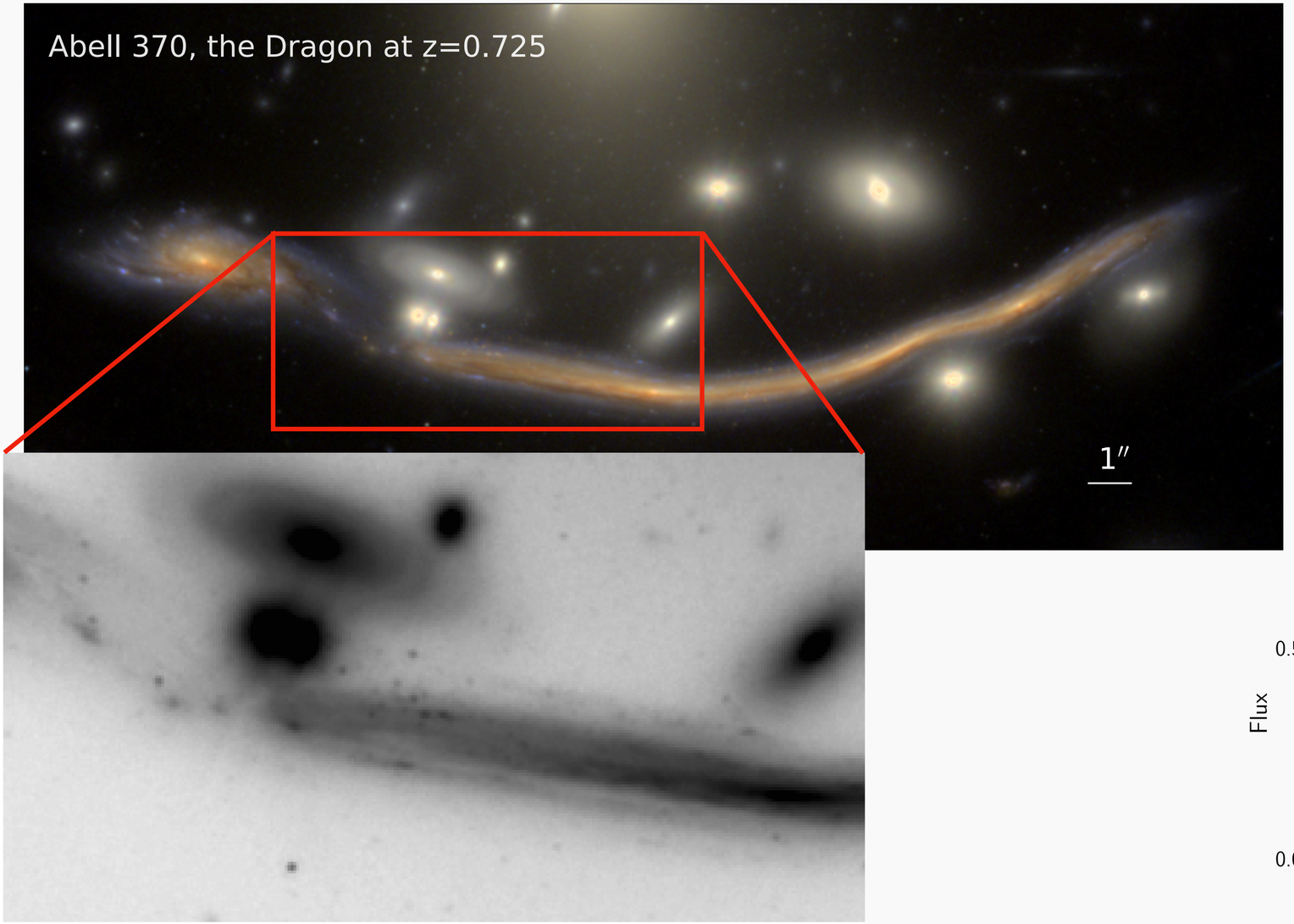

Kelly+ (incl. MO) Nat. Ast. **2**(2018)334

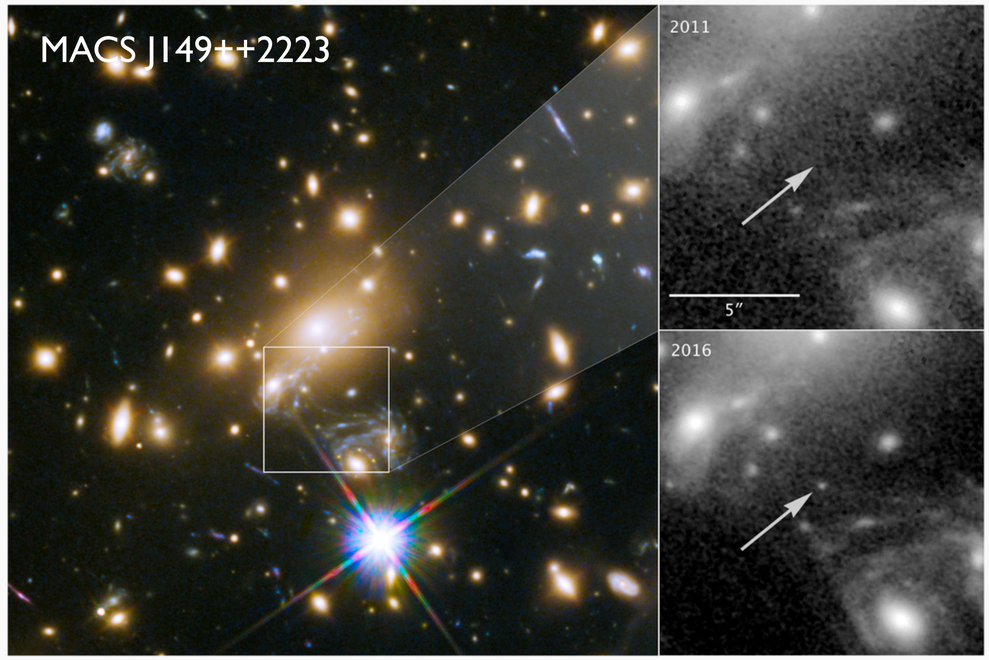

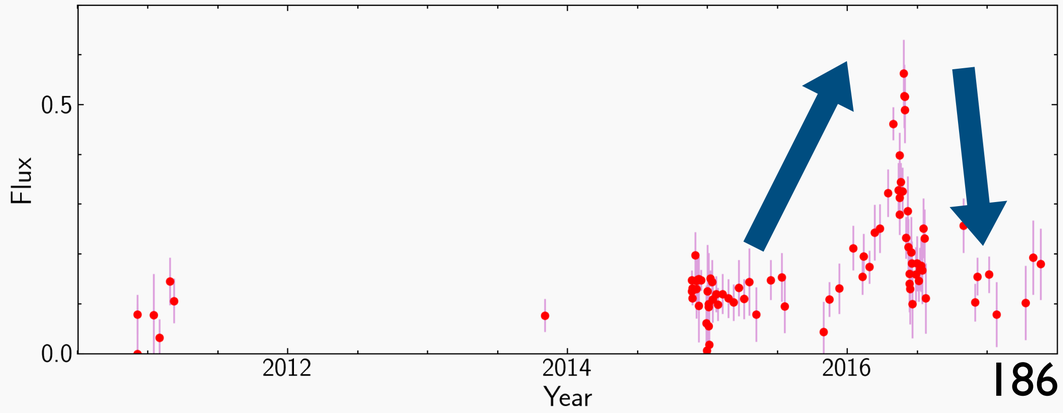

Summary

- from observation of magnification curve, information on impact parameter and Einstein time are obtained
- degeneracy can be broken by finite source size effect or microlensing parallax
- microlensing probability constrains fraction of compact dark matter

7. Weak lensing

Principle of weak lensing measurement

- each galaxy has intrinsic shape (ellipticity), but assume its orientation is random
- by taking average of galaxy shapes in some region, intrinsic shapes are average out, and shear in that region can be inferred

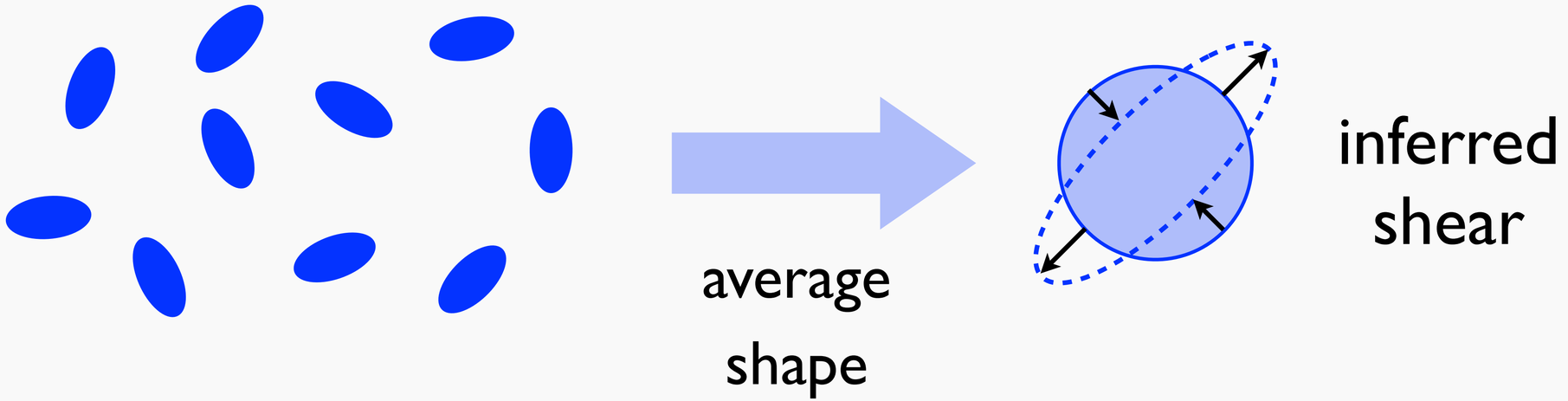

Shape measurement method (I)

- define galaxy shape by 2nd moment of intensity $I(\boldsymbol{\theta})$

$$Q_{ab} = \frac{\int d\boldsymbol{\theta} I(\boldsymbol{\theta}) \theta_a \theta_b}{\int d\boldsymbol{\theta} I(\boldsymbol{\theta})}$$

coord. origin = galaxy center

- define complex ellipticity and shear for convenience

$$\epsilon = \frac{Q_{11} - Q_{22} + 2iQ_{12}}{Q_{11} + Q_{22}}$$

complex ellipticity

$$\gamma = \gamma_1 + i\gamma_2$$

complex shear

Shape measurement method (II)

- from $\delta\boldsymbol{\beta} = A(\boldsymbol{\theta})\delta\boldsymbol{\theta}$, relation between intrinsic shape $Q_{ab}^{(\mathrm{s})}$ and observed shape Q_{ab} is

$$Q_{ab}^{(\mathrm{s})} = \frac{\int d\boldsymbol{\beta} I(\boldsymbol{\beta})\beta_a\beta_b}{\int d\boldsymbol{\beta} I(\boldsymbol{\beta})} \simeq A_{ac}A_{bd}Q_{cd}$$

A: Jacobi matrix

intensity conserved $I^{(\mathrm{s})}(\boldsymbol{\beta}) = I(\boldsymbol{\theta})$

small galaxy shape $\int d\boldsymbol{\beta} = \int d\boldsymbol{\theta} \, |\det A| \simeq |\det A| \int d\boldsymbol{\theta}$

Shape measurement method (III)

- inserting expression of Jacobi matrix to compute

$$\epsilon^{(\mathrm{s})} = \frac{(1-\kappa)^2\epsilon - 2(1-\kappa)\gamma + \gamma^2\epsilon^*}{(1-\kappa)^2 + |\gamma|^2 - 2(1-\kappa)\mathrm{Re}(\gamma\epsilon^*)}$$

$$= \frac{\epsilon - 2g + g^2\epsilon^*}{1 + |g|^2 - 2\mathrm{Re}(g\epsilon^*)}$$

$$g = \frac{\gamma}{1-\kappa}$$

reduced shear

inverse

$g \to -g$

$$\epsilon = \frac{\epsilon^{(\mathrm{s})} + 2g + g^2\epsilon^{(\mathrm{s})*}}{1 + |g|^2 + 2\mathrm{Re}(g\epsilon^{(\mathrm{s})*})}$$

Shape measurement method (IV)

- ignoring higher order terms and take average

$$\langle \epsilon \rangle \simeq \langle \epsilon^{(\mathrm{s})} + 2g \rangle \simeq 2\langle g \rangle \simeq 2\langle \gamma \rangle$$

average of observed galaxy ellipticity in some region on the sky

average shear in that region

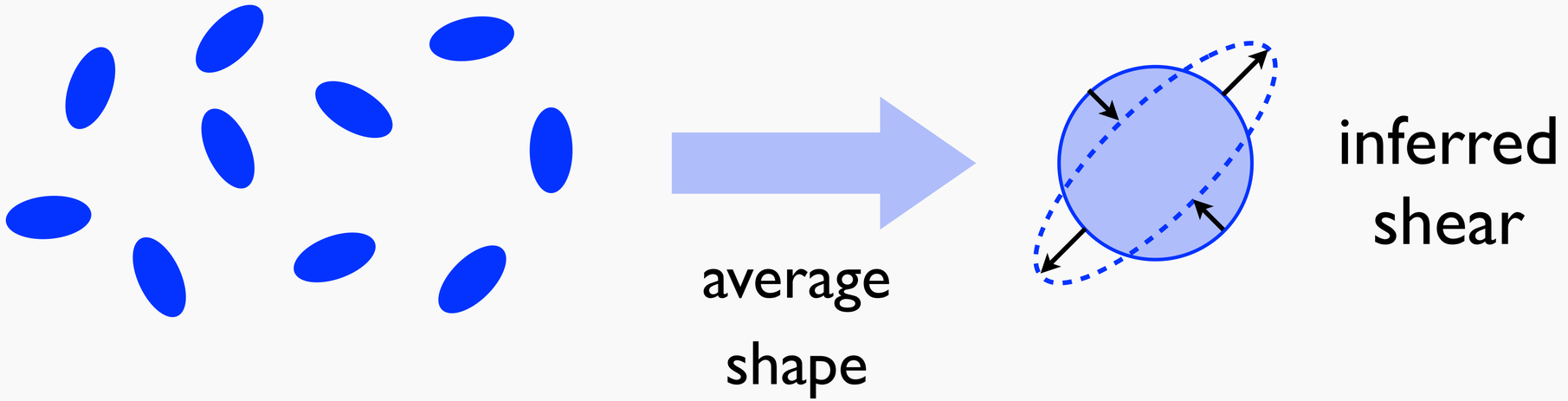

Noise of weak lensing measurement

- ignoring higher order terms and take average

$$\langle \epsilon \rangle \simeq \underbrace{\langle \epsilon^{(s)} \rangle}_{\text{noise}} + \underbrace{2\langle \gamma \rangle}_{\text{signal}}$$

$$\sim \sigma_{\epsilon/2}/\sqrt{N}$$

$$\frac{S}{N} \sim \frac{\sqrt{N}\gamma}{\sigma_{\epsilon/2}}$$

$\gamma \sim 0.03$ (galaxy, cluster) 0.003 (cosmic shear)

shapes of $N \sim 10^3 - 10^5$ galaxies needed

intrinsic ellipticity $\sigma_{\epsilon/2} \sim 0.3$

Measurement in real data

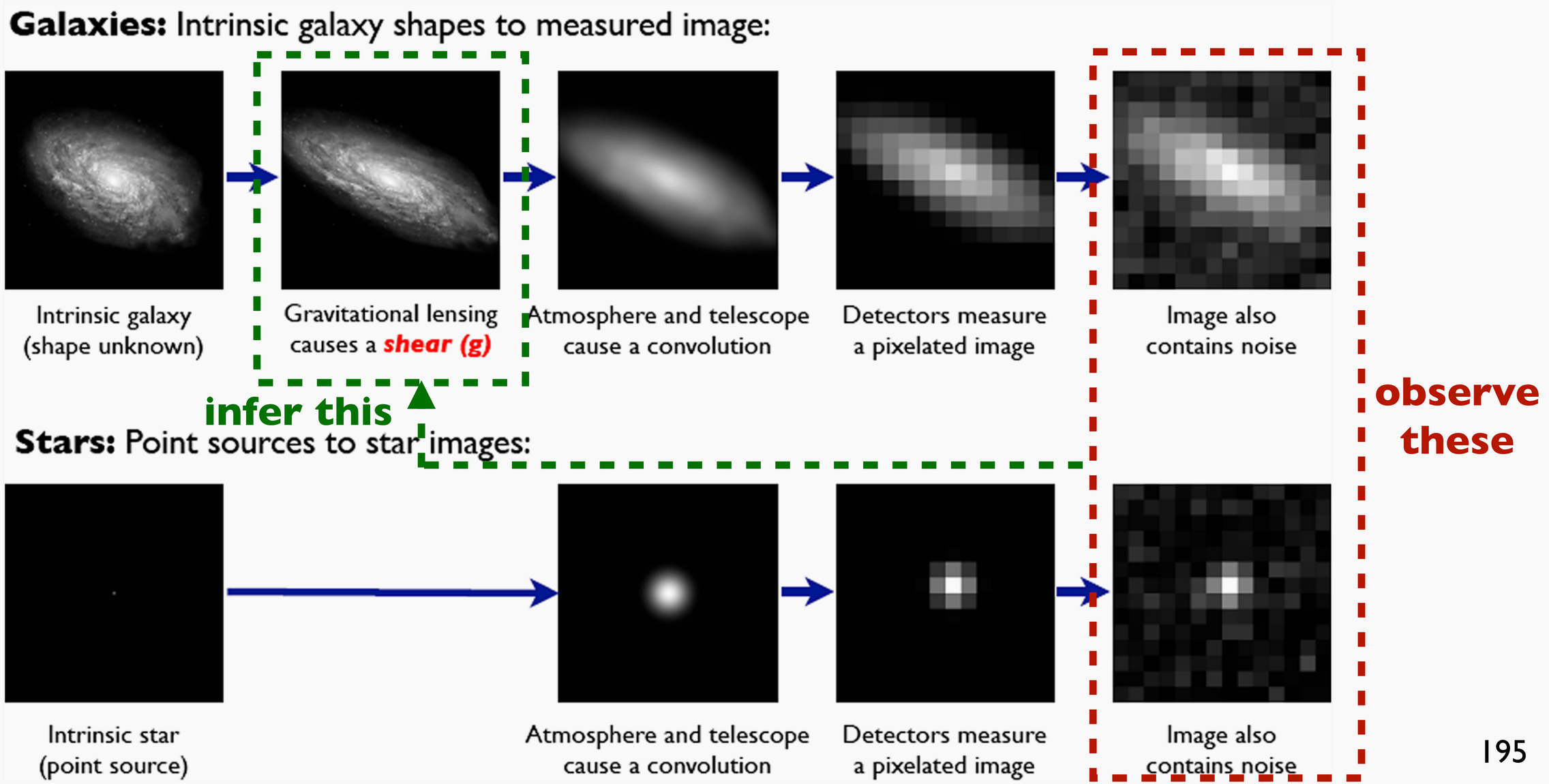

Tangential shear analysis

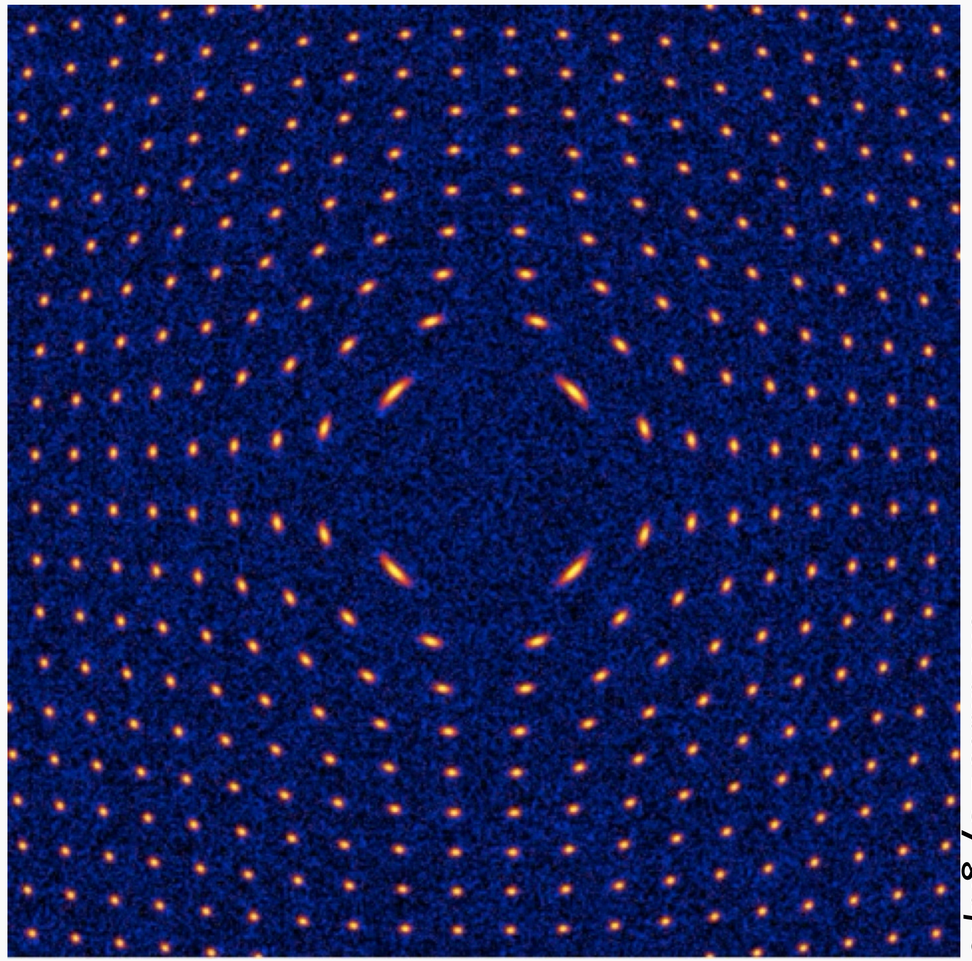

simulated by *glafic*

lens object at the center

- determine origin, and measure tangential shear γ_+ and cross shear $\gamma_\times$ around it
- lens signal corresponds to γ_+

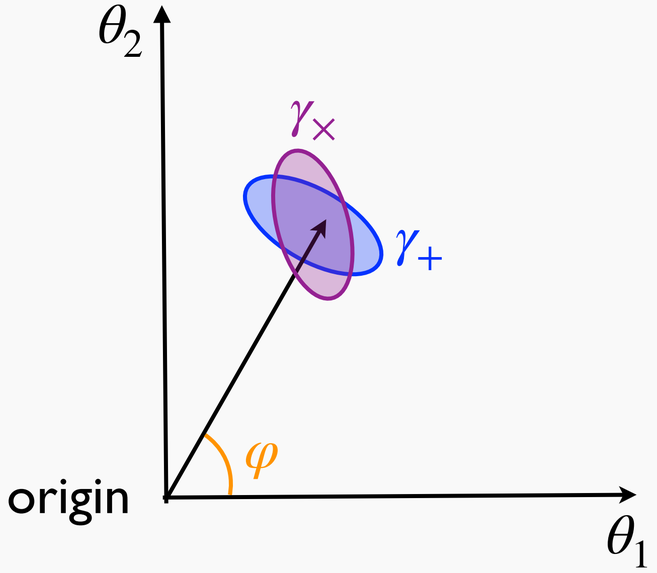

Tangential shear analysis

- definition of tangential shear γ_+ and cross shear $\gamma_\times$

$$\gamma_+(\boldsymbol{\theta}) = -\gamma_1(\boldsymbol{\theta})\cos 2\varphi - \gamma_2(\boldsymbol{\theta})\sin 2\varphi = -\,\mathrm{Re}\left[\gamma(\boldsymbol{\theta})e^{-2i\varphi}\right]$$

$$\gamma_\times(\boldsymbol{\theta}) = \gamma_1(\boldsymbol{\theta})\sin 2\varphi - \gamma_2(\boldsymbol{\theta})\cos 2\varphi = -\,\mathrm{Im}\left[\gamma(\boldsymbol{\theta})e^{-2i\varphi}\right]$$

- for spherically symmetric lens (Chap. 4)

$$\gamma_+(\theta) = \bar{\kappa}(<\theta) - \kappa(\theta)$$

$$\gamma_\times(\theta) = 0$$

More general (non spherically symmetric) case

- average convergence $\bar{\kappa}(<\theta)$ and azimuthally averaged convergence $\kappa^{\rm ave}(\theta)$ for general mass distribution

$$\bar{\kappa}(<\theta) = \frac{1}{\pi\theta^2}\int_{|\boldsymbol{\theta}'|<\theta} d\boldsymbol{\theta}'\kappa(\boldsymbol{\theta}') = \frac{1}{2\pi\theta^2}\int_{|\boldsymbol{\theta}'|<\theta} d\boldsymbol{\theta}'\nabla^2_{\boldsymbol{\theta}'}\psi(\boldsymbol{\theta}')$$

$$= \frac{1}{2\pi\theta}\int_0^{2\pi} d\varphi\frac{\partial\psi}{\partial\theta}$$

2D Gauss's theorem

$$\bar{\kappa}^{\rm ave}(\theta) = \int_0^{2\pi}\frac{d\varphi}{2\pi}\kappa(\boldsymbol{\theta})$$

Tangential (cross) shear in general case

- by taking azimuthal average, relation similar to that in spherically symmetric case holds in general

$$\gamma_+^{\rm ave}(\theta) = \int_0^{2\pi} \frac{d\varphi}{2\pi} \gamma_+(\boldsymbol{\theta}) = \bar{\kappa}(<\theta) - \kappa^{\rm ave}(\theta)$$

$$\gamma_\times^{\rm ave}(\theta) = \int_0^{2\pi} \frac{d\varphi}{2\pi} \gamma_+(\boldsymbol{\theta}) = 0$$

Tangential shear analysis

- define annulus with radius θ
- take average of tangential shear of each galaxy j in the annulus

$$\bar{\gamma}_+(\theta) = \frac{\sum_j w_j \gamma_{+j}}{\sum_j w_j} \qquad w_j : \text{weight}$$

- compare observed $\bar{\gamma}_+(\theta)$ with theoretical model to infer physical quantities of lens such as mass

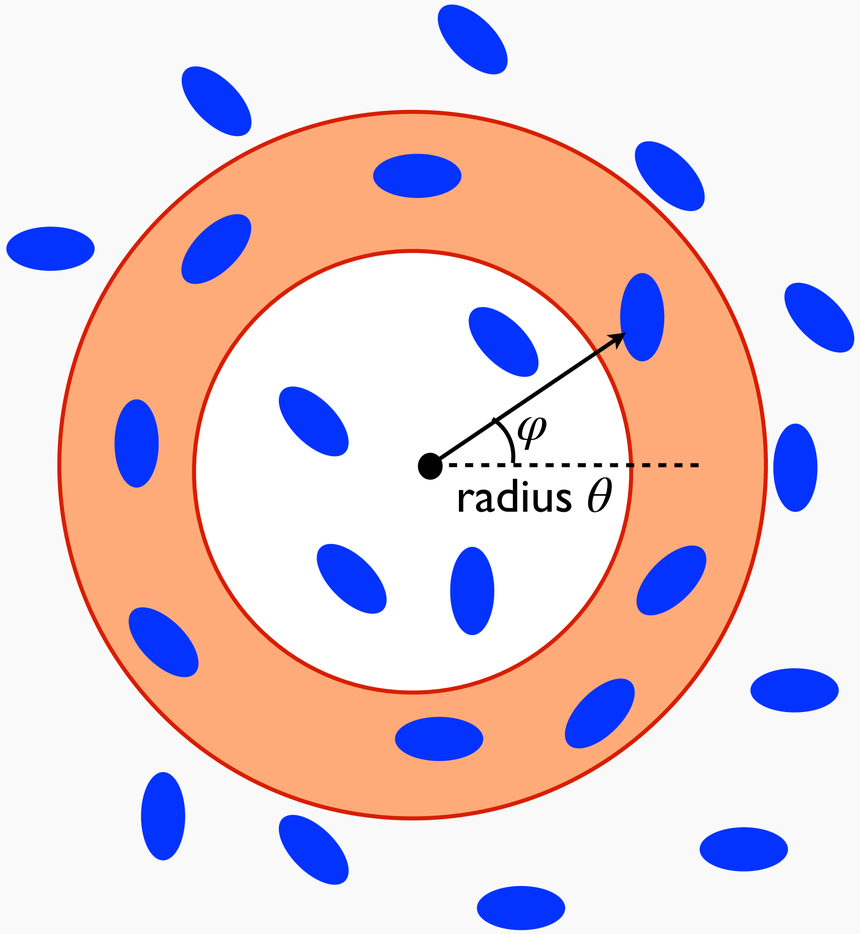

Example of analysis: SDSSJ1138+2754

Subaru/Suprime-cam gri-band

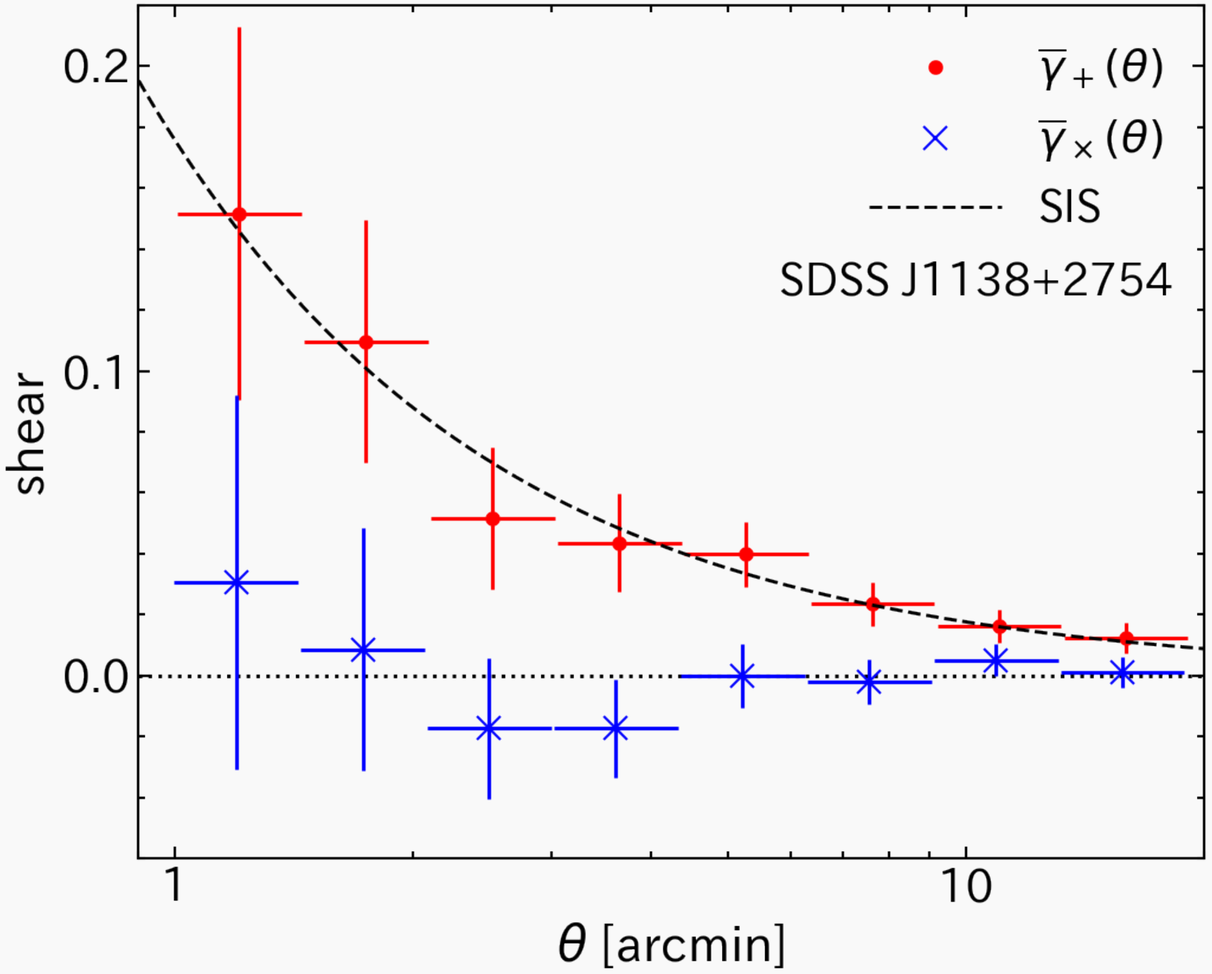

Differential surface mass density

- when redshift of each source galaxy is known, one can multiple tangential shear by critical surface density to obtain differential surface mass density

$$\overline{\Delta\Sigma}_{+}(R) = \frac{\sum_j w_j \gamma_{+j} \Sigma_{\rm cr}(z_{\rm l}, z_j)}{\sum_j w_j}$$

- additionally can take average of lens i

$$\overline{\Delta\Sigma}_{+}(R) = \frac{\sum_i \sum_j w_{ij} \gamma_{+ij} \Sigma_{\rm cr}(z_i, z_j)}{\sum_i \sum_j w_{ij}}$$

Stacked weak lensing analysis

MO+ MNRAS **420**(2012)3213

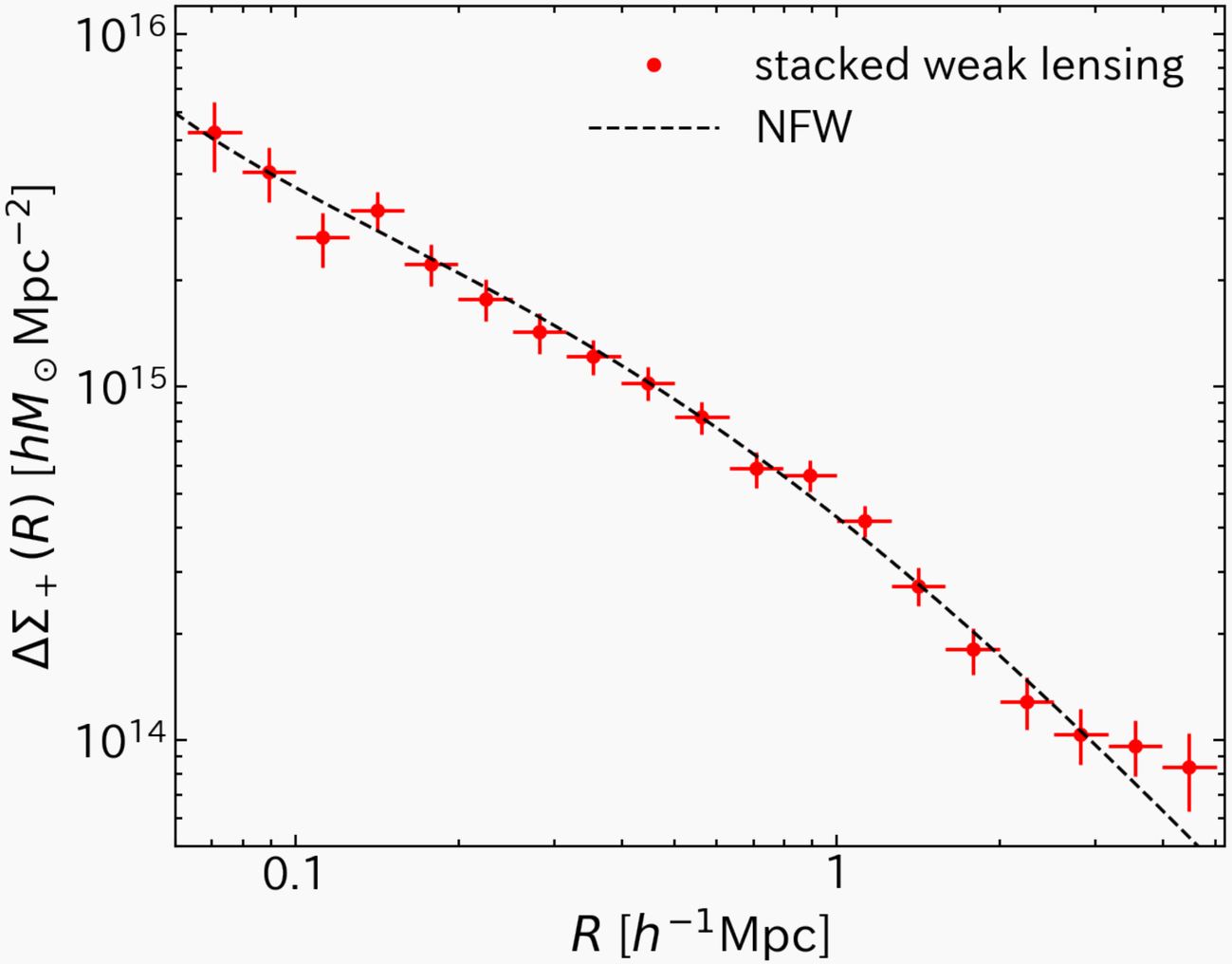

- average of differential surface mass density of 25 clusters
- precise measurement of dark matter distribution

Stacked weak lensing analysis in 2D

- stacking shear field in 2D aligning major axis from strong lensing
- significant project ellipticity (non-sphericity) with axis ratio of 2:1 detected
- confirm important cold dark matter prediction

MO+ MNRAS **420**(2012)3213

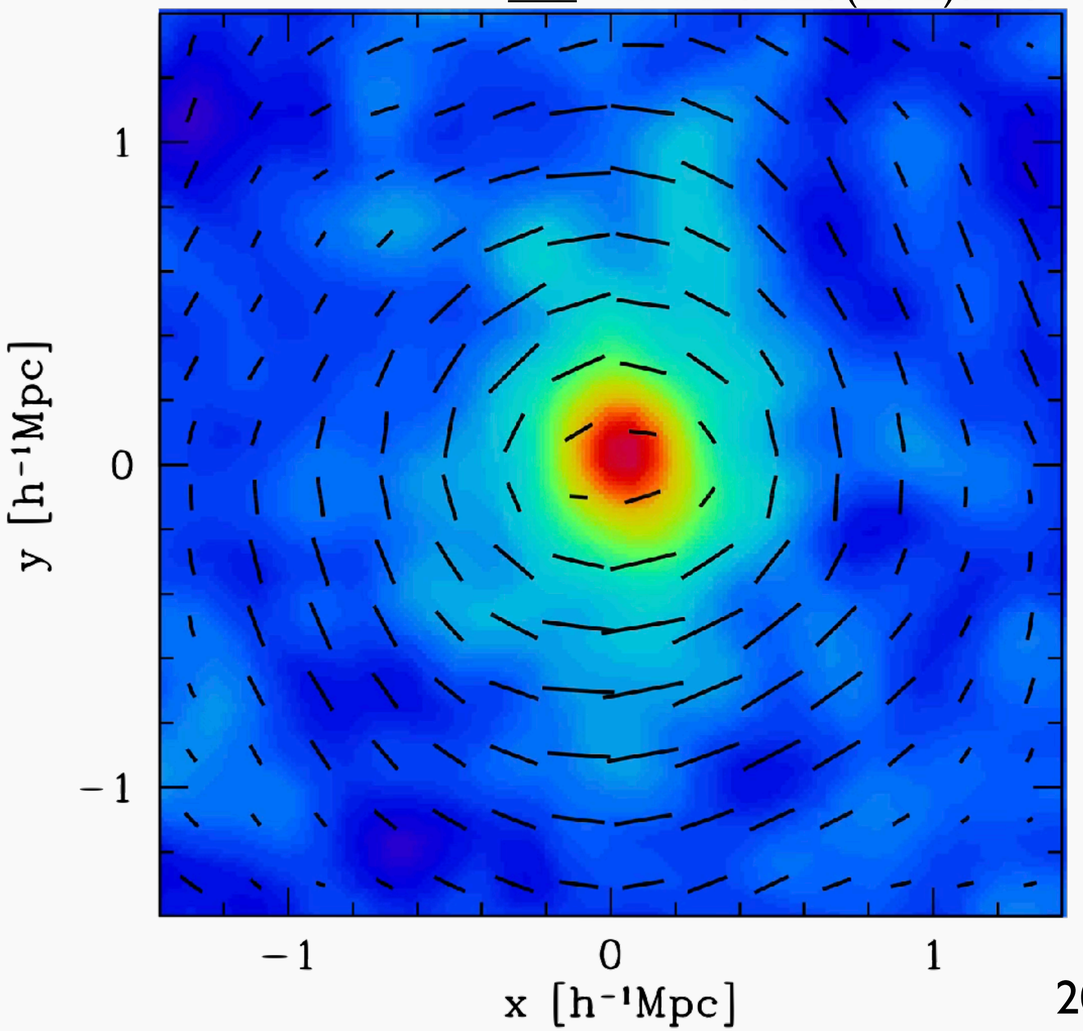

Detailed analysis of dark matter distribution

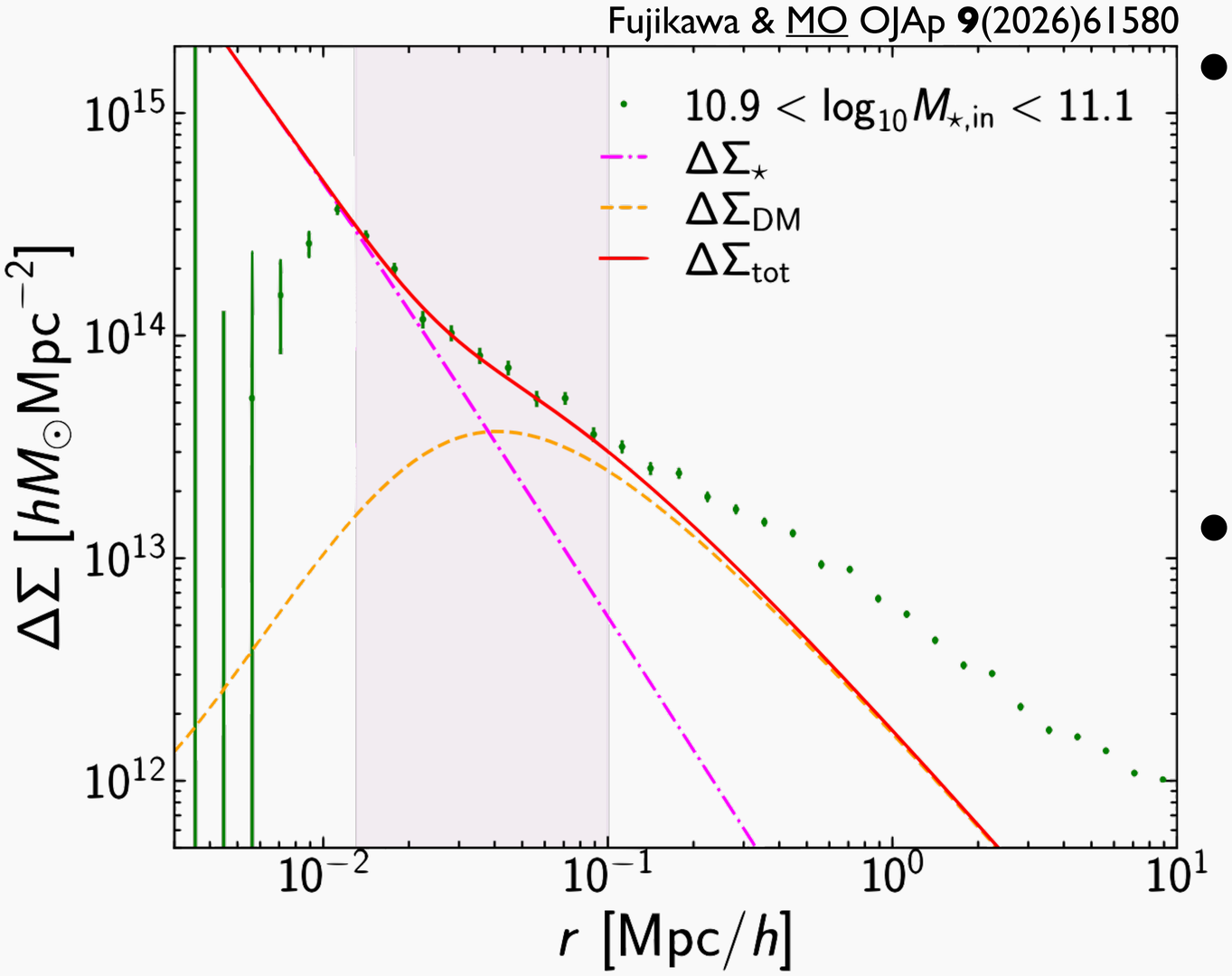

- differential surface mass density analysis using 30 million source galaxies and 1 million lensing galaxies from Subaru HSC survey data
- detect signals down to ~10 kpc, allowing analysis of central dark and stellar mass distributions of galaxies with weak lensing

Halo mass-stellar mass relation, stellar IMF

both directly measured by weak lensing

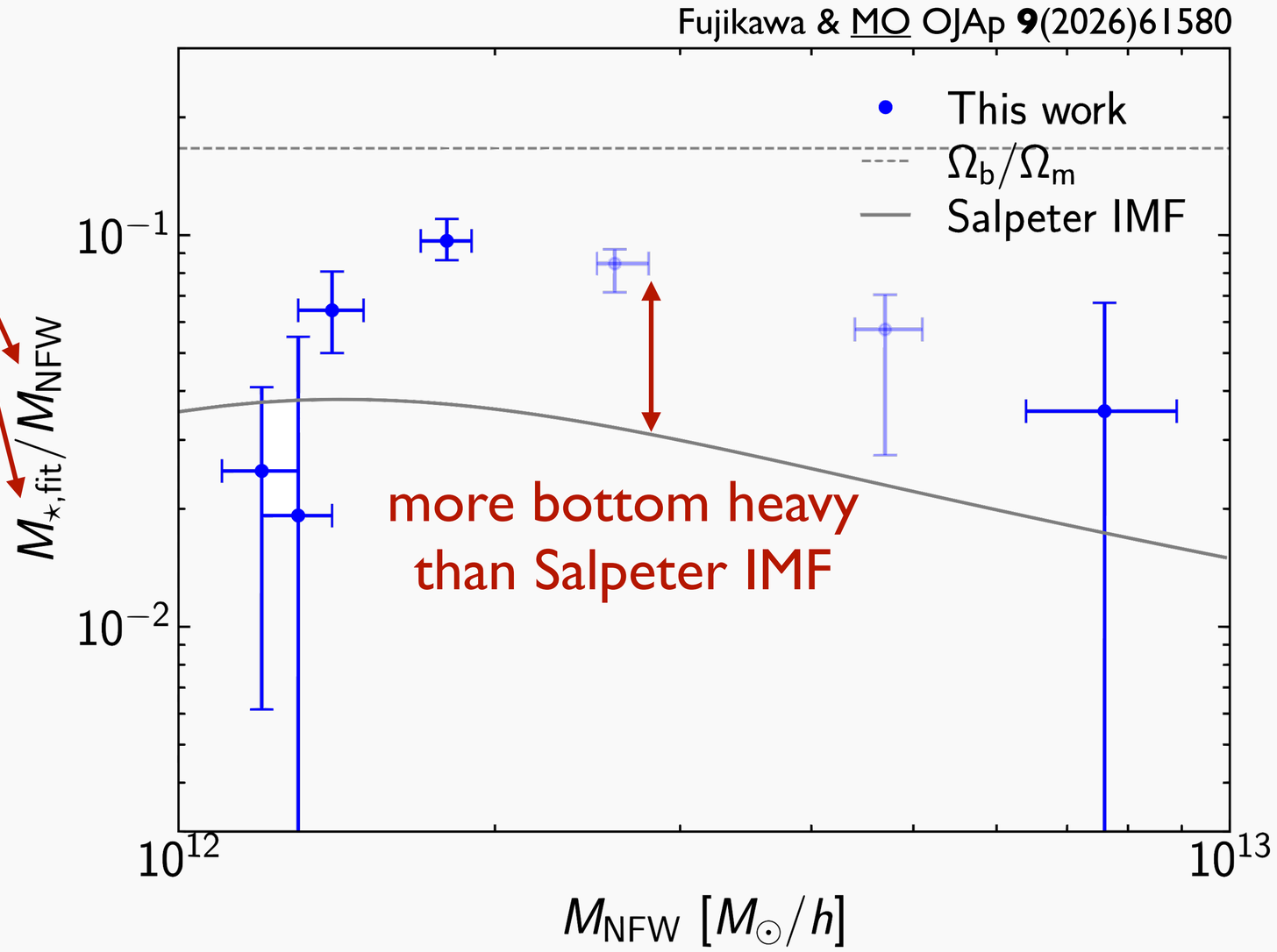

Dark matter map

- tangential shear analysis requires assumption on lens center
- it is possible to reconstruct dark matter distribution without any assumption → dark matter map

Kaiser-Squires method (I)

- relation between complex shear $\gamma(\boldsymbol{\theta})$ and convergence $\kappa(\boldsymbol{\theta})$

$$\psi(\boldsymbol{\theta}) = \frac{1}{\pi}\int d\boldsymbol{\theta}'\kappa(\boldsymbol{\theta}')\ln\left|\boldsymbol{\theta}-\boldsymbol{\theta}'\right|$$

$$\gamma(\boldsymbol{\theta}) = \frac{1}{\pi}\int d\boldsymbol{\theta}'\kappa(\boldsymbol{\theta}')D(\boldsymbol{\theta}-\boldsymbol{\theta}') \qquad D(\boldsymbol{\theta}) = \frac{\theta_2^2-\theta_1^2-2i\theta_1\theta_2}{\left|\boldsymbol{\theta}\right|^4}$$

- Fourier transform (convolution→product)

$$\tilde{\gamma}(\boldsymbol{\ell}) = \frac{1}{\pi}\tilde{\kappa}(\boldsymbol{\ell})\tilde{D}(\boldsymbol{\ell}) \qquad \tilde{D}(\boldsymbol{\ell}) = \pi\frac{\ell_1^2-\ell_2^2+2i\ell_1\ell_2}{\left|\boldsymbol{\ell}\right|^2}$$

Kaiser-Squires method (II)

- expression of convergence in Fourier space

$$\tilde{\kappa}(\boldsymbol{\ell}) = \frac{1}{\pi}\tilde{\gamma}(\boldsymbol{\ell})\tilde{D}^*(\boldsymbol{\ell})$$

- expression of convergence in real space

$$\kappa(\boldsymbol{\theta}) - \underline{\kappa_0} = \frac{1}{\pi}\int d\boldsymbol{\theta}'\gamma(\boldsymbol{\theta}')D^*(\boldsymbol{\theta}-\boldsymbol{\theta}')$$

constant

(mass-sheet transform) correspond to $\ell = 0$

reconstruct mass distribution $\kappa(\boldsymbol{\theta})$ from observation of galaxy shape $\gamma(\boldsymbol{\theta})$

EB mode

- rewrite equation of convergence (κ) reconstruction

$$\kappa(\boldsymbol{\theta}) - \kappa_0 = \underbrace{\frac{1}{\pi}\int d\boldsymbol{\theta}' \frac{\gamma_+(\boldsymbol{\theta}';\boldsymbol{\theta})}{\left|\boldsymbol{\theta}-\boldsymbol{\theta}'\right|^2}}_{\text{E-mode } \gamma_{\rm E}(\boldsymbol{\theta}) \text{ (convergence)}} + i\underbrace{\frac{1}{\pi}\int d\boldsymbol{\theta}' \frac{\gamma_\times(\boldsymbol{\theta}';\boldsymbol{\theta})}{\left|\boldsymbol{\theta}-\boldsymbol{\theta}'\right|^2}}_{\text{B-mode } \gamma_{\rm B}(\boldsymbol{\theta}) \text{ (zero)}}$$

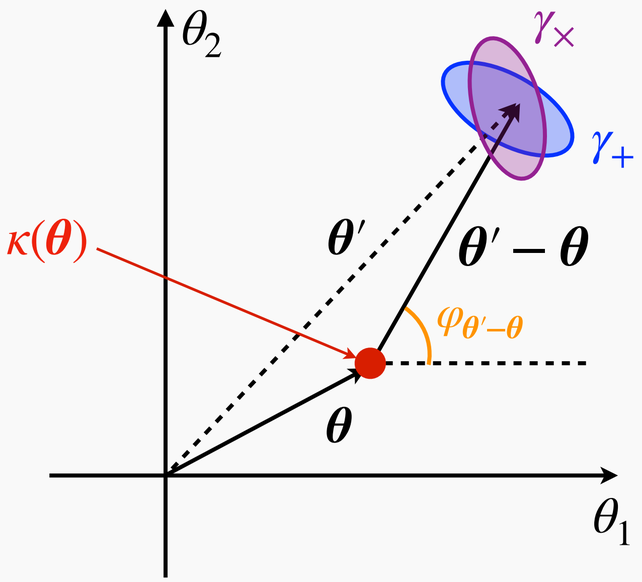

$$\gamma_+(\boldsymbol{\theta}';\boldsymbol{\theta}) = -\gamma_1(\boldsymbol{\theta}')\cos(2\varphi_{\boldsymbol{\theta}'-\boldsymbol{\theta}}) - \gamma_2(\boldsymbol{\theta}')\sin(2\varphi_{\boldsymbol{\theta}'-\boldsymbol{\theta}})$$

$$\gamma_\times(\boldsymbol{\theta}';\boldsymbol{\theta}) = \gamma_1(\boldsymbol{\theta}')\sin(2\varphi_{\boldsymbol{\theta}'-\boldsymbol{\theta}}) - \gamma_2(\boldsymbol{\theta}')\cos(2\varphi_{\boldsymbol{\theta}'-\boldsymbol{\theta}})$$

κ reconstruction = EB mode decomposition

convergence
$\kappa(\boldsymbol{\theta})$

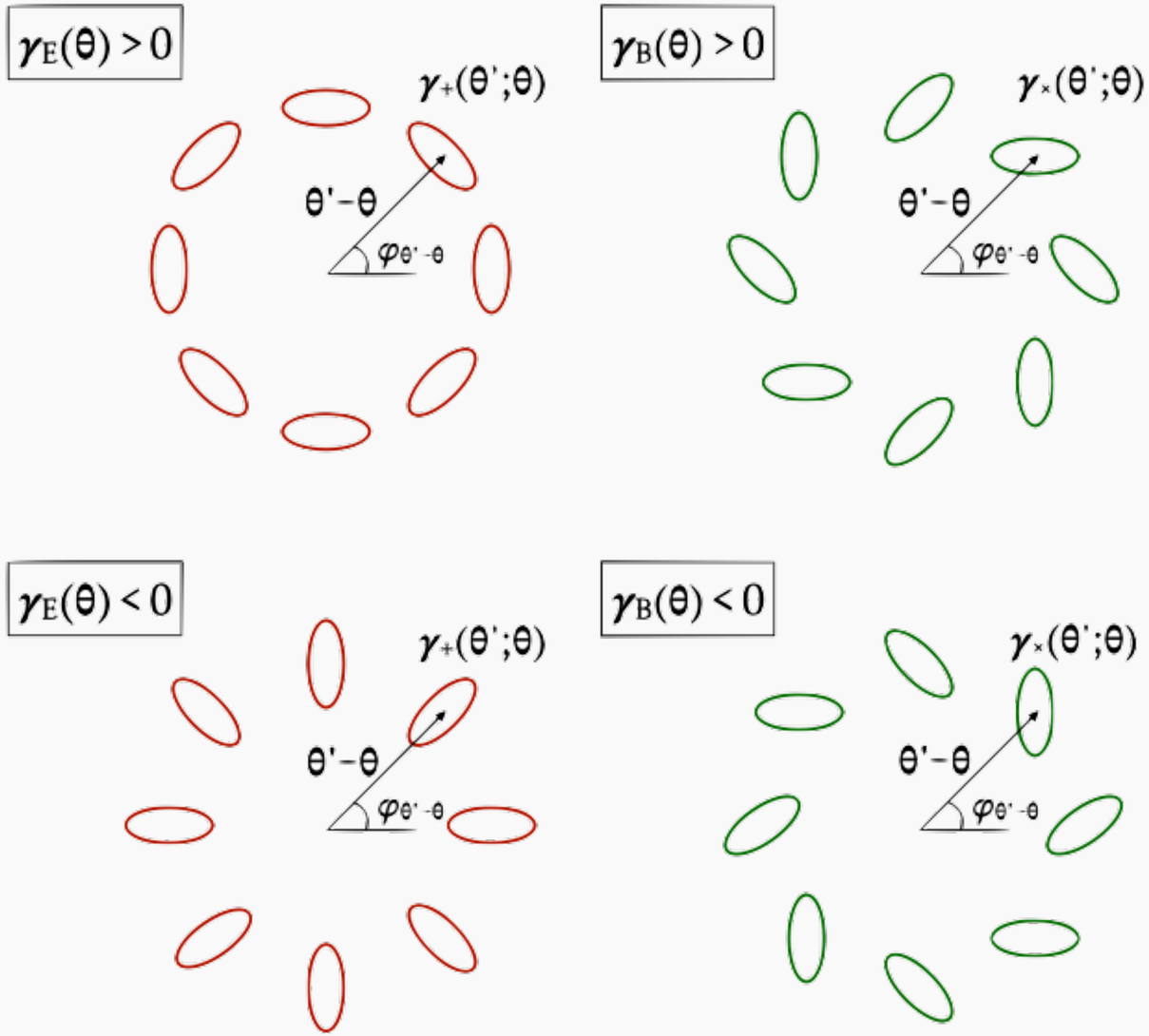

zero
(check for systematics)

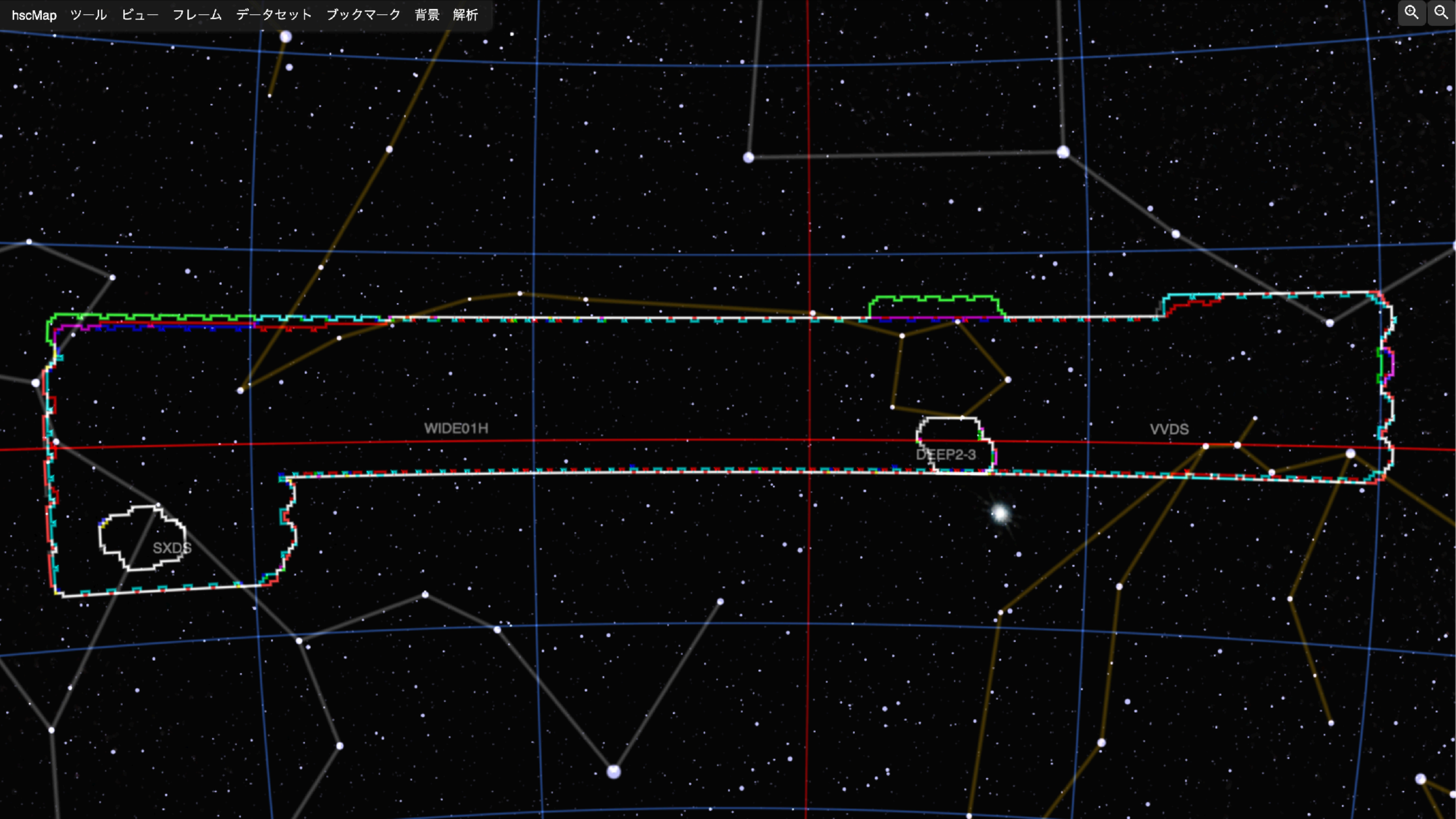
hscMap ツール ビュー フレーム データセット ブックマーク 背景 解析
WIDE01H
DEEP2-3
VVDS
SXDS

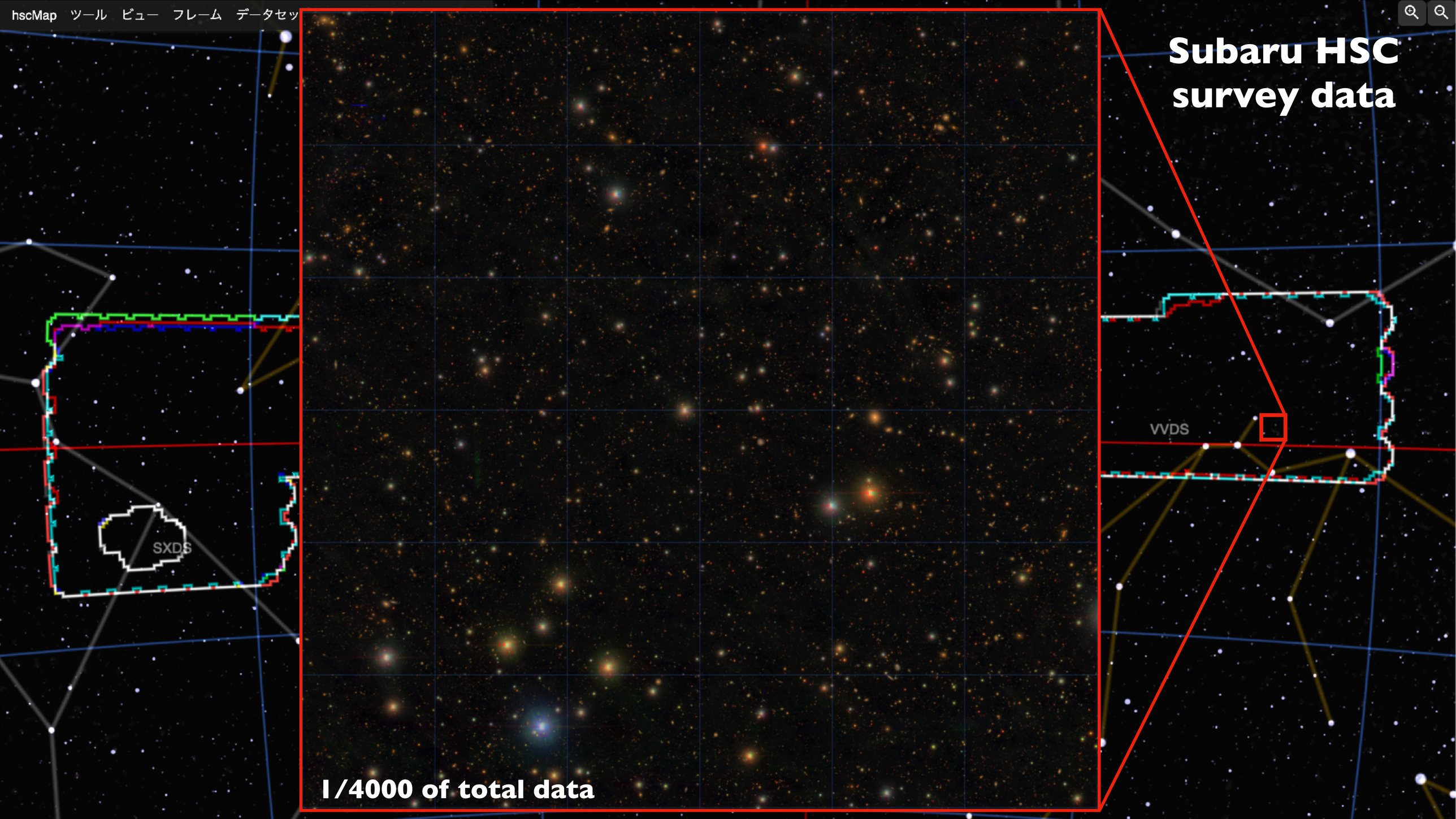
hscMap ツール ビュー フレーム データセッ
Subaru HSC
survey data
SXDS
VVDS
1/4000 of total data

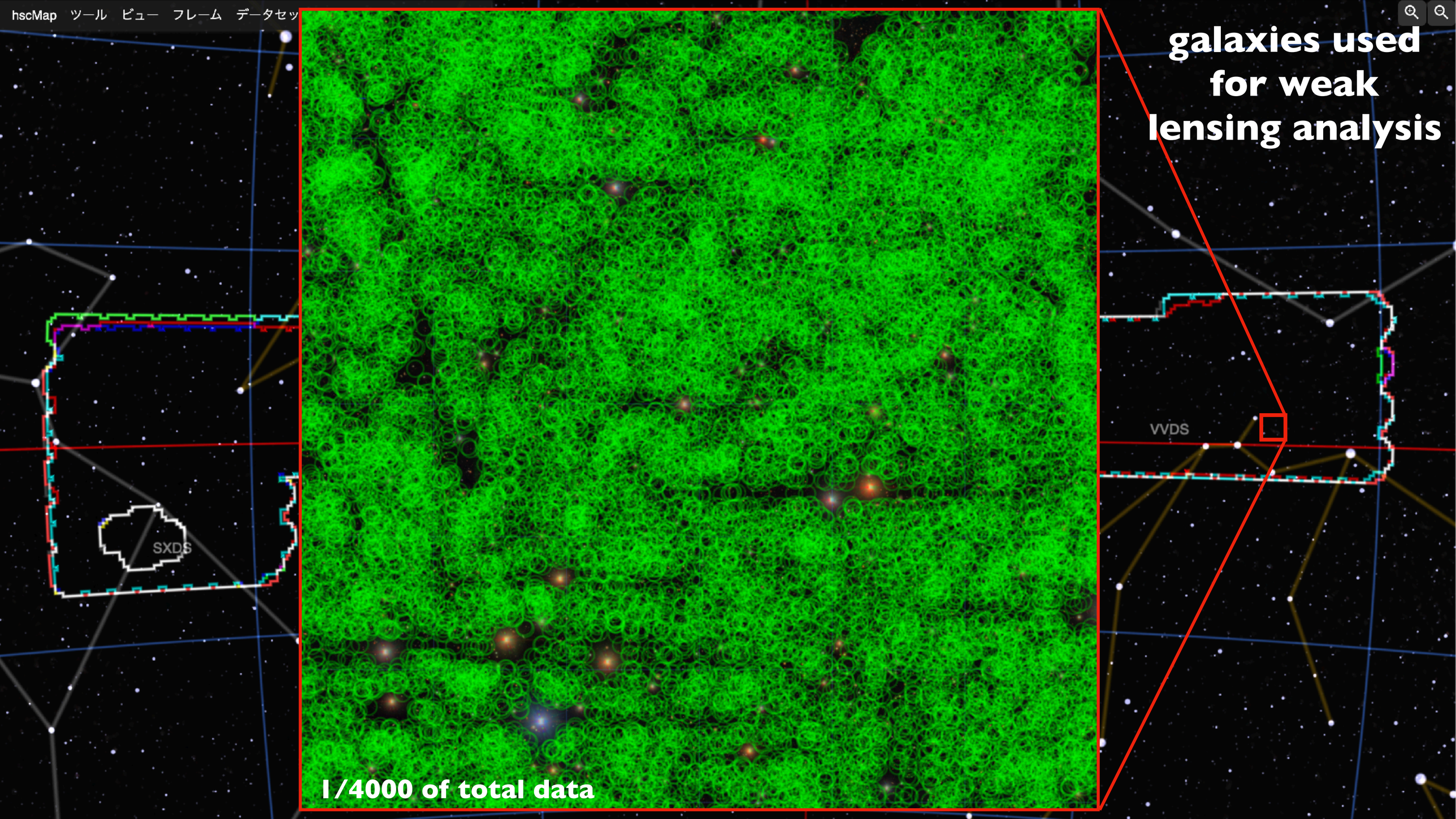
hscMap ツール ビュー フレーム データセッ
SXDS
VVDS
galaxies used for weak lensing analysis
1/4000 of total data

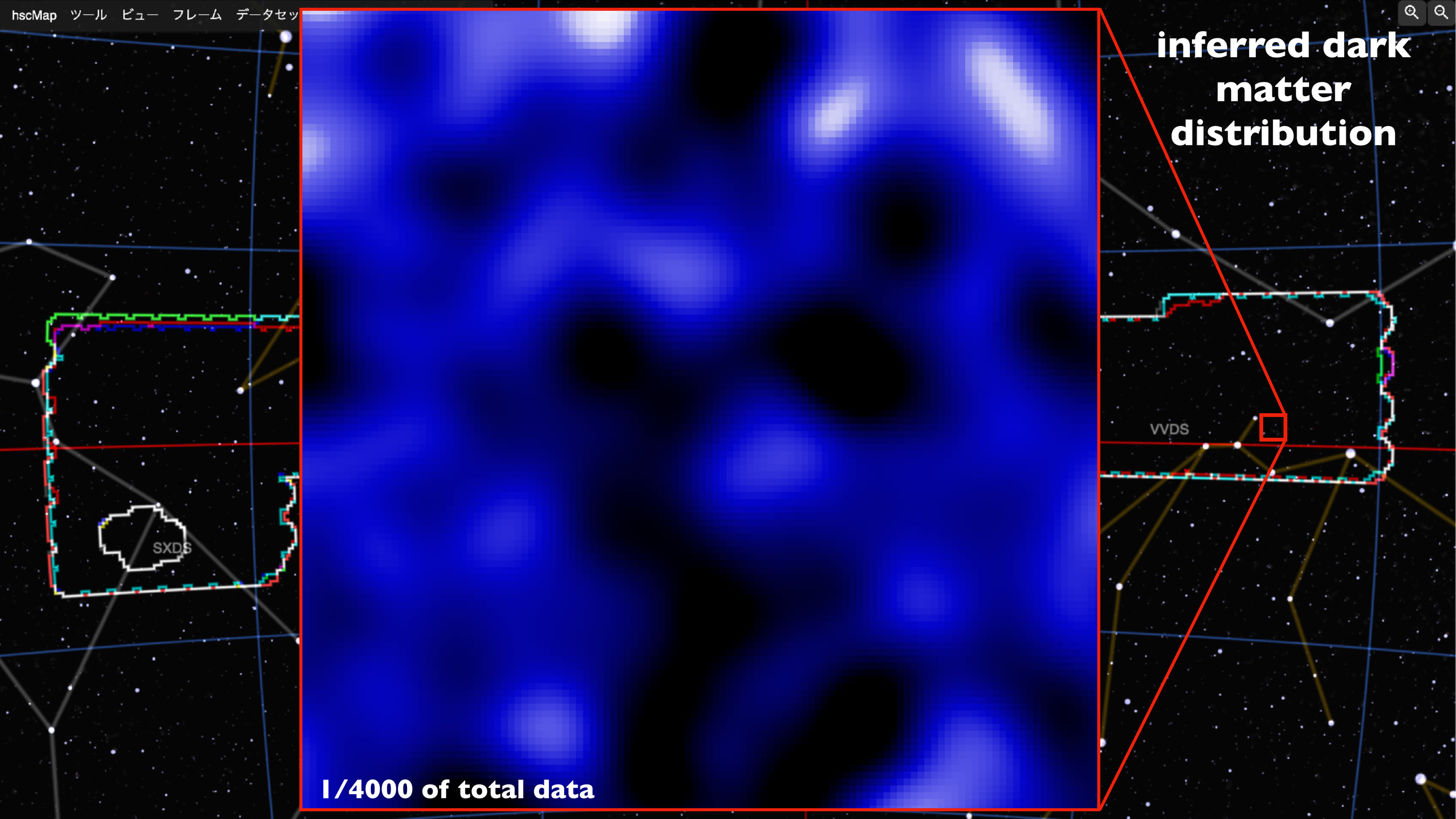
hscMap ツール ビュー フレーム データセッ
inferred dark matter distribution
SXDS
VVDS
1/4000 of total data

Cluster search using dark matter map

MO, Miyazaki+ PASJ **70**(2018)S26

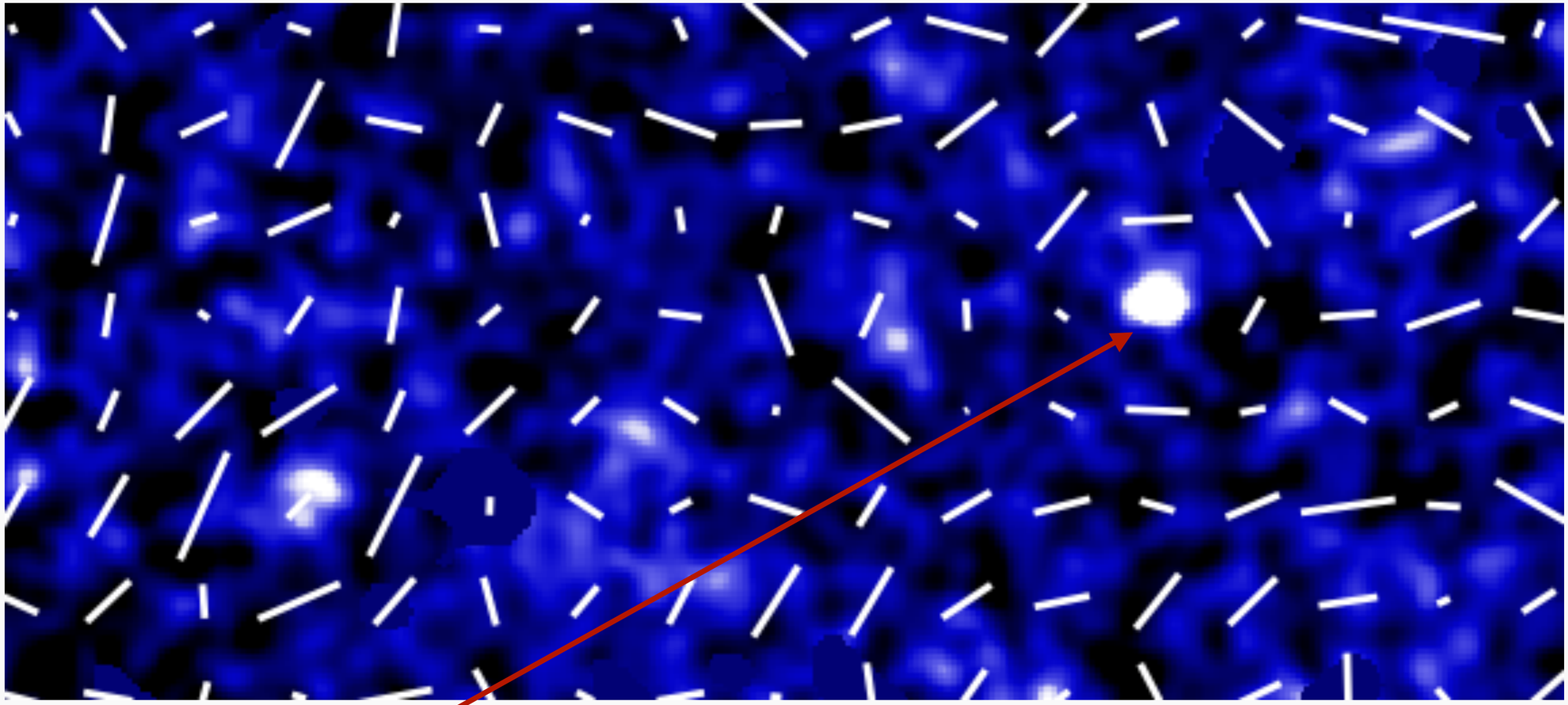

bar: shear
color:
convergence

can search clusters (peaks in map) from purely gravitational effect

Density distribution from weak lensing

- relation between κ and $\delta_{\rm m}$

$$\kappa(\boldsymbol{\theta}) = \int_0^{\chi_{\rm s}} d\chi\, W(\chi)\delta_{\rm m}(\chi, \boldsymbol{\theta})$$

$$W(\chi) = \frac{3\Omega_{\rm m0}H_0^2}{2c^2}\frac{f_K(\chi_{\rm s}-\chi)f_K(\chi)}{a f_K(\chi_{\rm s})}$$

- integration along line-of-sight with weight that depends on source redshift

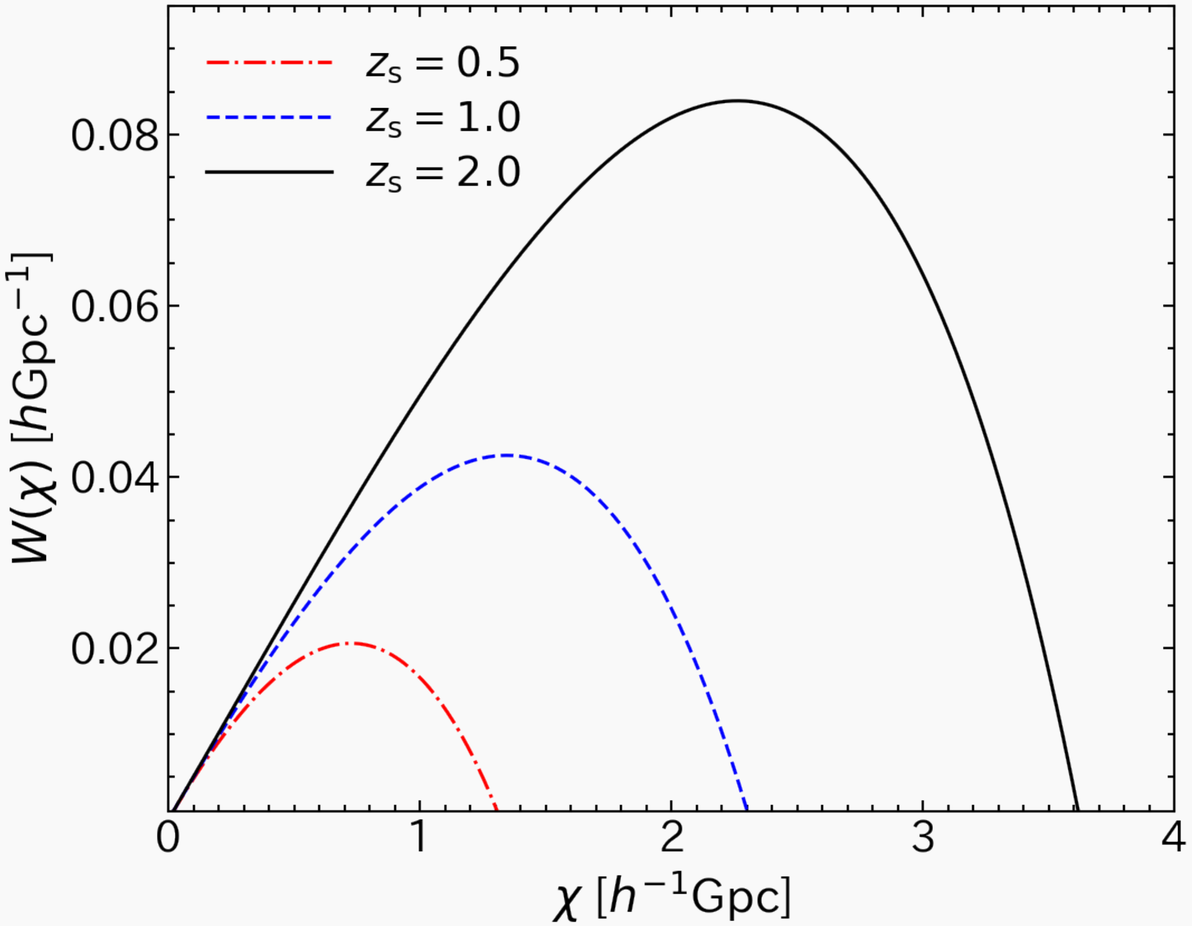

Reconstruction of 3D density distribution

- from convergence with different source redshift $\kappa(\boldsymbol{\theta}; z_{\mathrm{s},i})$

$$\kappa(\boldsymbol{\theta}; z_{\mathrm{s},i}) \simeq \sum_j \Delta\chi_j \, W(\chi_j; z_{\mathrm{s},i}) \delta_{\mathrm{m}}(\chi_j, \boldsymbol{\theta})$$

$$\Rightarrow \quad \delta_{\mathrm{m}}(\chi_j, \boldsymbol{\theta}) \simeq \sum_i \left[\Delta\chi_j \, W(\chi_j; z_{\mathrm{s},i}) \right]^{-1} \kappa(\boldsymbol{\theta}; z_{\mathrm{s},i})$$

3D reconstruction possible

Example of 3D reconstruction

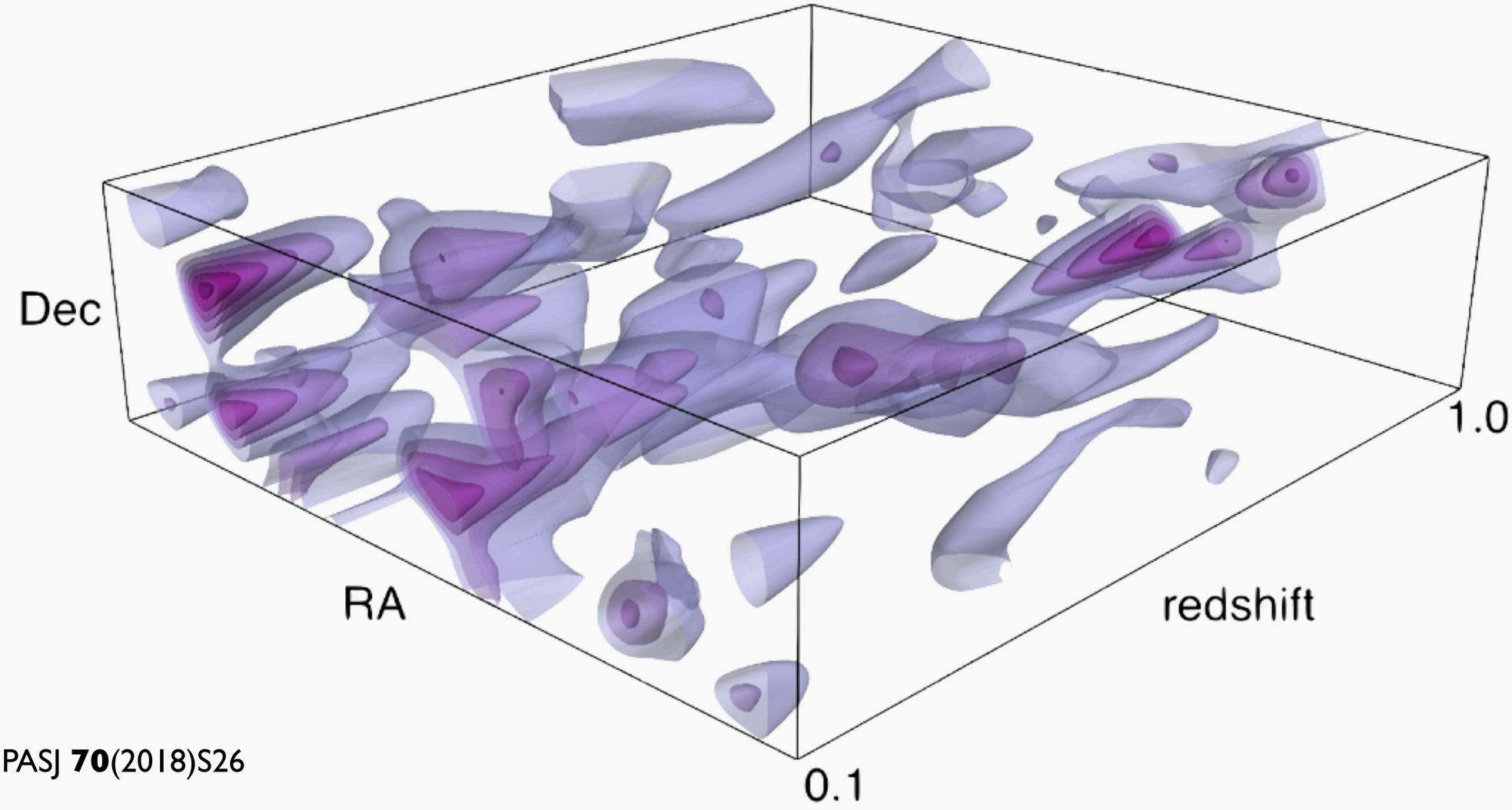

MO, Miyazaki+ PASJ **70**(2018)S26

Quantify density fluctuations

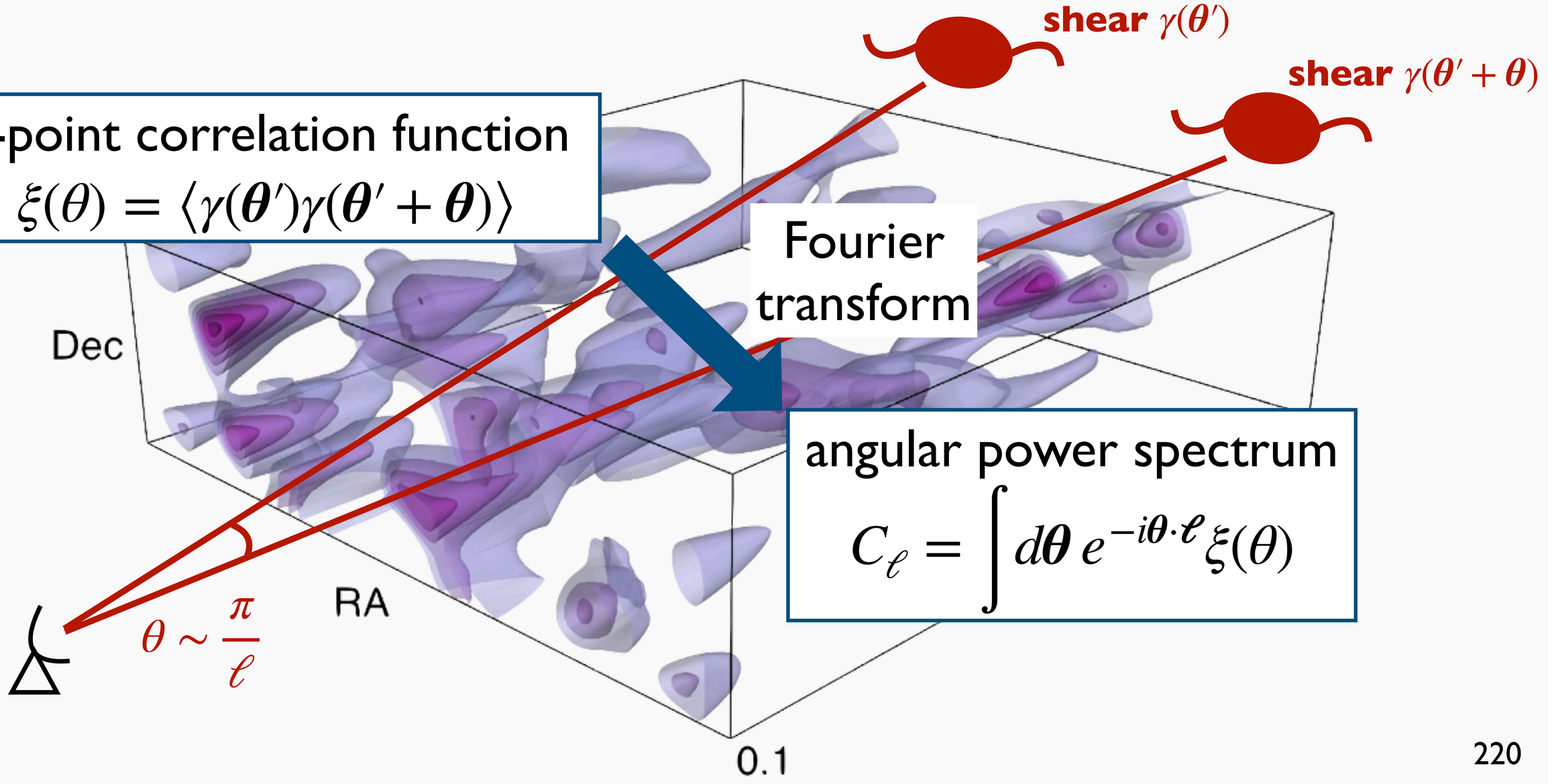

Cosmic shear power spectrum

- with Limber's approximation, angular power spectrum of convergence is

$$C_\ell^{\kappa\kappa} = \int_0^{\chi_\mathrm{s}} d\chi \left[\frac{W(\chi)}{f_K(\chi)}\right]^2 P_\mathrm{m}\left(\frac{\ell + 1/2}{f_K(\chi)}\right)$$

cosmic shear power spectrum

Calculation of cosmic shear power spectrum

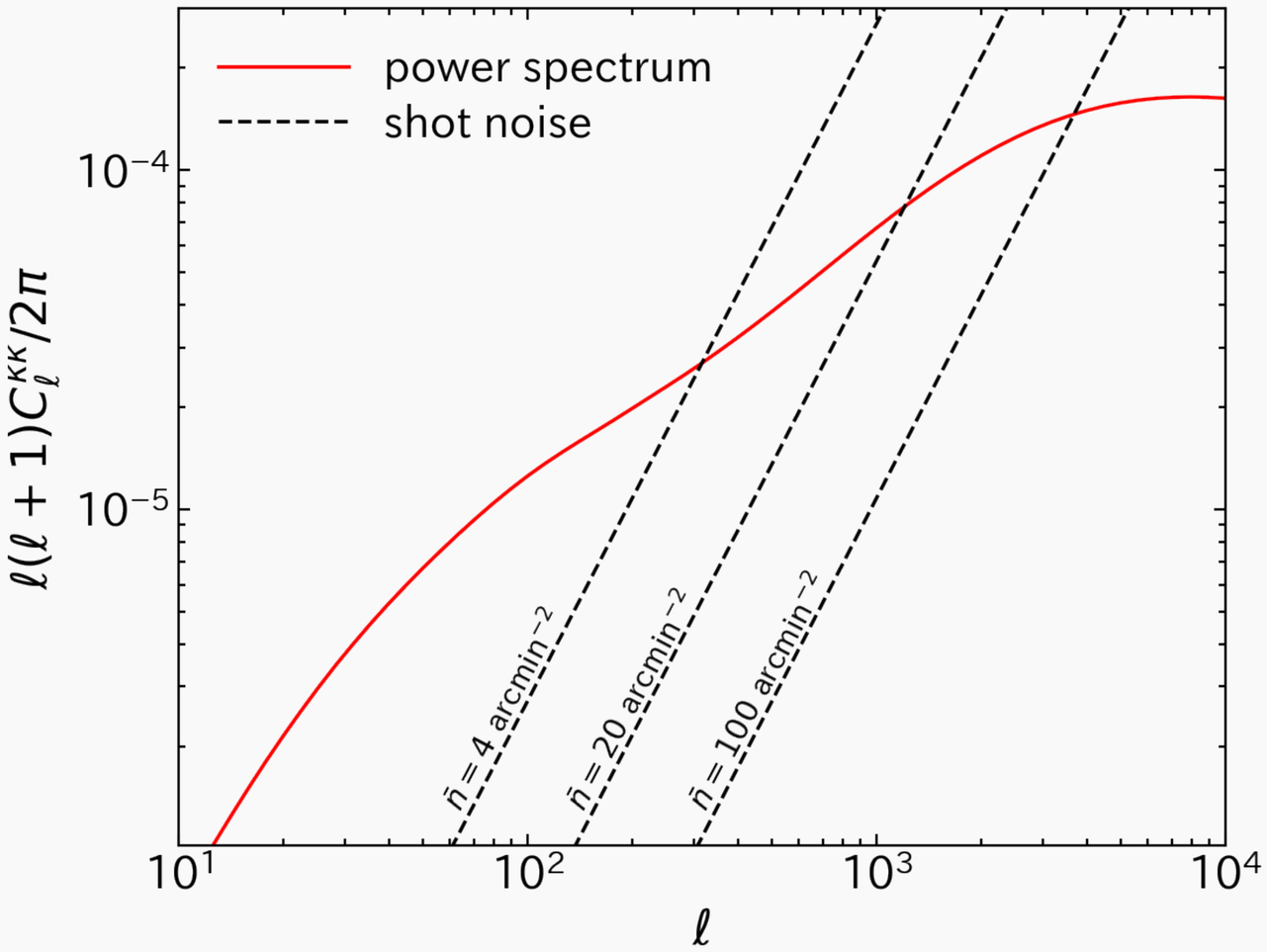

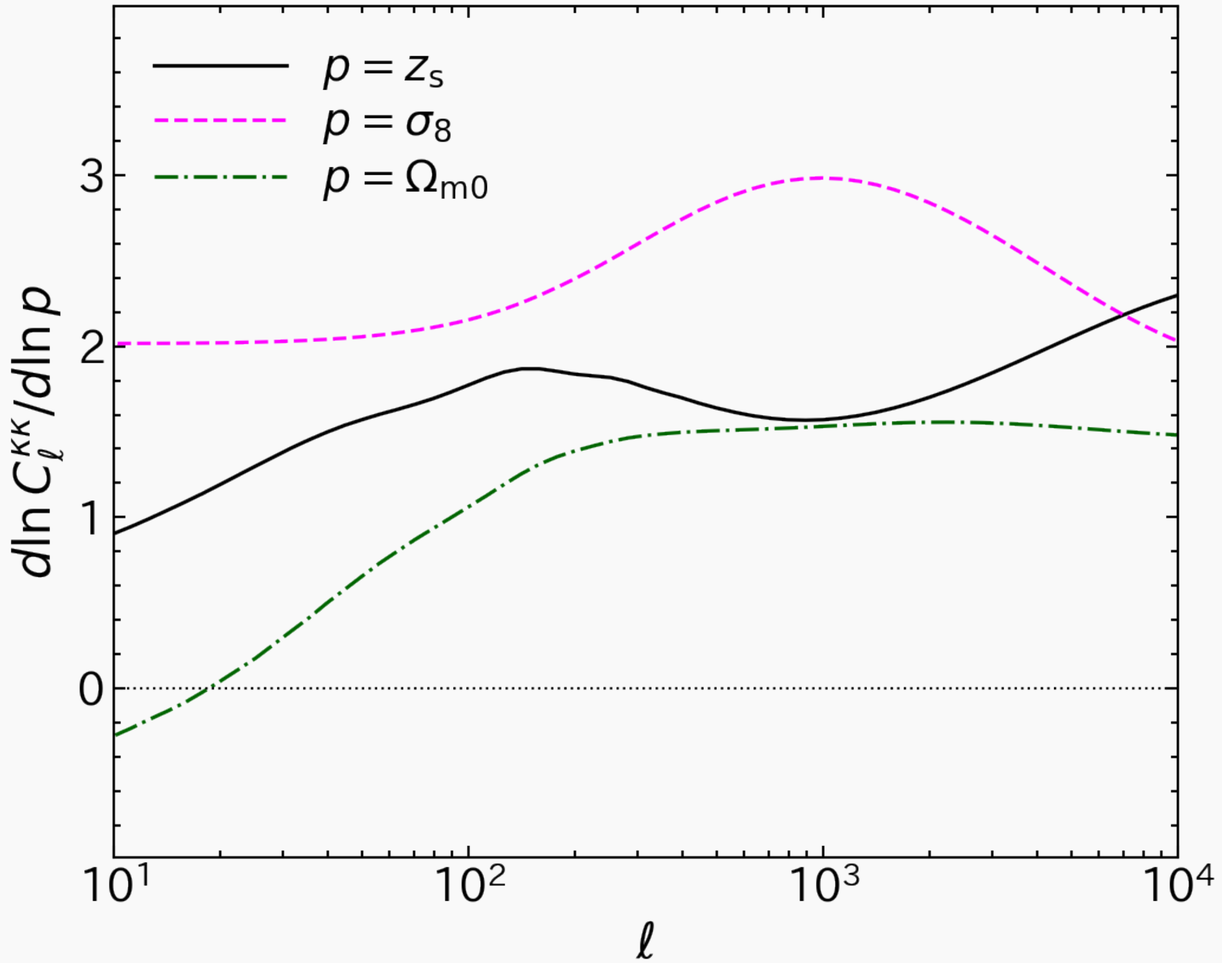

Example of observation and analysis

Hikage, MO+ PASJ **71**(2019)43

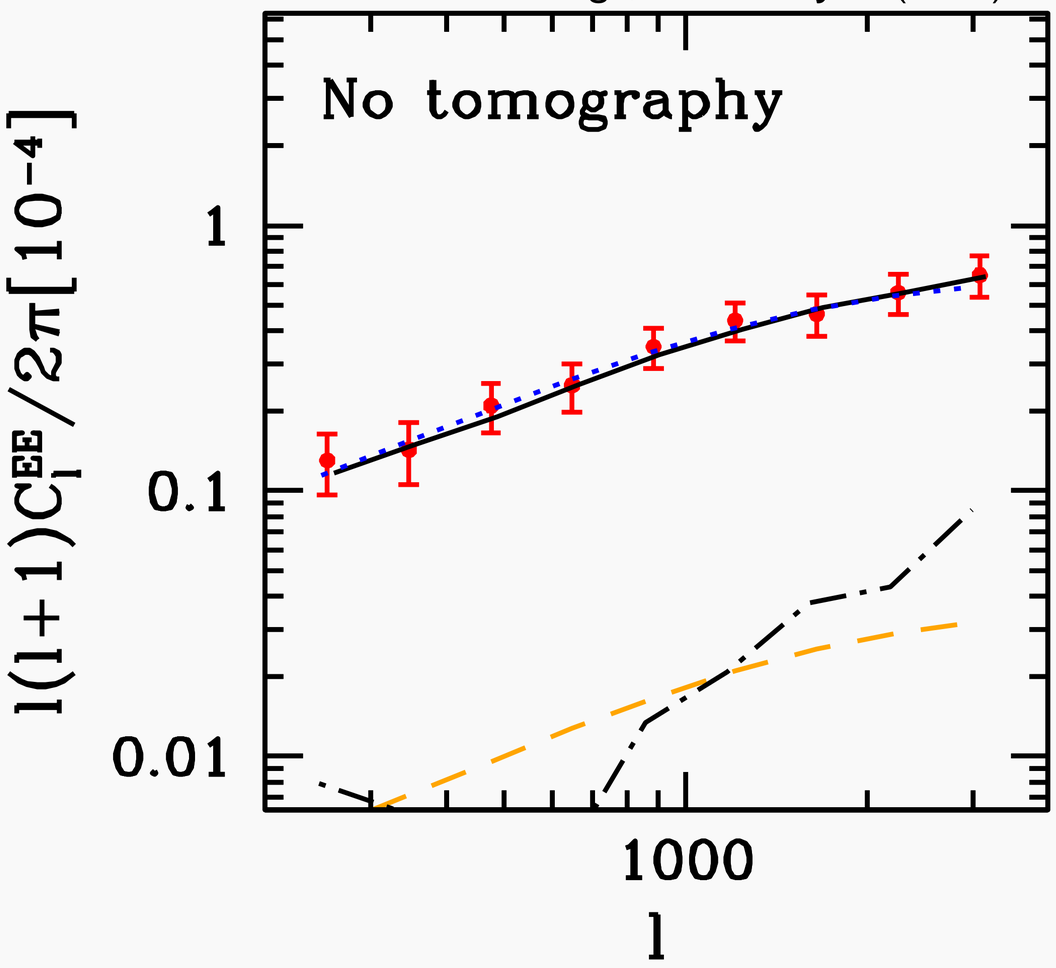

Hikage, MO+ PASJ **71**(2019)43

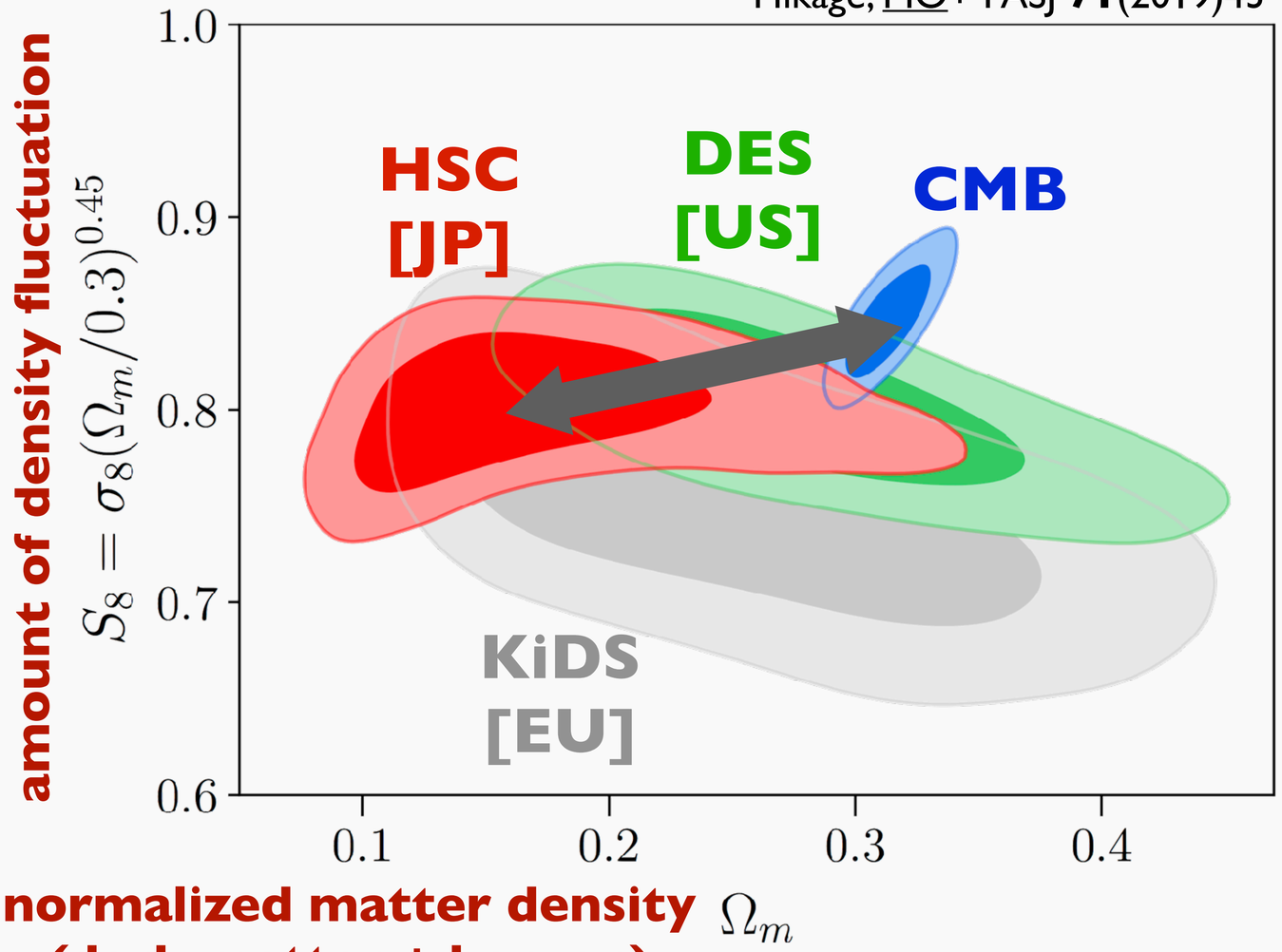

Summary

- weak lensing shear can be measured by taking average of shapes of many galaxies
- when lens objects are a priori identified, their mass distribution can be analyzed by tangential shear analysis
- mass reconstruction without any assumption is also possible